THE STRUCTURE OF BRAID BARS:

FACIES RELATIONSHIPS OF PLEISTOCENE

BRAIDED OUTWASH DEPOSITS, PARIS, ONTARIO

THE STRUCTURE OF BRAID BARS: FACIES RELATIONSHIPS OF PLEISTOCENE BRAIDED OUTWASH DEPOSITS, PARIS, ONTARIO

By

GEORGE EYNON, B.Sc.

A Thesis

Submitted to the Department of Geology

in Partial Fulfilment of the Requirements

for the Degree

Master of Science

McMaster University

1972

MASTER OF SCIENCE (1972)

McMASTER UNIVERSITY
Hamilton, Ontario.

TITLE: The Structure of Braid Bars: Facies Relationships of Pleistocene Braided Outwash Deposits, Paris, Ontario.

AUTHOR: George Eynon, B.Sc. (London University)

SUPERVISOR: Professor R. G. Walker

NUMBER OF PAGES: xii, 235

ABSTRACT

A large gravel pit at East Paris exposed 14m of Pleistocene braided outwash. Large scale longitudinal bars (30 - 400m long) were developed utilising irregular topographic highs (4 - 6m) of the basal gravels as Bar Cores. These bars prograded downstream by means of larce-scale cross-strata, periodically interupted by reactivation surfaces. Contemparaneous upstream addition of material took place by the migration of mixed sand and gravel bed-forms on the stoss-side of the bars. The gravel supply to the avalanche face of the major bars took the form of imbricated gravels which passed from the Stoss-side, through the Bar Top, onto the Bar Front. Adjacent, sandy side-channels (4 - 6m deep) exhibit a fining upward fill of trough cross beds, planar lamination and ripples; and interdigitated with the gravel bars alongside.

Aggradation of the flood plain led to the extension of the Bar Top facies over the length of the bars, and then to the development of a Shallow-braided stream facies over the whole system. The latter is recognised by its smaller (less than 1m) bar forms composed of cross-bedded gravel supplied by an imbricate gravel, and numerous small, sandy channel forms.

At West Paris another large gravel pit exposed 6m of sandier, but stratigraphically equivalent deposits. Large scale side-bar accumulations (200-300m across) of gravel developed from river bank lateral accretion deposits. The downstream progradation was by lobes of cross-stratified and imbricated gravels, alternating with sand drapes of low flow stages. Sandy Side-channels (4m deep) developed between the gravel lobes and the accreting river bank.

The concept of braid bar growth from a pre-existing form (bar core or river bank) is in contrast to the classic theory of development from a gravel lag. The differences may be due to depth relationships of the systems, which in this case may be the effect of position on the sandur surface.

ACKNOWLEDGEMENTS

The author particularly wishes to thank Dr. Roger G. Walker, his supervisor, for the aid and encouragement he has given throughout this study.

Messrs. Colin C. Turner and Ian C. Davies, and Professor G. V. Middleton provided useful discussions and suggestions. Messrs. Bill Day and Larry Bourke ably assisted with the field and laboratory work, and drafting and computing respectively.

The text was expertly translated from my handwritten manuscript by Miss Lynn Pickering.

LIST OF CONTENTS

			Page
Abstract			iii
List of contents			vi
List of figures			viii
List of tables			xi
Chapter One	The Problem		1
Chapter Two	The Literature		7
Chapter Three	The Pleistocene History		12
Chapter Four	The Local Stratigraphy		21
Chapter Five	Introduction to the Facies		28
Chapter Six	The Facies at East Paris		30
	Bar Core Facies		30
	Occurrence	30	
	Stratification	32	
	Fabrics and Palaeocurrents	33	
	Grain Size	35	
	Bar Front Facies		39
	Occurrence	39	
	Sedimentary Structures	40	
	Fabrics and Palaeocurrents	47	
	Grain Size	50	
	Stoss-side Facies		53
	Occurrence	53	
	Stratification and Sed. Structures	54	
	Fabrics and Palaeocurrents	55	
	Grain Size	57	
	Bar Top Facies		57
	Occurrence	57	
	Stratification	59	
	Fabrics and Palaeocurrents	60	
	Grain Size	62	
	Side-channel Facies		64
	Occurrence	64	
	Sedimentary Structures	67	
	Palaeocurrents	68	
	Grain Size	70	
	Shallow Braided Stream Facies		73
	Occurrence	73	
	Stratification and Sed. Structures	74	
	Fabrics and Palaeocurrents	76	
	Grain Size	78	
	The Facies at East Paris: Interpretation		81
	Basal Gravels	81	
	Erosion of the Basal Gravels	82	
	Bar Front Growth	84	
	Stoss-side addition	85	
	Sed. transport through the system	87	
	Side-channel infilling	91	
	Shallow Braided Stream	91	
	Summary of Longitudinal Braid Bar 'Model'		92

Chapter Seven	The Facies at West Paris		94
	Bar Front Facies		94
	Occurrence	94	
	Sedimentary Structures	96	
	Palaeocurrents	106	
	Grain Size	108	
	Lateral Accretion Facies		111
	Occurrence	111	
	Stratification and Sed.Structures	112	
	Fabrics and Palaeocurrents	113	
	Grain Size	117	
	Side Channel Facies		119
	Occurrence	119	
	Sedimentary Structures	120	
	Palaeocurrents	121	
	Grain Size	125	
	The Facies at West Paris: Interpretation		125
	Type of Bar Form	126	
	Bar Origins	128	
	The Side-channel Facies	129	
	The multilobate advance	131	
	Summary of the Side Bar 'Model'		133
Chapter Eight	Synthesis		135
	Channel Depth	135	
	The Origins of Braid Bars	137	
	Braid Bar Migration	139	
	Proximal-Distal Relationships	141	
	Sandar Zones at Paris	142	
	The Fining Upward Sequence	144	
Reference List			146
Appendix A:	Sand and Gravel Pits in the Area		152
Appendix B:	Grain Size Methods and Data		160
	Methods	160	
	Data for East Paris	164	
	Data for West Paris	189	
Appendix C:	Palaeocurrent Methods and Data		204
	Methods	204	
	Data for East Paris	209	
	Data for West Paris	223	
Map A		(back pocket)	
Photolog: East Paris		"	"
Photolog: West Paris		"	"

LIST OF FIGURES

Figure No.		Page
1.	Map of the ice front position at the time of the Paris moraine and Late Whittlesey	14
2.	Part of the δO^{18} curve for Camp Century ice core from Greenland, with interpretation for southern Ontario.	16
3.	Ice movements and moraines in the area west of Lake Ontario.	18
4.	The ice front and drainage pattern at the time of the Moffat moraine.	19
5.	Map of the bedrock topography in the Paris-Brantford area.	22
6.	Simplified geological section through the moraine-outwash complex at Paris.	24
7.	Stratigraphy of the outwash gravels at East Paris	26
8.	Map of East Paris pit.	31
9.	Palaeocurrents of the Bar Core Facies.	34
10.	C-M diagrams of the outwash gravels.	36
11.	Grain size scales for clastic sediments.	37
12.	Grain size distributions for Bar Core Facies.	38
13.	Bar Front Facies and its component parts.	41
14.	The Orientation of pebbles on the foreset slopes.	43
15.	Photograph of gravel foresets of Bar Front Facies.	44
16.	Types of cross-strata in the Bar Front Facies.	45
17.	Geometry of the Reactivation surfaces.	48
18.	Dimensions of the advancing Bar Front Facies.	49
19.	Palaeocurrents of the Bar Front Facies.	51
20.	Grain size distributions of the Bar Front Facies.	52
21.	Palaeocurrents of the Stoss-side Facies.	56

22.	Grain size distributions of the Stoss-side Facies.	58
23.	Palaeocurrents of the Bar Top Facies.	61
24.	Grain Size distributions of the Bar Top Facies.	63
25.	Type-exposure of Side-channel Facies.	66
26.	'Pebble Clusters' in Side-channel Facies.	69
27.	Palaeocurrents of the Side-channel Facies.	71
28.	Grain size distributions of the Side-channel Facies.	72
29.	Palaeocurrents of the Shallow Braided Stream Facies.	77
30.	Grain size distributions of the Shallow Braided Stream Facies.	79
31.	Summary of the palaeocurrents at East Paris.	83
32.	Flow stage fluctuations and reactivation surfaces.	86
33.	Map of the West Paris pit.	95
34.	The Bar Front Facies and its component parts.	97
35.	Measured section through Sand Drape (b).	103
36.	Measured section through Sand Drape (c).	105
37.	Palaeocurrents of the Bar Front Facies gravels.	107
38.	Palaeocurrents of the Bar Front Facies sand drapes.	109
39.	Grain size distributions of the Bar Front Facies.	110
40.	Palaeocurrents of the Lateral Accretion Facies imbrication.	115
41.	Palaeocurrents of the Lateral Accretion Facies cross-beds.	116
42.	Grain size distributions of the Lateral Accretion Facies.	118
43.	Side channel complex at West Paris.	122
44.	Palaeocurrents of Side-channel Facies.	123

45. Grain size distributions of Side-channel Facies. 124

46. Map of palaeocurrent data at West Paris. 127

47. Reconstruction of palaeoflow conditions at West Paris. 130

48. Table of depths of rivers in the literature. 136

49. Sandar zones, ice recession and channel 'switching' at Paris. 145

50. Photograph of instrument used to measure pebble orientations. 205

LIST OF TABLES

Table No.		Page
	Grain size data for East Paris	
1.	Bar Core Facies	164-168
2.	Bar Front Facies	164-168
3.	Stoss-side Facies: Cross-bedded gravels	169-173
4.	" " " Imbricate gravels	169-173
5.	Bar Top Facies: Sands	174-178
6.	" " " Gravels	174-178
7.	Side Channel Facies: Trough cross-beds	174-178
8.	" " " Planar lamination	179-183
9.	" " " Rippled sands	179-183
10.	Shallow Braided Facies: Imbricate gravel	179-183
11.	" " " tabular cross-bedded gravel	184-188
12.	" " " channel infilling	184-188
13.	" " " sands	184-188
	Grain size data for West Paris	
14.	Bar Front Facies: sand drape (a)	189-193
15.	" " " " " (b)	189-193
16.	" " " " " (c)	189-193
17.	" " " gravel cross-strata	194-198
18.	" " " imbricate gravel	194-198
19.	Lateral Accretion Facies: gravels	194-198
20.	" " " transition sub-facies	199-203
21.	" " " sands	199-203
22.	Side-channel Facies.	199-203
	Palaeocurrent Data for East Paris	
23.	Bar Core Facies	209
24.	Bar Front Facies: gravel cross-strata	210
25.	" " " side-channel sand body	211
26.	Stoss-side Facies: imbrication	212
27.	" " " cross-strata	213
28.	Bar Top Facies: reworked bar core	214
29.	" " " sand lenses	215
30.	" " " imbrication	216
31.	Side-channel Facies: trough cross-strata	217
32.	" " " rippled sands	218
33.	Shallow Braided Facies: imbrication	219
34.	" " " channel infill	220
35.	" " " tabular cross-strata	221
36.	" " " cross-bedded sands	222

Palaeocurrent data for West Paris

37.	Bar Front Facies: imbrication	223
38.	" " " gravel foresets	224
39.	" " " minor bars	225
40.	" " " sand drape (a)	226
41.	" " " " " (b)	227
42.	" " " " " (c)	228
43.	Lateral Accrection Facies: imbrication (i)	229
44.	" " " " (ii)	230
45.	" " " cross-strata	231
46.	" " " transition sub-facies	232
47.	" " " cross-bedded sands	233
48.	Side Channel Facies: ripples	234
49.	" " " cross-bedded sands	235

CHAPTER ONE

THE PROBLEM

CHAPTER ONE

THE PROBLEM

Several problems related to braided streams and their deposits were set up when approaching this study. First of all there was relatively little data or literature available on braided streams generally; this situation was particularly noticeable when searching for work on coarse braided stream deposits. The literature has little on the relationships of the sands and gravels in the systems, and virtually nothing on the gross facies relationships laterally and vertically, despite the fact that bar development had been observed in the modern environment, recorded (by time-lapse-photography), and simulated experimentally.

Almost regardless of scale, (an important factor which will be discussed in Chapter 8) braid bars were regarded a few years ago as being all of the same type, and as having a set pattern of development, however imperfectly understood that might be. Writing about braided channels tributary to the Green River near Daniel, Wyoming, Leopold et al (1964, p.284) "... noted the following characteristics. The several channels in a given reach were separated by vegetated islands whose upper surfaces tended to be at the same level as small unvegetated central bars obviously in the process of being built .... The ages of vegetation taking hold on the new gravel bars indicated that the bars tend to build by additions at the downstream end and probably also on some parts of the lateral boundaries, but not on the upstream tip." Once initiated such

a mid-channel bar (Morisawa 1968, p. 146) ..."also deflects the current against the side walls of the channel causing erosion."

These two descriptions constitute the classic geomorphological concept of braided channels and their bars, and indicate some of the limits of our knowledge. Not all bars in braided systems are "mid-channel" bars. Smith (1970,1971) recognised two types, relating them to downstream decrease in sediment grain size. Longitudinal bars were found to occur nearer the source area and transverse bars downstream of them. Similarly, Collinson (1970), working on the Tana River in Norway divided the features into banks and islands, side-bars and linguoid-bars.

However, many questions still remain to be answered. How does the "mid-channel bar" itself originate? Does the "mid-channel bar" cause channel widening or is the feature itself a response to widening? How does the addition of material onto the growing form take place? What are the relationships of the "bar" to the sediments in the channels on either side?

To date all braided stream gravel accumulations have been termed "bars" - but can anything more definite be said about them? It was hoped the relationships investigated in this study would form a model for braid-bar development, enabling us to understand better the present day braided streams and more readily identify their deposits in the geological record.

The lack of data on gross facies relationships can be attributed to the predominance of studies in the modern environment. The very nature

of the braided stream system, being highly mobile and generally coarse grained,precludes work on the internal structures of deposits, especially below the level of low stage flow. In addition, the most active period of any braided stream is at the high water stage, but this is the most difficult period to observe and record. Consequently, it becomes virtually impossible to see a bar originate, and then grow and develop in its early stages, so rapid are the changes taking place (Smith, 1972). This restriction on field observation places similar restrictions on the conclusions that can be drawn.

It is fully realised that the modern environment provides the best basis for the study of process, and of the relationships of the sediment in the system to the transporting medium; but the "fossil flume" nature of the glacial outwash gravels of the Pleistocene make them the ideal object of study for establishing facies relationships. All that is lacking is the water, but it may be possible to partially remedy that situation by the reconstruction of palaeoflow parameters (see works by Schumm, 1967, 1968a, 1968b, 1969 and Jopling 1964, 1965, and 1966; and a recent paper by Cotter 1971, in which such palaeoflow reconstructions are discussed and made).

Three dimensional views of the internal structures, the facies and their relationships can be relatively easily obtained in these generally unconsolidated deposits, particularly in areas where the sand and gravel industry is important. It was for this reason that southern Ontario in general, and the Paris region in particular, was chosen as the field area.

The deglaciation of southern Ontario has left large areas of outwash deposits in ice-marginal channelways. A complex of parallel

moraines which run approximately north to south in the area west of the Niagara Escarpment has been a major control of the outwash deposition at several periods during the ice-front fluctuations. These deposits are exploited commercially and the exposures provided were thought to afford answers to the problems and questions posed.

Reconnaissance was undertaken during August and September 1970, to locate suitable outcrops. Several possible areas were investigated, and locations of all pits examined are shown on Map A. To the south of Breslau a small area with several pits was located adjacent to the present day Grand River. A second area to the north east of Preston, along side the Speed and Grand Rivers with several well exposed pits was also considered; while a continuous "sand" plain west of Galt has some six or eight pits within about 10 square miles which could have provided the basis for a study.

Further south in the moraine/outwash complex, at a position north of Paris, the Paris moraine appears to have been obliterated by the outwash system, and large gravel deposits laid down in its place (Cowan, 1970, p. 54-55). This area provided very good exposures in two pits belonging to Consolidated Sand and Gravel Limited, who are the only operators working the area. The main body of the industry is located nearer to Preston and Galt in the north, or to Brantford in the south.

C. S. & G's East Paris pit provided some 1,000 metres of horizontal faces. Two walls in particular provided what are interpreted to be the cross-section of a side channel and the longitudinal section through a large braid bar.

The longitudinal bar model proposed in this thesis was developed from these two faces, and it was used as a predictive model for other

pit exposures to reconstruct and interpret the palaeomorphology.

The second working pit (C. S. & G's West Paris pit) was also investigated in the light of the model proposed. What is interpreted to be a side-bar is exposed in this pit; the two types were compared and contrasted, and some general comments will be made regarding braid bar modelling in Chapter 8.

The longitudinal bar model (see Fig. 7 and Photolog) is basically very simple, comprising five constituent parts:

A coarse core from which the bar grows;

A stoss-side addition of sediment to the upstream end;

A bar-front with slip-face avalanche deposits downstream of the core;

A bar-top representing the gradual accretion of the "through-flow" of gravel in the bar; and

A lateral sandy deposit interfingering with the bar form, and representing sediments of the side channel.

The side-bar model (see Fig. 47 and photolog) is slightly more complex This is no directly comparable core, growth taking place from a laterally accreting river bank. No separate stoss-side facies is present either, and the sandy channel bed-load grades into the bar-top bed load with no distinct break. Equivalent bar front, bar top, and side-channel facies are present but they differ in their internal organisation.

The bar top facies of the longitudinal bar model compares quite closely with what is interpreted as a shallower braided stream deposit, (Smith, personal communication, 1972), located stratigraphically above the main unit in which the longitudinal bar model is developed. (see Fig. 7). However, the internal organisation of this system has not been established,

though some facies have been recognised (see pages 73 to 80). These are comparable to facies of the Kicking Horse River, in British Columbia (Smith, 1972) and to the Pleistocene deposits adjacent to the Red River, Texas (Waechter, 1970).

CHAPTER TWO

THE LITERATURE

CHAPTER TWO

THE LITERATURE

Already some mention has been made of the paucity of literature on braided streams generally, and of coarse braided streams in particular. A comprehensive bibliography of the existing literature can be found in the list of references.

The purpose of this review is to examine some of the ways in which braided streams have been studied, pointing out one or two undeveloped approaches and thereby setting the present study in its context.

Apart from isolated early work on braided streams, valley trains and sand plains, such as the papers by Davis (1889) and Salisbury (1892), the first work on braided channels was an integral part of the inquiry into river channels in toto. Variously, channel-pattern, -form and -geometry, longitudinal profile and base level, have all been studied and applied to meandering, braided and straight channels. The most conspicuous success has been achieved in the field of meandering streams, not surprisingly, since as Leopold et al. (1964, p. 295) state "... nearly all natural channels exhibit some tendency to develop curves." It is doubtful whether straight channels actually exist in nature and the term straight may simply refer to irregular, low sinuosity or non-meandering reaches.

Undoubtedly the regularity of meandering systems attracted attention initially, and the ancillary studies of other channel patterns and their

deposits followed as a logical consequence. Leopold and Wolman (1957) studied channel patterns and tried to distinguish between the three categories on the basis of a "sinuosity index". Mackin (1956) looked at the relationships between braiding and the graded river and Schumm and Kahn (1972) related channel patterns slope and sediment size.

Simultaneously, detailed descriptions of braided rivers were being made, presumably with the assumption that good physical descriptions had to be made before the processes and mechanics could be understood. As has already been noted, Davis and Salisbury pioneered this work, but a spate of such "good physical descriptions" appeared in the late 1950's and early 1960's. Hjulstrom (1952) investigated Icelandic sandar; Sundborg (1952) analysed the River Klaralven in a classic monograph; Arnborg (1955) looked at the River Austerflojt; Fahnestock (1959) examined the White River; Doeglas (1962) compared the Durance and the Ardèche; and Brice (1964) studied the River Loup. Many of these are classic studies, and combined they describe the braided stream environment under various climatic and hydrologic regimen.

Subsequently, the attention of investigators has turned to a different scale of phenomena. Attempts to define the bedforms and their development were made, both from direct observation of modern braided streams and flume experimentation. In the latter case, Leopold et al (1964, p285-288) reported the development of bar-like forms in flume runs and refer to the work of Fahnestock (1963) by way of comparison. In their flume "the introduction into the flowing water of poorly sorted debris at the upper end produced, with time, forms similar to those observed in the field." The coarser grains, after several hours, accumulated as a coarse "lag" in the middle of the channel, and this lag initiated the development

of a small-scale braid bar complex. This at least provides one theoretical answer to question posed earlier regarding the origin of the mid-channel bars. The implication of this idea will be answered in some detail in Chapter 8 and the interpretive sections.

The direct observation of bed forms and their development, rather than the complete braided stream system, is a more recent type of study, though both Chien (1961) and Doeglas (1962) looked at the problems. The most recent studies are those of Ore (1964) who investigated modern braided streams in Wyoming, Colorado and Nebraska; Coleman (1969) who looked at large bedforms on the Brahmaputra River; Williams and Rust (1969) who made observations in the Donjek River; Smith (1970) who continued Ore's work on the Platte River and made some comparisons to some Silurian clastic rocks; Church (1971) who studied Baffin Island sandar; and McDonald and Bannerjee (1971) who examined outwash plains in the Rocky Mountains.

Two of these studies in particular have already been mentioned with regard to bar types and classification. Between them, Collinson (1970) and Smith (1970) recognised longitudinal bars, transverse bars, side bars, linguoid bars, and "banks and islands".

Ancillary to work on braided streams directly is the analysis of primary sedimentary structures and their hydrodynamic significance (Middleton, 1965, and the extensive bibliography contained therein). Much of this work has been used in the study of palaeoflow parameters, the papers by Jopling (1964, 1965, 1966) being good examples.

However, despite this body of literature, some obvious gaps exist in our knowledge. Four deficiencies can be seen. There is i) little data on coarse deposits; ii) virtually nothing on the

facies relationships; iii) only minimal studies of'ancient' braided streams; and iv) an absence of any sort of predictive model.

The first of these problems has had only one really extensive investigation, that of Church (1971). This however was essentially part of a much larger project and as such contains a good deal of raw data but few widely applicable results. The system of deposits reported in the present study contains an admixture of sands and silts with gravels. Hopefully, the data will complement that of Church in filling in this particular gap.

Secondly, the dominance of studies of modern streams has led to an almost complete lack of knowledge of gross structures within the deposits, and of the facies relationships both vertically and horizontally. The limitations placed on trenching and other field techniques by the modern stream environment are easily overcome in the Pleistocene, where essentially undisturbed sediments can be studied to depth with little hinderance. Consequently the present study will hopefully establish facies relationships in braided streams and at the same time produce a link between the modern and ancient examples.

Few ancient conglomerates have been identified as braided stream deposits, the best examples being associated with alluvial fans as with the Pottsville conglomerates (Meckel, 1967) and the Van Horn Sandstone (McGowan and Groat, 1971). Other Pleistocene examples have been recognised, and Waechter (1970) has recognised deposits which "display characteristics of braided streams".

Whilst there is still an absence of any sort of predictive model, some work has been carried out on facies relationships. Recent studies by Costello (1970) and Costello and Walker (1972) have suggested that

a coarsening-upwards channel fill sequence may be diagnostic of the sandy braided stream system. The coarsening upwards denotes increasing flow power and implies through-flow of water. The channel is interpreted as a braid channel abandoned previously but later re-occupied and brought back into the system with rising stages of the water. The same situation could not exist in the "cut-offs" of a meandering stream since through-flow does not occur.

The work in this thesis is a direct continuation of Costello and Walker's work, with special reference to the facies relationships of coarse braided streams.

CHAPTER THREE

THE PLEISTOCENE HISTORY

CHAPTER THREE

THE PLEISTOCENE HISTORY

The general sequence of events in the Pleistocene has been described many times before. A comprehensive, but somewhat dated, outline of the effects on southern Ontario is that of Chapman and Putnam (1966), and a recent summary can be found in Costello (1970). This section will, therefore, be a brief explanation of the salient features affecting the study area.

Within the Pleistocene Succession of North America four major Glacials are recognised - the Nebraskan, Kansan, Illinoisan and Winconsinan. As each succeeding major glacial occurred there was almost total destruction of the deposits of the previous one. Consequently the Winconsinan Glaciation is the one which has had the most effect on the present day topography and physiography of southern Ontario, and it is not surprising that little evidence has been found of Pre-Wisconsinan deposits or erosional forms. Three climatic subdivisions have been recognised in the Wisconsinan (Goldthwait et al, 1965; Dansgaard et al, 1971). The early Wisconsinan (73,000 - 59,000 BP) comprising the main cooling period from the Sangamon interglacial; the Middle Wisconsinan (59,000-32,000 BP) with generally more stable conditions; and the late Wisconsinan (32,000-11,000) comprising the coldest part of the glaciation and further characterised by greatly varying conditions.

The study area was most affected by the late Wisconsinan period, the shape of the ice sheet margin during this time being shown in Fig. 1.

This diagram is a generalised view of the ice-front showing the various lobes which exerted their influences in southern Ontario.

The three major lobes of Huron Ice, Georgian Bay - Lake Simcoe Ice, and Erie - Ontario Ice played major roles in the development of the topography of southern Ontario in Wisconsin times. As the three retreated from the centre of the area the so-called "Ontario Island" began to be uncovered. This developed from a narrow ridge trending north-east to south-west from Orangeville to Ridgetown (Chapman and Putnam, 1966, p. 38), into the larger area shown in Fig. 1. This land mass development is also shown in the summary diagram, Fig. 3. This study deals with the drainage between the east flank of the Ontario Island and the Ontario Ice lobe.

Dating of the Pleistocene events has been done conventionally by the carbon - 14 method and pollen analysis of materials found within the Pleistocene sediments. More recently another method employing the oxygen - 18 isotope concentration in ice has been devised. Consequently, the deposits of the Greenland ice sheet have yielded palaeoclimatic information applicable to both Europe and North America. The index of concentration, δ, of oxygen 18 (Dansgaard et al, 1969 and 1971) in high latitude precipitation is mainly determined by the temperature of formation (Dansgaard, 1954, 1964 and Picciotto et al 1960). This causes both seasonal and long term variations in δ, the latter due to climatic changes, (Dansgaard et al, 1969). Increasing δ's upwards on ice core indicate a warming climate, and decreasing values indicate a cooling climate over the course of time. By taking into account the rate of ice accumulation, the rate of plastic deformation, and the horizontal velocity component, the age-depth relationships of the ice can be calculated. The validity of the resulting time scale, and of assumptions

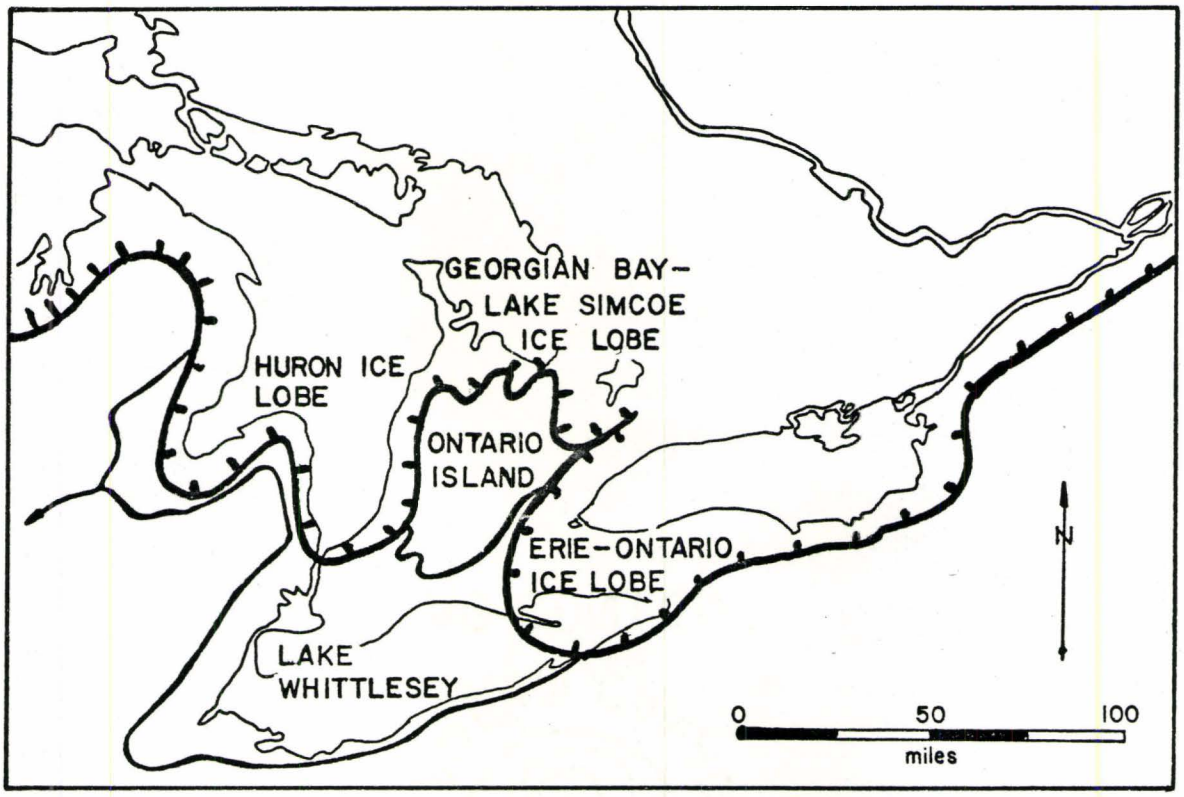

Fig. 1 The ice front positions at the time of the Paris moraine and Lake Whittlesey (approximately 12,800 years B.P.)

made in its calculation can be estimated by applying the δ measurements and Fourier power spectral analysis. Dansgaard et al (1971 p. 38-54) have done just this for the Camp Century Ice Core from Greenland, and Fig. 2 shows an enlarged portion of their δ-curve. If this method is combined with conventional Pleistocene stratigraphy, carbon 14 analysis and palynology (Hancock, 1971) a dated stratigraphy can be built up. This has been done in Fig.2 for the period of interest to this study.

The oldest event represented in the area is probably the Canning "Clay" till which is early Wisconsin. What are thought to be undisturbed portions of this are found in the Nith River section at Canning, four miles west of Paris, (Karrow, 1963, p. 33.) The Catfish Creek Till may also be present in this section though Karrow states that there is some difficulty in distinguishing it from the Port Stanley Tills.

The Erie-Ontario ice lobe then experienced an interstadial condition (i. e. Lake Erie interstade) which at its type locality is dated at 16,700 BP. The subsequent glacial substage produced the "Dorchester" Till, which is not exposed in the field area, and an imbricate series of Port Stanley Tills. The latter are marked by terminal moraines named the Ingersoll, Tillsonburg and Norwich, trending North East to South West, (of Port Stanley I) and the Breslau Moraine (of Port Stanley II). Originally Karrow (1963) mapped Wentworth Till to the west of the Paris Moraine, including the Breslau moraines in this classification. However, a recent revision (Karrow, 1970) defines the Wentworth Till as the Paris Moraine and moraines east of it, and the Port Stanley II as that area west of the Paris Moraine previously designated as Wentworth Till.

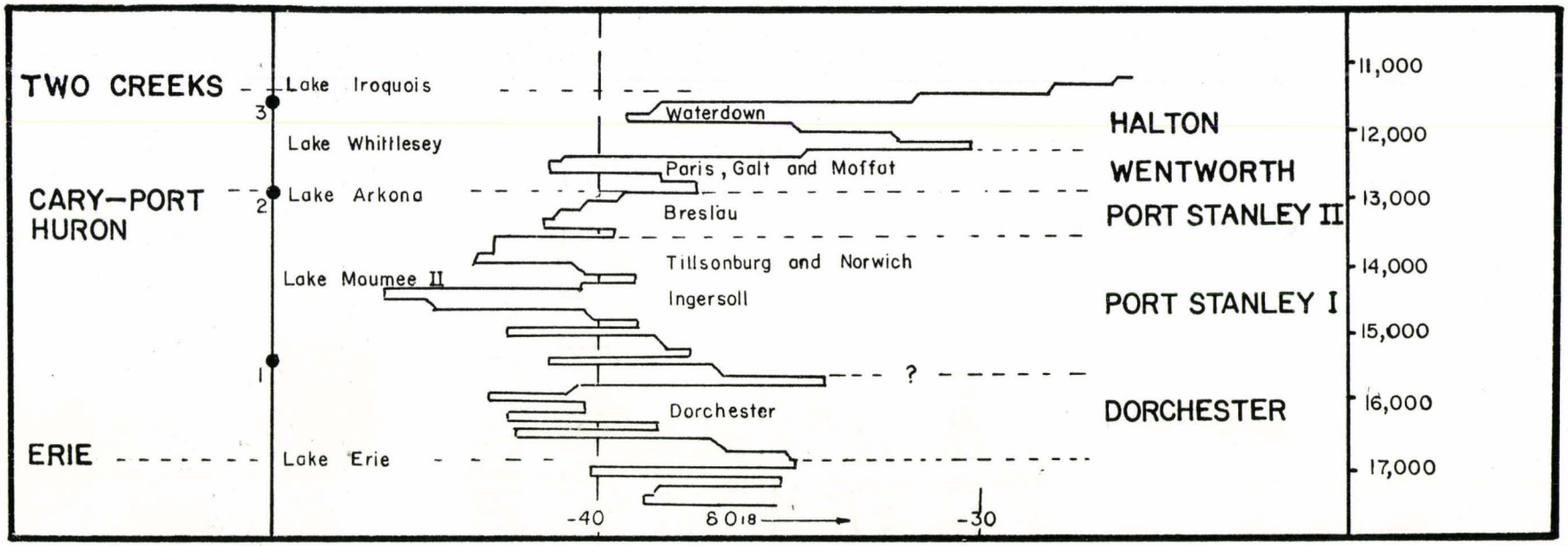

Fig. 2 Part of the $\delta\ O^{18}$ curve for the Camp Century ice core from Greenland (Dansgaard et al, 1971) with interpretation for Southern Ontario (after Hancock, 1971)

Radiocarbon dates (●)

1	OWU-83	14.780 ± 192	(Ogden and Hoy, 1965)
2	Y240 _____	12,800 ± 250	(Barrendsen et al 1957)
3	_____	12,600 ± 440	(McCallum et al, 1955)
	_____	11,840 ± 100	(Farrand et al, 1969)

The Port Stanley Tills were deposited in the period 14,780 to 12,800 B. P. based on Carbon - 14 dates OWU - 83 (Ogden & Hay, 1965) and S-240 (Barrendsen et al, 1957). The Lake Arkona or Cary-Port Huron Interstade has been dated from 12,800 to 12,660 B.P (McCallum, 1955) by which time the Wentworth Till advance of the Ontario lobe, had spread westwards into the middle of southern Ontario producing what are the freshest moraine features in the study area - the Paris, Galt and Moffat moraines. From 12,660 to approximately 12,200 B.P. this advance coexisted with Lake Whittlesey (Figs. 1 and 2) and it is at this time that the outwash gravels which are the subject of this study must have been formed.

Lakes Warren, Wayne ,Grasmere and Lundy all existed during the deposition of the Halton Till. This ice advance lasted only some 200 years from 12,200 to 12,000 B.P. and produced the Niagara, Trafalgar, Waterdown, Oak Ridges and Upper Leaside Moraines. The maximum retreat coincided with the maximum of glacial Lake Iroquois at about 11,500 B.P.

Fig. 3 is a summary of some of the ice movements and their associated moraines in the area, during Lake Wisconsin times, and shows the relationship of the study area to the emergent Ontario Island and the retreating ice lobes.

The drainage network which must have existed within the complex of moraines and outwash channel ways adjacent to the ice-sheet, is reconstructed in Fig. 4. The overall drainage pattern is ice marginal along the top of the escarpment in the area to the north, being deflected south-westwards by the arcuate ice-front in this area. The braided channel-way pattern breaking up the moraine ridges has a focus at the region to the north of Paris where the Paris Moraine appears to be absent. This is

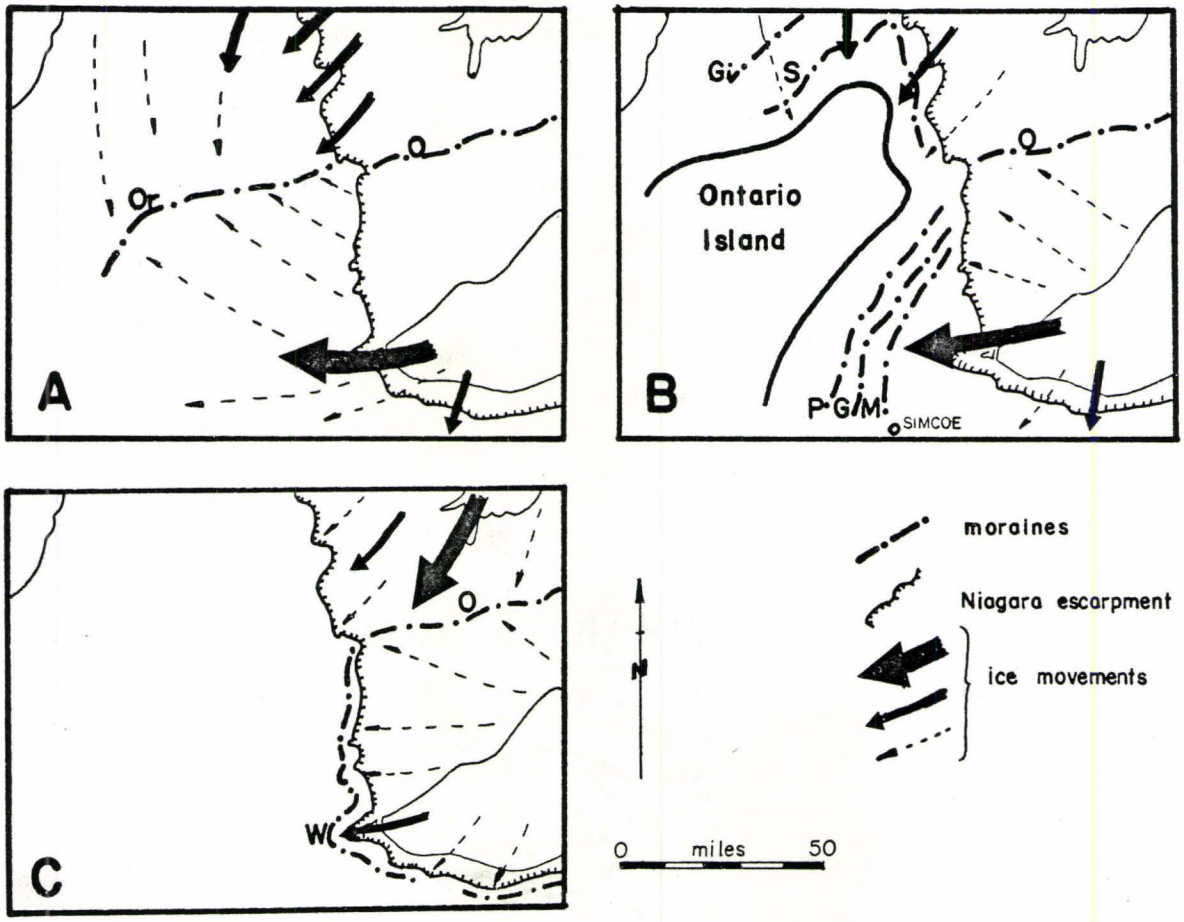

Fig. 3 Ice movements and moraines in the area West of Lake Ontario.

A During maximum of Lake Wisconsinan glaciation

B At time of Moffat moraine

C At time of Waterdown moraine

(after Straw, 1968)

Or. Orangeville moraine
O. Oakridges "
Gi. Gibraltar "
S. Singhampton "
P. Paris "
G. Galt "
M. Moffat "
W. Waterdown "

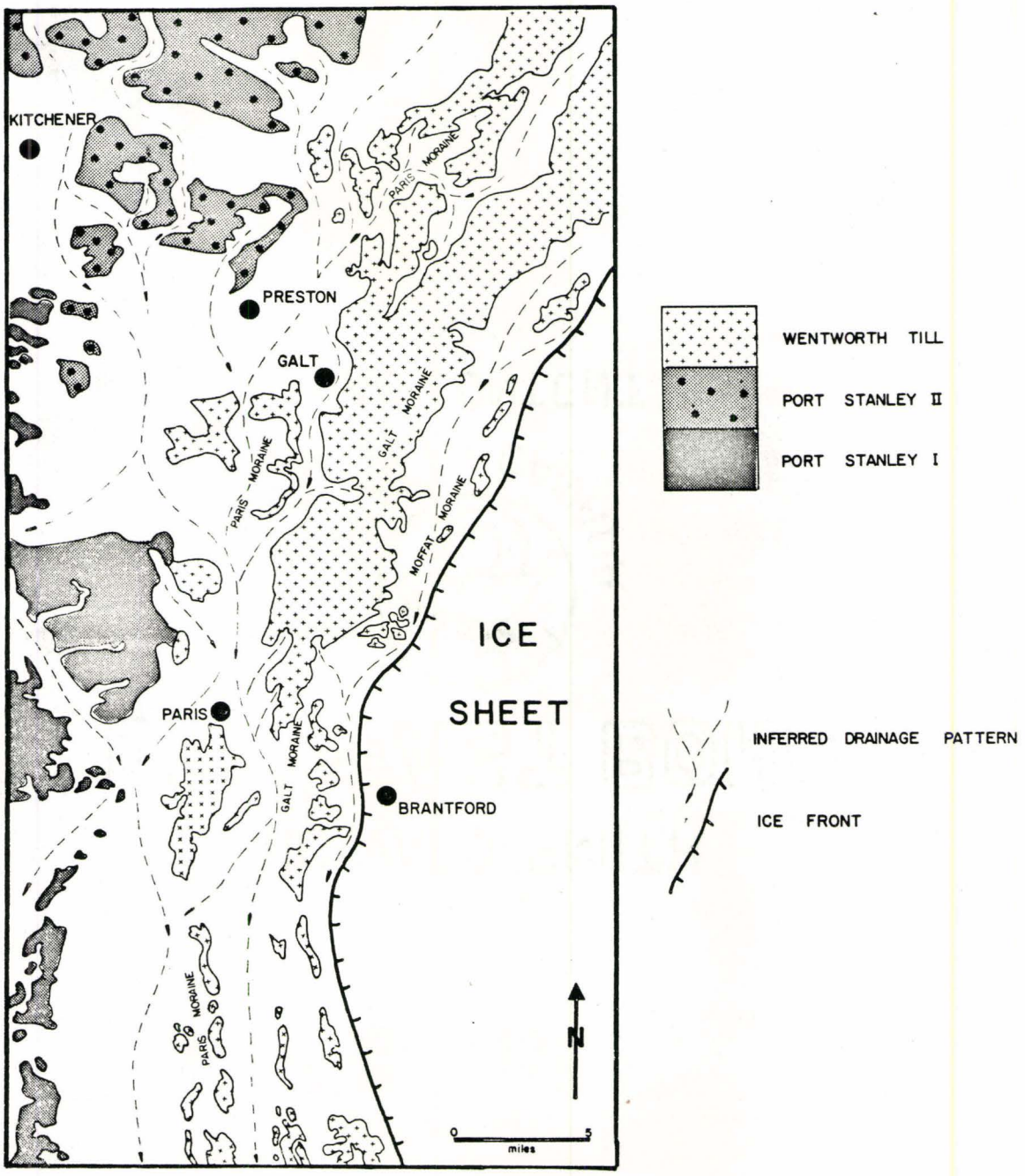

Fig. 4: Ice front at the time of the Moffat moraine with drainage patterns inferred for the moraine-outwash complex.

the exact location of the two pits which form the basis of this study. The whole system drained southwards into Lake Whittlesey, whose position has not been determined with any degree of accuracy for this time. The lake shoreline would have migrated from a position near to a line through Otterville, Delhi and Simco northwards to somewhere north of Waterford. The local stratigraphy of the gravels suggest a retreat of the ice and a probable transgression of the lake shore (see Chapters 4 and 8 for a more complete analysis).

CHAPTER FOUR

THE LOCAL STRATIGRAPHY

CHAPTER FOUR

THE LOCAL STRATIGRAPHY

The bedrock of the field area is of Silurian age, and is the Salina Formation. Exposures are found in the valley side of the Grand River quite close to the East Paris pit. The outcrops are 5-7 m thick and consist of dolomite strata upto 35 cms thick, and shaly dolomite with thin seams of gypsum which are up to 5 cms thick

The bedrock topography has been mapped (Karrow, 1963), and this provides a useful tool for determining drift thickness when used in conjunction with a standard topographic map. A map (Fig. 5) of the bedrock topography has been taken from Karrow's map. Around Brantford the bedrock is at less than 550 feet above sea level, while to the west of Burford it reaches more than 825 feet above sea level.

Just to the north of Paris (at the approximate location of the section in Fig. 6.) a spur of bedrock runs west-northwest - east-southeast dividing tributaries of the Dundas Buried Valley. To the west of Brantford other tributary-like depressions in the bedrock link with a depression under the site of Brantford itself. This depression appears to connect (at about 575 feet above sea level) with the Dundas Buried Valley system. Karrow (1963) considers the Dundas Buried Valley to be an ancestral Grand River.

Overlying the bedrock is a sequence of Pleistocene drift deposits varying from 250 feet thick in south west Brantford to less than 50 feet thick in many parts of the southern area around Scotland and Oakland.

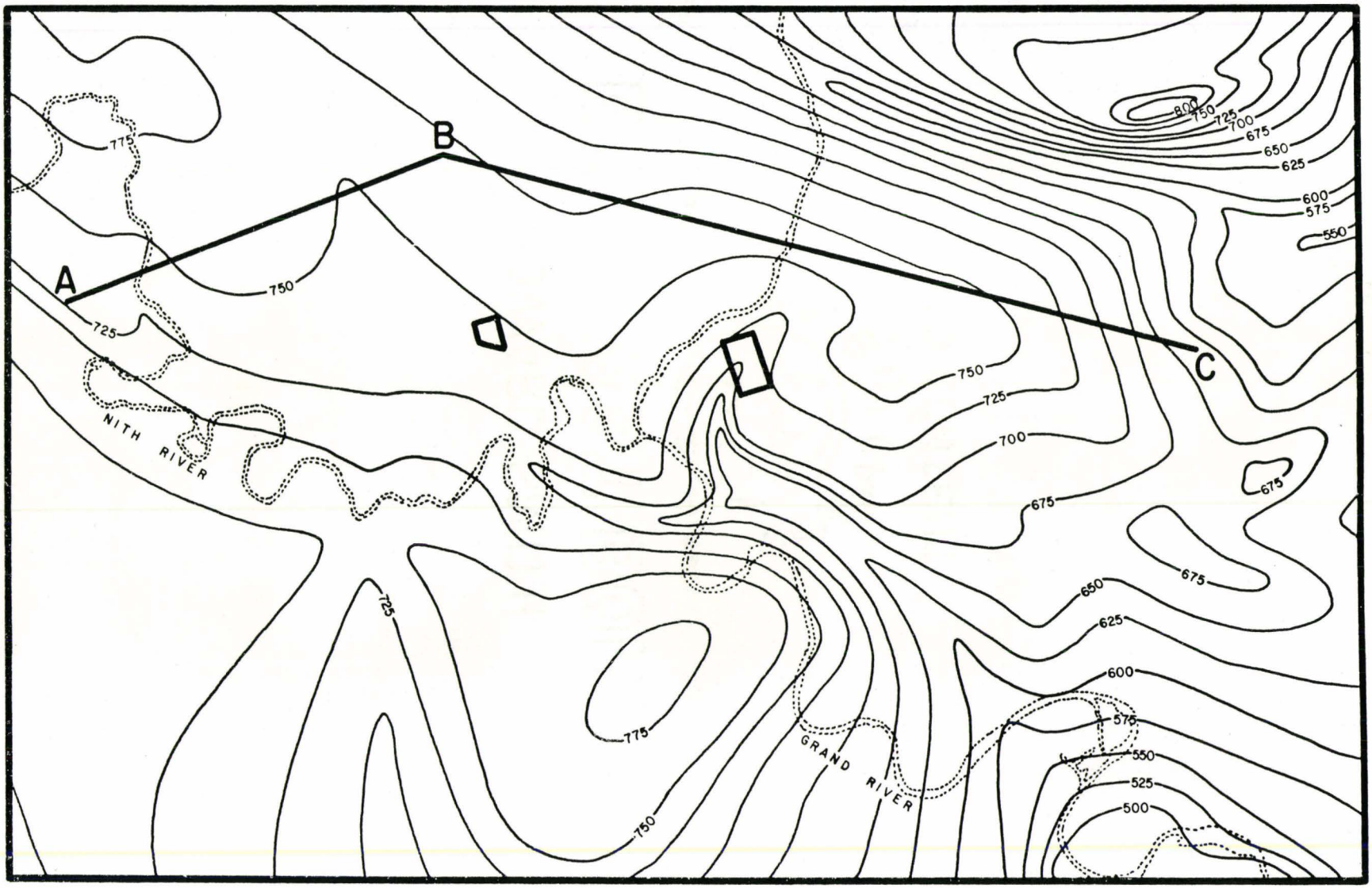

Fig. 5: Map of the bedrock topography in the Paris-Brantford area (after Karrow, 1963)

In and around the two pits the drift averages about 100 feet in thickness: at HWY 5 2 miles east of Paris it is 75-100 feet thick; at the East Paris pit 110-125 feet thick; at the West Paris pit 95 feet thick; 2 miles south from Paris in the Paris Moraine it is 100 feet thick; and at Burford it is 105 feet thick.

The drift stratigraphy is shown in Fig. 6, on a section through the area north of Paris and just north of the two pits belonging to C.S.&G. Ltd. The line of the section is approximately along the crest of the bedrock spur referred to above.

The oldest drift deposit exposed, the Canning Till, is found in the Nith River north of Falkland. This is a clay till with occasional pebbles, and at present it forms part of the slip-off, or lateral accretion, surface of the inside of a large meander bend in the river. Stratigraphically above this, is the Catfish Creek Till, exposed at the Canning Section of Karrow (1963). Both of these are probably laterally discontinuous eastwards, having been removed by later ice advances.

The Port Stanley Till, forming the Norwich, Ingersoll and Tillsonburg moraines and ground moraines between them, extends at least as far as the Grand River north east of Paris, where it is exposed in the riverside directly overlying bedrock.

The Wentworth Till lies to the east of, and stratigraphically above the Port Stanley Till, and forms the Paris, Galt and Moffat moraines and ground moraines between them. On the line of the section the Paris moraine forms a small topographic feature immediately adjacent to the Tillsonburg moraine, but its extent at this point is considerably less than elsewhere to both the north and south. It is probable that the moraine was initially much larger at this point, but that it has been obliterated by the outwash

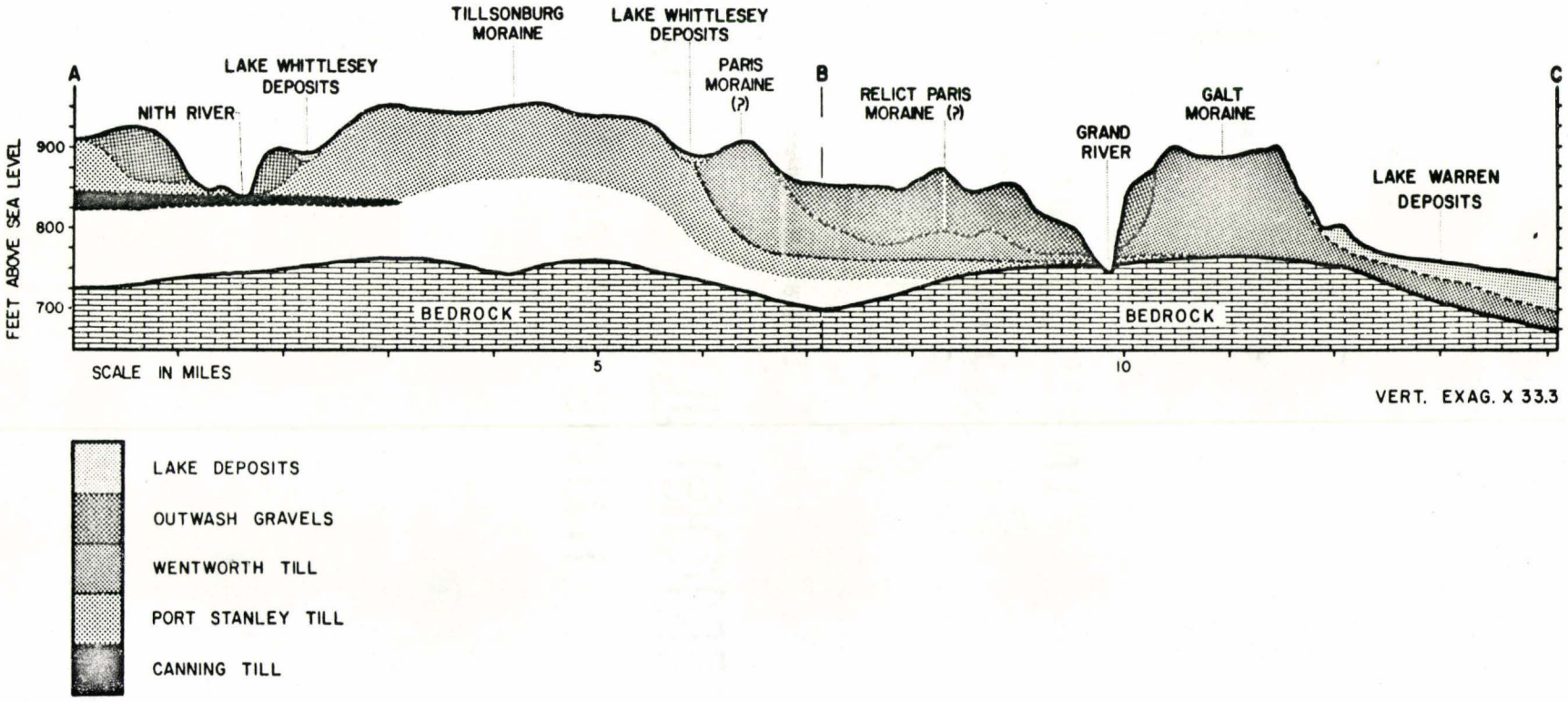

Fig. 6: Simplified Geological section through the moraine-outwash complex north of Paris.

activity, the gravels of which now occupy a large area north of Paris.

The outwash gravels themselves, exposed in the East and West Paris pits, can be divided stratigraphically into three units (see Fig. 7). The basal part, unit 1, is coarser than the other two and consists of crudely horizontally stratified coarse gravels which are dominantly imbricated. There are also thin horizons (5-25 cms) of sandier material which are laterally discontinuous (1.5-10m) giving the unit its crudely horizontally stratified appearance. The whole unit is L 10 m thick in the pit, but it is probably considerably thicker, underlying the base of the pit in some parts. At the south end, however, the base of the pit appears to be actually at the contact between the outwash gravel and the Wentworth Till, the working level being floored by a continuous bouldery layer which acts as a natural pavement. At this point unit 1 directly overlies the till.

The contact between units 1 and 2 is quite irregular, there being channels cut down into the underlying unit in some parts, and additions of material intimately related to topographic highs of the underlying unit in other parts. The whole internal organisation of unit 2 is completely different from that of unit 1. As already mentioned there are commonly channels cut into the basal unit, which are 30-100 m. wide. These channels are composed of dominantly sandy material which is normally trough cross-bedded. The material associated with the topographic highs of unit 1 is coarse gravel and is normally cross-bedded on a large scale, with foresets 2-3m high. In other parts the material is not as coarse forming pebbly tabular cross-bedded sets. Unit 2 is completed vertically by crudely horizontally stratified coarse gravels which are dominantly imbricated, with a large number of sandier lenses

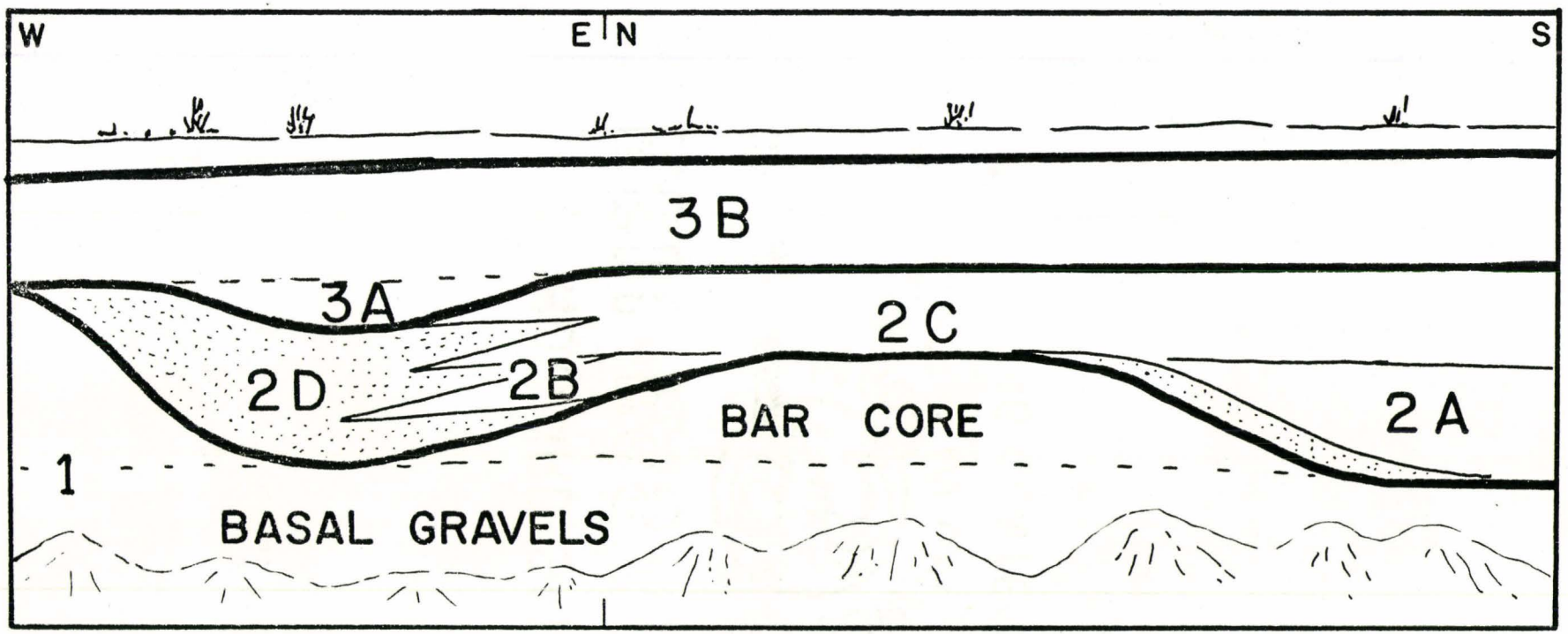

Fig. 7 Stratigraphy of the outwash gravels of East Paris (diagrammatic)

unit 3B Shallow Braided Facies proper

3A Shallow Braided Facies channel infill

unit 2D Side Channel Facies

2C Bar Top Facies

2B Stoss-side Facies

2A Bar Front Facies (section 15m thick)

with planar and low angle laminations. The percentage and type of sand bodies, and the stratigraphic position distinguishes this from unit 1.

The topmost unit of gravels exposed, unit 3, has an appearance similar to the top of unit 2, but is sandier. There are large beds of horizontally stratified coarse gravels (dominantly imbricated), which alternate randomly with tabular cross-bedded and trough cross-bedded sands and pebbly gravels, and thin sandy lenses with planar and low angle laminations.

The basic interpretation of these three units is as follows. The overall sequence of units 1 through 3 has a fining upwards component which suggests a receding of the source area, and probably a change from more ice-proximal conditions in unit 1 to less ice-proximal conditions in unit 3. As will be shown in more detail in Chapters Six and Eight the basal unit has a relict topography and palaeocurrent orientation distinctly different from the upper two units and may represent an outwash system separate from the one which deposited units 2 and 3. Unit 2 is interpreted to be a deep-channel and stable-bar braided system establishing itself on the relict topography of unit 1. Unit 3 is thought to be a shallow-water, mobile-bar braided system, analogous to the Kicking Horse River, British Columbia (Smith, 1972, and personal communication).

The exposed gravels in the West Paris pit are confined to the unit 2 of the outwash stratigraphy. It is probable that unit 1 is either absent or quite thin here, because Hewitt and Karrow (1963) report that a red clay till (possibly Port Stanley drift) underlies the gravel not far below the base level of the pit. Unit 3 is not represented.

CHAPTER FIVE

INTRODUCTION TO THE FACIES

CHAPTER FIVE

INTRODUCTION TO THE FACIES

The overall simplicity of the stratigraphy in this thin vertical sequence of deposits, allows a series of facies to be recognised and defined by their textures, bedding and assemblages of sedimentary structures. The facies have been interpreted and given genetic names (rather than facies A, B etc.), to make the text easier to read. Nevertheless, the description of each facies is separate from its interpretation. The facies recognised are as follows.

Bar Core facies (unit 1 of Fig. 7.). The topographic highs of this facies form the cores of the braid bars in stratigraphic unit 2, and the facies also totally comprises stratigraphic unit 1.

Bar Front facies (2A of Fig. 7) This facies consists of large scale cross-strata developed downstream from the bar core.

Bar Stoss-Side facies (2B of Fig 7). This facies consists of coarsening-upwards cross-bedded sandy gravels and imbricate pebble and cobble gravels, developed on the upstream side of the bar core.

Bar Top facies (2C of Fig. 7). This facies consists of crudely horizontally stratified coarse, imbricated gravels with thin sands , developed vertically above the bar core, the bar front and the stoss-side facies.

Side-channel facies (2D of Fig . 7). This facies consists of trough cross-bedded, ripple- and plane-laminated sands with occasional gravel interbeds, developed adjacent to the first four facies.

Lateral Accretion facies (found only at west Paris). This facies consists

of strata dipping gently streamward, with imbricated gravels, low angle cross-strata, and thin sand lenses, developed adjacent to the side channels.

Shallow braided stream facies (unit 3 of Fig. 7). This facies is similar to the bar top facies, having imbricated gravels and sand lenses, but is sandier with cross-lamination and plane-bedding developed in the lenses.

The following two chapters will contain descriptions of the various facies recognised at each of the pits, and will build each group into separate interpretive models. Finally, a synthesis will be made of the East and West Paris systems, along with examples of braided systems in the literature, some generalisations will be made and some conclusions drawn.

For both grain sizes and palaeocurrents, the methods of sampling and the tabulation of the data obtained, are given in the respective appendices (Appendix B: Grain size , and Appendix C: Palaeocurrents).

CHAPTER SIX

THE FACIES AT EAST PARIS

CHAPTER SIX

THE FACIES AT EAST PARIS

Each of the facies recognised at East Paris will be described separately, and each description will include their occurrence, stratification, fabric and palaeocurrents, and grain size data. Interpretation will be deferred until the conclusion of the chapter where all the facies will be tied-in to an interpretive model. The pit map (Fig. 8) and the localities marked, will serve as a guide to the positioning of the facies described. The face (2)-(3) is approximately transverse to the inferred palaeocurrent direction, and the face (3)-(4) is roughly parallel to it. These are the two faces depicted on the photolog.

BAR CORE FACIES: OCCURRENCE

This facies comprises (i) basal gravels (which are continuous across the pit) with (ii) preserved topographic highs above the basal gravel which are the cores from which the braid bars grew in stratigraphic unit 2. The basal gravels are 4m thick in the pit but probably extend to unknown, and irregular depths below the pit base level. The topographic highs rise above the basal gravel to a height of 6 m (location (2) Fig. 8; and left end of first strip of photolog), and 4m (between locations 3 and 4, Fig. 8; and third and fourth strips of photolog).

The contact between unit 1 and unit 2 is generally sharp and erosional, particularly where it underlies the side channel facies (E of photolog) and the bar front facies (R of photolog). Elsewhere it can be

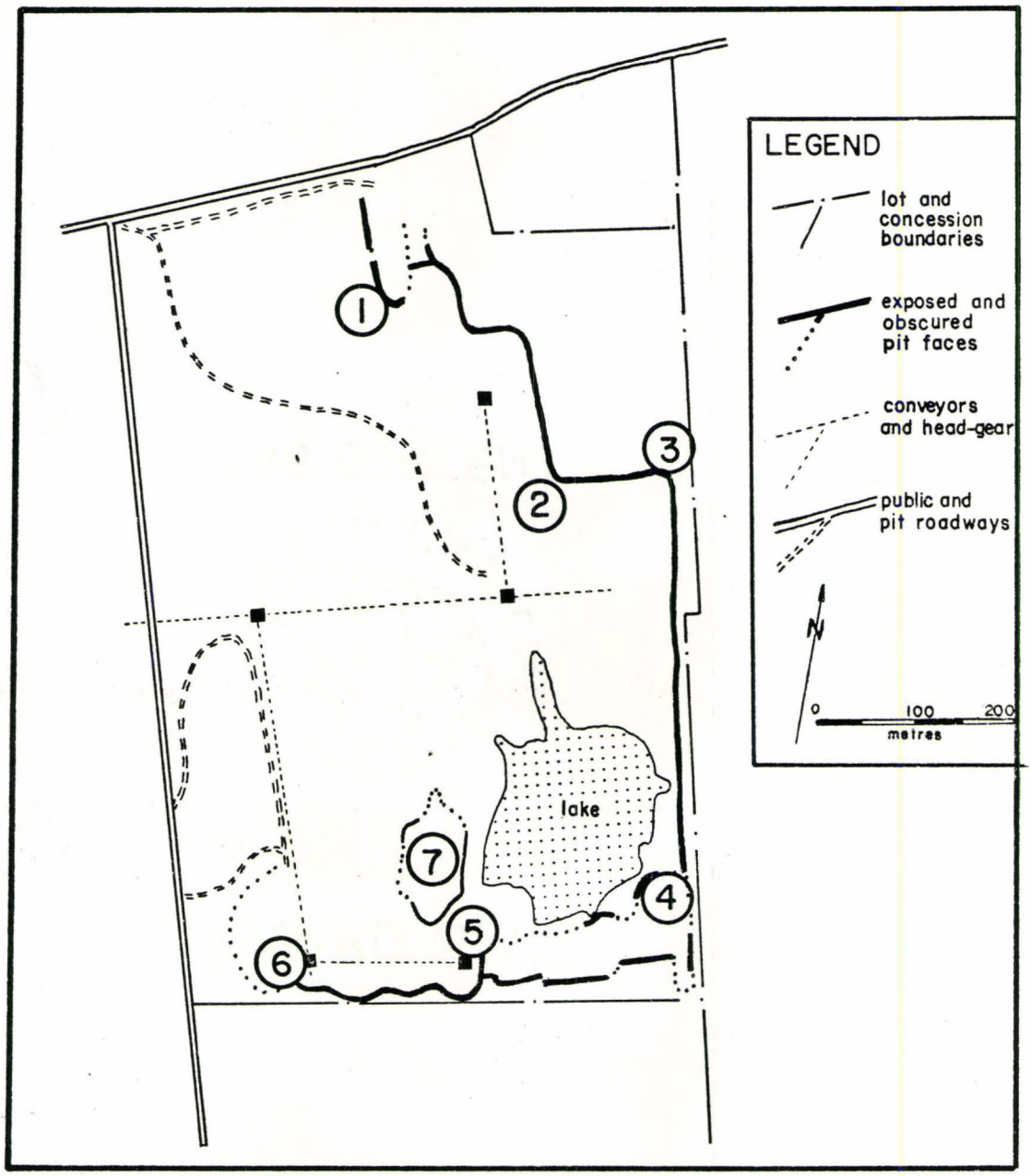

Fig. 8 Map of the East Paris pit (C.S. & G. Ltd.) with numbered locations used in the text.

gradational as with the contact of the bar core and the bar top facies (O of photolog), or erosional where the bar core underlies the bar stoss-side facies (M of photolog).

BAR CORE FACIES: STRATIFICATION

This facies is predominantly composed of coarse gravels which are crudely horizontally stratified and moderately well imbricated. There is no apparent overall sequence in this facies, the fabrics, structures and stratification remaining similar throughout. The crudely horizontal nature of the deposit is imparted by a series of features:-

(i) Discrete sand lenses (B of photolog), 5 to 25 cms thick and 1.5 to 4m wide, which are concave upwards and appear as channel like depressions. These exhibit planar lamination, low angle cross lamination and trough cross lamination, singly or in combination. The trough cross lamination is usually small scale (1.5 to 4 cms) though some larger scale structures (up to 10 cms) do occur in places.

(ii) Thin discontinuous horizons, 5 to 25 cms thick and 3 to 8 m wide, with higher than average matrix content. These occur variously as concave upwards or convex upwards bodies, and there does not appear to be a predomincance of either type.

(iii) Thin discontinuous horizons, 5 to 20 cms thick and 2 to 9 m long, with finer than average matrix content, which are easily located because of their capacity to retain moisture. These are usually concave upwards (see C and P of photolog), and have a thin silt drape at the top.

(iv) Horizons with little or no matrix (the true openwork gravels), 5 to 15 cms thick and 2 to 6 m long. In these horizons the sand content

usually increases upwards, finally closing off and sealing the gravels against further sand infiltration.

BAR CORE FACIES: FABRIC AND PALAEOCURRENTS

The coarse gravels of the bar core facies are moderately well imbricated. The angle of dip of the pebbles and cobbles (see Table 23 Appendix C), has a mean of 24 degrees, and the modal class (taken from stereoplot of Fig, 9) is 20 to 30 degrees. The histograms of the dip angles of the 5 samples shows the modal class variously as 20 to 24 degrees and 25 to 29 degrees, with no predominance of either class. Angles of imbrication within this range (20 to 29 degrees) have been reported in other studies dealing in part with the imbricate nature of Pleistocene gravels (Rust, 1972).

The imbrication of the gravels was used primarily as a palaeocurrent indicator. All the pebbles and cobbles measured had a ratio of b:c axes of greater than 3:1, and a b axis of 5 cms or more. In nearly all cases the a axes were oriented transverse to the inferred palaeocurrent direction, and the a-b planes of the pebbles dipped upstream. The exceptions to these conditions, which were relatively few, were those pebbles with a b:c ratio closest to 3:1 (i.e. the more spherical particles). These were oriented at varying angles filling the void spaces between larger and flatter pebbles, and tend to have their a axes distributed equally between transverse-to and parallel-with the inferred palaeocurrent direction.

Fig. 9. shows a plot of 119 readings from 5 samples of imbricate pebbles and cobbles taken in various parts of unit 1. Of the 5 samples one is from the bar core at location (2) (Fig. 8.), two are from the bar core between locations (3) and (4), and two from below the channel facies between locations (2) and (3).

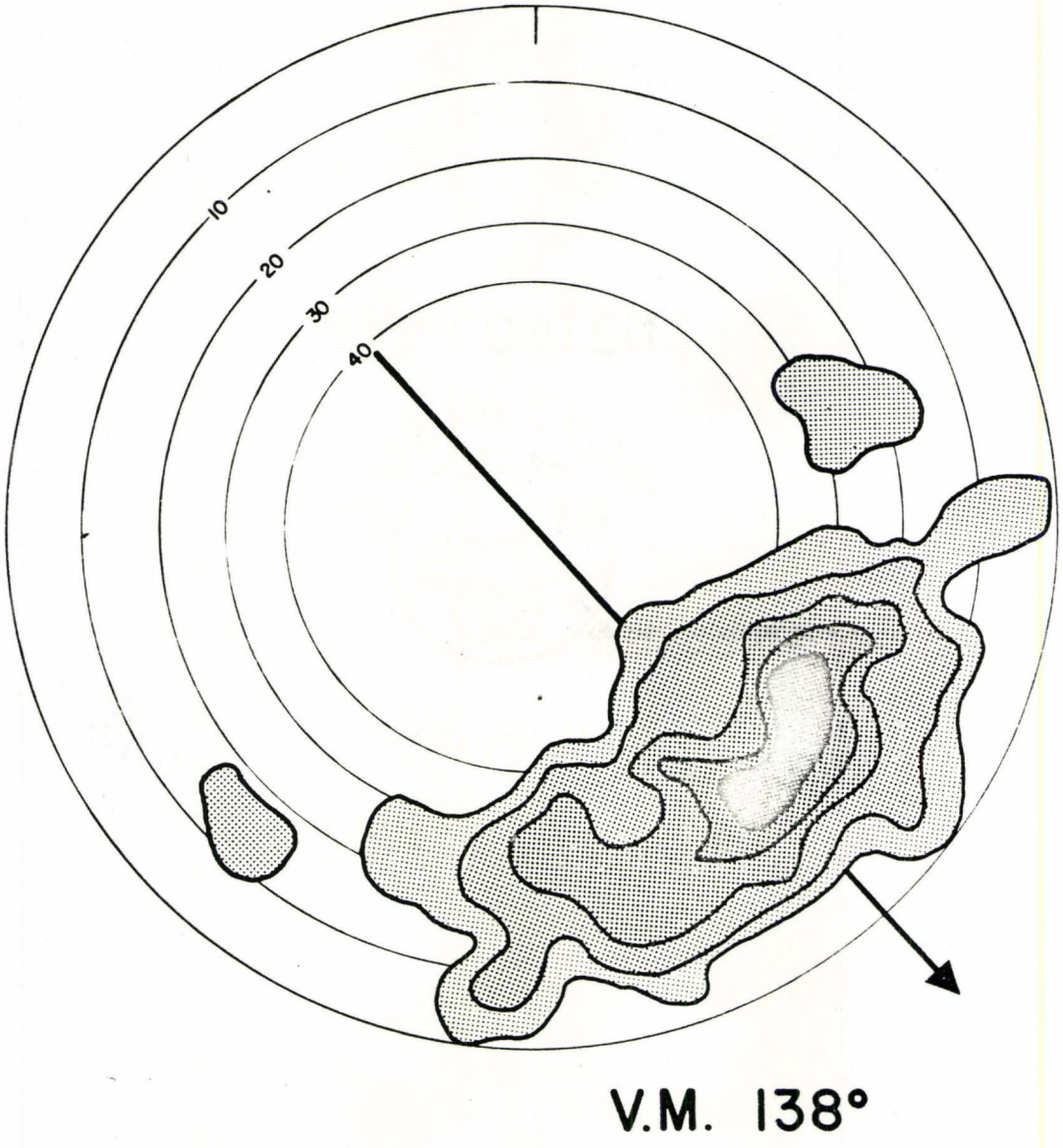

Fig. 9: Stereoplot of the imbricate fabric of the Bar Core facies.

Table 23 in the palaeocurrent data appendix (p.209), shows the measured dips and inferred palaeoflow directions for this facies; the dips are about 24 degrees, and the inferred palaeocurrent grand vector mean is about 140 degrees. The two cores have the same palaeocurrent directions as each other, and as the basal gravel. Visual comparison of rose diagrams of dip directions indicates a close similarity in distributions between the 5 samples. The vector means of the samples (139, 140, 135, 140, 136) are also very close. Therefore, all the samples are probably from the same braided system, there being no essential differences between the parts of unit 1 which form the topographic highs (and bar cores) and those which form the underlying basal gravels. The whole of unit 1, therefore, belongs to a system whose palaeocurrent direction was south east.

BAR CORE FACIES: GRAIN SIZE

This facies is the coarsest deposit overall in the outwash system (see Fig. 10.) Isolated boulders of 50 to 72 cms in diameter are found in this and other facies (R and T of photolog), but they do not represent the normal particles moved by the stream. Bradley et al (1972) refer to these as "oversized particles", and the remaining sediment as "coarse particles readily moved", by the stream system. The second of these categories in the Bar Core facies has a mean grain size ranging from -3.25 to -4.0 phi. The mean of the 10 largest particles, an approximation of the coarsest percentile (see Appendix B for brief discussion of methods used and for all grain size data), is in the range - 7.25 to -7.5 phi (i.e. cobbles of the Wentworth (1922) scale; see Fig. 11.)

Fig. 12 shows the grain size distributions of a typical basal gravel sample of the Bar Core facies. There are three gravel modes and

CHAPTER ONE

THE PROBLEM

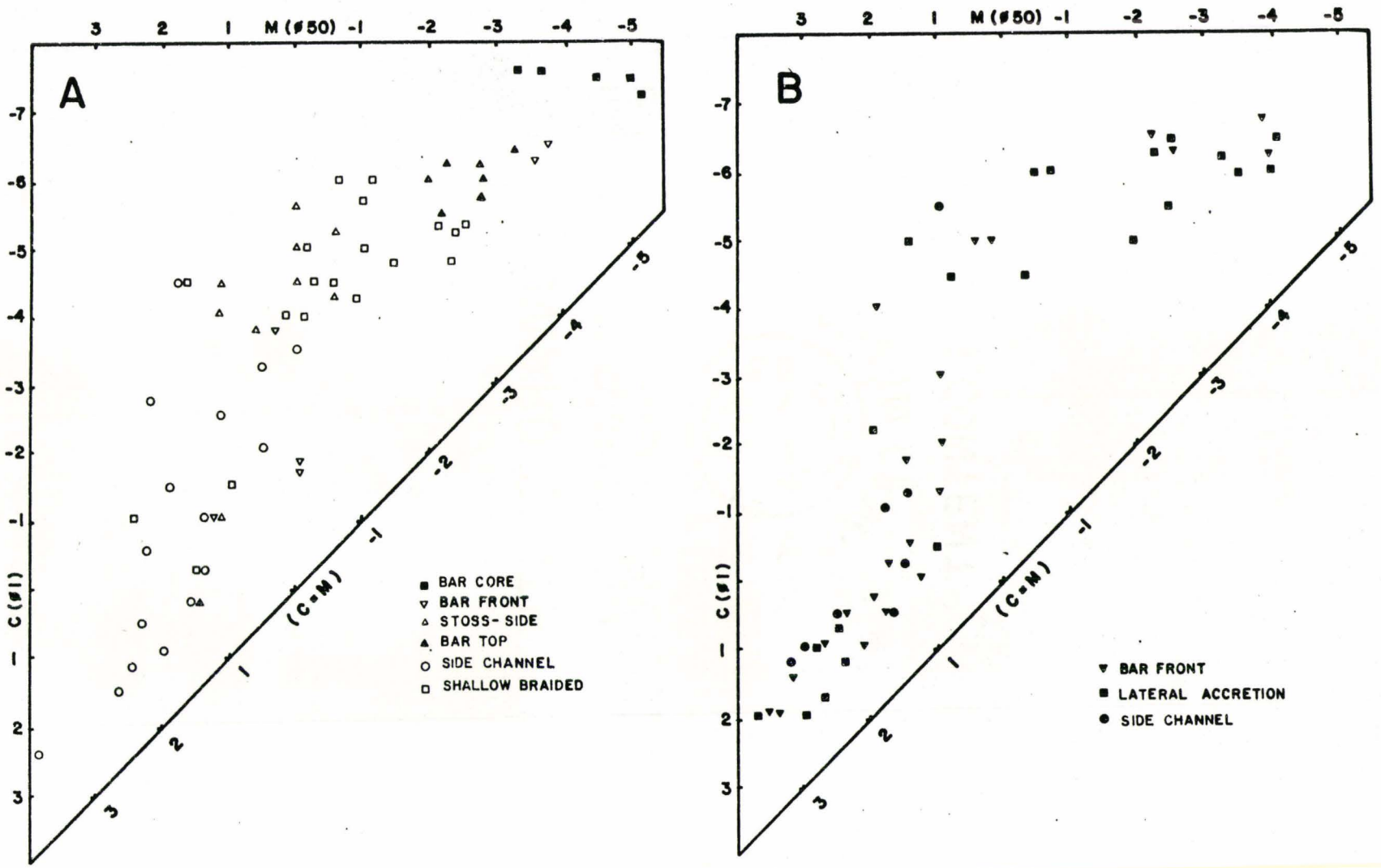

Fig. 10: Passega type C-M diagram for samples of the Pleistocene outwash at Paris. (The number of samples is not representative of the relative abundance of the facies, but is chosen to show the spread of the samples).

A. East Paris B. West Paris

mm	microns	phi	Wentworth
			Boulders
256		-8	
			Cobbles
64		-6	
			Gravels
16		-4	Pebbles
4		-2	
			Granules
2		-1	
			V. coarse
1	1000	0	
			coarse
0.5	500	1	
			Sands
			medium
0.25	250	2	
			fine
0.125	125	3	
			V. fine
0.0625	62.5	4	
			coarse
	31.0	5	Silts
			Med. & fine
	3.9	8	
			clay

Fig. 11 Grain size scales for clastic sediments.
(after Folk, 1968)

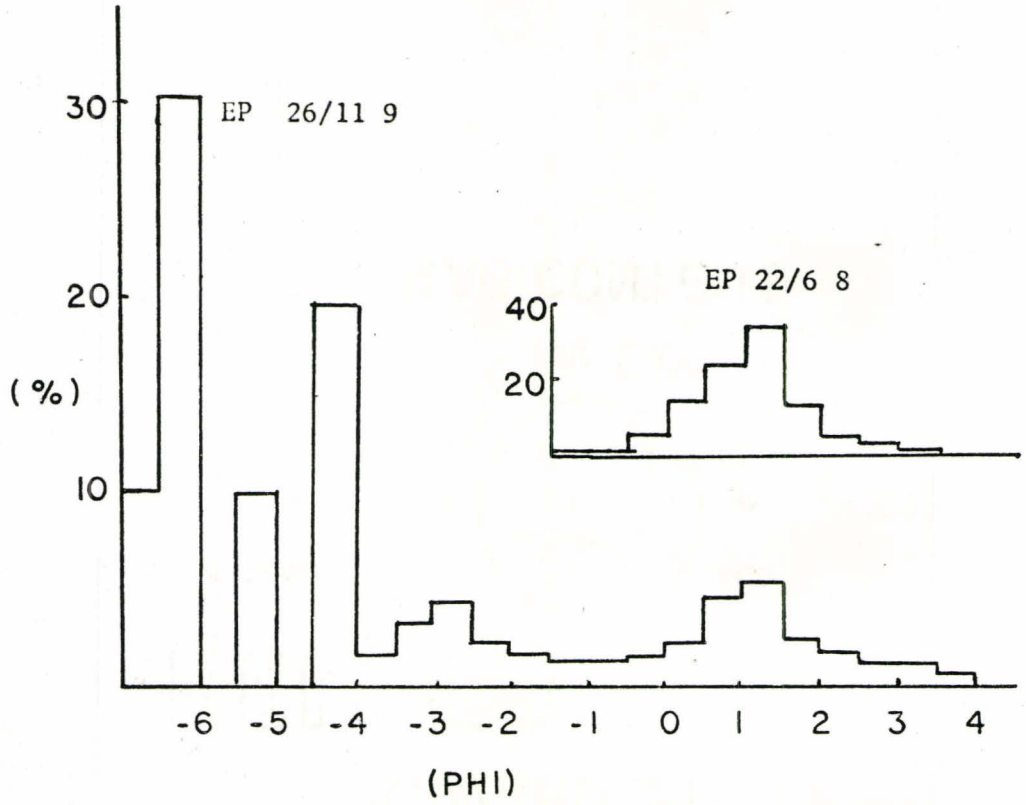

Fig. 12 Histogram of size distribution of samples from Bar Core Facies: gravel and sand (insert)

one medium sand mode. The inset of Fig. 12 shows a sand sample from a lens (at B on photolog) within the bar core facies. Its distribution is comparable to that of the sand fraction of the matrix of the coarse gravel sample.

The sand in the gravel sample comprises approximately 20% of the total sediment, (using the gravel/sand boundary at -1.0 phi after Wentworth, 1922). Plumley (1948) demonstrated that loosely packed gravels could accommodate 32% sand, and closely packed gravels could accommodate 22% sand. Sample EP 26/11-9, which is typical of the Bar Core facies, has a sand content of approximately 20%, which would seem to indicate that the fabric of the original gravel was closely packed.

The standard deviation values of the gravel samples range from 2.6 to 3.3. These high values reflect a very poor sorting (Folk, 1968) which is also reflected in the polymodal distribution. The skewness values of the samples are all positive, indicating excess fine material in the distribution. The kurtosis values range from 0.591 to 1.215 (very platykurtic to keptokurtic). The combination of large standard deviation values and predominantly platykurtic values of kurtosis reflects a history of the sediments which involves little effective sorting.

BAR FRONT FACIES: OCCURRENCE

This facies derives its name from its position in relation to the bar core, and is best exposed in association with the bar core between locations (3) and (4) (see Fig. 8.). The facies has a maximum thickness of 4m, which is controlled by the original relief of the core, and an exposed length of 150m.

A sand body lies between the bar core itself and the Bar Front facies (see R to U of photolog). This is actually part of the side

channel facies, but is described in this section because it initiates the downstream addition of material to the bar core. The contact between the sand body and the Bar Front facies is sharp and erosional (see U of photolog).

Further exposures of the Bar Front facies occur in places amongst the stock piles between locations (4) and (5) of Fig. 8, and more continually at and around location (5) itself. Here the facies has prograded over a sandy deposit of the side channel sands. In all cases the Bar Front facies is overlain by the Bar Top facies and the shallow braided stream facies in succession.

BAR FRONT FACIES: SEDIMENTARY STRUCTURES

This facies is composed of (i) coarse gravels with large scale cross strata, (ii) imbricated coarse gravels, and (iii) a series of reactivation surfaces which interrupt the cross strata, and which have sands associated with them in places. The imbricate gravels represent a continuation of the Bar Top facies along the reactivation surface and down the avalanche face, and as such will be described later. Thus the Bar Front facies grades upwards into the Bar Top facies and no distinct boundary between the two can be drawn (see Fig. 13.).

The angle of dip of the cross strata was measured in 7 sampling locations. 20 pebbles and cobbles lying with the plane of the foreset were measured for angle and direction of maximum dip at each sampling location (see table 24 Appendix C). The values range from 6 to 49 degrees in total, but the mean of each sample falls within the range of 27-29 degrees. In 5 cases the modal class is 25-29 degrees, and in 2 cases it is 30 to 40 degrees.

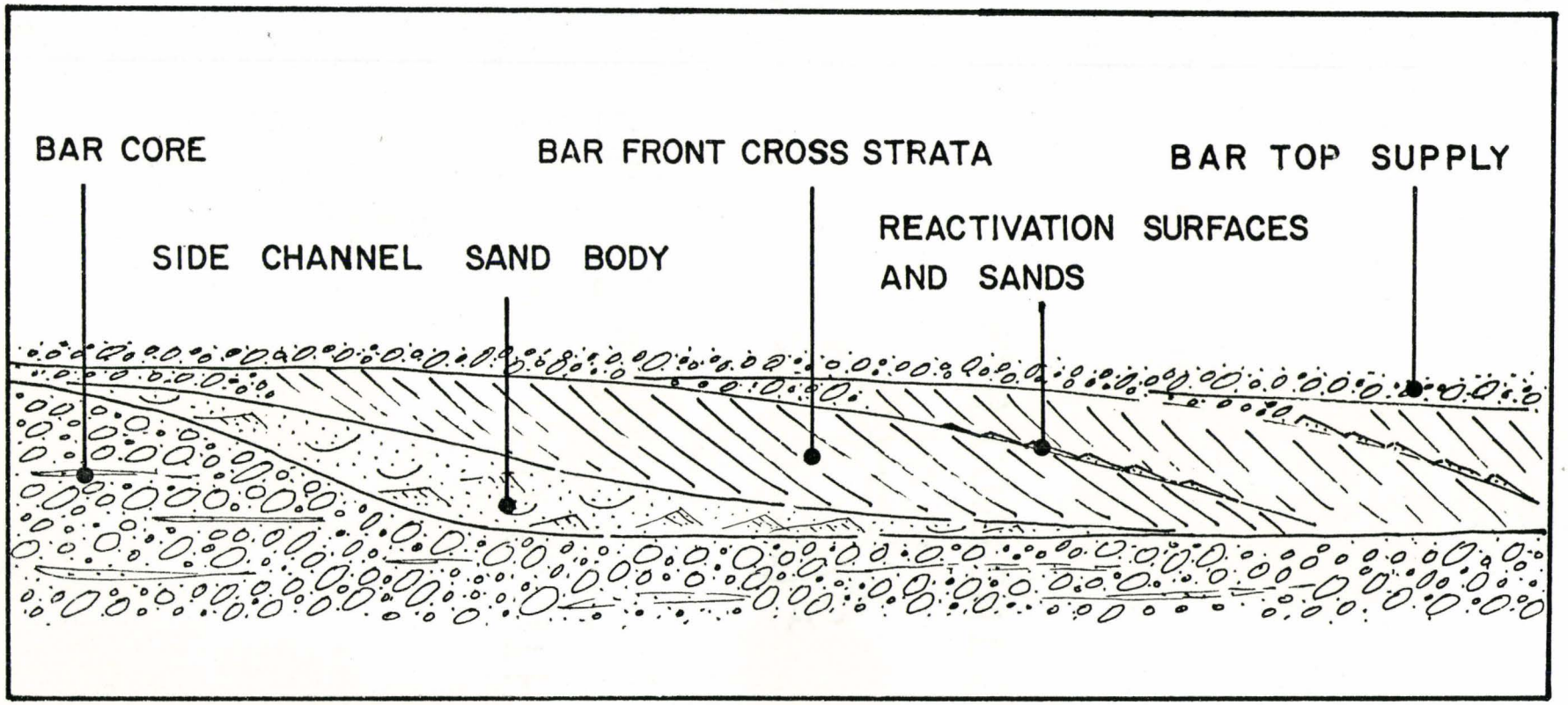

Fig. 13 Diagrammatic representation of the Bar Front Facies and its component parts

The foreset slopes not only have pebbles and cobbles lying within the plane of the foreset but a form of imbrication also occurs with those particles that avalanche down the foreset slope. By definition, imbrication is taken to be the stacking of particles with their maximum projection planes dipping upstream relative to the depositional surface. Thus pebbles and cobbles on a foreset slope which are actually dipping downstream relative to the channel substrate, can be imbricated relative to the foreset slope (see Fig. 14). This was commonly the case in some of the cross strata of this facies.

The coarse gravels form two distinct types of cross-strata:-

(i) This type is formed by the pebble/cobble fraction of the gravel with little or no matrix and constitutes an openwork gravel (see Fig. 15). The foresets are from 5 cms to 45 cms thick and commonly wedge and thicken down the foreset slope. The top of the foreset is composed of pebbles and cobbles. This fining up the foreset slope is marked by a fining upwards perpendicular to the plane of the foreset, again from pebbles and cobbles to granules and pebbles (see (i) of Fig. 16). This openwork gravel type of foreset is commonly followed by a thin (15 to 60 cms) development of type (ii).

(ii) This type of foreset is composed of heterogeneous gravel, in which there is little or no grain size segregation. In places the largest particles (of cobble size) are found as the upper half of the foreset slope having not had sufficient time to slide further before burial. A whole range of grain sizes is present, from coarse sands, through granules and pebbles, to cobbles. The thickness of the laminae is indeterminate because of the heterogeneous nature of the gravel. The laminae can be straight or convex

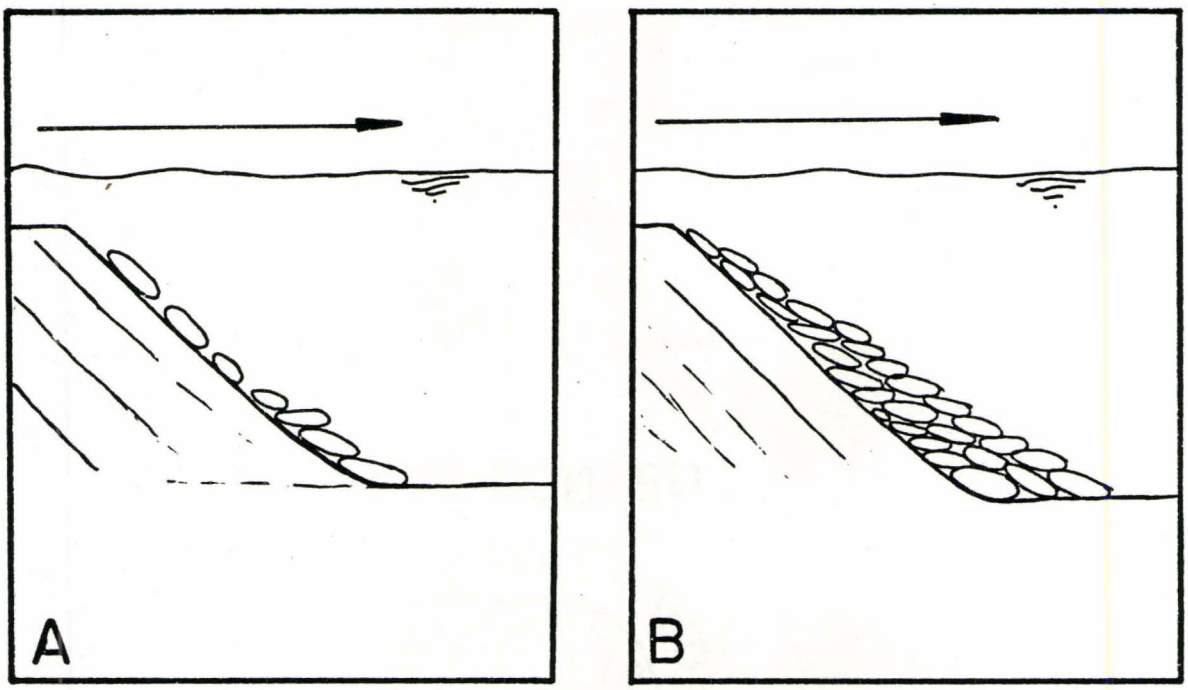

Fig. 14 The orientation of pebbles on foreset slopes

A Sliding down parallel to the foreset slope and stacking at base.

B Composite layers of pebbles and cobbles with varying orientations due to sliding and stacking

Fig. 15: Gravel foresets of Bar Front facies.

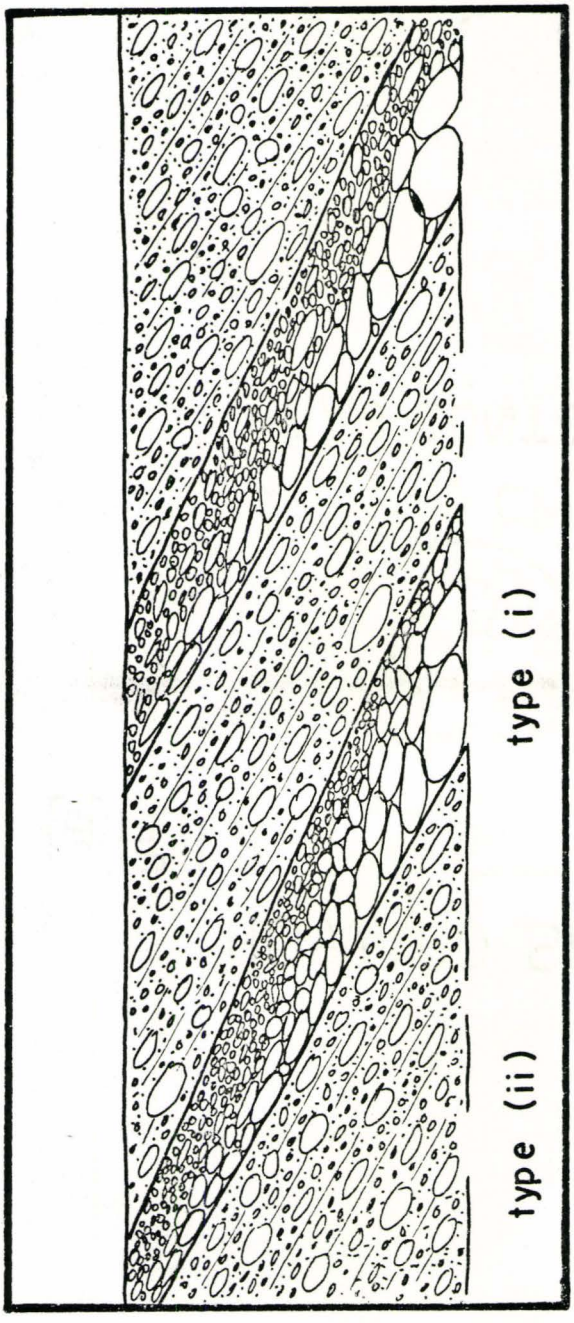

Fig. 16 Type of cross strata in the coarse gravels of the Bar Front Facies

upwards, and occur in bundles 1 to 3 m thick (see photolog at V), or in a thinner series alternating with type (i).

The alternations of types (i) and (ii) (openwork gravel foresets and heterogeneous gravel foresets) constitute a series of cross strata which appear to be fining upwards. The top of the openwork gravel becomes sealed off against infiltration of matrix sized particles because of burial by the heterogeneous gravels. Another feature of the openwork gravels at the base of the foreset slope is the occurrence of Mn-rich and Fe-rich chemical sedimentary deposits as fine grained coatings on the pebbles and cobbles. These coatings both appear black in fresh exposure, but the Fe-rich one quickly oxidizes to a rust brown colour, while the Mn-rich one eventually turns a dull ash grey. The chemical tests of these deposits were carried out using the procedure laid down by Wolf et al (1967). The two chemically deposited sediments were invariably found separate from each other, though in places they were in adjacent foresets. Similar deposits occur in openwork gravels throughout the fluvio-glacial system from Preston to Oakland.

The sand body, between the coarse gravels of the Bar Front and the bar core, ought properly to be described as a side channel facies. However it initiates the downstream addition of material onto the bar core, therefore could be considered as a constituent of the Bar Front facies. As such it will be described here. It is composed dominantly of trough-cross bedded sands, with troughs of various sizes from 3 cms deep by 20 cms wide to 30 cms deep by 140 cms wide. Rippled sands are also developed at the base of the sand body. The palaeocurrent and grain size data are described below, and the significance of the sand body's divergent palaeocurrent (217 degrees compared to 177 degrees) is discussed at the end of the chapter.

In the 110 m of cross strata exposed north of location (4) (Fig. 8), there are 10 or 11 reactivation surfaces. The letters V, W and Z of the photolog are located near to three of the better examples. These surfaces are convex upwards, with an angle of 0 to 5 degrees near the top, increasing to 15 to 20 degrees at the base (see Fig. 17). Even at their steepest these surfaces rarely match the angle of dips of the cross strata, and nearly always truncate them at a lower angle. The surfaces are 10 to 15 m long and from 3 to 13 m apart, (see Fig. 17), with the exception of the most northerly part of the cross-stratification. Immediately after the sand body there is at least 30 m of progradation by gravel cross strata before interruption by a reactivation surface. Fig. 18 shows the complete Bar Front exposure and the distances between reactivation surfaces.

On several of the reactivation surfaces, such as those at W and Z on photolog, thin sands are developed. These have an internal sedimentary structure of medium-scale cross lamination, and the partially preserved external morphology of dunes. These dunes are 8 to 15 cms high, with a wavelength of 30-35 cm and an inferred palaeocurrent direction opposite to that of the cross-strata.

BAR FRONT FACIES: FABRICS AND PALAEOCURRENTS

The pebbles and cobbles measured in an attempt to determine the cross strata dip direction (see Table 24 , Appendix C) have a range of directions from 085 to 274 degrees. However the mean values of the sample fall in the range from 169 to 187 degrees, and the standard deviation values range from 33 to 45 degrees. Fig. 19 (A) shows a stereoplot of the 140 readings from the 7 samples. The Bar Front advance as indicated by the cross strata is almost due south.

The sands on the reactivation surfaces could not be measured accurately

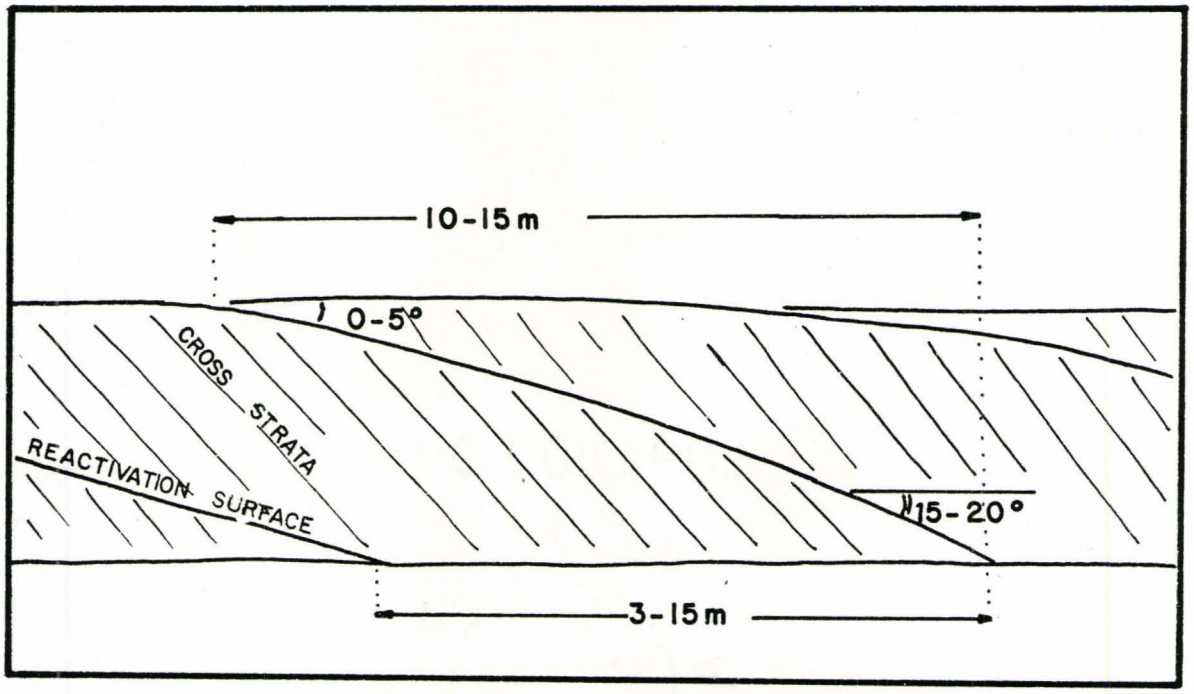

Fig. 17 Geometry of the reactivation surfaces of the Bar Front Facies

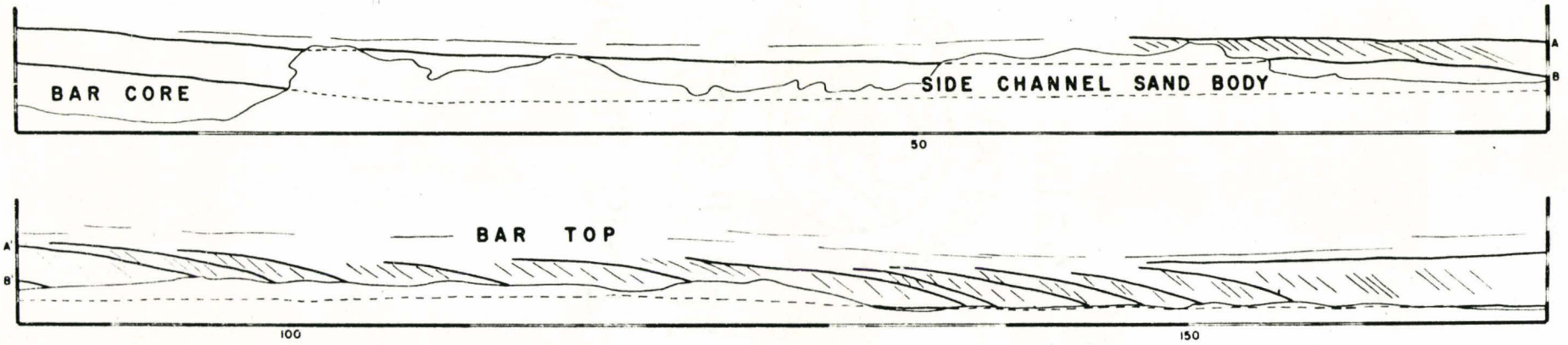

Fig. 18: The dimensions of the advancing Bar Front exposures in simplified form. (Vertical and horizontal scales in metres.)

but the direction of flow indicated by their foresets and the dune asymmetry was opposite to that of the large scale gravel cross strata. The imbricate gravel of the Bar Top, forming the top set of the whole Bar Front, has palaeocurrents similar to those of the large scale cross strata. These are discussed in detail in the Bar Top facies section.

The side channel sand body was measured at 3 localities and 40 palaeocurrent readings taken in total (see Table 25, Appendix C). The 10 trough axes measured gave a palaeocurrent flow toward west-southwest (255 degrees), and the crest-lines of medium scale foresets gave a palaeocurrent flow toward south-southwest (205 degrees.) The readings are plotted on Fig. 19 (B), and the grand vector mean for the sand body palaeocurrents is 217 degrees (southwest).

BAR FRONT FACIES : GRAIN SIZE

This facies is one of the coarsest in the outwash system (see Fig. 10). Two samples of the gravel cross-strata, two of the reactivation sands, and two of the side channel sandy body were sieved. Fig. 20 gives histograms for each of these and table 2 gives the raw data.

In both the gravel samples the mean grain size if -3.0 phi, and the mean of the 10 largest particles is -6.25 and -6.5 phi (i.e. cobbles of the Wentworth (1922) scale: see Fig. 11). Standard deviation values are 1.73 and 2.06 phi, indicating poor sorting. For the reactivation sand samples the means are 0.0 phi and 1.1 phi; the standard deviation values of 0.81 to 1.96 indicate moderate to poor sorting. The modal classes of the gravel samples occur in the pebble range, and in the coarse-sand range. The one mode in the reactivation sands is comparable to the coarse sand mode of the gravel samples.

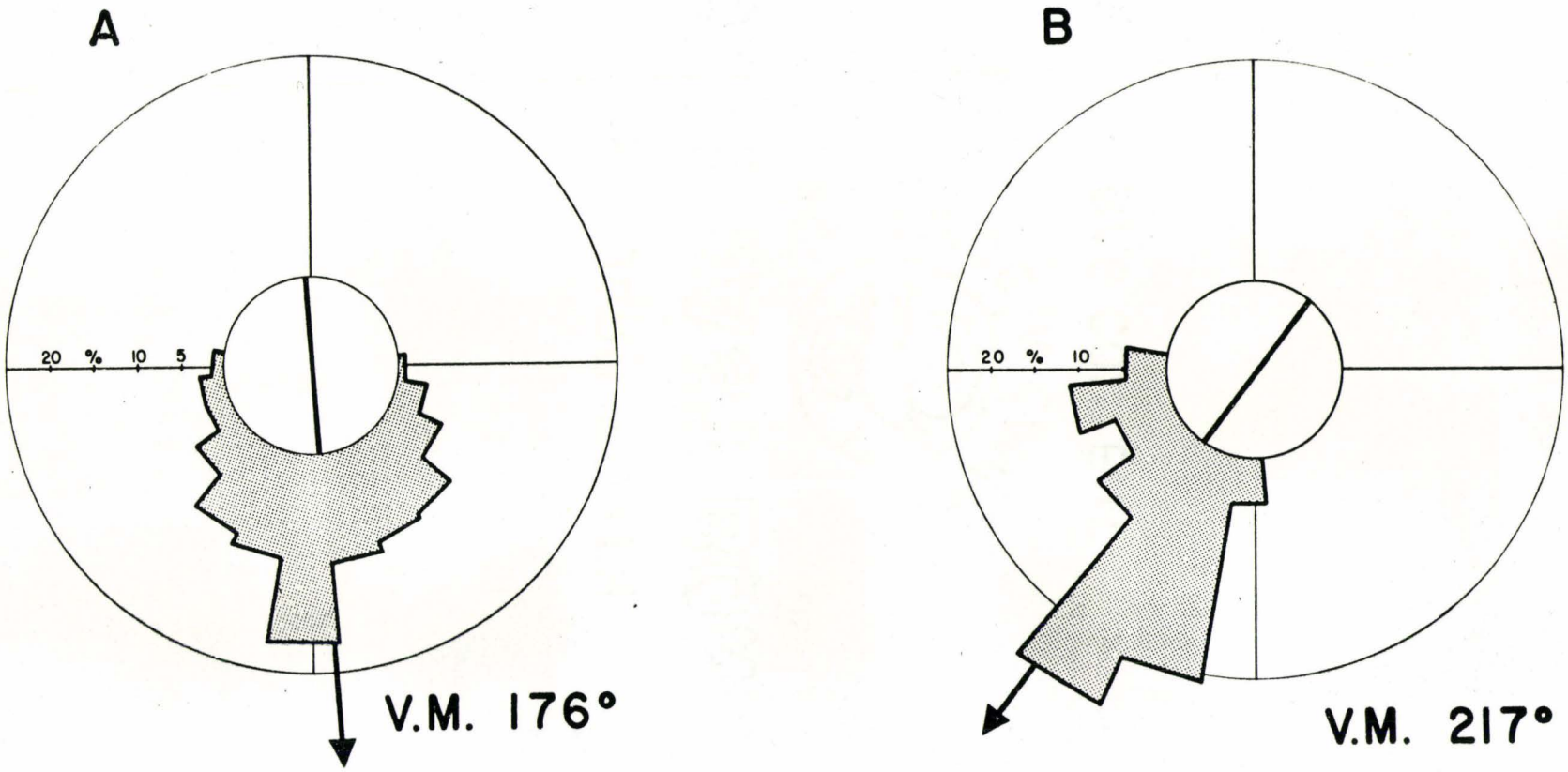

Fig. 19: Palaeocurrents of the Bar Front facies at East Paris.

A. cross-strata

B. side channel sand body

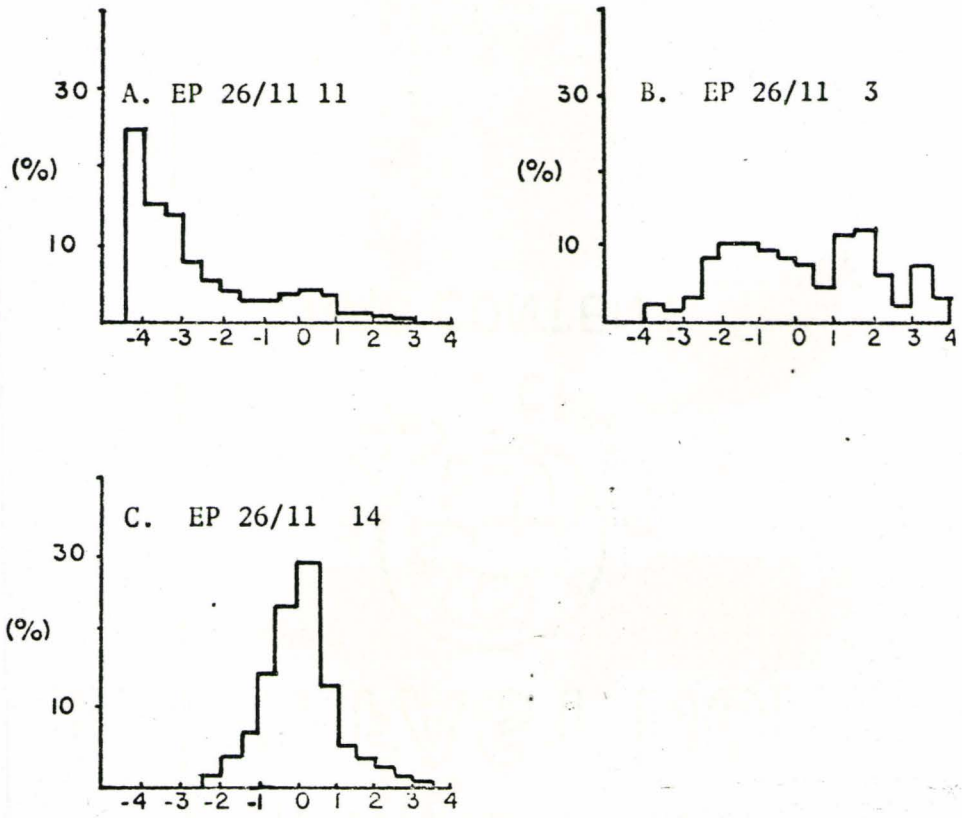

Fig. 20 Histograms of size distributions from Bar Front Facies

A Cross-bedded gravels

B Side Channel sands

C Reactivation Surface sands

The sands of the side channel sand body have mean grain sizes of 0.3 phi and 1.2 phi, and the mean of the 10 largest grains is -3.75 and -1.0 phi respectively. Both of the sands have a single mode at the medium sand range, and one of them has an additional minor mode in the granule range. Standard deviation values of 0.7 and 1.9 indicate moderate to poor sorting. Skewness values vary from -0.238 to 0.510 (coarse skewed to strongly fine skewed). Both sands sampled on the reactivation surface display a near symmetrical distribution. Kurtosis values range from 0.799 to 1.379 (platykurtic to leptokurtic).

BAR STOSS-SIDE FACIES: OCCURRENCE

As the name suggests, this facies is developed upstream of the topographic high of unit 1, which is the bar core. It is best exposed along the north part of the face between locations (3) and (4) (see Fig. 8). The facies has a maximum thickness of 4m, controlled by the thickness of the core, and and exposed length of 150m. It consists of coarsening upwards units (see G of photolog) composed of tabular cross bedded coarse sands and granules, grading into well imbricated coarse gravels in the cobble size range.

The contact between the stoss-side facies and the underlying basal gravels of the bar core facies is sharp and erosional where the tabular cross-bedded sands and granules are in direct contact (H of photolog), and gradational where the coarse gravels are in direct contact (below F of photolog). Where contact with the bar core proper occurs the junction is erosional (H of photolog). Laterally in the system the stoss-side facies is found interfingering with the side channel facies (see F of photolog). The stoss-side facies is overlain gradationally by the Bar Top facies. The

The shallow braided stream facies follows in succession.

A further exposure of the stoss-side facies at location (1) of Fig. 8, where it is seen overlying the basal gravels, and laterally adjacent to another exposure of side channel facies.

BAR STOSS-SIDE FACIES: STRATIFICATION AND SEDIMENTARY STRUCTURES

In places this facies is developed in upstream-dipping inclined strata which are most prominent (a) where the facies interfingers with the side channel, (here a maximum angle of 10-12 degrees is recorded) and (b) where the facies comes into contact with the bar core (here the maximum angle is 9-10 degrees). Elsewhere the angle is much lower and the facies stratification is sub-horizontal.

Basically the facies is composed of coarsening upwards units which have two component parts:-

(i) tabular cross bedded coarse sands and granule gravels, in wedge shaped and parallel sided sets. Each coset of this type coarsens upwards becoming more pebbly towards the top (see H of photolog). This part of the facies can be up to 2.5m thick. The individual sets are commonly 20 to 35 cms thick, but occasionally are 50 to 55 cms thick. The angle of dip of the cross-bedding was measured at 4 sampling localities with 46 readings in total (see table 27 of Appendix C). The dip angle varied in total from 6 to 34 degrees, and the means of the 4 samples ranged from 18 to 23 degrees.

(ii) A well imbricated coarse gravel capping to each coarsening-upwards unit, which is predominantly cobble size material. This part can be anything from a one-pebble thick unit, up to 1.5m thick (see I of photolog). It is this part of the facies which interfingers with the side-channel facies

(see F of photolog).

The whole coarsening-upwards unit is commonly topped by a cobble lag of one particle thickness. In some places the upper part of the coarsening upwards unit (i.e. - part (ii) and the cobble lag), is less well developed or missing altogether.

A repeated sequence of coarsening-upwards units is exposed in places (see L of photolog), which has both the tabular cross-bedded and the well imbricated gravel parts.

BAR STOSS-SIDE FACIES: FABRICS AND PALAEOCURRENTS

Two types of palaeocurrent data are available for this facies. The imbricate fabric of the coarse gravels in the upper part of the facies was measured, and the direction of the maximum dip of the cross beds in the lower part was also measured.

The palaeocurrents inferred from the cross-bedding are slightly more variable than those from the imbrication. The mean directions of 4 samples of cross strata (46 total readings, table 27 Appendix C), range from 155 to 200 degrees. Fig. 21(A) shows the rose diagram of the cross-bedding which has a vector mean of 176 degrees, roughly due south.

The imbricate fabric was examined at 6 localities (150 readings - table 26 Appendix C). The means of the dip angles range from 22 to 26 degrees but the modal classes are less consistent, with samples having modes variously from 10 to 14 degrees to 30 to 34 degrees. In fact only one of the samples has a mode in the 20-24 degrees class where most of the means fall.

The mean inferred palaeocurrent direction for the sampling locations range from 161 to 194 degrees. The grand vector mean for the 150 readings is 182 degrees, also roughly due south. (see Fig. 21 (B)).

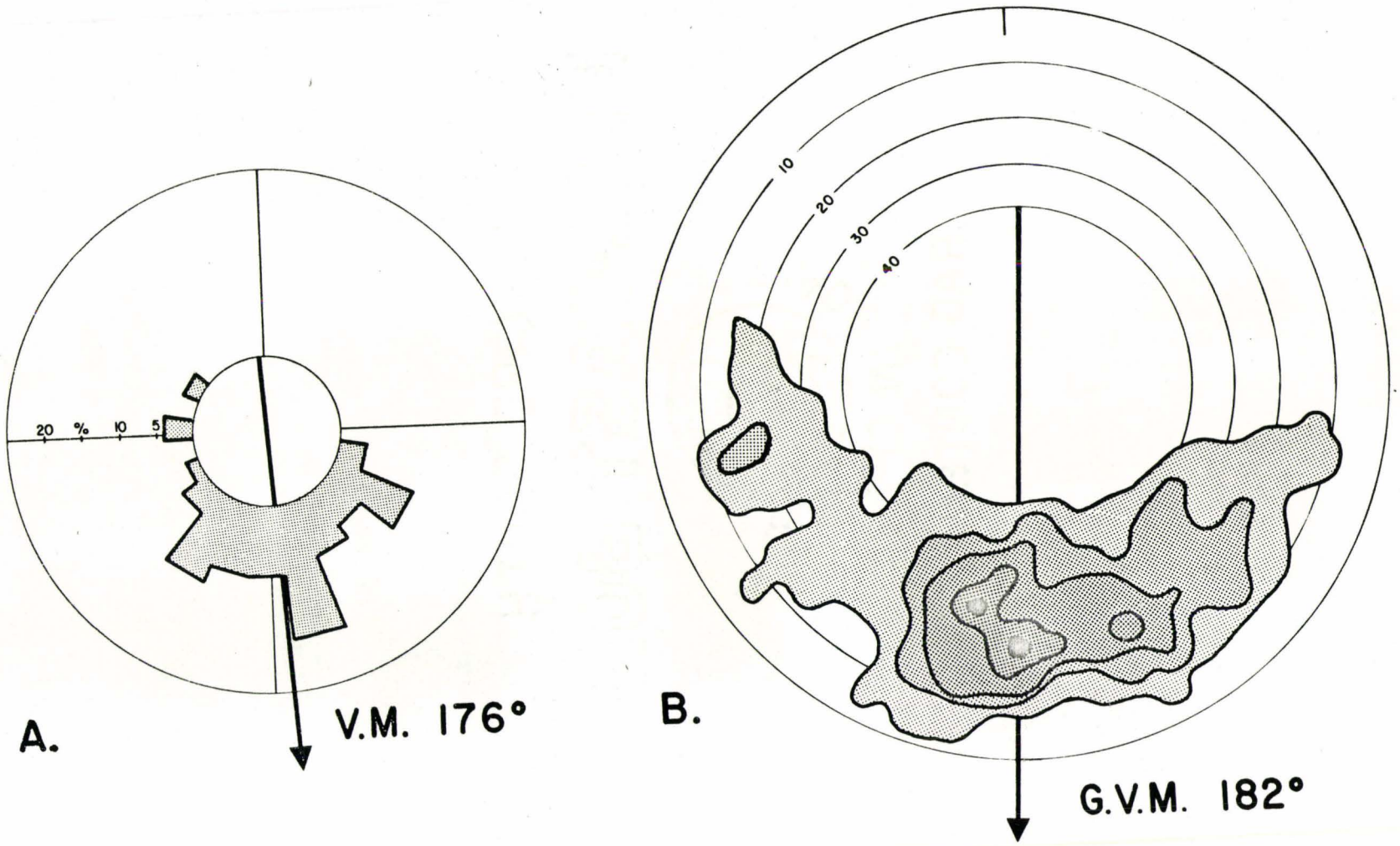

Fig. 21: Palaeocurrents of the Stoss-side facies at East Paris.

A. cross-bedding B. imbrication

BAR STOSS-SIDE FACIES: GRAIN SIZE

The cross-bedded sands and gravels were sampled at 16 sites (see table 3 Appendix B). The mean grain size ranges from -0.79 to 1.33 phi, and standard deviation values of 0.88 to 2.16 indicate moderate to very poor sorting. The gravels of the imbricate beds were sampled at 3 sites (see table 4 Appendix B). The means of the 10 largest particles at these sites range from -6.0 to -6.25 phi (cobbles of the Wentworth (1922) scale; see Fig. 11). The mean values range -2.11 to -2.33 phi, and the standard deviation values of 2.07 to 2.35 indicate very poor sorting.

Fig. 22 shows two coarsening upwards sequences with 3 samples from each, taken in the same unit approximately 40m apart. In both cases the coarsest sample is an imbricate gravel, and the other two in each are cross-bedded gravels. The sand modes for those six samples range from 0.0 to 2.5 phi, but most of them (5 out of 8) are in the range 0.0 to 0.5 phi coarse sand. The gravel modes vary from -2.5 to -5.0 phi pebbles.

Virtually all the stoss-side samples exhibit negative skewness indicating an excess of coarse material. The imbricate gravel samples (Table 4, Appendix B) are exceptions with near symmetrical to strongly fine skewed distribution. The kurtosis values of the cross-bedded gravels indicated predominantly leptokurtic distributions. The imbricate gravel distributions are platykurtic, and the combination of these values with large standard deviaiton values indicates that little effective sorting has been experienced.

BAR TOP FACIES: OCCURRENCE

The bar top facies is exposed along the length of the face between locations (3) and (4) of Fig. 8, on top of the Bar Core, Bar Front and

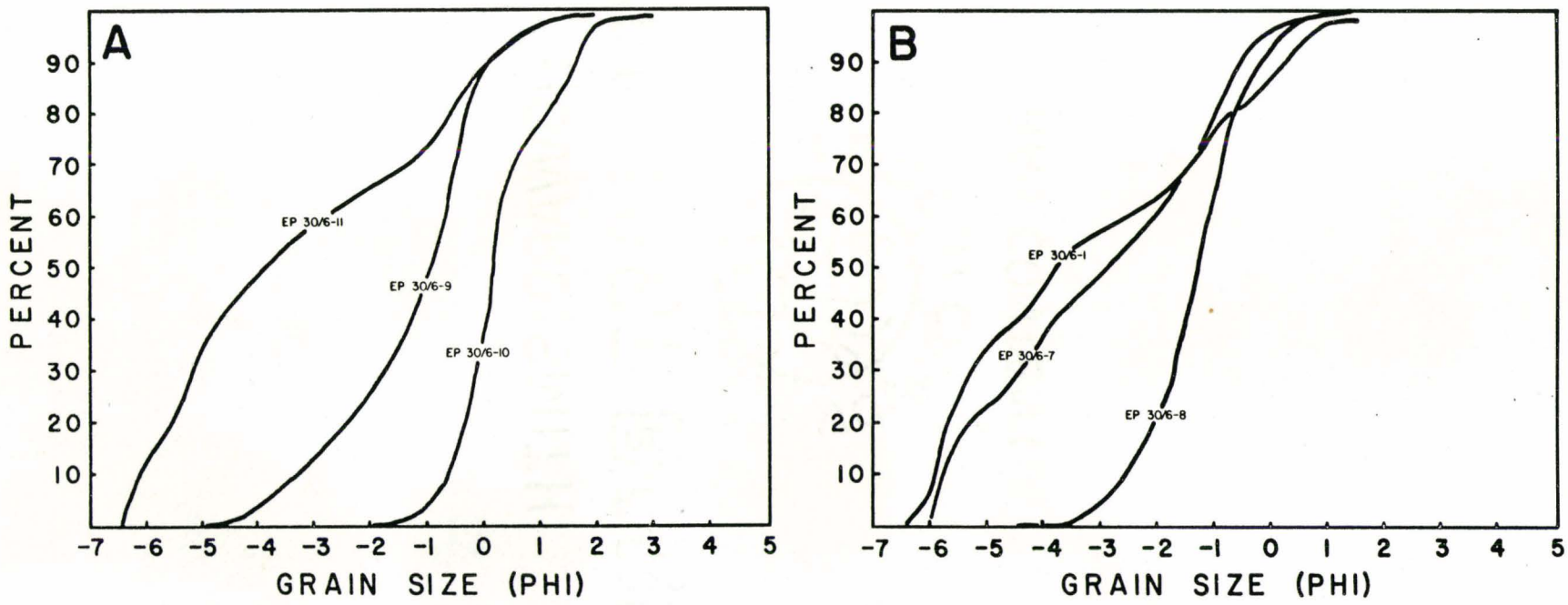

Fig. 22: Cumulative Curves (arithmetic ordinate) of grain size distributions for samples from the coarsening upwards units of the Stoss-side facies.

A. 10m to the left of H on the Photolog

B. 15m to the right of I on the Photolog

Bar Stoss-side facies. Where the Bar Top and the Bar Core are in direct contact, the transition is a zone of reworked core gravel (see O of photolog). This zone has particular significance regarding the reconstruction of the sequence of events of bar formation, and will be discussed fully at the end of the chapter. Contact with the Bar Front gravel is gradational (see above) because the Bar Top imbricate gravel also forms the Bar Front gravel supply. The Shallow Braided-Stream facies follows above the Bar Top throughout the system, and the transition is everywhere gradational, and normally very difficult to determine exactly.

Other exposures of the facies occur between location (1) and (2), and (5) and (6), where they variously overlie Bar Front and Bar Stoss-side facies exposures.

BAR TOP FACIES: STRATIFICATION

This facies has two constituent parts:-

(i) The upper surface of the bar core topographic high is reworked and forms part of the Bar Top facies. A relatively thick (1 to 1.5m) unit of undulatory appearance marks this zone. This configuration is due to shallow trough or channel-like depressions from 3 to 5 m wide. The whole zone is exposed from H to R, and one trough-like depression is labelled at O on the photolog.

(ii) The bulk of the facies is composed of coarse gravels which are crudely horizontally stratified and moderately well imbricated. The crude horizontal stratification of the deposit is imparted by a series of features comparable to those described in the Bar Core facies section. They are:- a) Discrete sand lenses (S of photolog) 5 to 20 cms thick and 3 to 6 m long, which are generally concave upwards and appear as channel-like depressions infilled by sand. These exhibit small to medium-

scale cross lamination of both low angle and trough types. In places the complete lens is one cross-laminated set. b) Thin discontinuous horizons 5 to 25 cms thick and upto 20 m long in the direction of flow, composed of sand-matrix-rich gravels. These normally occur as slightly concave upwards forms, and can be seen at X of photolog. c) Horizons with little of no matrix 5 to 15 cms thick and 2 to 10 m long. The sand content of these horizons normally increases upwards closing off and sealing the gravels against further sand infiltration.

The silt matrix horizons described in the Bar Core facies section are not present here.

BAR TOP FACIES: FABRICS AND PALAEOCURRENTS

Three types of palaeocurrent data are available for this facies. The low angle trough cross-bedded gravels of the reworked top surface of the bar core were sampled at 2 sites (51 readings); the discrete sand lenses with cross-lamination were sampled at 5 sites (70 readings); and the moderately well imbricated coarse gravels were sampled at 4 sites (95 readings). Fig. 23 shows a rose diagram or a contoured stereoplot for each group.

The reworked core gravels were measured at a location 8 m to the right of P of photolog. An approximately equal number of readings (25 and 26) was taken from each side of a shallow trough-like structure. The two parts of the distribution are reflected in the bimodality of the rose diagram (see Fig. 23). The inferred palaeocurrent direction is 249 degrees. The divergence of this direction from the others of this facies is discussed in the interpretive model developed at the end of this chapter. The dips of the cross strata varied from 3 to 41 degrees, and the means of the two samples were 23 and 22 degrees.

The cross laminations within the sand lenses (see also table 2

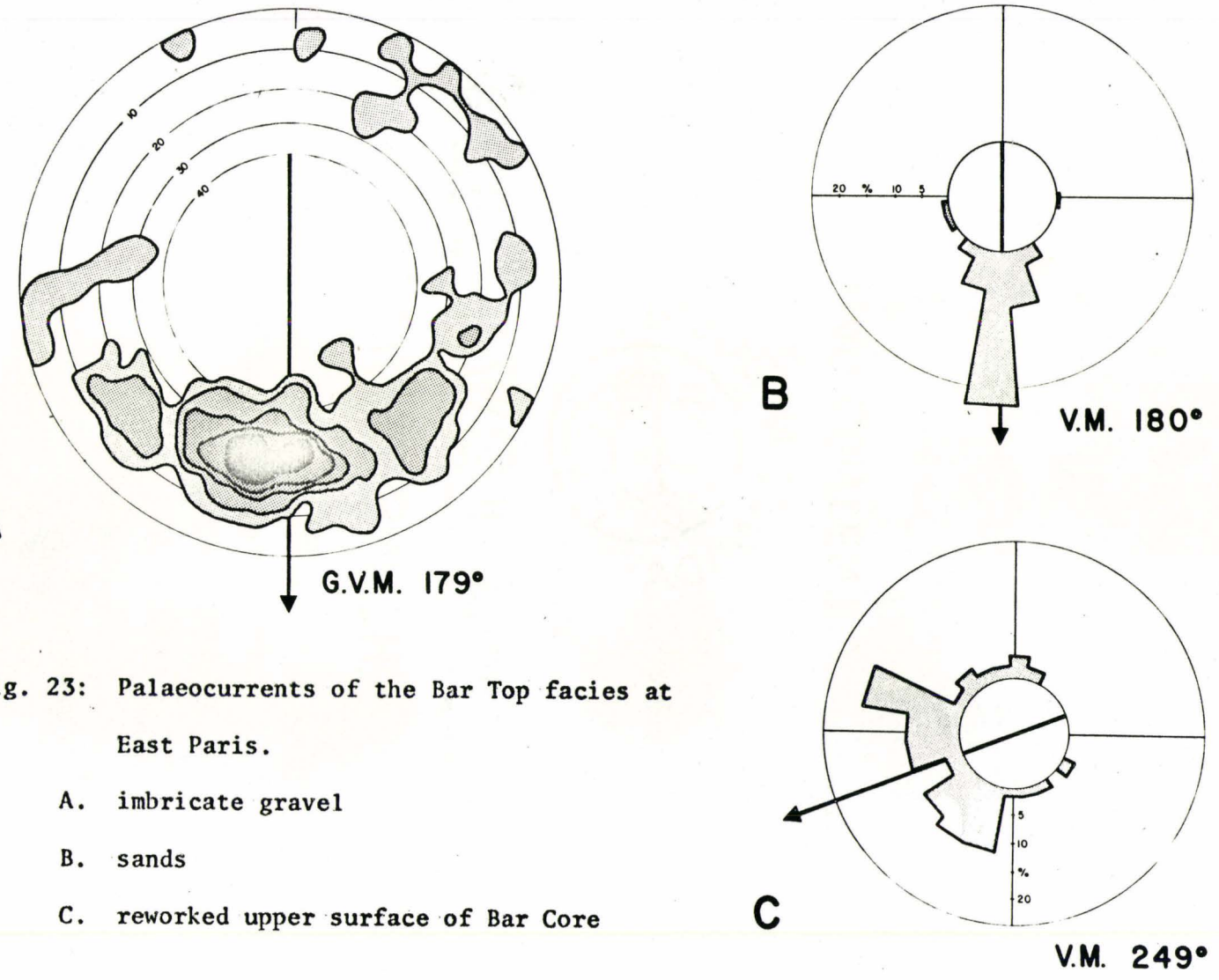

Fig. 23: Palaeocurrents of the Bar Top facies at East Paris.

A. imbricate gravel

B. sands

C. reworked upper surface of Bar Core

Appendix C) gives a range of inferred palaeocurrent directions from 096 desgres to 268 degrees, with a grand vector mean of exactly 180 degrees, due south. The individual means of the 5 samples range from 170 to 188 degrees.

The moderately well imbricated gravel was sampled at 4 sites and Fig. 23 shows a stereoplot of these measurements. The mean angle of dip of the samples ranges from 18 to 26 degrees, while the total range is 3 to 48 degrees. The grand vector mean and inferred palaeocurrent direction is 179 degrees, almost due south, while the vector means for the samples range from 157 to 204 degrees (see table 30 , Appendix C). These imbricate gravels also represent the gravel supply to the Bar Front (see above). The inferred palaeocurrent of the Bar Front cross strata (177 degrees), the imbricate gravels (179 degrees) and the sand lenses (180 degrees) all agree very closely.

BAR TOP FACIES: GRAIN SIZE

Isolated boulders 50 to 72 cms in diameter are found in this and other facies of the system (R and T of photolog; and see above Bar Core facies: Grain Size), but do not represent the normal particles moved by the stream. The normal particles of the Bar Top facies are coarse gravels (see Table 6 Appendix B). The mean grain size of the samples ranges from -2.0 to -2.2 phi, and the mean of the 10 largest particles ranges from -5.5 to -6.25 phi (pebbles and cobbles of the Wentworth (1922) scale: see Fig. 11.). The sands observed in the discrete sand lenses have a mean grain size of 1.5 phi. (medium sand, see Table 5, Appendix B).

Fig. 24 shows histograms of the 4 samples. The sand sample has a mode at 1.5 phi, while the sand fraction of the gravels has modes from -0.5

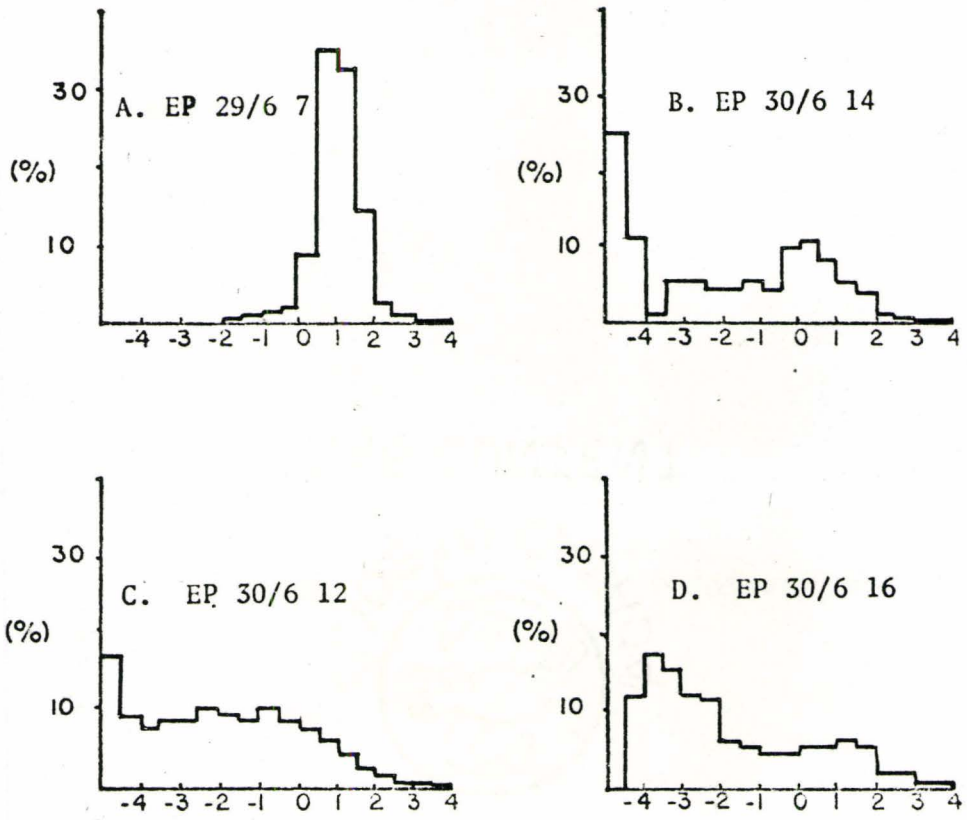

Fig. 24 Histogram of size distributions of samples from Bar Top Facies

A Sand

B-D Gravels

(very coarse sand) to 1.5 phi (medium sand). Gravel modes occur at -4.5, -3.5 and -2.0 phi (all in the pebble size-class). The sand content of the gravel samples is between 25 and 36 percent of the total sample, which implies a moderately loose packing (Plumley, 1948). The standard deviation values for the gravels range from 1.99 to 2.27 (poorly to very poorly sorted), and for the sands are 0.54 (moderately well sorted). Skewness values indicate excess fine material in the gravels and in the sand. The gravels have kurtosis values indicating platykurtic distributions which together with the high standard deviation values suggest that little effective sorting has been experienced. The leptokurtic value of the sand sample reflects its unimodal distribution.

SIDE-CHANNEL FACIES: OCCURRENCE

The deposits of the side channels are some of the finest in the whole outwash system, and the finest at East Paris (see Fig. 10). There are 5 exposures of the facies:-

i) Near location (1) (Fig. 8), between a deposit of stoss-side facies on the west and an exposure of a bar core on the east.

ii) Along the face between locations (2) and (3), where a large (100m by 6m) exposure is located. This is the type example.

iii) Between the bar core and the bar front facies along the face (3) to (4) of Fig. 8. (see above: Bar Front facies.)

iv) At location (5) subjacent to Bar Front facies deposits, and

v) At location (6) where it overlies basal gravels of the Bar Core facies and is laterally adjacent to cross-strata of the Bar Front facies.

In all cases the contact between the side-channel facies and the Bar Core facies is sharp and erosional. This relationship is particularly well illustrated in the face between (2) and (3) (near B and C, and at E of photolog). The contact with the stoss-side deposits displays an interpenetrating relationship, with thin-lenses of stoss-side gravel pinching out across the channel (see F of photolog). Contact with the Bar Front facies is generally sharp and erosional when the bar front cross strata overlie the channel sands (as at V of photolog), and is sharp where the two are laterally adjacent.

The type example of the side channel facies is exposed along the face (2) to (3) (Fig. 8). Here the channel form has a maximum depth of 6 m and a width of 100 m. It is illustrated in the first strip of the photolog, and a diagrammatic representation is given in Fig. 25. On the west side of the channel, a portion of a bar core is exposed adjacent to the channel deposits and forming one bank. Basal gravels of the Bar Core facies underlie the channel, and stoss-side and bar top deposits form the eastern side of the channel.

The channel itself displays a fining upwards sequence from large scale trough cross-bedding in granule gravels, to smaller scale trough cross bedding, to plane lamination at the sides of the channel inclined up the sloping edges, and finally rippled and ripple drift cross-laminated fine sands.

Elsewhere the channels are of a smaller scale (3-4m deep and 25-50m wide), and exhibit no such sequence, having dominantly rippled and plane laminated sands.

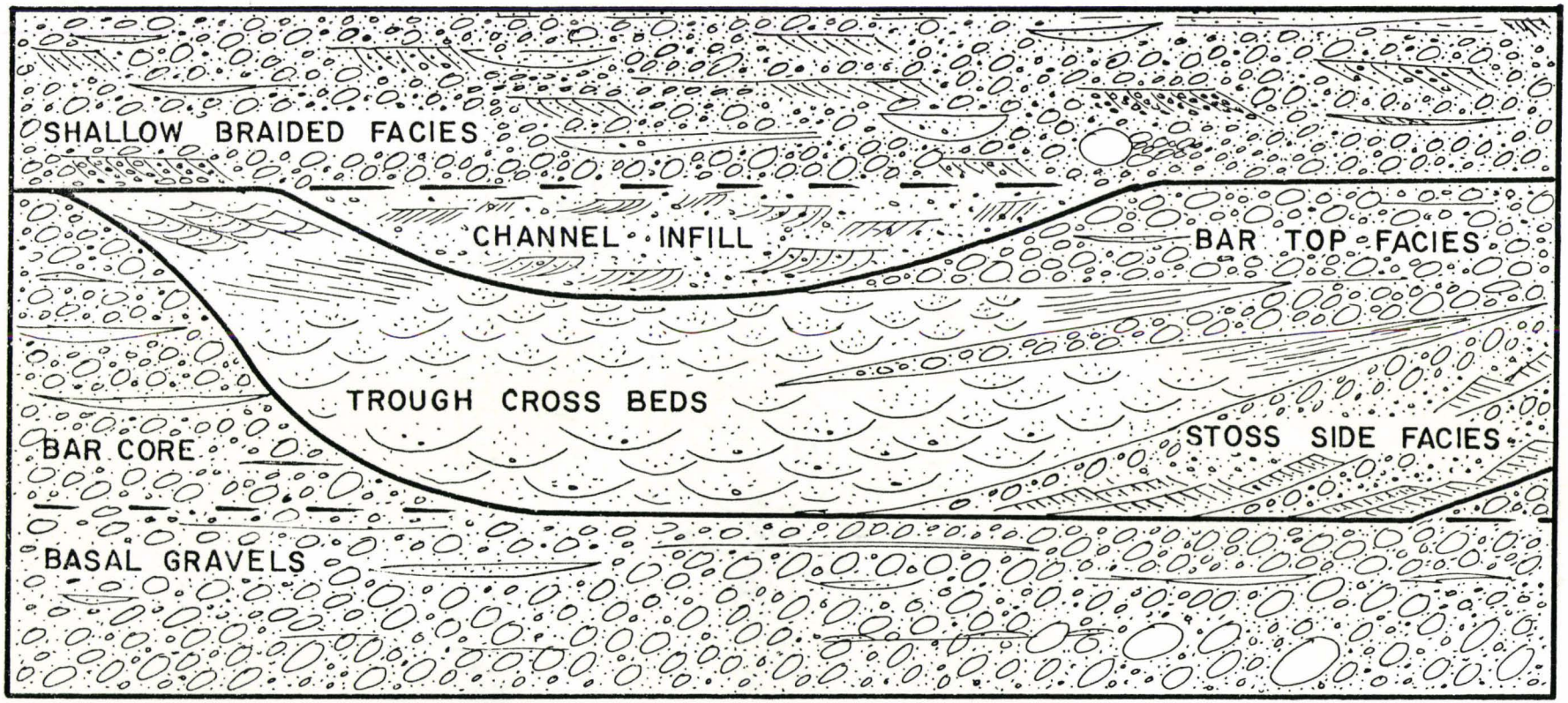

Fig. 25: Diagrammatic representation of the Side Channel facies type-exposure (between locations (2) and (3) of Fig. 8).

SIDE-CHANNEL FACIES: SEDIMENTARY STRUCTURES

There are basically three types of sedimentary structures: trough cross bedding, planar lamination, and ripple lamination.

The trough cross-bedding and trough cross lamination are best exhibited in the central portions of the channel forms. There are two directional components of fining exhibited by these structures in the channels. The troughs get smaller and the material finer both upwards and outwards from the centre and base of the channel forms. The trough sizes vary from 450 by 35 cms to 50 by 8 cms in the granule gravels and coarse sands, but are considerably smaller in the fine sands where they are as small as 7 cms by 2 cms. The latter constitute part of the rippled deposits. Because of the nature of the exposure the length of the troughs in the direction of flow was not observed.

The width-depth ratios range from 4:1 to 18:1, and there does not appear to be an overall change through the fining upwards sequence. Trough cross-bedding in granule gravels is seen in three of the channels (those in the north of the pit, and the one along the east face). In the south face the channels are developed in coarse to medium sands, and are associated with considerably more planar lamination.

The plane lamination occurs in two situations. Firstly, inclined plane laminae are found in the extremities of the larger channel forms. They are located on the east side of the channel in the portion of the sandy deposit which interfingers with the stoss-side of the adjacent bar form (above F on photolog); and on the west of the channel higher up the side, below the rippled sands (above B of photolog).

In other channels the planar lamination is predominantly horizontal. In some places there is a segregation of the heavy mineral grains and the

quartz grains into thin (2 to 5mm) laminae. Elsewhere the planar lamination is dominantly quartz sand, but commonly has isolated pebbles and pebble clusters in assocation with it. The nature of these coarser features give a crude palaeocurrent indication. The isolated pebbles on a plane bed tend to be oriented dipping upstream, which agrees with the observations made by Fahnestock and Haushild (1962). Where associated pebble clusters occur, two types are observed, which Dal Cin (1968) also noted (see Dal Cin, 1968 Fig. 2, p. 235; and Fig. 26 of this volume). In the one case (Dal Cin's "normal" case), the so called wake of pebbles associated with a cobble is found on the upstream side; while the other case (Dal Cin's "exceptional" case), the cobble is upstream of the pebble wake. At East Paris both were observed and neither was apparently dominant.

Sands which are rippled or ripple drift cross-laminated, occur at the top of the main channel fining-upwards sequence, and in the shallower and sandier channels elsewhere. The direction of climb of the ripple drift cross-lamination is oblique to the main palaeocurrent of the channel. In the main channel ripples only occur on the west side (see Fig. 27), but this may be the only half preserved of a symmetrical pattern as occurs in the smaller channels. Individual sets have thicknesses ranging from 0.6 to 5.1 cms, and cosets can be upto 45 cms thick.

SIDE CHANNEL FACIES: PALAEOCURRENTS

Quantitative data is available for the trough cross-bedded and the ripple laminated deposits. The pebble clusters give only a crude palaeocurrent indication which was neither easily nor accurately measured. 6 sampling sites of the trough cross-beds were measured (a total of 124 readings, see table 31 , Appendix C). Readings were taken of the cross-beds themselves

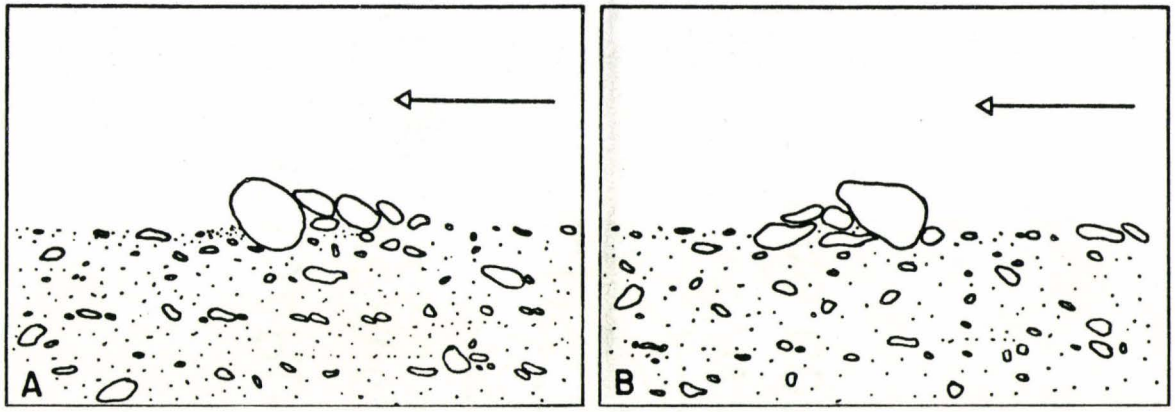

Fig. 26 Types of "pebble clusters" occurring in the Side Channel Facies sands (A) normal (B) exceptional (after Dal Cin, 1967)
Note also the isolated pebbles dipping upstream

where they were partially cemented and weathered out, and of the discoid pebbles lying in the plane of the foreset slope as an approximation of the cross-beds elsewhere.

The directions obtained ranged from 070 degrees to 294 degrees, with mean values for the samples from 171 to 221 degrees. The number of readings taken was considered sufficient to obtain a valid palaeocurrent direction despite the trough like nature, and therefore inherent variability, of the cross strata. The angle of dip varied from 3 to 36 degrees, with a range for the means of the 6 samples of 15 to 27 degrees. Fig.27 (A) shows a rose diagram of the cross strata with a vector mean of 182°, almost due south.

The rippled sands were measured at 4 sampling sites, where "rib and furrow" directions and directions perpendicular to measured crest lines were noted. A total of 56 readings was obtained in the main channel from the western side where they are well preserved, and these have been plotted on a rose diagram (Fig. 27 (B)). The means of the samples varied from 186 to 236 degrees, with a total range of 148 to 306 degrees, the two sets of data are somewhat comparable and have been combined to give a grand vector mean in Fig. 27 (C).

SIDE-CHANNEL FACIES: GRAIN SIZE

This facies constitutes the finest deposit in the East Paris Pit. Fig. 28 shows cummulative curves for 4 samples of the facies. The complete data for the 25 samples are listed in tables 7, 8 and 9, Appendix B.

The trough cross bedded deposits have mean grain size values from -0.59 to 1.39 phi, with the mean of the 10 largest particles ranging from -3.0 to -5.0 phi. Gravel modes are rare occuring in only two out of 12 samples, at -4.0 and -2.5 phi (pebble size class). Sand modes range from

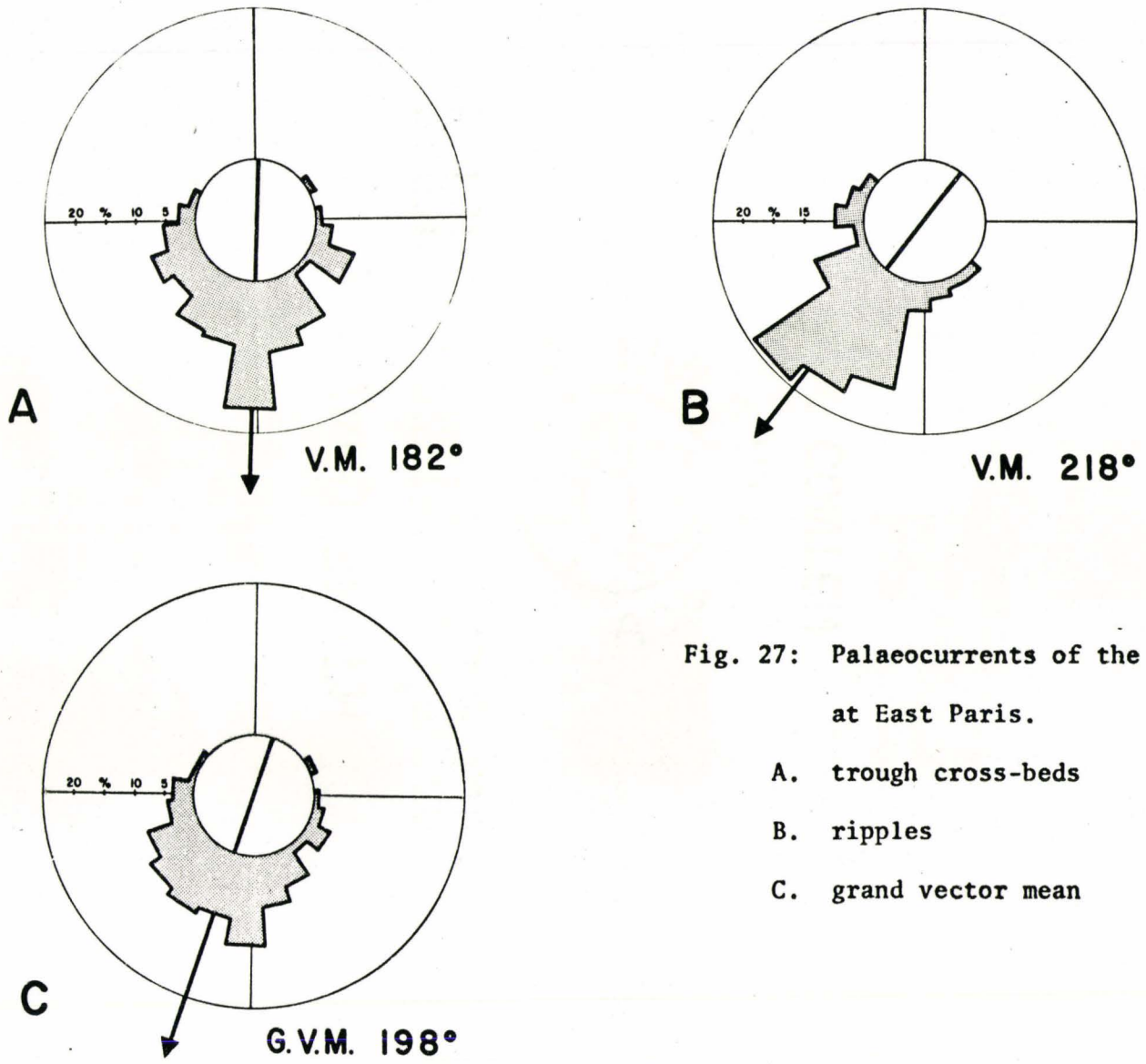

Fig. 27: Palaeocurrents of the side channel facies at East Paris.

A. trough cross-beds

B. ripples

C. grand vector mean

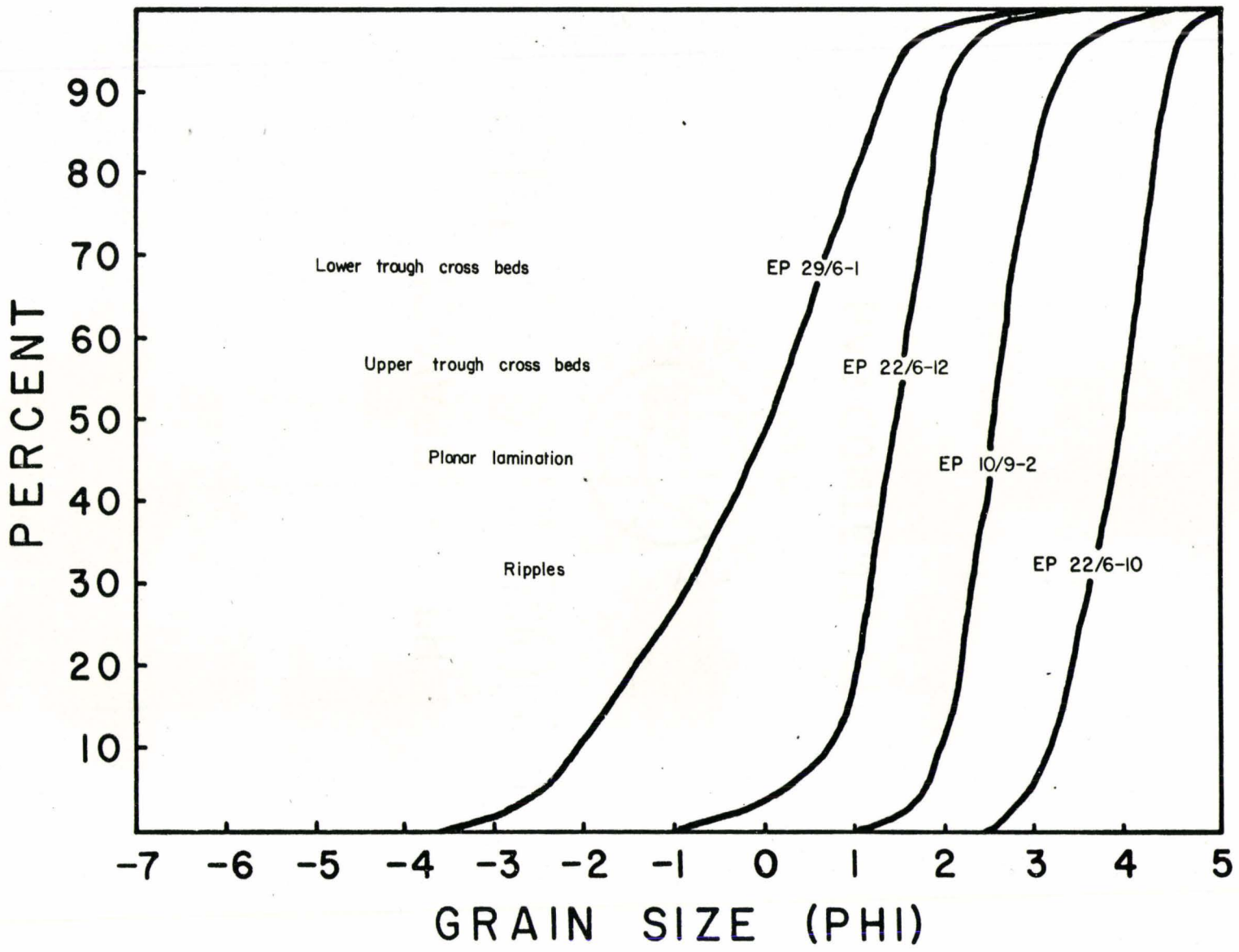

Fig. 28: Cumulative curves (arithmetic ordinate) of the grain size distributions of samples from the side-channel facies.

-0.5 to 2.5 phi, but are mainly in the range 1.0 to 2.0 phi (medium sand class). The standard deviation values of 0.57 to 1.48 indicate moderately well-to poorly-sorted deposits.

The planar laminated sands have mean grain size values of 1.78 to 2.62 phi. Modes occur from 2.0 to 3.0 phi (fine sand), and all samples are unimodal. Standard deviation values of 0.45 to 0.70 indicate well- to moderately well-sorted sands. The rippled sands have mean grain size values of 1.58 to 3.8 phi. The latter, upper value is not strictly correct because the sample had 40 per cent finer than 4.0 phi (silt size) and its upper limit was not determined. At one locality at the top of the main channel a thin (1.5 to 3.5 cms) seam of clay size particles was observed "pinching and swelling" through the rippled sands and silts. Standard deviation values ranged from 0.41 to 0.82 (well sorted to moderately sorted).

Skewness values for the trough cross-bedded material and for the rippled sands were dominantly negative, while for the planar laminated they were almost all positive. In the latter the negative value of the skewness is associated with a gravel size C (phi 1). Kurtosis values range from mesokurtic to very leptokurtic.

SHALLOW-BRAIDED STREAM FACIES: OCCURRENCE

The shallow braided stream facies totally comprises stratigraphic unit 3, (see Fig. 7), and has two constituent parts. The lower part consists of cross-bedded granule gravels which are the final infilling of the side-channel depression. This is not part of the side-channel facies however, and can be distinguished from it by two criteria. Firstly, this part of unit 3 is considerably coarser than the channel deposits immediately underlying it; and secondly, the contact with the channel depsoits below

is erosional while the contact with the rest of unit 3 above is gradational.

The upper part of unit 3 is composed of crudely horizontally stratified gravels with imbrication, gravels with medium scale tabular cross-stratification, and small sand bodies and lenses of varying nature. It is this part from which the facies derives it name. The contact of this part of the facies with unit 2, is always gradational with the Bar Top facies, and commonly difficult to delineate precisely.

The facies in total constitutes a 'blanket' cover of gravel over the entire outwash system at East Paris, and at most locations can be found at the top of the outcrop face. The upper part of this facies also has a fining upwards component, and a thin sandy horizon below the top soil can be commonly observed at most points.

SHALLOW BRAIDED STREAM FACIES: STRATIFICATION AND SEDIMENTARY STRUCTURES

The facies will be described in terms of 4 distinct sub-facies (i) the trough cross-bedded gravels of the lower part of the unit; (ii) the imbricated gravels with crude horizontal stratification; (iii) the tabular cross-bedded gravels; and (iv) various sandy horizons and small scale sand bodies.

(i) The trough cross-bedded gravels of the main channel infill are in sets of 20 to 35 cms, and in one coset of 1.5m maximum thickness (see D of photolog). The troughs crop out in oblique section, but can be excavated to give transverse sections. These widths vary from 0.75 to 4.15m, and the elongation downstream is commonly 4 to 8m. The cross-strata are generally asymptotic and have dip angles ranging from 13 to 35 degrees, with means at the 5 sampling locations of 25 to 29 degrees (see Table 34, Appendix C).

(ii) The imbricate gravels occur in two situations. The first is as a thick (commonly 3m) accumulation of crudely horizontally stratified gravels (see above Q of photolog), with associated thin sand horizons and lenses, and matrix free horizons (see (iv) below); and secondly as thin 10 to 20 cm) beds in assocation with the tabular cross-bedded gravels. Both imbricate gravel situations have similar fabrics. The angle of dips of the pebbles and cobbles (125 readings, 5 samples) varied from 3 to 42 degrees, with a range slightly less than this in each of the 5 samples. The mean angles varied from 12 to 22 degrees (see table 33 , Appendix C). The palaeocurrents are discussed below.

(iii) The tabular cross-bedded gravels have angular to slightly asymptotic bases to the foresets, which occur in sets of 25 to 40 cms in thickness (see J of photolog). Each set, some 5 to 20m long, is usually found with an associated thin imbricate gravel bed (see above) directly above the foresets. The foresets dip at 16 to 35 degrees (47 readings from 3 sample locations), and the mean angle for each sample, is 24, 25 and 26 degrees. The palaeocurrent data for these features are discussed below

(iv) This sub-section includes a widely diversified group of sandy features. They are:-

a) Thin discontinuous sand-matrix-rich horizons within the thick imbricate gravels which together with the thin discontinuous matrix-free horizons, impart the curde horizontal stratification to the gravels. These are 5 to 12 cms thick and 1 to 3m long.

b) Thin sandy horizons, 10 to 15 cms thick, but continuous in direction of flow for up to 25m. Some pebbles also occur in those sandy seams. They are commonly planar laminated internally, and horizontal in total aspect.

c) Thin discrete sand lenses 10 to 35 cms thick and 1.5 to 4.5m long. These are concave upwards and appear as small channel-like depression infillings. Their internal structure varies with size. The smaller ones are normally planar laminations or cross-stratified on a small scale, whereas the larger ones have small scale cross-stratification or trough cross-bedding.

d) The top 20 to 100 cms of the ourcrop has a sandy capping in some places (see T and Y of photolog), with planar lamination, low angle-, tabular-, and trough cross-bedding variously exposed.

SHALLOW BRAIDED STREAM FACIES: FABRICS AND PALAEOCURRENT

The palaeocurrent data for this facies can be classified into 4 groups: the imbrication of the gravels; the cross-bedding of the channel infill; the cross-bedding of the tabular sets; and the cross-lamination of the sandy lenses. These are illustrated in Fig. 29. For the imbricate gravels (5 samples, 125 readings; see table 33, Appendix C), the directions vary from 093 to 353 degrees. The means for each sample range from 182 to 227 degrees, and the vector mean is 196 degrees. (see Fig. 29 -A).

The cross-bedding in the lower part of the facies, the channel depression infill, ranges in inferred palaeocurrent direction from 188 to 266 degrees. The means of the 5 samples (21 readings see table 34, Appendix C) range from 208 to 245 degrees, and the vector mean is 229 degrees. (see rose diagram Fig. 29 -C).

The cross-bedding of the tabular sets (3 samples, 47 readings - see table 35, Appendix C), has inferred palaeocurrent directions ranging from 178 to 235 degrees. The means of the samples are from 202 to 207 degrees; and the vector mean for all 47 readings is 205 degrees (see

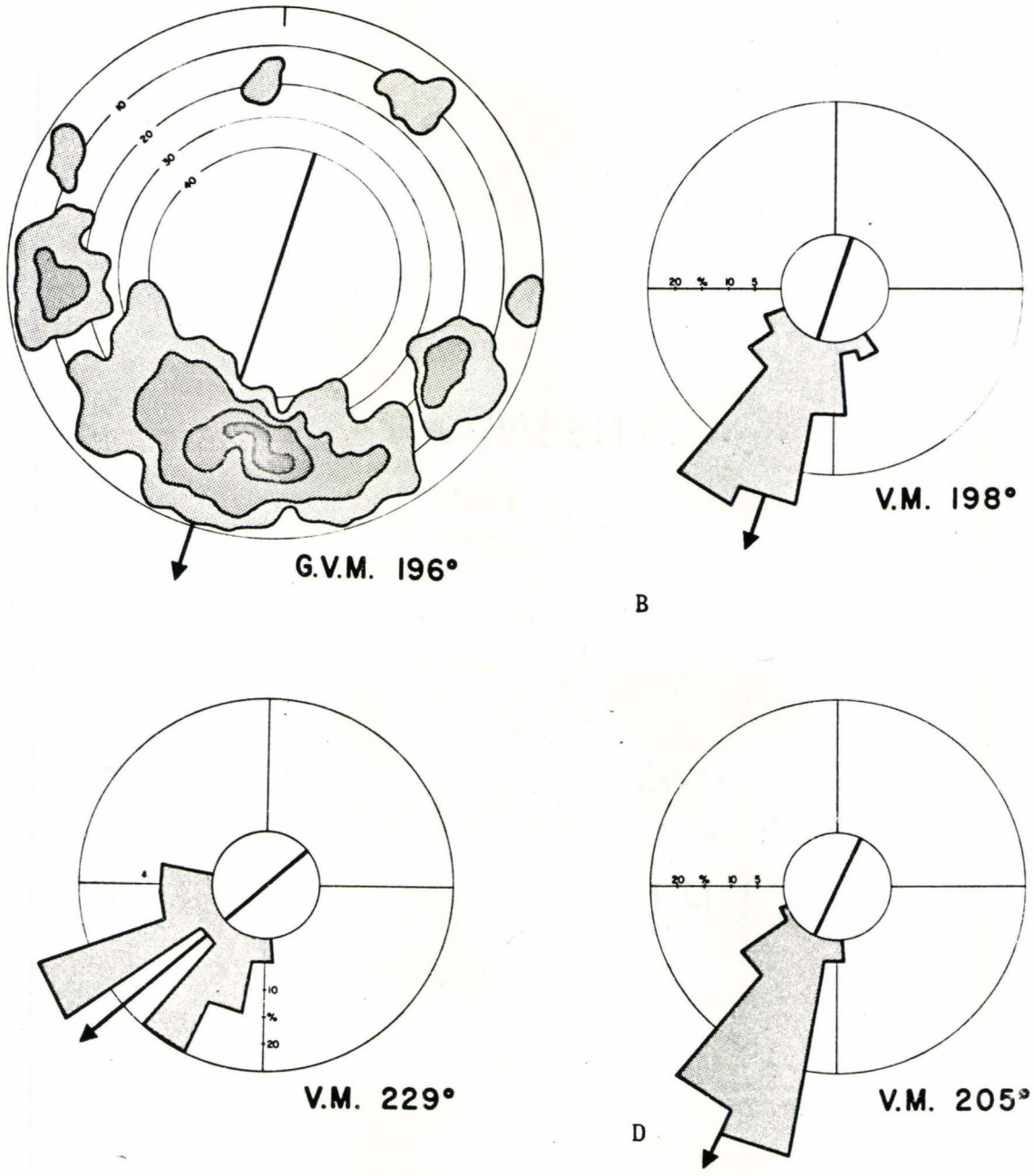

Fig. 29: Palaeocurrents of Shallow Braided Stream Facies.

A. Imbricate gravels

B. Cross-bedded 'bar' gravels

C. Channel-fill cross-beds

D. Cross-bedded sands

Fig. 29 -B).

The cross lamination in the sandy lenses of this facies was measured at 3 sampling sites (48 readings; see table 36 , Appendix C). The palaeocurrent directions obtained range from 153 to 235 degrees. The means of the 3 samples are 193, 200, and 203 degrees; whilst the vector mean of all readings is 198 degrees. (see Fig. 29. D).

The imbrication, gravel foresets and sand lenses all give similar vector mean palaeocurrent directions (196, 198, 205 degrees). The channel infill appears to have a different direction (229 degrees), probably due to the inherited form of the channel.

SHALLOW BRAIDED STREAM FACIES: GRAIN SIZE

The 20 grain size samples and analyses have been divided into the classes outlined above in the palaeocurrent section. Fig. 30 shows cumulative curves and histograms for the grain size distribution of samples selected from each group (see tables 10 to 13 , Appendix B, for data).

The imbricate gravels are bimodally distributed with a gravel mode at -3.0 to -4.0 phi, and a sand mode at 1.0 to 1.5 phi (coarse to medium sand). The means of the 3 samples range from -1.43 to -2.30 phi, and the mean of the 10 largest particles is -5.25 in all three cases (cobbles of Wentworth (1922) scale; see Fig. 11). Standard deviation values of 2.42 to 2.52 denote very poor sorting. These are illustrated by histogram A of Fig. 30.

The tabular cross-bedded gravels (Fig. 30 -B) have a mean grain size ranging from -3.32 to 0.01 phi. The mean of the largest 10 particles varies from -4.0 to -4.75 phi. The gravel modes occur variously at -4.0, -3.5, -2.5 and -2.0 phi, while further modes occur at -1.0, -0.5

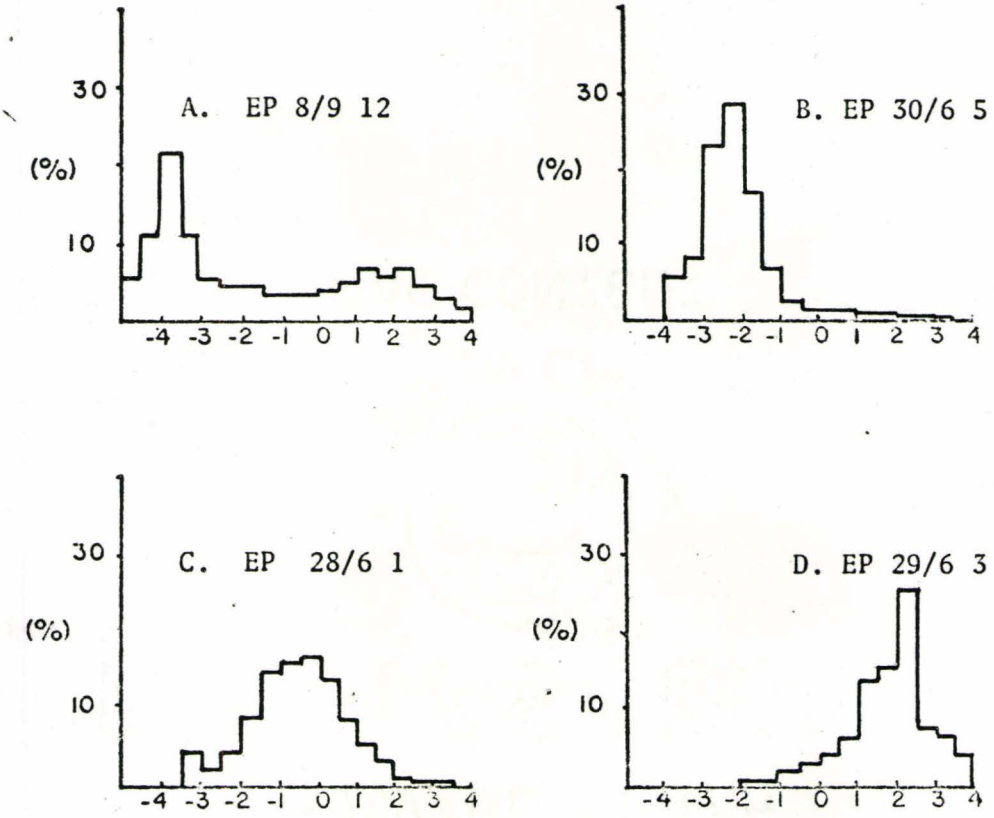

Fig. 30 Histograms of size distribution of Shallow Braided Facies

A. imbricate gravel

B. tabular cross-beds

C. channel infill cross-beds

D. sands

0.5, 1.5 and 2.5 phi, the most common sand mode being at 0.5 (coarse sand). Standard deviation values range from 0.98 to 1.55, and indicate moderate to poor sorting.

The trough cross-bedded deposits of the channel infill (Fig. 30 -C), the lower part of the facies, have a mean grain size between -1.46 and 0.97 phi (very coarse sand/granule gravel boundary). The mean of the 10 largest particles has values from -0.5 to -6.0 (pebbles and cobbles of Wentworth (1935) scale), the largest occurring at the bottom of the sub-unit. There are minor modes in the pebble range but major sand modes occur from very coarse sand to medium sand. Standard deviation values of 1.27 to 1.79 indicate poor sorting.

The sand samples of this facies (Fig. 30-D) have mean grain size values from -0.62 to 2.13 phi (i.e. from very coarse sand to fine sand). Some of the coarser samples have values for the mean of the 10 largest particles of -4.25 and -4.5 phi (pebbles). Standard deviation values of 0.78 to 1.23 indicate moderate to poor sorting.

The skewness values range considerably. The imbricate gravels all have positive skewness and excess fine material, and the channel infill samples are predominantly coarse skewed. The other two groups have no dominance of either. Again the imbricated gravels have low kurtosis values (playkurtic distributions) and high standard deviation values which reflect a history of little effective sorting. For the rest of the samples the distributions vary from platykurtic to very leptokurtic, with a predominance of leptokurtic values.

THE FACIES AT EAST PARIS: INTERPRETATION

At this stage a detailed interpretation of the facies will be made, and it will be related to the sequence of events at East Paris. This account will of necessity include the growth and development of the longitudinal braid bar, so to facilitate the reading a brief summary of the salient features will conclude the chapter.

BASAL GRAVELS

The basal gravels were described earlier as the Bar Core facies and stratigraphic unit 1. They exhibit crude horizontal stratification with moderately well imbricated coarse gravels and various sandy horizons. The direction of palaeoflow inferred from the imbrication data is towards the southeast (140 degrees). Bearing mind that (i) the palaeoflow inferred for unit 2 is predominantly southward or south-southwestward, and that (ii) the contact between the two units is generally erosional, it is concluded that there is no direct or intimate relationship between them. The stratigraphic units 1, 2 and 3 need not necessarily be part of a single fining-upwards sequence.

Consequently the basal gravels (unit 1) must be interpreted on their own merits since their context is obscurred by the erosional contact above. The horizontal stratification and the well-developed imbrication both suggest that the deposits are waterlain. Their coarse grain size and overall position in the stratigraphic sequence suggest an ice-proximal position in the outwash system. It is probable that these gravels were deposited by the initial meltwater run-off in the form of repeated sheet floods. Certainly the crude horizontal stratification and thick sequence of predominantly well imbricated gravels

which are exhibited, and the absence of any large or medium scale channelling at the exposed sections, could be explained by this hypothesis. (Bull, 1968 and 1972).

The basal gravels exhibit none of the features, except imbrication, held to be characteristic of shallow braided stream deposition, such as tabular cross-bedded gravels, and trough cross-bedded sands in frequent channel forms (Waechter, 1970; Smith, 1972, and personal communication). It is quite possible that major channelized flow occurred elsewhere on the outwash plain and that these gravels represent the overbank sheet flood deposits of a deep-channel braided system.

EROSION OF THE BASAL GRAVELS

The interpretation of the erosional history of the basal gravels, and of the contact between units 1 and 2, rests on the palaeocurrent data derived from the two units. There are 3 sets of significant data (see Fig. 31):

(i) The flow direction of the current depositing unit 1 was southeastward (140 degrees)

(ii) The flow directions given by Side Channel sand body at the downstream end of the Bar Core and the reworked Bar Core top surface were towards the southwest quadrant (205 and 255 degrees; and 249 degrees)

(iii) The flow direction given by the Bar Front, Stoss-Side and Bar Top deposits of the longitudinal bar were towards the south (177, 182 and 179 degrees).

The data are interpreted as follows. An initial period of repeated sheet flooding developed by a southeastward flowing current produced a flat

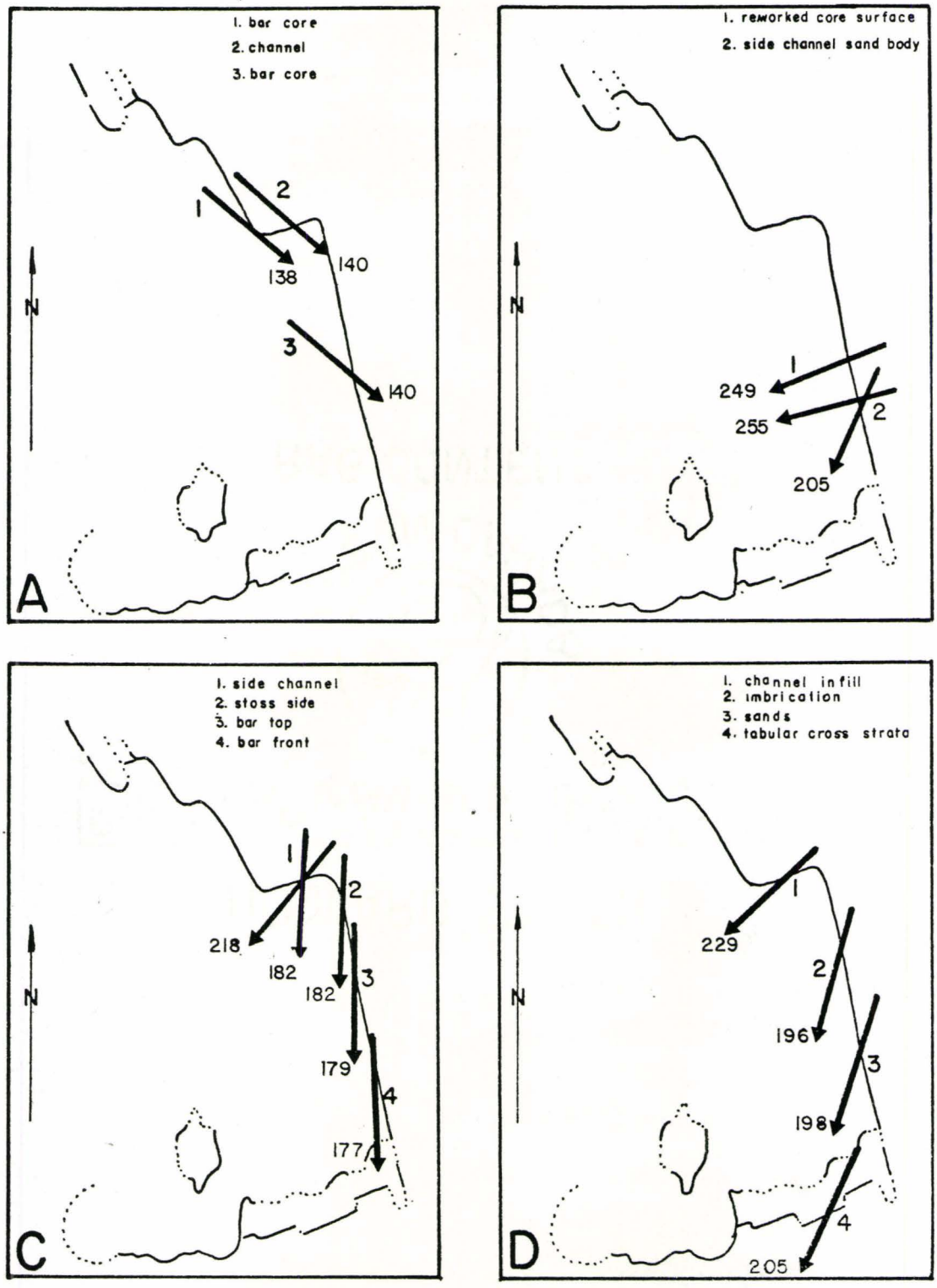

Fig. 31: The palaeocurrent at East Paris.

A. unit 1 deposition

B. unit 1 incision

C. unit 2 bar progradation and aggradation

D. unit 3 aggradation

surface of gravels with thin sandy patches . This flat surface was dissected by a subsequent flow toward the south, producing remnant topographic highs, the major channel forms and the erosional contact. This second period of activity was erosional rather than aggradational, therefore there was probably relatively little sediment input into the system at this time. It is suggested that this imposition of a new flow direction is the consequence of a major "switching" of the braided channel system from another part of the outwash plain, an hypothesis which would explain the different palaeocurrent directions obtained from the unit 1 basal gravels and the deposits of unit 2.

The apparently anomalous palaeocurrent directions to the southwest (see (ii) above) are interpreted as diagonal flows within the southward flowing channel system. These deposited sand around the angled downstream end of the bar core to initiate growth of the bar form, and flowed over the topographic high of the bar core gravels reworking the top surface. This type of diagonal flow is well documented in the literature (Hjulstrom, 1952; and Krigstrom, 1962), and there is no need to invoke a separate and intermediate period of flow towards the southwest to account for these local palaeocurrents.

This interpretation suggests that the channels in the new system were first transporting only sand and were partially sand plugged, and that the newly formed bar cores began to grow downstream by sand addition.

BAR FRONT GROWTH

For the major part of the bar front growth the channel system was capable of transporting gravel, but of preserving it only on the bar forms. The Bar Front growth is in the form of large scale coarse gravel

cross strata, periodically interrupted by lower angle planes termed reactivation surfaces, which have associated sands in dune forms on them. This series of sedimentary structures is interpreted in terms of flow stage fluctuations (see Fig. 32). The cross beds are the product of high flow conditions, the reactivation surfaces are the product of low stage conditions, and the upstream moving dune sands are the product of the rising flow stage. The low stage activity had to be of sufficient intensity and duration to round off these large scale cross-strata, and then to sweep sands onto the resultant reactivation surfaces at the rising stage. The Bar Top was exposed for a period equal to the time taken to produce each reactivation surface, that is the low flow stage.

The fact that some of the groups of foresets (a group comprises the foresets between two successive reactivation surfaces) can be traced upstream into Bar Top deposits, means that some vertical aggradation must have taken place during bar front progradation. Conversely, the fact that most of the groups of cross-strata do not pass upstream into Bar Top deposits, means that most of the time any gravel was moved right across the bar top and over the bar front.

STOSS-SIDE ADDITION

The stoss side facies has been shown to consist of a series of coarsening-upwards units. These have tabular cross-bedded sets of sands and granule gravels at the base, becoming more pebbly upwards, and passing into imbricated coarse gravels, which are topped off by a cobble lag. These parts can be 2.5 m and 1.5 m respectively at maximum, but in successive coarsening upwards sequences either can be very thin or non-existent.

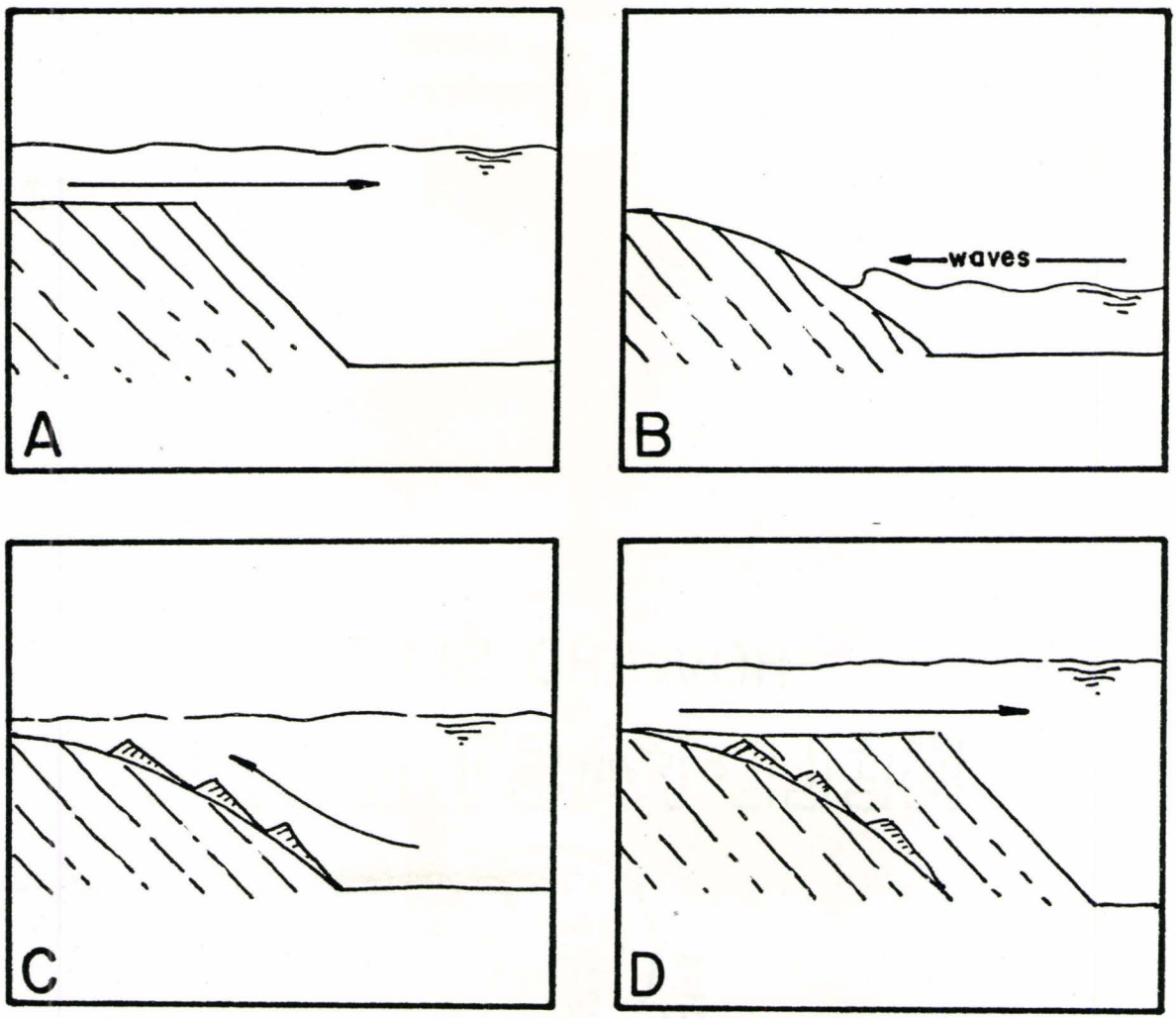

Fig. 32 Flow stage fluctuations after their effects on the Bar Front Facies

A High Stage
B Low Stage
C Rising Stage
D Subsequent High Stage

The parts of these coarsening upwards units are also related to stage changes in the interpretation placed on them. The sandy tabular cross bedding represents low flow stage, the increasing pebble content represents the rising stage, and the coarse imbricate gravel bed represents the high flow stage. The cobble lag when present is the product of the falling stage.

However, it is doubtful that one coarsening-upwards sequence is related to a single cycle of fluctuation in the stages of flow. Indeed, because of their thickness, and the smaller number of these stage change sequences than at the Bar Front, it is suggested that they may reflect either (i) isolated and unusual events at the ice front as opposed to seasonal events for the bar front reactivation, or (ii) incomplete records of several periods of stoss-side aggradation in any one coarsening upwards sequence. The first of these alternatives implies a very rapid aggradation, while the second implies intermittent aggradation alternating with through-flow and/or removal of sediment from the stoss side.

SEDIMENT TRANSPORT THROUGH THE SYSTEM

As has already been noted the paleocurrents of both the Bar Front and Stoss side facies agree closely (177 and 182 degrees respectively), and neither can be considered without reference to the Bar Top facies (palaeo-current 179 degrees). It is difficult to deduce the relationships between the three parts, but it can be reasonably concluded that they are not completely synchronous. For example, the initial, large progradational phase of the bar front cross strata (see Fig. 18) cannot be related to a similar large aggradational deposit at the stoss-side, or on the bar top.

Indeed it is impossible to equate the whole bar front sequence with comparable deposits of the other facies.

The interpretation placed on these various parts in such that the cross-strata and reactivation surfaces at the Bar Front probably represent a more or less complete sequence of the progradational events, but that stoss-side and bar top deposits are an incomplete record of their respective aggradation. In the case of the stoss-side the deposits may even represent isolated and abnormal events at the ice front, such as jokulhlaups or glacier bursts (Rist, 1955). This is unlikely, however, since such events would affect the whole of the sandur plain and would not just be reflected in any one facies.

In any event it seems likely that the gravel supplied to the bar front must have come from the stoss-side, passing through the bar top, into the avalanche face cross strata, and there stored before removal of some of it to supply the next bar downstream.

In channels adjacent to the bar core, bar front, stoss-side, and bar top facies there was more or less continuous movement of sand through the system. These sediments represent the bed load of the channels in the form of large dunes with scalloped fronts, preceded by ellipsoidal scours (the trough cross-bedding ; Harms and Fahnestock, 1965; McGowan and Garner, 1970), and channel side ripples (the ripple drift cross-lamination) oblique to the main current (182 degrees). A feature of considerable importance in these channels is the interfingering of the gravel units of the bar form, especially the stoss-side (location (3), Fig. 8 ; and F of photolog). Here a wedge of gravel extends from the adjacent bar form and pinches out on the flank of the channel. The lack of any gravel in the base of the channel system except on the gently sloping flanks (less than 10 degrees)

of the channels is important for the interpretation. Two possible situations could have existed:

1) The gravel formed a continuous lag right across the channel at periods of flow when the stream was not competent to move it. Subsequently the gravel was flushed out of the channel bed at periods of flow of higher competence. If this were so, channel gravel lags would be preserved in the deposits, and such is not the case.

2) The gravel moved through the system exclusively as bar-forming material, passing across intermediate levels in the channel from bar form to bar form, and never in the main channels. This would appear to be the case, but the hydrodynamic conditions for this situation are difficult to envisage.

Similar situations to the latter ((2) above) have been reported in the literature. Leopold and Wolman (1957, p. 47) state that " the band of principal bed load transport lies on top of the submerged central bar. The grain movement in the deeper parts of the channel adjacent was negligible in the early stage of island development. The central bar continued to build closer to the water surface yet the principal zone of movement remained for a time along the top of the building bar"

It seems likely that gravel movement occurred only at high stages of flow when the bar form was covered. The coarse gravels therefore moved in shallow flow across the bar top where the imbricate gravels with their associated thin sand bodies, are interpreted as thin sheets of gravel bedload material with shallow depressions anastomosing across the surface. The facies is thought to be so thin vertically as to preclude the formation of cross-strata in the gravels. The flanks of

the bars were not steep enough for gravity rolling to be sufficiently active, so that the gravels never rolled or moved completely into the channels and the interdigitations of gravel and sand were produced.

At this point it is instructive to make a comparison with the Donjek River, in the Yukon (Williams and Rust, 1969). The four levels of channel and bar-island forms reported by Williams and Rust, attest to the rivers' degradational history, and the existence of the gravel bars as erosional remnants. This is to be contrasted with outwash at East Paris where, after the initial downcutting of the post unit 1 period, the bars were active during channel sand movement, as is shown by the interfingering relationships.

Another problem in the reconstruction of the outwash conditions and the movement of sediment, is that of the movement of gravel from one bar form to the next. Can cobbles get from one bar front avalanche face to another bar via a deeper part of the channel system at high flow, or do they have to wait and be transported at falling or low stage? The nature of the bar front foresets suggests that the material is buried rapidly and that little or no wholesale movement of gravel takes place in the channel at high flow stage. However the suggestion of Leopold, Wolman and Miller (1964, p. 285) that "when mixed with smaller material larger grains may be moved under flow conditions incapable of transporting them when concentrated with grains of a similar size", means that individual large particles could move in the channel system.

Hence it is possible that the gravel moves from bar to bar mixed with finer material, not in the deepest parts of the system, but from bar front to succeeding bar stoss-side via an area of intermediate depth. The intensity of the low stage activity in the model has to be sufficient

to reduce the avalanche face to a lower angle reactivation surface, and it is probable that this intensity of activity is also capable of moving gravel in the system between the bars. Further it is likely that sand and gravel moves together at this time in the form of stoss-side dunes, and then at high stage the sand is winnowed out and swept onward while the gravel remains as imbricate bed load on the stoss-side and bar top.

SIDE CHANNEL INFILLING

The deposition of unit 2 must have ended with a waning of flow depositing only sand, because the final deposit of the major side channel is the top most part of an overall fining upwards sequence in the channel. It seems probable that the gravel supply or movement temporarily ceased for this period, beginning again with the deposition of stratigraphic unit 3. Initially the reoccurrence of the gravel as bed load material in the system served to infill the remnant topography of unit 2 as the flow was probably confined to the channel forms. This was described earlier as the lower part of the shallow braided stream facies. The infilling of the stream topography left the sandur plain area again as a flat surface on which the shallow braided facies developed.

SHALLOW BRAIDED STREAM

The facies derives its name from the upper part, the major portion, which completes the exposed products of sedimentation at the East Paris Pit. There are several sedimentary structures which lead to the interpretation of unit 3 as the product of a shallow braided stream environment.

(i) sets of tabular cross bedded gravels 25 to 40 cms thick, which are thought to represent the bar progradation.

(ii) imbricate gravels, often located immediately above the bars and interpreted as the bar top supply to the avalanche face of (i) above.

(iii) adjacent sandy channel like forms, up to 1.5m deep, with trough-cross bedding and other structures similar to those of the smaller channels in unit 2.

The question of the origin and development of braid bars of this scale is not satisfactorily answered. Nowhere in these deposits was there observed a "bar core" comparable to that of unit 2 bars, from which the small (25 to 40 cm) bars could have prograded. It seems likely that several phenomena are capable of inducing braid bar growth. In one instance a small bar formed downstream of a large boulder 52 cm in diameter. In another case in similar facies in a pit near Galt, the tabular cross-bedding and imbricate gravel supply was seen to develop downstream of what was interpreted as a frozen mass of boulders, sand and silt (possibly a till block), 2m across. However, these are the exception rather than the rule, and little conclusive evidence for any are mechanism of shallow braid bar initiation was found.

The whole outwash period represented here apparently ended with a further period of waning currents and the deposition of sandy material as the last phase of sedimentation.

SUMMARY OF THE LONGITUDINAL BRAID BAR 'MODEL'

(1) The bars are developed from topographic highs produced by the erosion of a flat outwash plain surface.

(2) Initial growth of the bar forms on these "cores" (the topographic highs) is in the form of sand addition at the downstream end.

(3) Major bar growth occurs at both the upstream and downstream ends and on top of the bar form over the whole period, but the addition of material to these parts is not synchronised. The Bar Front cross-strata, reactivation surfaces and associated sands are a more or less complete record of progradation and stage changes, whereas the other two facies display a somewhat incomplete record of all the events.

(4) Gravel movement in the system occurs over the bar surface from the stoss-side, through the bar top to the bar front, while sand moves in the channels. A satisfactory hydrodynamic explanation for this situation has not been established.

(5) Gravel movement between bars is in the form of mixed sand and gravel dunes of the stoss-side facies.

(6) Side channel sediment transport is in the form of sand dunes with scalloped fronts proceded by ellipsoidal scours, and channel-edge ripples oblique to the main channel direction.

CHAPTER SEVEN

THE FACIES AT WEST PARIS

CHAPTER SEVEN

THE FACIES AT WEST PARIS

The West Paris Pit was studied with the data and interpretation of East Paris in mind, as a test for the model proposed. Major differences were observed between the two pits, particularly the sandier nature of the West Paris system, and a divergence of the palaeocurrents both in direction and variability. However, underlying similarities were noticed especially with reference to the geometry and downstream growth of bars. A complete comparison of the two systems will be given in chapter eight as a concluding synthesis.

The facies defined at West Paris are:-

The Bar Front facies

The lateral accretion facies, and

The Side Channel facies.

All of these are part of the equivalent of stratigraphic unit 2 at East Paris. As has already been noted, there is an underlying basal gravel on top of a clay till, and these may be the equivalents of unit 1 and the underlying till at East Paris.

THE BAR FRONT FACIES: OCCURRENCE

The exposures of this facies occur from the mid-point of the embayment between locations 5/5′ and 6/6′ (see pit map; Fig. 33), northeastwards to beyond location 4′. This facies was only exposed north of location 4 on the face first examined in 1970. From the mid-points of the successive embayments to locations 5 and 5′ the facies is seen in

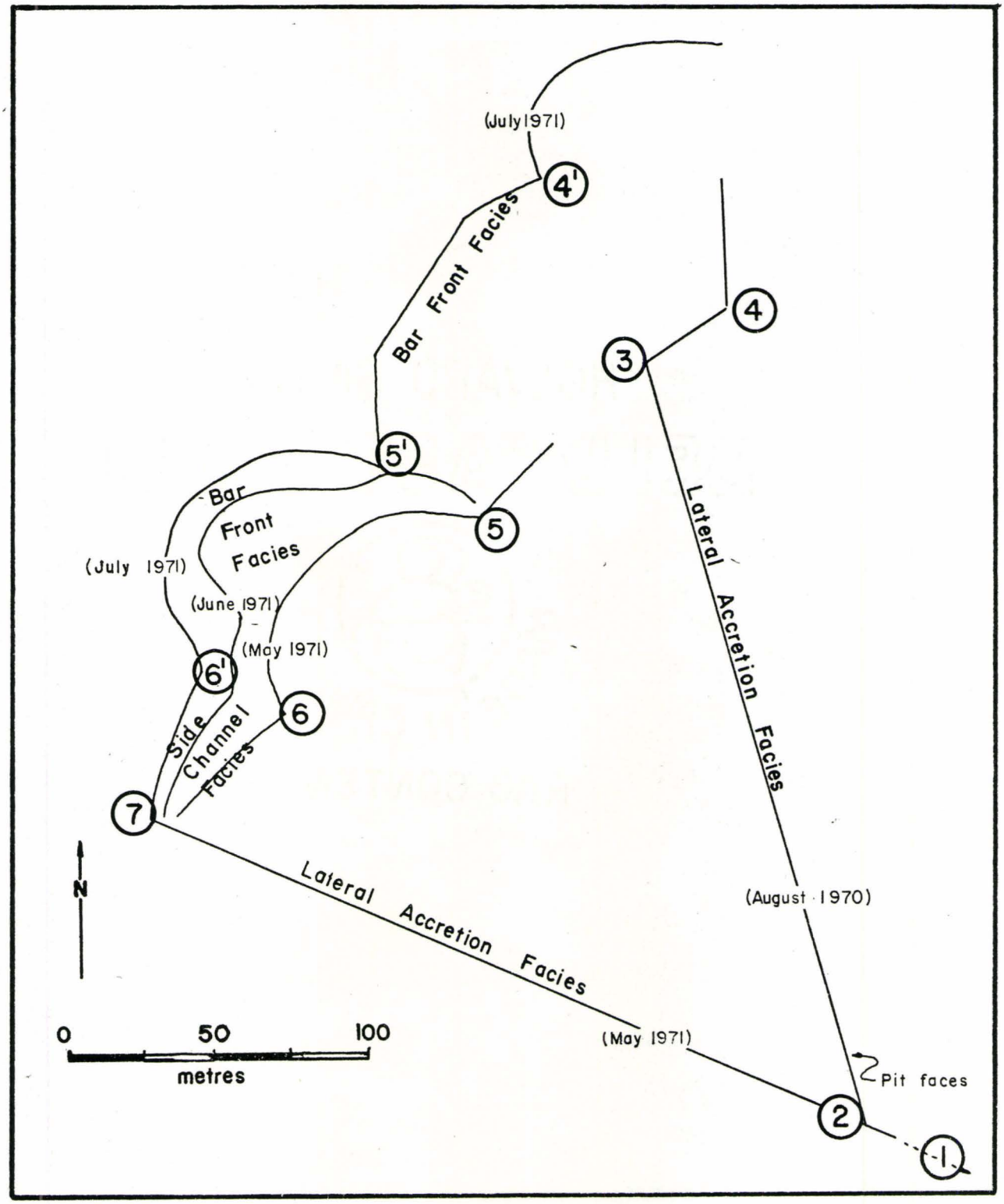

Fig. 33: Map of the West Paris Pit indicating positions of facies exposures and location numbers used in the text.

longitudinal section slightly oblique to the inferred overall palaeocurrent direction of west-southwest. From location 5' to 4' the face gives a transverse view of the facies, though not exactly perpendicular to the flow direction. These two types of faces enable a three-dimensional reconstruction of the facies.

Laterally adjacent, to the southwest (from (6) and (6') to beyond (7)), the side channel facies was exposed. The passage into this facies is via a narrow transition sub-facies (see lateral accretion facies below). In the upstream direction the lateral accretion facies was exposed in the wall from locations (2) to (3), but nowhere was the junction between these two facies seen.

The bar front facies is 4 to 5m thick, and underlain by a coarse gravel deposit which has thin sandy lenses. The underlying gravel goes down below pit base level for an indeterminate depth; though probably not more than a few metres because Hewitt and Karrow, 1967 report that a 'clay till' lies below the gravel and produces a water table which is at pit base level. The clay till was not exposed at West Paris.

BAR FRONT FACIES: SEDIMENTARY STRUCTURES

The facies has four constituent parts:-

i) Thick units of imbricate course gravels,

ii) Large-scale cross bedded, coarse gravels,

iii) Cross-bedded, coarse gravels as minor bars,and

iv) Downstream-dipping sand beds, here termed 'sand drapes'.

These subdivisions of this facies can be seen in the line-drawing of the facies, Fig. 34.

i) The imbricated gravel units range from 30 cm to 150 cm in thickness and are upto 35m long. Two of these can be seen directly above

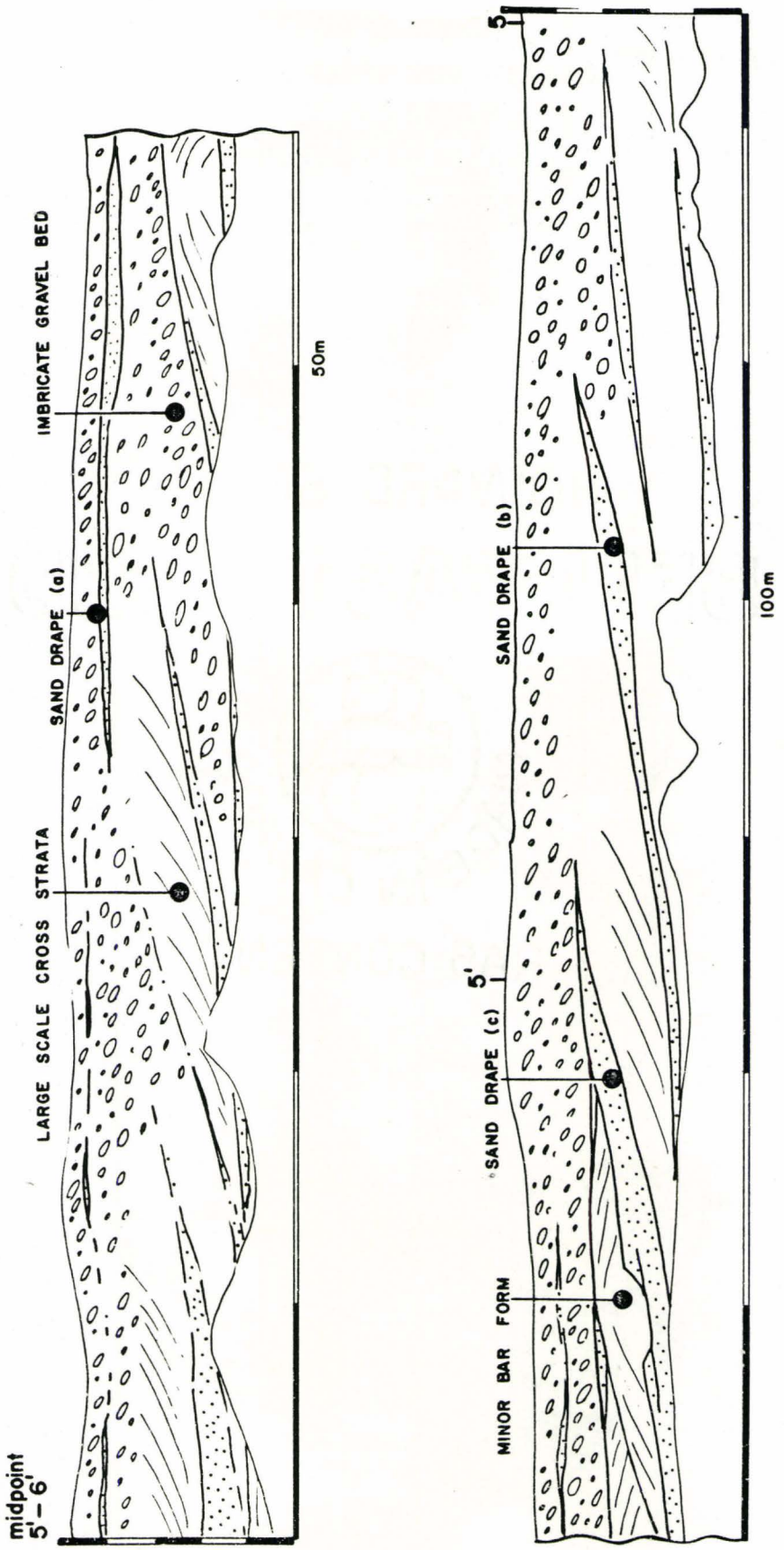

Fig. 34: The advancing Bar Front facies and its component parts.

P and above the sand lens at Q on the photolog. The gravel units are only poorly imbricated for the most part, although isolated patches have well-developed imbrication. In both the examples cited the imbricate unit is horizontal and near the top of the facies at its upstream end, passing downstream and down slope over a subjacent sand drape. In one case the unit develops into large scale cross-bedding downstream, while in the other the imbrication persists down to the toe of the sand drape (left of P), where both the gravel and the sand approach the horizontal again.

This latter imbricate unit was measured at 3 sampling sites. (see table 37, Appendix C). The angle of dip of the pebbles and cobbles, with reference to the horizontal, ranged from 5 to 44 degrees, from 6 to 39 degrees, and from 10 to 43 degrees. The mean dips were 22, 24 and 22 degrees respectively, and are comparable to those measured at East Paris. The samples have a closer agreement of dip angles when the angle of dip of the base of the unit is taken into account. The imbricate bed from which the measurements were taken has an inclination of 5-6 degrees at its steepest, levelling out upwards to the horizontal uppermost portion. Where the dip is 5-6 degrees the imbrication mean angle (with reference to the horizontal) is 22 degrees. When the substrate dips at 2-3 degrees the imbrication mean angle is 24 degrees, and on the horizontal part the imbrication mean angle is 27 degrees. Allowing for the dip of the substrate, and rotating around to the horizontal, all 3 samples have mean angles of imbrication relative to the base of the bed at 26-28 degrees.

The contact with the other parts of the facies are variable. Already noted is the downstream gradation of one imbricate unit into large-scale cross-bedding. The contact with the underlying sand drapes is commonly

sharp and erosional. In one case (see P of photolog), the contact is knife edge sharp. Pebbles and cobbles of the gravel bed rest directly on a sand bed which has parallel lamination and very little disturbance of the contact is to be seen. One or two of the larger gravel particles (approximately 8-15 cm in diameter) project slightly below what is otherwise a perfectly straight contact with no intermixing of the two deposits. On close examination the parallel lamination of the sands was seen to be slightly disturbed in places but the contact was preserved These disturbances took the form of tiny (less than 2 cm) flame structures on the flanks of the downward projecting cobbles.

The imbricate gravels can be succeeded immediately by another sand drape, in which case the contact can be either sharp or gradational, or by the large-scale cross-bedded gravels, in which case the contact is invariably gradational.

ii) The large-scale cross-bedded, coarse gravels occur in units up to 2m thick, and persist downstream for up to 25m. Two examples of this structure can be seen at N and O on the photolog, and the structure also occurs north eastwards of location 4 (see Fig. 33). The cross-bedding is recognisable by two features; firstly a grain size segregation of the foresets whereby open work gravels alternate with relatively pebble-and cobble free laminations; and, secondly, the orientation of the discoid pebbles dipping downstream in the plane of the foreset slope of a heterogeneous gravel. Examples are shown adjacent to N on the photolog.

The foresets are concave upwards, being truncated at the top and asymptotic at the toe, in the case of the grain-size-segregation cross-beds; but are generally more planar where they are composed of heterogeneous gravel.

The foresets were measured at six sampling sites, (165 readings

see table 38 , Appendix C), the total range of dip angles was 3 to 48 degrees, and the mean angle of dip of the samples ranged from 21 to 28 degrees.

The foresets commonly overlie and pass upstream into one of the imbricate coarse-gravel beds, both contacts being gradational. Where the foresets are underlain by a sand drape the contact is usually quite sharp and erosional. Vertically the foresets may be succeeded by either a sand drape which is usually dipping downstream, or by an imbricate gravel which may be either horizontal or dipping downstream. In both cases the contact is usually erosional but not always sharp because there is some reworking of the tops of the foresets.

iii) Cross bedded coarse gravels also occur as minor topographic highs on the advancing bar front. Two examples can be seen at R and S on the photolog. Both types of cross-bedding referred to earlier are exhibited, but the size-segregated foresets are more common. These structures appear as small (140 cm high at maximum) domed structure resting on a sand drape. The foresets dip outwards from the centre in both cases at angles ranging from 7 to 44 degrees, with means of 24 degrees. The direction of advance of the bars was found by bisecting the bimodal distribution obtained from measuring each flank of the structures (see Fig. 38 C and D) giving palaeocurrent directions of 196 degrees and 317 degrees. The shape of these topographic highs can only be guessed at, but it seems likely that they are lobate.

Both examples rest on a sand drape with a knife edge sharp contact between the units. Both are succeeded by a sand drape, but this has been eroded in places by an imbricate gravel unit which now rests on the minor bars.

iv) The sand drapes or their eroded remnants occur more or less regularly throughout the exposures of the bar front facies. At least 7 occur from location 5, through location 5, to the midpoint of the embayment (see Fig. 34). The upstream end of each longitudinally exposed sand drape is almost always truncated by the succeeding gravel unit, whether it is cross-bedded or imbricated. The latter is more commonly associated with this erosion. The downstream end of each sand drape is invariably asymptotic.

These sand bodies range from few centimetres in thickness where they have been severely eroded by the succeeding gravel unit, to 150 cm in thickness where the minor topographic highs have afforded some protection. (see S on photolog). A whole range of sedimentary structures indicative of varying flow regimes and sediment supply conditions occur within the sand bodies. These are:-

Planar laminated sands, with and without pebbles;

small-scale ripple cross-laminated sands and silts;

ripple-drift cross-laminated sands and silts;

medium scale cross-laminated sands;

trough cross-laminated sands and granule gravels;

wavy laminated sandy silts; and

thin single-layer pebble horizons.

These structures and features will be described in the context of the sand drapes in which they occur.

Three sand drapes will be detailed here and in later sections:

a. A horizontal sand layer (see Q on photolog);

b. A sand drape in traverse section (see V and several metres below X on photolog), and

c. A longitudinal section through a downstream dipping sand drape (see below R and S on photolog).

a) This sandy layer has a maximum thickness of 35 cm and a total exposed length of 35m along the pit face, though it is not continuous for this distance. It consists of two parts, a lower section of ripple drift cross laminated sands and an upper part of medium scale cross-bedded sands with pebbles, separated by a thin pebble and cobble layer. The contact of this sand layer variously with the large scale cross-bedded gravel and the imbricate gravel below is fairly sharp, with a few centimetres of sand infiltration into the gravel, filling in the void spaces and sealing off the gravel against further sand infiltration. The ripple drifted portion of the sand layer is upto 15 cm thick and is composed of type A ripple drift, of Jopling and Walker (1968), in fine sand (sample WP 2/9-2). The angle of climb varied only slightly and was estimated to be 8-10 degrees. The medium scale cross-bedded part is up to 20 cms thick, and composed of medium sand, with granules and small pebbles occurring on the foreset slopes. The foresets themselves are low angle and asymptotic. The unconsolidated nature of the deposit made measurement difficult, but the angle of dip of the foresets slopes was estimated to be between 10 and 20 degrees.

b) The sand drape seen in transverse section has two types of sedimentary structures. Firstly, the lower part is composed of trough cross-bedded sands with occasional granules, and is from 30 to 90 cms in thickness. This passes gradationally into various types of ripple-drift cross-lamination in fine sands and silts, varying from 30 to 60 cm in thickness. Fig. 35 shows a vertical measured section through this sand drape. The trough cross-bedded lower part thins in a southerly direction

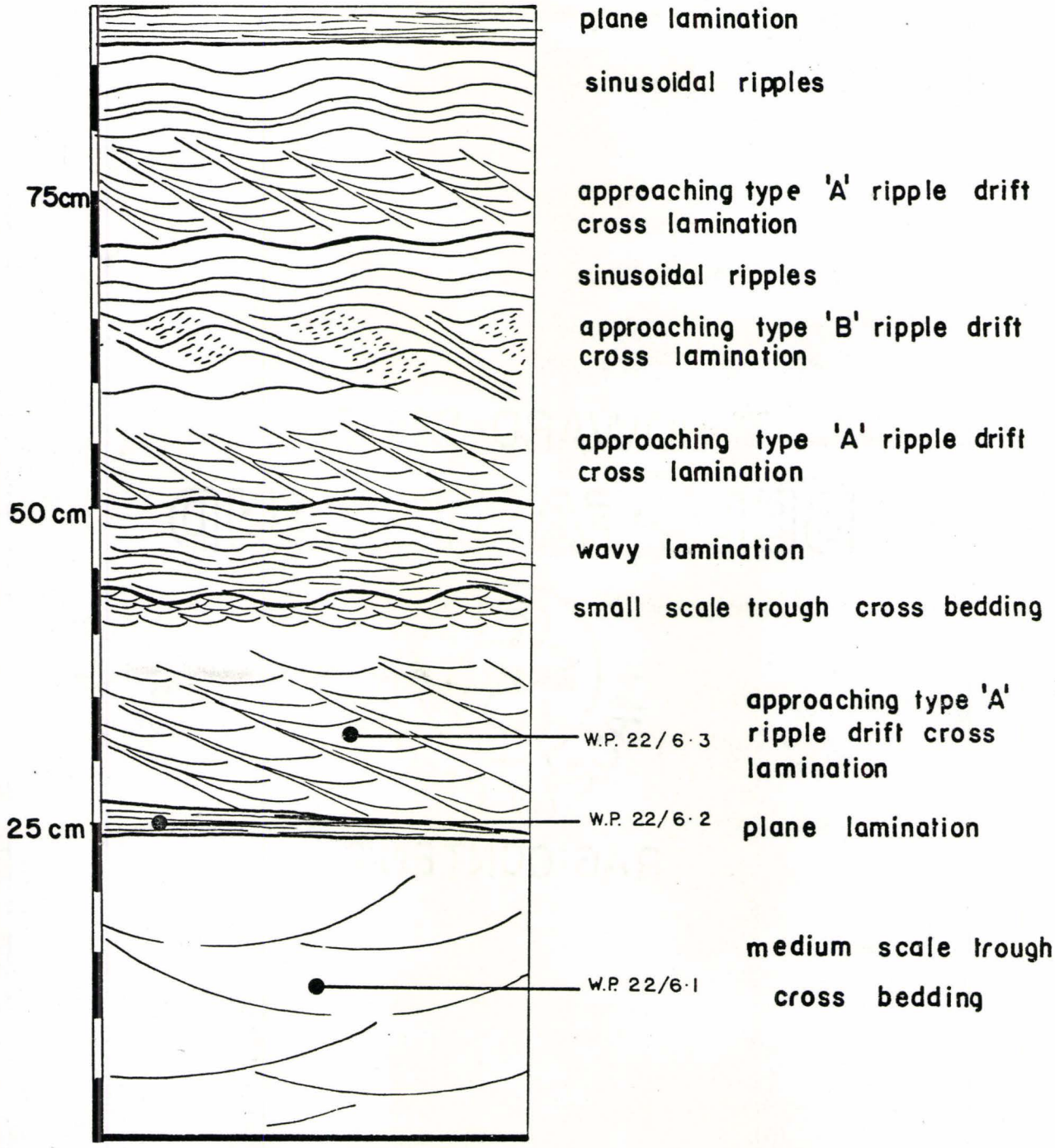

Fig 35 Measured section through sand drape (b)
(Sample numbers refer to Fig. 37 (b))
(Ripple drift cross lamination types after Jopling and Walker, 1968)

and is eroded away completely by a succeeding sand body in one place. The ripple drifted upper portion dips gently to the south testifying to a slightly oblique transverse section, and is finally truncated by the gravel initiation of the same succeeding sand body.

c. This sand drape was the thickest observed reaching 150 cms at one position, and extending along the pit face far over 30m. Two parts were again noticed. The lower part (see Fig. 36) was coarser grained and consisted of a thick unit (upto 60 cms) of trough cross-bedded coarse to medium sands passing into small scale trough cross-bedding, and finally into a unit of wavy lamination and/or sinusoidal rippling. Thus the whole of the lower part fined upwards. The upper portion began with an erosional contact overlain by small scale trough cross-bedded sands. Ripple drift cross-lamination followed, which climbed both upstream and downstream, and passed upwards into small scale trough cross bedding again. The sequence was finished by wavy to planar laminated sands and silts, again an overall fining upwards.

Not all of the sand drapes were composite in nature as the 3 described. One of two of the thinner ones (less than 20 cms), were comprised totally of planar lamination, usually with pebbles associated with the laminae. However, a more complex composition was the general rule.

An important feature seen in the face from (5') to (4') is the channel-like form at X on the photolog. Features such as these were commonly observed, and were normally 4 to 9m wide and up to 1m deep. The structures exhibited in these sands were planar lamination, rippling, and medium scale cross-bedding. The planar lamination was the most abundant. The significance of these sand bodies is discussed at the end of the chapter.

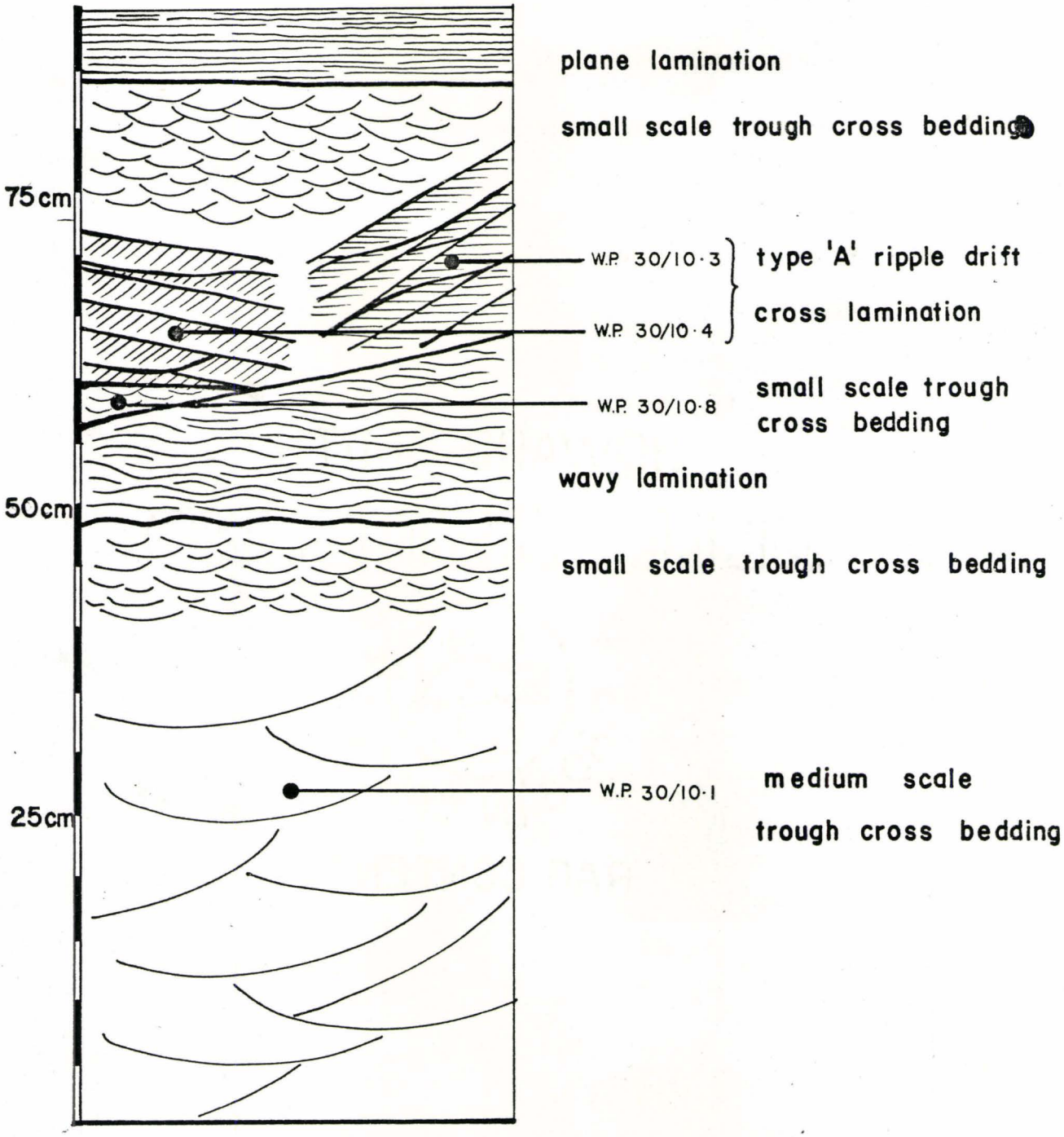

Fig. 36 Measured section through sand drape (c)
(Sample numbers refer to Fig. 39 (c))
(Ripple drift cross lamination types after Jopling and Walker, 1968)

BAR FRONT FACIES: PALAEOCURRENTS

Palaeocurrent data is available from 4 types of features; the cross-bedded gravels, the minor bars, the imbricate gravels and the sand drapes. Fig. 37 shows rose diagrams or stereoplots for the first 3 of these. It is immediately obvious that the palaeocurrents are more variable here than in the East Paris Pit. The overall direction of advance, indicated by the foresets, is westwards; the minor bars pass obliquely across the bar front face north westwards and south-southwestwards; and the imbricate gravel supply gives a southwesterly direction, surprisingly diverging from the foresets.

The data for the cross-beds was obtained from 6 sampling sites (165 readings: see table 38 , Appendix C), 4 taken in one cross-bedded unit and 2 in another. There was a total range of directions from 170 to 084 degrees. The mean directions ranged from 246 to 320 degrees, and the grand vector mean was 274 degrees.

The imbricate gravels were sampled at 3 sites (85 readings; see table 37, Appendix C) , all in the one bed above P on the photolog. The total range of inferred palaeoflow directions was 122 to 349 degrees, but the means of the samples occurred at 242, 242, and 206 degrees.

Both minor bars were sampled, with 28 readings taken on each (see table 37 , Appendix C). The ranges were 208 to 087 degrees, and 103 to 279 degrees, with vector means of 317 and 196 degrees respectively. The bimodality displayed by the rose diagram is probably a function of the sampling procedure whereby the apparent cross-strata on the flanks of the structure were measured, but the central area was omitted.

The palaeocurrent data for the sand drapes are given in tables 40, 41 and 42 (Appendix C), and are illustrated in Fig. 38. For sand drape (a)

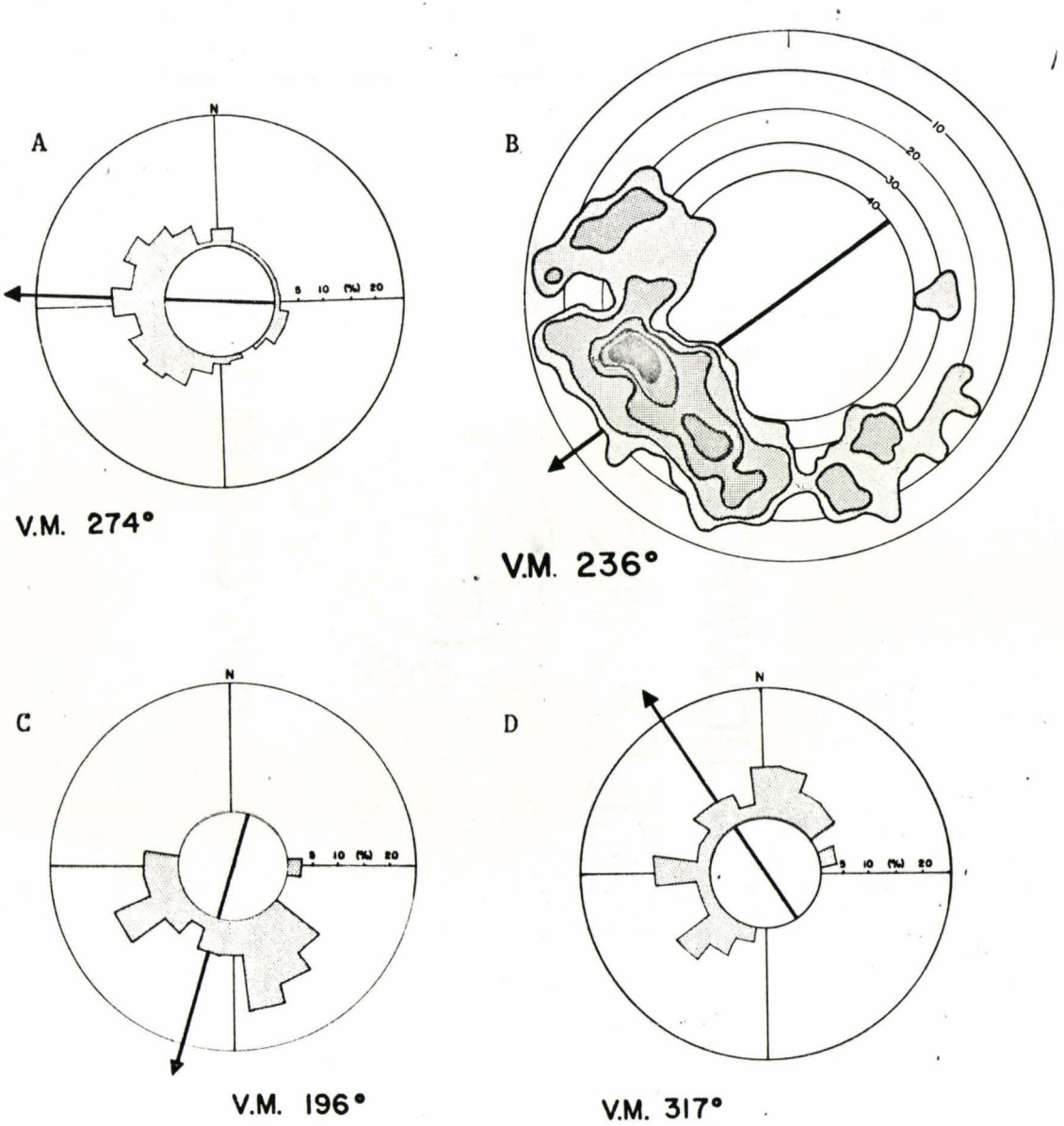

Fig. 37: Palaeocurrents of the Bar Front Facies

A. Cross-strata B. Imbricate gravels

C. Minor topographic high at R on photolog. D. Minor topographic high at S on photolog

5 sampling sites were selected and a total of 62 readings taken. Fig. 38 A shows the resulting rose diagram. The modal class marked (i) represents the readings taken in the ripple drift cross-lamination in the lower half of the drape, and (ii) represents the readings taken from the medium scale cross-bedding in the upper half of the drape. Fig 38 B shows the plot of 60 readings taken at 7 sampling sites in sand drape (B). The mode at (i) represents the predominant ripple drift cross lamination palaeocurrent direction, and the mode marked (ii) represents the thin layer of small scale trough cross lamination (see 40 cm mark on Fig. 35.). Fig. 40 C shows the plotted data for sand drape C. Four modes are visible. At (i) the mode represents the reattachment part of the current over the crest of the bar, producing ripple drift cross-lamination (approx 70 cms, left hand side of Fig. 36). Mode (ii) represents the counter current eddy also producing ripple drift cross-lamination (approx. 70 cms; right hand side Fig. 36). Mode (iii) represents the major transverse current parallel to the bar front found by measuring ripple cross-lamination, and mode (iv) its complementary minor transverse current.

Fig. 38 D is a rose diagram showing the total 225 readings plotting together. The same four modes evident in Fig. 38 C, are still apparent, but the dominance of the major transverse current, and the over-bar flow is clearly demonstrated.

BAR FRONT FACIES: GRAIN SIZE DATA

Tables 14 - 18 (Appendix C) contain the grain size data for the foreset groups; imbricate gravels and the sand drapes. Fig. 39 displays cumulative curves of some representative samples. Both the cross-bedded gravels

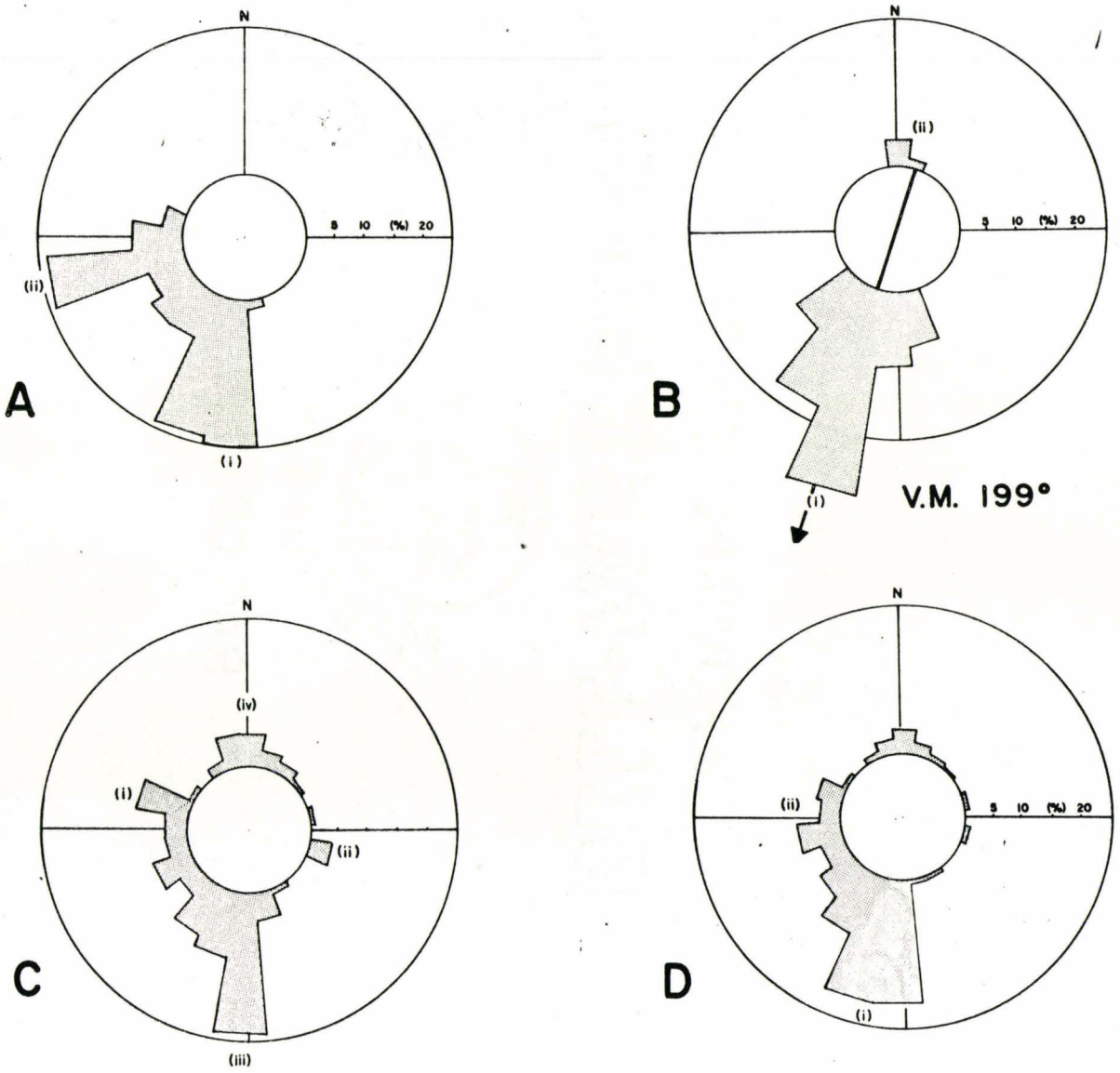

Fig. 38: Palaeocurrents of the sand drapes of the Bar Front facies at West Paris

A. sand drape (a)

B. sand drape (b)

C. sand drape (c)

D. A, B and C combined

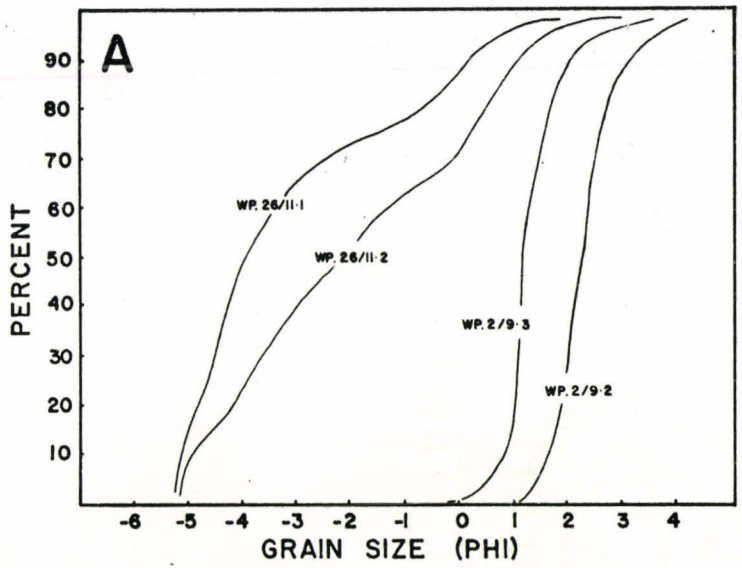

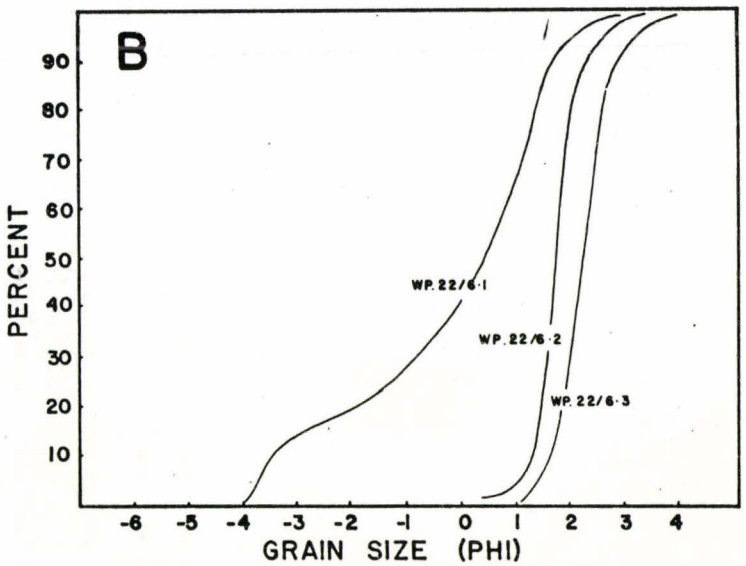

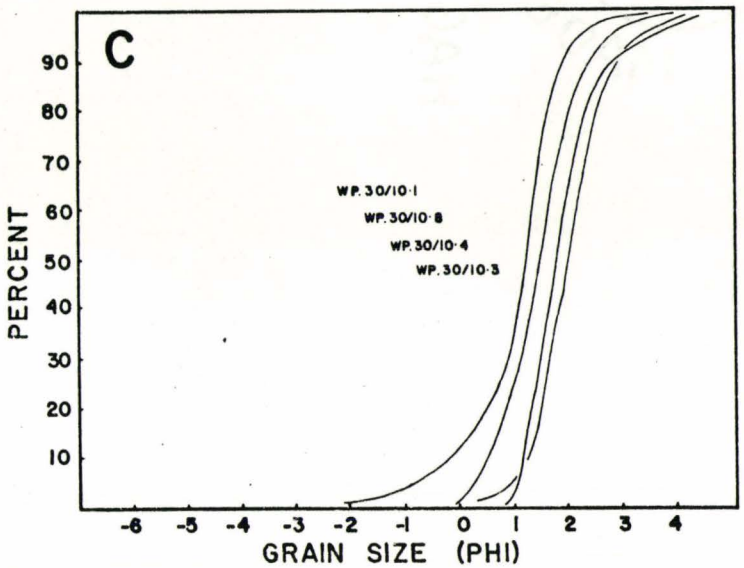

Fig. 39: Cumulative Curves (arithmetic ordinate) of the grain size distributions of samples from the Bar Front facies at West Paris.

A. finer samples from sand drape (a)

WP26/11.2 from imbricate gravels

WP26/11.1 from cross-bedded gravels

B. sand drape (b)

C. sand drape (c)

(Fig. 39 A), have a mean grain size of -3.0 phi and a standard deviation value of 2.1 indicative of poor sorting. Modes occur at -4.0, -2.0 and 0.0 to 0.5 phi in the two samples. The mean of the largest grains is -6.25 and -6.75 phi. Skewness values are 0.49 and 0.52, indicating an asymmetry towards the fine end of the distribution.

The imbricated gravels (Fig. 39 A), have mean grain sizes of -1.96 and -2.19 phi, and standard deviation values of 2.2 and 2.1. Again the high values of standard deviation indicate very poor sorting. Modes occur at -4.0, -2.5 and 0.5, and at -4.0, -2.5 and 0.5 in the two samples. Skewness values of 0.11 and 0.16 indicate near symmetry in the distributions.

Samples from the individual sand drapes detailed above are shown separately in Fig. 39 A, B and C. In total the sediments of these sand bodies range in mean grain size from -0.3 (very coarse sand) to 3.59 phi (very fine sand) and also into the silt size range. Standard deviation values fall in the range from 0.48 to 1.91, with a predominance of values in Folk's "moderately well sorted" and "moderately sorted" classes. Skewness values range from -.39 to 0.52, most falling in the "near-symmetrical" class. Kurtosis values fall in the mesokurtic and leptokurtic classes predominantly.

The mean of the ten largest grains can be as high as -5.0 phi where pebbles occur in the deposit, but can be 2.25 phi in fine, well-sorted sands.

LATERAL ACCRETION FACIES: OCCURRENCE

This has been designated a separate facies because of its distinctive characteristics. There are long low-angle surfaces in the direction of the main stream (approximately west-northwestward), which are marked by thin sandy horizons or a change in the type of sedimentary structure within

the gravels. This is a distinctive facies and, whilst not occurring at East Paris, it has been noted elsewhere in the overall outwash system (Flintkote Co. of Canada Pit No. 27 , Appendix A).

The lateral accretion facies at West Paris comprised almost all of the exposed pit face in 1970 (from (1), through (2) to (3); Fig. 34); and almost the whole of the face from (2) to (7) in 1971. Near location (7) the facies passes laterally into the side channel facies via a transition sub-facies. Despite the fact that the bar front facies was exposed north of location (4), nowhere was the junction between the lateral accretion facies and the bar front facies seen. A pit road had been constructed at this point in 1971, and by the 1972 field season any trace of a contact has been removed completely.

The lateral accretion facies is approximately 6m thick, and apparently underlain by the same coarse gravels and clay till that was associated with the bar front facies.

LATERAL ACCRETION FACIES: STRATIFICATION AND SEDIMENTARY STRUCTURES

The first strip of the West Paris pit photolog gives a good indication of this facies. The apparent dip of the long low angle features was 5 to 7 degrees, and they are asymptotic at the base, at the same hight above pit base level as the sand drapes of the bar front facies. However, there is much less sand in this facies than in the bar front facies, and the heterogeneous nature of the gravels gives an altogether less organised appearance.

The gravels exhibit 2 types of structures or fabrics. There are poorly-to moderately-imbricated beds and poorly-to moderately-cross stratified beds. The sands exhibit planar lamination and medium-scale cross bedding.

The fabric of the imbricated gravels (see F on photolog), was sampled at 7 sites, and the 2 samples with a moderately imbricated fabric were found to differ in inferred palaeocurrent direction from the other 5 samples which were only poorly imbricated (see below). The angle of dip did not differ noticeably, however, the means of all 7 samples falling in the range 18 to 24 degrees. The total range for all 185 readings was 3 to 55 degrees.

The cross-bedded gravels, were measured at 2 sites (50 readings; see table 45 , Appendix C). The mean angle of dip of the foresets was 25 and 21 degrees, with ranges of 8 to 46 and 5 to 29 respectively. These foresets ranged from well-developed structures with a small amount of grain size segregation on the foreset slopes, to poorly developed structures in a heterogeneous gravel indicated only by the orientation of the discoid pebbles and cobbles. The various states of the development of the cross bedding are shown by location C, D and E on the photolog. Cross-bedding also occurs in the transition sub-facies which marks the passage into the side-channel facies. Here the range of dips (for 25 readings) is only 9-31 degrees, with a mean dip angle of the foresets of 19 degrees.

The sands in the lateral accretion facies are either parallel and planar laminated, or medium scale cross-bedded. The foresets had a range of dip angles from 21 to 32 degrees, and a mean of 27 degrees, (15 readings; see sample DW 27, table 47 , Appendix C). Pebble clusters on the planar laminations also occurred. (see side-channel facies East Paris, above; and side channel facies West Paris, below).

LATERAL ACCRETION FACIES: FABRICS AND PALAEOCURRENTS

Palaeocurrent data is available from 4 of the sedimentary structures

described: the imbrication, the large scale cross-stratification; the medium-scale cross-stratification and the transition sub-facies cross-strata. Fig. 40 A and B shows the imbrication. As previously mentioned there are two separate palaeocurrent directions indicated by this fabric and they have been plotted separately in the figure. They are plotted separately because they come from different parts of the pit face between (2) and (7), and because they produce a definite bimodality when plotted together. The two modes of the distributions can be seen better when plotted separately. Fig. 40-A represents 5 samples (135 readings) with vector mean directions of 180, 180, 185, 188 and 209; and Fig. 40-B shows 2 samples (50 readings) with vector mean directions of 247 and 248. Those samples with a south-southwest palaeocurrent direction were located in the bottom 2m of the face and from location 2 to mid-way along the southern face (see Fig. 33). The other two samples are from the top half and the western end of the same face. The significance of the two palaeoflow directions is discussed at the end of the chapter.

The large scale cross-stratification in the gravels was measured at two sites (50 readings; see table 45, Appendix C), and the data are plotted in Fig. 41-A. A wide spread of the data and directions is clearly indicated with two modes at approximately 265 to 280 and 325 to 340 degrees. The vector mean and inferred palaeocurrent direction for the cross-strata is 317 degrees.

The interbedded sand and gravel cross-stratification of the transition sub-facies has a similar pattern, Fig. 41-B shows the 25 readings (see table 46, Appendix C) plotted on a rose diagram. The modes occur again, this time at 265 to 280 and 340 to 355 degrees. The

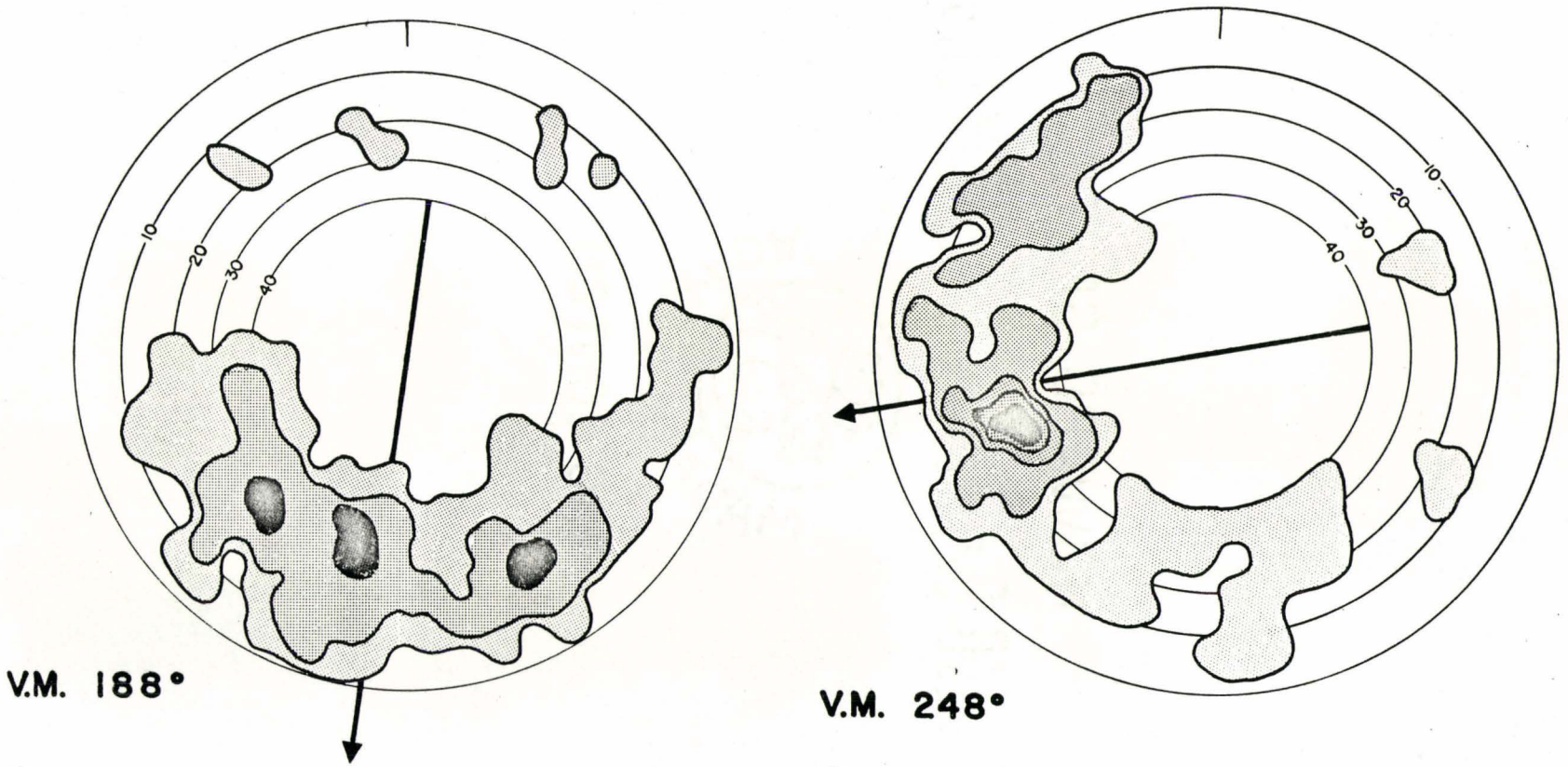

Fig. 40: Palaeocurrents of the Lateral Accretion Facies imbricate gravels

A. Samples F9, F11, F12, F13, F14 and F20

B. Samples F10 and F17.

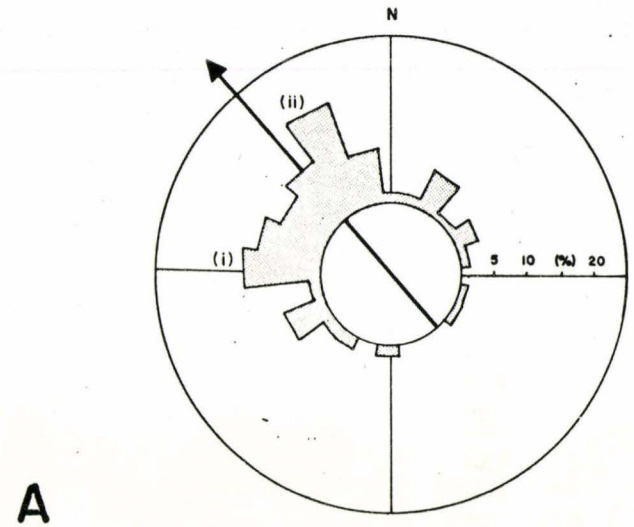

A

V.M. 317°

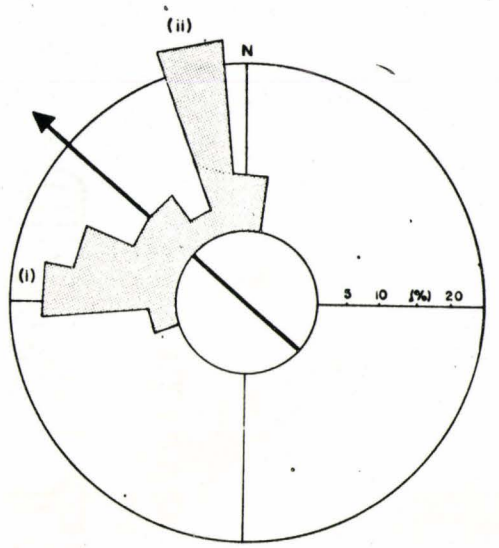

B

V.M. 311°

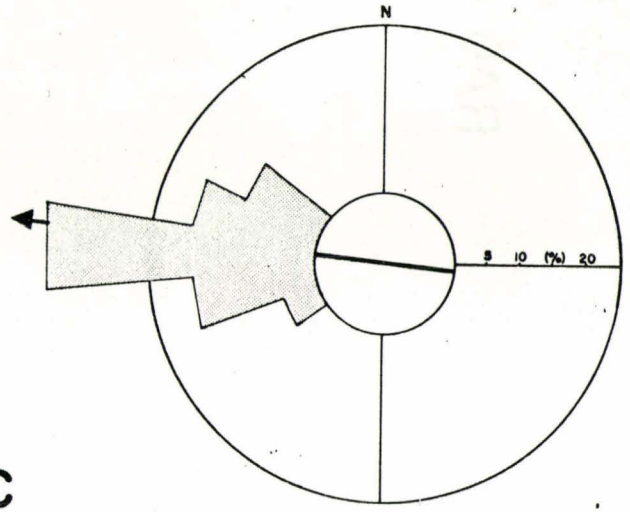

C

V.M. 276°

Fig. 41: Palaeocurrents of the lateral Accretion facies at West Paris.

A. large scale gravel cross-beds

B. transition sub-facies

C. medium scale cross-bedded sands

vector mean and inferred palaeocurrent direction in this case is 311 degrees. The significance of the two modes in both these structures will be discussed at the end of the chapter.

The sands of the lateral accretion facies have medium scale cross-bedding shown in Fig. 41-C (15 readings; table 47 , Appendix C). The distribution is unimodal, and the inferred palaeocurrent direction is 276 degrees, almost due westwards.

LATERAL ACCRETION FACIES: GRAIN SIZE

The grain size data for this facies are given in tables 19, 20 and 21 (Appendix C), and are shown by selected examples in Fig. 42.

The two types of gravels described previously (cross-bedded and imbricated), show very little difference in grain size parameters and data, and are thus shown in the same table and the same diagram (Fig. 42-A). The gravels range in mean grain size from -0.6 to 3.0 phi (very coarse sand to pebbles), and have standard deviation values from 1.646 to 2.702 indicating poor to very poor sorting. This is also reflected in the predominantly bimodal or even polymodal nature of the distributions of the samples and the kurtosis values from 0.52 to 1.13 (very platykurtic to mesokurtic). The modes are spread throughout the gravel sizes with a large number in the -4.0 to -5.5 phi range. The major sand mode falls in the range from 0.5 to 1.5 phi. Two-thirds of the samples are fine- or strongly fine-skewed, and the other one-third is coarse- or strongly coarse skewed.

The transition sub-facies with its interbedded sands and gravels in cross-bedded deposits was sampled in two places. Fig. 42-B shows both samples plotted, and indicates the bimodal nature of the gravel member.

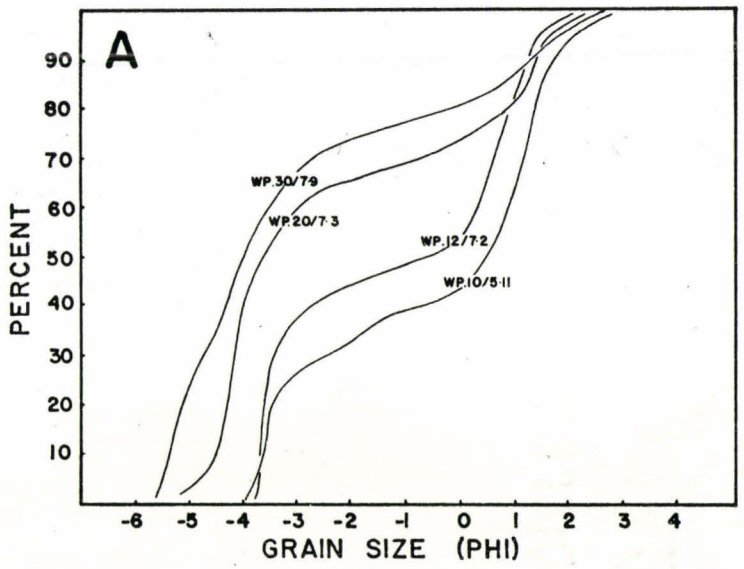

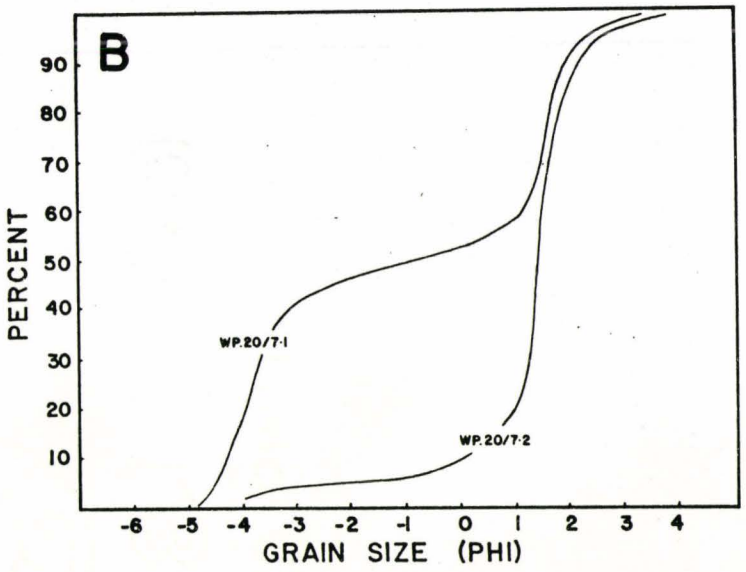

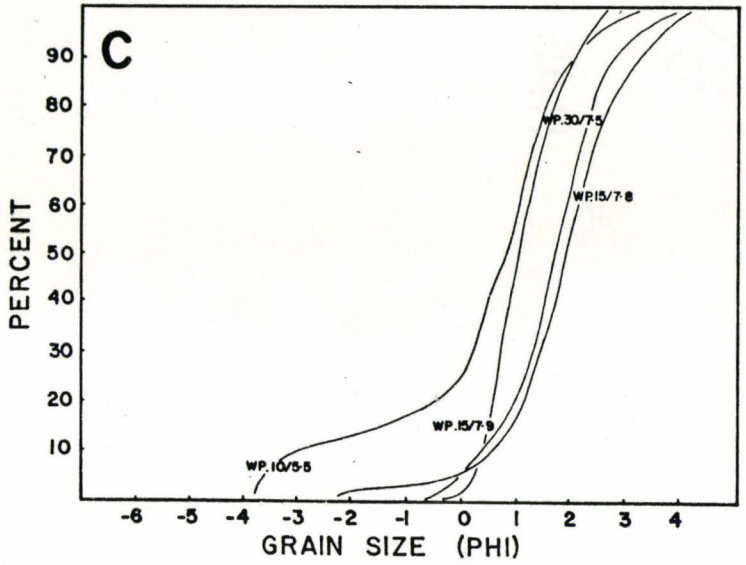

Fig. 42: Cumulative curves (arithmetic ordinate) of the grain size distributions of samples from the Lateral Accretion facies.

A. cross-bedded gravels (WP30/7.9 and WP12/7.2) imbricate gravels (WP20/7.3 and WP10/5.11)

B. transition sub-facies

C. sands

The sand member bears a close resemblance to the sands of the facies (see Fig. 42-C). In the transition sub-facies the mean grain size is from 1.34 and -1.05 phi, the gravel modes occurs at -4.0 phi, and both sand modes occur at 1.5 phi. The standard deviation value for the gravel is 2.60 indicating very poor sorting, and for the sand is 1.21 indicating poor-sorting respectively. The skewness values indicate excess coarse material or near symmetry in the distributions.

The sands of the lateral accretion facies (see table 21, Appendix B), are illustrated in Fig. 42-C. Their mean grain sizes range from 0.33 to 1.95 phi, and the standard deviation values fall in the range from 0.587 to 1.733 (moderately well-to poorly-sorted). The samples are predominantly unimodal, and all the sand modes fall in the range 1.0 to 2.5 phi (medium to fine sand). One sample has a gravel mode at -2.5. Kurtosis values indicate distributions which are mesokurtic to leptokurtic, reflecting the unimodal character of the samples.

SIDE CHANNEL FACIES: OCCURRENCE.

Sufficient similarity was seen between these dominantly sandy exposures in trough-like depressions here at West Paris and the smaller side channels at East Paris to give the facies the same name. The facies occurs at only one place at West Paris, where a series of channel forms comprise a complex of dominantly sandy trough-like infills. This complex is situated from a position just to the east of location 7, through to locations 6 and 6'. The second strip of the photolog gives a good representation of this facies. Laterally to the south and east the facies passes into the lateral accretion facies; and laterally to the

north into the bar front facies via a transition similar to the one described above (see page 113). The facies is underlain by the same gravel deposit outcrop of 'clay till' as underlies the bar front and lateral accretion facies. Vertically the channel deposits pass directly into top soil.

SIDE CHANNEL FACIES: SEDIMENTARY STRUCTURES

Medium scale cross-bedding occurs and commonly takes the form of dunes, which can be seen climbing up the stoss-side of the previous dunes at the base of the channel form marked by K on the photolog. These dunes are upto 30 cms thick and pass across the complete width of exposure of the channel form.

The dunes pass vertically into rippling and ripple drift cross lamination which is the predominant structure of the facies. At one point (K on photolog) the ripple drift cross lamination is 2m thick and consists of alternations, type A, type B, and sinusoidal ripples (of Jopling and Walker, 1968) although no pattern to the alternations could be observed.

Planar and low-angle cross-lamination occurs throughout the facies, normally in association with the gravels. Consequently pebbles and pebble clusters occur which are similar to those described in the side-channel facies at East Paris (see Pages 68-69).

The gravel associated with the side channel facies can be seen as interfingering beds of gravel upto 45 cm thick. These normally thin towards the centre of the channel form but occasionally pass right across the channel as a pebble/cobble lag. These gravels bear a close

resemblance (see below) to the gravels of the transition sub-facies found on either side (previously described above).

The side channel complex can be simplified into a number of distinct channel forms (see Fig. 43), indicating that the channellized flow was confined to a limited area between the lateral accretion facies and the bar front facies during aggradation.

SIDE CHANNEL FACIES: PALAEOCURRENTS

The pebble clusters found in the planar laminated sands provide only a crude palaeocurrent indicator. However, the ripple drift cross-lamination and the medium-scale cross bedding provide quantitative data (see Fig. 44; and tables 48-49 , Appendix C). It is quite clear (Fig. 44-A) that the ripple drift cross-lamination has two modes, with two directions of flow indicated. The mode marked (i) on the diagram is close to the direction given for both modes (ii) of Fig. 44 A and B is the lateral accretion facies. Similarly the mode marked (ii) of the ripple drift cross-lamination is close to the mode for the imbrication shown in Fig. 44-A of the lateral accretion facies, and the south-southwestly modes of the 3 sand drapes detailed (Fig. 44 A, B and C) in the bar front facies. The vector mean of the 20 readings comprising mode (i) in 325 degrees, and the vector mean of the other 20 readings for mode (ii) is200 degrees.

The medium-scale cross-bedding was measured at two locations (30 readings), and a vector mean of 253 degrees was obtained. This coincides approximately with the bisector of the two modes for the ripple drift cross-lamination (253 vs 264 degrees).

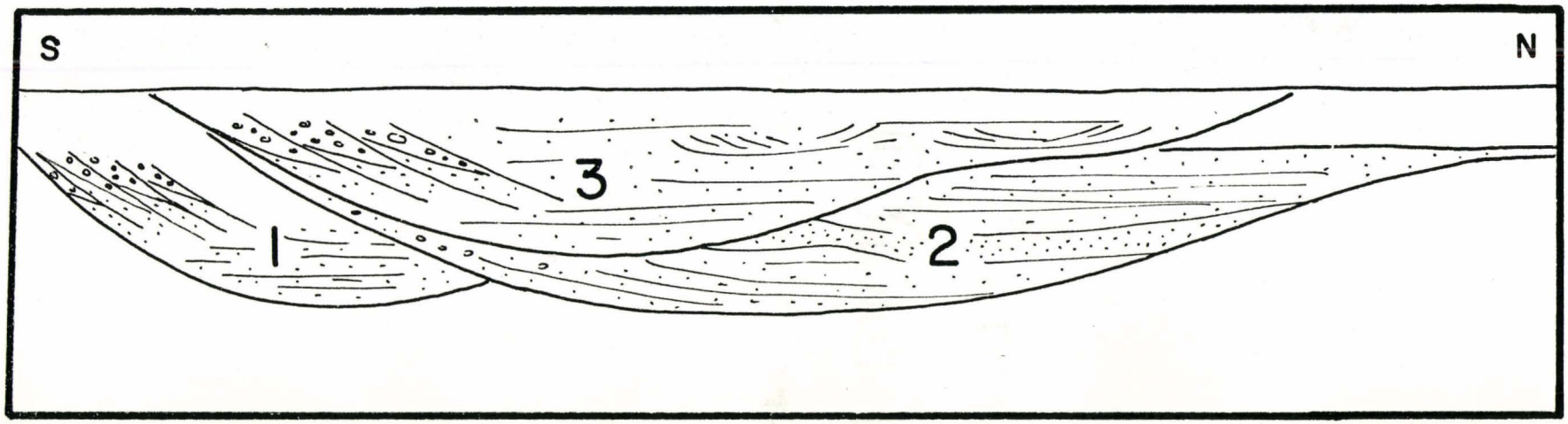

Fig. 43 The channel complex of the Side Channel Facies at West Paris (Note: width of outcrop 120m; depth of channel complex 4m)

Comparison of gravels of Side-channel and transition sub-facies

	mean	st. dev.	skew.	kurt.	median	c(phi.1)
WP 20/7.1	-1.05	2.60	-0.17	0.55	-0.66	-5.25
WP 30/7.7B	-0.33	2.45	-0.65	0.54	1.04	-5.5

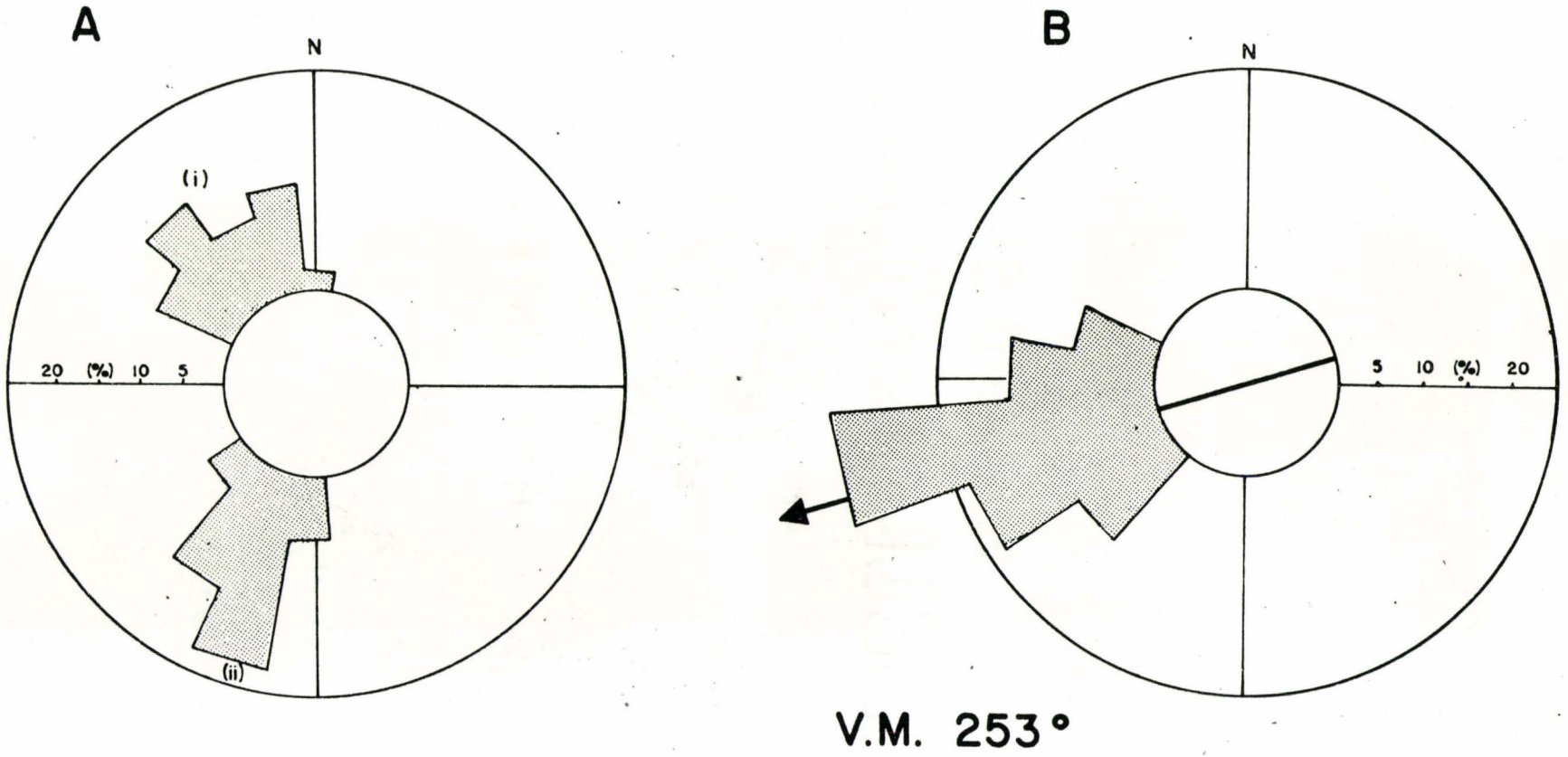

Fig. 44 Palaeocurrents of the side channel facies at West Paris.

A. ripple drift cross-lamination

B. medium scale cross-bedded sands

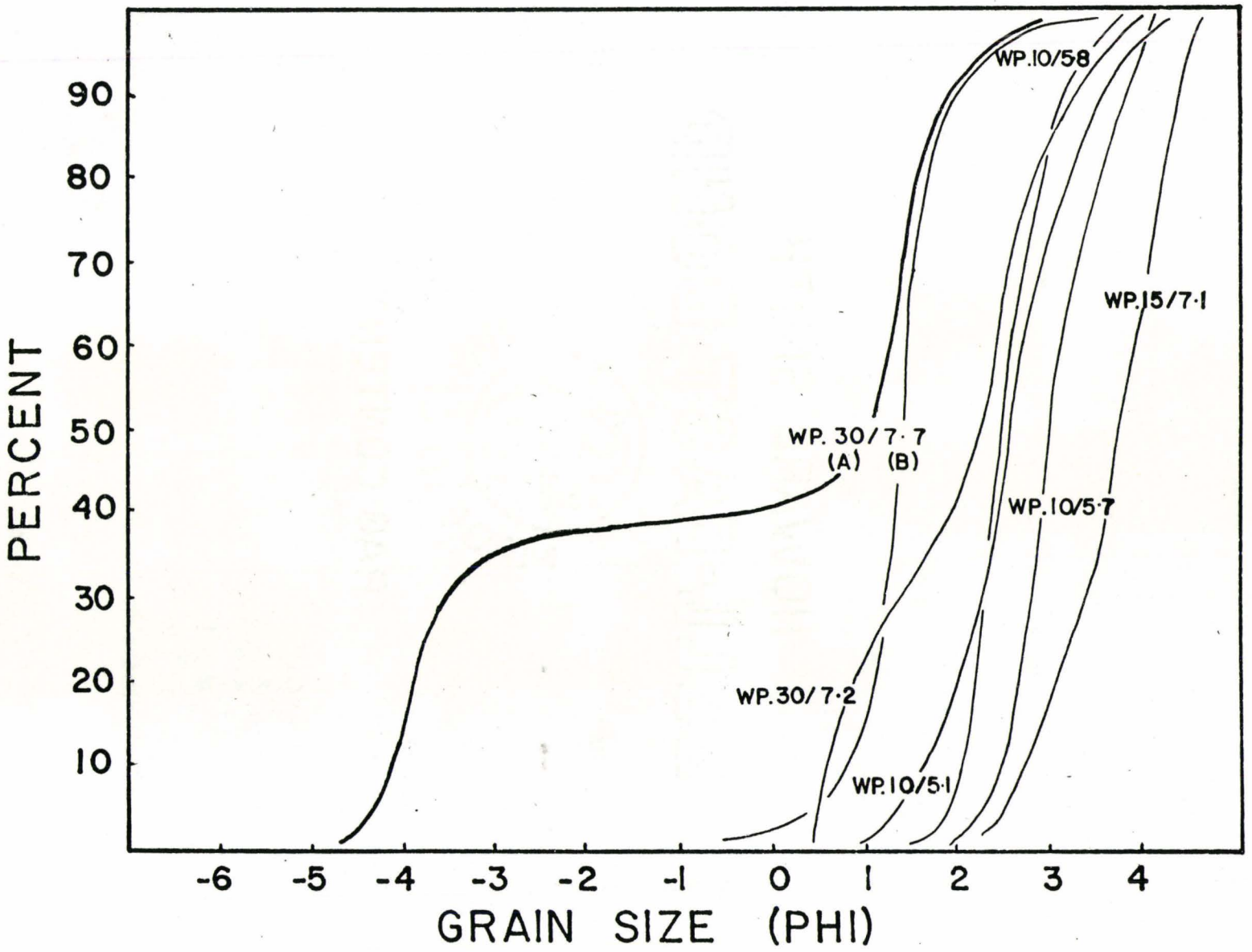

Fig. 45: Cumulative Curves (arithmetic ordinate) of the grain size distributions of selected samples from the side-channel facies at West Paris.

SIDE CHANNEL FACIES: GRAIN SIZE

A total of 14 samples (see table 22 , Appendix B) were analysed from this facies. The mean grain sizes ranged from -0.33 to 3.64 phi, and standard deviation values were predominantly in the moderately well sorted to moderately sorted classes (0.46 to 1.045, with one value at 2.45). The skewness values were predominantly in the near-symmetrical/fine-skewed classes, with the one gravel sample strongly coarse-skewed. The kurtosis values ranged from 0.54 to 1.61 and were predominantly mesokurtic to leptokurtic. The distributions were practically all unimodal with the mode in the fine and very fine - sand classes (2.5 to 3.5 phi). The mean of the 10 largest grains (or in this case, the actual coarsest one percentile) fell in the range -0.25 to 2.0 phi, with the gravel sample again very different at -5.5 phi.

The gravel sample (WP 30/7 7B) bears a striking resemblance in practically all its aspects to the gravel member of the transition sub-facies of the lateral accretion facies (see table adjacent to Fig. 43). The cumulative curves shown in Fig.45 also compares closely with that of the gravel sample in Fig. 42-B

THE FACIES AT WEST PARIS: INTERPRETATION

As has already been noted the stratigraphic sequence at West Paris is an attenuated one. It seems that the exposed deposits all belong to the equivalent of stratigraphic unit 2 at East Paris, and that unit 3 is missing completely. The basal gravels at West Paris may be the equivalent of stratigraphic unit 1 at East Paris, but more than a tentative correlation is unwarranted.

TYPE OF BAR FORM:

The major differences observed between the two pits suggest a different bar form for the production of these deposits. In particular the whole system is somewhat sandier, the Bar Front facies has a different organisation, the palaeocurrents generally are more variable (see Fig. 46), a new facies is defined (the lateral accretion facies), and other facies are absent. Consideration of these features has led to the interpretation of the West Paris deposits as the product of a Side-Bar type of sedimentation. Side-Bars have been reported in the literature by Znamenskaya (1962), Popov (1964), and Collinson (1970) who have described grouped cuspate or linguoid sand bodies in the form of large sand banks adjacent to the river banks. The present description is probably the first of such a feature is dominantly coarse grained material.

The most complete description is that of Collinson (1970, P. 38) in which he notes: "In plan they are often pointed at the upstream end... (and) ... gradually widen downstream before the margins slope rather sharply back to the river bank. The bars do not have individual slip faces at their downstream ends, but, being complexes of smaller forms pass gradually into deeper water... The surface morphology of the side bars, particularly the larger ones, is a complex of smaller forms of which linguoid bars dominate, ... which are arranged in a very clear en echelon offsetting". Collinson further recgonises modification made by changing flow stages with differing flow patterns, deposits and erosional agents at high-and low- water stages.

The facies and their relationships exhibited at West Paris have features which fit very well into a "Side-bar" interpretation.

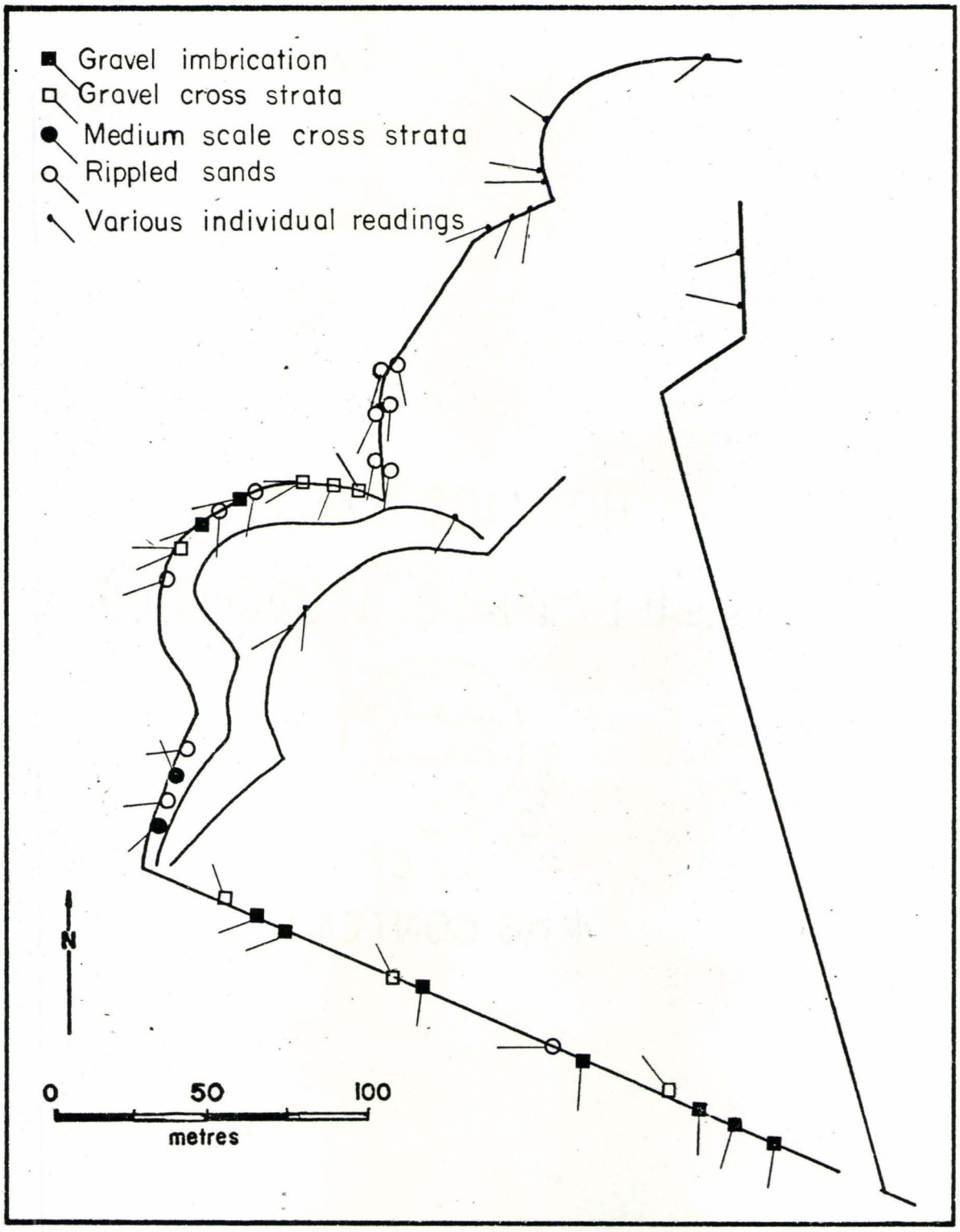

Fig. 46: The palaeocurrent data at West Paris.

The widely varied palaeocurrent data obtained from the bar front facies cross-strata suggest advance of the gravel accumulations in lobate form; the sandy channel-like deposits within the bar front facies suggest low-water stage flow between the gravel lobes; the sand drapes are interpreted as the immobile front of the bar at low water stage; and the adjacent lateral accretion facies suggests growth of the bar outward from the river bank toward the main channel.

BAR ORIGINS

With sand bar accumulations of this type the growth of the bar takes place from some channel-bank irregularity such as a headland (Collinson, 1970, P. 38). At West Paris the lateral accretion facies is interpreted as the channel bank from which the growth took place, the low-angle surfaces dipping in the direction of the main channel being the lateral accretion surfaces of the advancing river bank (see photolog at E or C). The accretion must take place primarily at times of high-water flow stages so that the gravel can be moved and supplied to the side-bar complex. The various channel-like sandy infills of the facies (see A of photolog) are interpreted as channelized flow at lower stages; either the falling stage in the case of the fining upwards lenses, or the rising stage in the case of the coarsening upwards lenses (Costello and Walker, 1972).

The relationships of the palaeoflow data to the low angle surfaces are not easy to determine. In the case of the lateral accretion surfaces on point bars, the flow is perpendicular to the direction of aggradation. But the flows indicated at West Paris are very variable (see Fig. 46). The data from sampling sites F10, F17, and DW27 appear to represent flow

in the same direction as the side channel; and data from sites at DW28, F18 and F19 seem to represent the flow into the channel from the river bank. These are probably the high and falling stage flows respectively. However, a different interpretation must be placed on the remaining data which are from the base of the face in its eastern half. These are thought to represent an earlier period of bank aggradation with the main channel in a somewhat different position.

The base level suggested by the horizontal basal sands, and the asymptotic bases of the accretion surfaces, is the local bed level in the stream. This coincides with the bed level associated with the bar gravels of the side-bar complex itself (see bar front facies above). The different heights of the pit faces , and the different thicknesses of the exposed sections of these two facies, would suggest that the bank (lateral accretion facies) was higher than the side bar (bar front facies) which is a logical and expected arrangement.

THE SIDE-CHANNEL FACIES:

The actual contact between the bar front facies and the lateral accretion facies, if it indeed occurred directly at all, was nowhere seen at West Paris. The two were separated at one point by the minor side-channel facies which intervened, and elsewhere the contact was obscurred by pit workings. However, it is quite likely that the two facies do not come into direct contact at all. The inferred flow pattern of Fig. 47 indicates the probability of a channelized flow between the bank and the side-bar complex. Such a situation is shown to exist on the Tana River by the diagrams and photographs of Collinson (1970, p. 34-39) Consequently the side channel facies

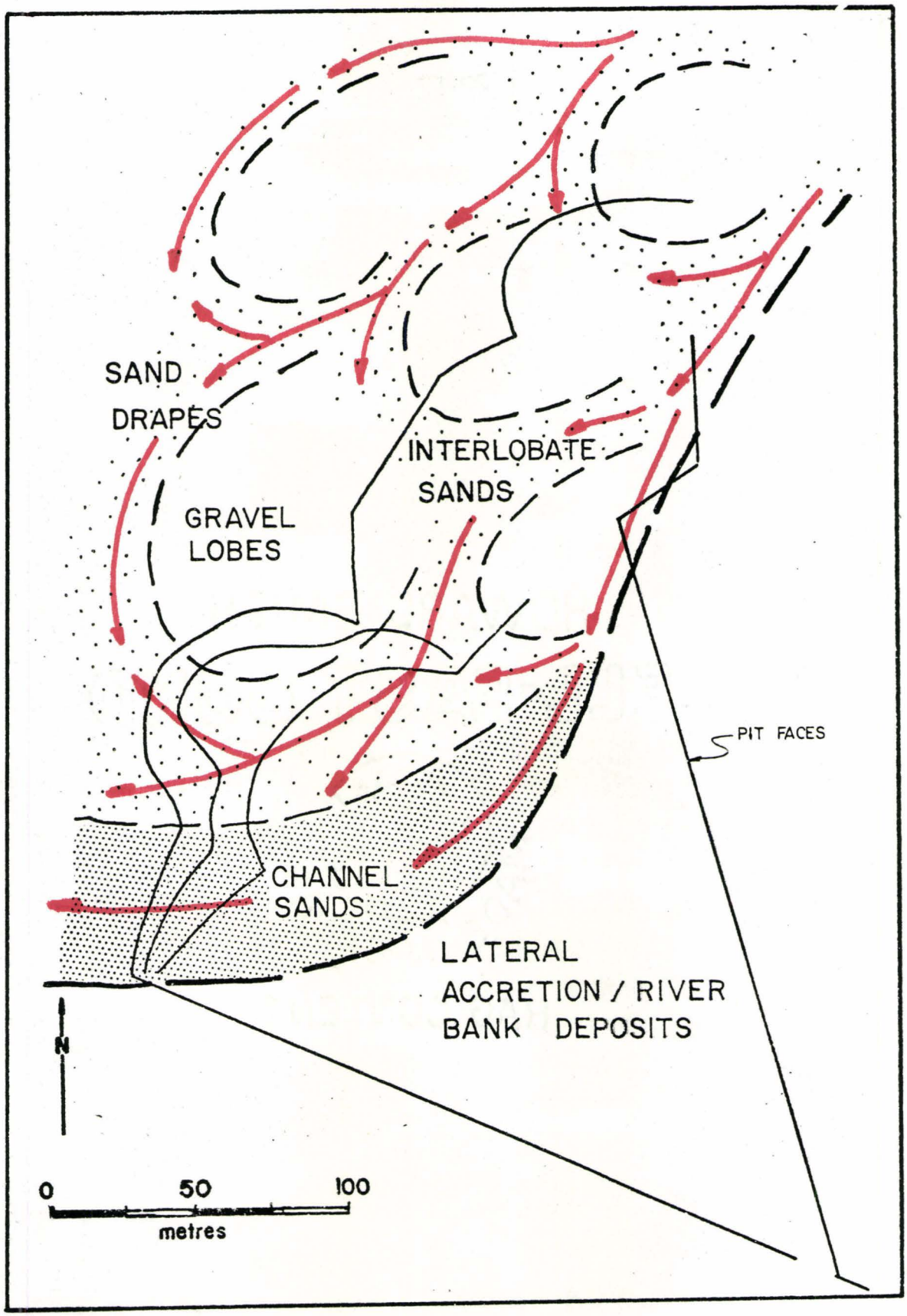

Fig. 47: Reconstruction of the Palaeoflow conditions in the West Paris pit.

described above is thought to be the sandy infilling, with gravel interdigitation, of a shallow depression between the laterally accreting bank and the side-bar complex. The fact that the gravels in the channels are found right across the trough shape suggests that the flanks of the channels were steep enough to permit gravity rolling to to move the cobbles, in contrast to East Paris where the slopes were not steep enough. The tops of the gravel lobes at West Paris are thought to have been under similar conditions to the bar top at East Paris - that is, shallow flow depth with relatively high velocity and gravel bed load movement.

THE MULTI-LOBATE ADVANCE

The bar front facies at West Paris has several features of side-bar complexes. Firstly, the spread of the palaeocurrent directions obtained from the cross-strata developed in the gravels, suggests a lobate advance of the gravels. The repeated pattern across the width of outcrop suggests not a single lobe but several together, constituting an advancing front some 200m or more across (see Fig. 47)

Secondly, the channel-like depressions (see X of photolog) suggest a flow pattern of interlobate sandy channels. During the formation of these sands at low water stage the tops of the gravel accumulations may have been covered by a very shallow depth of flowing water, or have been partially exposed. If the latter were the case the gravels would quite likely exhibit the products of winnowing by aeolian action. One would expect to find openwork gravels, devoid of sand matrix to at least one-pebble-depth - the socalled gravel pavements. It is difficult to tell whether or not these existed since the next

high stage would probably obliterate them. Nevertheless, the same type of openwork gravels occur at East Paris indicating that they do have preservation potential. Their complete absence in the bar front facies at West Paris would seem to indicate that they had never been formed, and consequently that the bar top was never quite exposed to aeolian action.

Corroboration of this hypothesis can be found in the form of the horizontal sandy units (such as Q of the photolog) at the top part of the bar front facies exposures. These suggest that flowing water was indeed present on the bar top surface at the low flow stage. The lower part of this particular sand is ripple drift cross-laminated and is interpreted as the product of the falling stage. The upper part is medium-scale cross-bedded and interpreted as part of the rising stage deposits, since it passes downstream into gravels of the high-flow stage. The contact of the two parts is marked by a thin pebble horizon and it is difficult to determine whether this signifies continuous flow or not.

Thirdly, the sand drapes (see N,O, and P of the photolog) are intimately related to the interlobate channels. They represent a sandy low stage deposit laid down in front of the large foresets of the gravel lobes, and are interpreted as the equivalent of Collinson's "downstream end which passes gradually into deeper water. Subsequent advances of the gravel lobes partially destroy the sand drapes, but in almost all cases there is some preservation. The deposits of the sand drapes are quite variable. There are fining upwards sequences of the falling stages, and coarsening upwards sequences of the rising stages. The opposed direction of ripple-drift cross-lamination (see Fig.44) attest to the position of the counter current eddy and the reattachment

zone of the separation flow. The wide spread of ripple orientations suggests a radial fanning out of the current emerging from the inter-lobate channels (see Fig. 47), and the formation of an apron-like drape wrapped around each adjacent lobe.

The contact between the upper surface of the sand drape and the succeeding gravels is often very sharp (see above, Page 98). The 'knife-edge' nature of the contact and the small scale 'flame' structures (interpreted as dewatering structures) suggest that the sand drape was frozen into a solid mass when the reactivation of the gravel lobes occurred. The surface was planed off and subsequent partial melting created the dewatering structures.

The development of sand drapes would occur only at the irregular slip-face frontal portion of the whole side-bar complex. Upstream the other gravel accumulations would have only adjacent interlobate sands.

The side-bar model used here necessitates a main channel talweg situated on the other side of the bar to be considered. Judging by the side bar to total channel width ratios of the Tana River (1 : 2) the main channel must be at least 100m wide , and be situated somewhere to the northwest of the present pit location.

SUMMARY OF THE SIDE-BAR MODEL:

(1) The side-bar consists of a series of lobate gravel accumulations advancing downstream by the avalanching of large-scale cross-strata, often supplied by imbricate gravel whose ultimate source is the adjacent river bank.

(2) The whole side bar complex probably originates at a change in direction of the river bank, which is formed of unconsolidated laterally

accreting gravels, and must be under water for the most part at high flow stage. It must also have ceased aggrading laterally when the side bar complex progrades forward over it.

(3) Between the gravel lobes of the side bar complex sandy channel deposits are formed, particularly at low flow stage feeding the sand drapes which accumulate at the irregular front of the bar.

(4) A minor sandy side-channel separates the side bar from the river bank deposits, at least at the downstream end, and the main channel talweg is situated on the other side.

CHAPTER EIGHT

SYNTHESIS

CHAPTER EIGHT

SYNTHESIS

This brief final chapter will attempt to draw from the observations at East and West Paris such features as appear to have general application to braided stream. In conjunction with the literature an appraisal will be made of some attempts to produce braided stream "models" Finally the gravels at Paris will be set in their context on the outwash plain.

CHANNEL DEPTH

The deposits at East and West Paris have been referred to in terms of 'deep' and 'shallow' braid streams with coarse gravel loads. To give some indication of what is meant by these conditions it is instructive to consider the depths of the systems inferred from the channel and bar sizes and to compare them to documented examples. In stratigraphic unit 2 at East Paris the major channel was 6m deep at its maximum (corresponding to the maximum depth of dissection of the surface of unit 1), and the 'core' was 4m high at its maximum. In the same stratigraphic unit at West Paris both the side channel (a minor side channel in the terms of the reconstruction) and the side-bar complex were 4m. The shallow braided system (unit 3 at East Paris) had channels and bars 1m deep and high respectively.

Fig. 48 shows a table of selected braided streams and their depths. In the Pleistocene this is one of the few parameters that can be measured

Ardeche River	Doeglas, 1962	6-8m in flood 3m high stage
Brahmaputra	Coleman, 1969	23m max. depth of scour
Donjek River	Williams & Rust, 1969 Rust, 1972	3m in flood
Durance River	Doeglas, 1962	1-4m
Green River	Leopold & Wolman, 1957	2m mean
Icelandic Sandar	Krigstrom, 1962	2-9m max.
Kicking Horse River	Smith, 1972	2m max.
New Fork River	Leopold & Wolman, 1957	1m max.
Platte Rivers	Smith, 1970 & 1971	0.3-0.6m
Slims River	Fahnestock, 1969	1.25m max.
Tana River	Collinson, 1970	1.5m plus
White River	Fahnestock, 1963	0.6m mean
* Van Horn Sst.	McGowan & Groat, 1971	3m plus
* Shawangunk Cong .	Smith, 1970	0.3-1.0m

Fig. 48 The depths of selected braided rivers from the literature

* Ancient example.

The rapidity of local and minor changes in the channel patterns of shallow braided streams has been demonstrated (Fahnestock,1963; and Smith, 1972). This means that the active bars often become dissected within the systems, and that their relict forms could become the framework of further bar development. Close studies of bar development over a long term period, and of the internal structures of bar forms and their palaeocurrent indicators, are needed to test this hypothesis. However, this will not yield data on the origins of the primary bar forms, a question which at present remains unanswered.

The braid bars studied at East and West Paris in stratigraphic unit 2 suggest forms of bar origin other than the classic "coarse lag" theory. In the case of the longitudinal Bar exposed at East Paris it has been demonstrated that the major bar forms grow from topographic highs of a dissected surface - the so-called "bar cores". Similarly at West Paris in the corresponding unit the Side-Bars are shown to develop from a channel bank. Both of these cases require a pre-existing form on which to develop the gravel bars, but in one it is a relict feature due to degradation, while in the other it is an active feature of aggradation.

The consequences of a mode of origin different from the classic Leopold and Wolman theory are considered here. With braid bar growth from a "coarse lag" it is implied that new bar growth is beginning within a channel in an active system. In the case of braid bar growth from a "bar core" it is implied that bars are being created in a new area with a pre-existing form to get them started. The side bar growth from a channel bank is an intermediate situation where the system is active, but the physical point of origin is to some extent pre-existent.

with any degree of accuracy and provides perhaps the best single point of comparison of the conditions when considering modern streams. However, it is apparent from the literature that often depth cannot be measured directly in modern stream, and in addition it is often reported in different ways.

Judging from the descriptions of these rivers in the literature, the shallow' and 'deep' systems at Paris can be equated to certain modern braided streams. The 'deep' braided system of unit 2 most closely resembles the Durance and Ardeche (Doeglas, 1962), and the "proximal zone" of the Icelandic sandar (Krigstrom, 1962); while the 'shallow' braided system of unit 3 most closely resembles the Slims River (Fahnestock, 1969), the Donjek River, (Williams & Rust, 1969 and Rust, 1972), the Kicking Horse River (Smith, 1972), and the 'zone further downstream' of the Icelandic sandar (Krigstrom, 1962).

THE ORIGINS OF BRAID BARS

The "Classic" theory of braid bar initiation is based on the experiments of Leopold and Wolman (1957). They suggested that bars are started by the selective deposition of the coarsest bed load fractions in the middle of stream channels. Subsequent growth of the bar form takes place by addition of finer material on the top and downstream portions. As Rust (1972) points out, the braided streams with relatively fine bed material tend to follow Leopold and Wolman's model, and he cites the Brahmaputra (Coleman, 1969) and the Yellow River (Chien, 1961) as examples.

In the coarse shallow braided system (unit 3 at East Paris) it was not possible to determine how the braid bars began (see above, page 92), and reports in the literature (Krigstrom, 1962; Fahnestock, 1963 and 1969; Smith, 1972 and Rust, 1972) give no indication either.

The question of generality as applied to the initiation of bar growth from relict of pre-existent topographic forms is an important one. It has already been suggested that this occurs in the shallow braided stream environment. In the deep braided system studied at East Paris, two contrasting situations are exhibited. There is a big different between (a) the seasonal or periodic emptying and filling of the channels with reoccupation on the same trends, displayed by the bar front cross-strata and reactivation surfaces, and (b) the major switching of channels with degradation and occupation of an area on a different trend, shown by the erosional contact between units 1 and 2, and the relict topographic highs as bar cores. Both are potentially preservable, one by virtue of its catastrophic nature and the other by virtue of more frequent occurrence.

BRAID BAR MIGRATION

In both the 'deep' and 'shallow' systems observed, the form of the braid bar migration was similar, with cross bedded gravels advancing downstream in tabular sets. The foresets were supplied with gravel moving over the tops of the bars. This is quite contrary to Rust't (1972) assertion that "the only directional property likely to be commonly preserved and observable in sediments of ancient gravel bars is the preferred orientation of platy or elongated clasts". (see also Waechter, 1970).

In the larger, deeper-water bar forms the advancing front was periodically interrupted by low water stage structures (the reactivation surfaces of East Paris, and the sand drapes of West Paris), but these were not observed in the shallow water braid bars.

There appears to be much generality in these bar migration patterns, similar structures having been reported in both sand- and gravel-dominant braided stream systems (Doeglas, 1962; Collinson, 1970; Waechter, 1970; and Smith, 1970). However, there are some major differences between the systems preserved at East Paris, and those reported in the literature. The bar forms at Paris, in both the 'deep' and 'shallow' braided systems have a sand-gravel-sand sequence laterally from channel to bar to channel. This is in direct contrast to other systems reported in the literature (for example, the Kicking Horse River, Smith, 1972), where the bars became sandier downstream and eventually are finer grained than their adjacent channels. The difference between this situation and the braided system of stratigraphic unit 2 at East Paris is probably a function of channel depth,but this arrangement obviously cannot apply to stratigraphic unit 3 - the 'shallow' braided system. It is thought that the preservation potential of such downstream fining is not very high, and that sands will be moved off the gravel bars into the channels before burial by aggradation.

A further feature of difference between the longitudinal bar forms at East Paris (in unit 2) and the bars reported in the literature concerns the stoss-side addition of material. This occurs in the longitudinal bars of the 'deep' system at East Paris and is in contrast to the description of Leopold and Wolman (1957) in which the bar "grows by successive additions at its downstream end, and presumably by some addition along its margins" Leopold and Wolman's observations are supported by Krigstrom (1962). Stoss-side addition at East Paris is demonstrably part of the active bar growth, since imbricate gravels of the stoss-side facies can be traced over the bar top into the bar front avalanche foresets.

Stoss-side addition is also proposed by Rust (1972) in which he envisages this to be the main aggradation of bars, with consequent upstream migration of the bar forms. He proposes such a situation because of the lack of downstream dipping strata at the downstream end of the bar, where he has only horizontal (± 3 degrees) strata. However, it seems possible from the descriptions he gives, and the observations made at Paris in this study, that Rust is looking at the dissection of a Bar Top facies of a larger preexisting bar form.

PROXIMAL-DISTAL RELATIONSHIPS

Perhaps the greatest single factor of similarity and generality regarding braided stream observations made to date, is the idea of a proximal-distal trend. Such a situation has been reported by Krigstrom (1962) an Icelandic sandar, Ore (1964) and Smith (1970) on the South Platte-Platte Rivers, Boothroyd (1970) on proglacial outwash in southeastern Alaska, Fahnestock (1969) on the Slims River, Bradley et al (1972) on the Knik River, and Rust (1972) on the Donjek River. The proximal-distal trend in sediments is by no means a new idea in geology having been applied to turbidites, alluvial plains and alluvial fans in the past; and it certainly appears to hold some validity in the search for a braided stream model.

Smith (1970) has shown that on the South-Paltte-Platte Rivers there is a downstream increase in

(i) the ratio of transverse to longitudinal bars

(ii) the size sorting of the bed load material, and

(iii) the proportion of planar cross-stratification to horizontal stratification.

and a similar downstream decrease in

(i) the bed relief index, and

(ii) the mean grain size.

Rust (1972) noted several of these same features on the Donjek River.

Krigstrom (1962) described 3 zones on Icelandic sandar. First there is a "proximal zone" nearest to the ice which is characterised by a few incised and gently sinuous channels, commonly with one main distinct channel. These are relatively deep (1-3m), well defined and parallel sided. In a "zone further downstream" occupying the major part of the sandar surfaces, the channels gradually widen and become shallower. The banks become less well-defined and the channel may merge into a plain on which the channels can no longer be kept together. Finally in a "zone furthest downstream" the intertwined channels merge into a shallow bay with streaming water.

Following Krigstrom's description, other instances of such zonation have been reported, notably Fahnestock's (1969) observations on the Slims River outwash plain in the Yukon, and more recently by Boothroyd and Ashley (1972) in southeastern Alaska.

SANDAR ZONES AT PARIS.

This type of zonation also fits well with the observed facts at East Paris. It seems likely that the coarsest deposits, those of unit 1 (see Fig. 7), belong to the very ice proximal position of the outwash, the deposits being laid down by the meltwater on its immediate contact with the proglacial environment. The change of stream conditions from steep gradients and efficient channels within or on the glacier, to less steep slopes and broader, shallower and less efficient channels of the outwash plain, is usually sufficient to cause the coarser part of the

stream load to be dropped and aggradation to be initiated (Flint, 1971, p. 186-187). Once the initial deposits have been laid down the sandar and their associated zones can be developed.

The major channels of the side-channel facies in stratigraphic unit 2, of both pits had a maximum depth of 6m, and an average depth of 3-4m, allowing for the periodic exposure of the bar surface. This is comparable to Krigstrom's "proximal zone", if one takes into account that the run-off from a continental ice-sheet such as that of Late Wisconsinan of Southern Ontario, was probably much greater than that from the present day Icelandic ice-fields such as Vatnajokull, Myradalsjokull and Eyrjaffjallajokull.

The interpretation of the erosional contact between unit 1 and unit 2 at East Paris (see Chapter 6; interpretation) gives us a more complete picture of the history of the sandur. It is suggested that the main drainage was on the Western part of the sandur surface initially, possibly at or near the West Paris pit. At this time the area at East Paris was aggrading by sheet flooding at high stage flow when the whole sandar was awash. A major "switching" of the drainage system to the eastern area dissected the plain surface there and produced deep braided channels, akin to the area in the western part, and longitudinal braid bars.

Similarly, the shallow braided stream facies (stratigraphic unit 3, Fig. 7) appears to be directly comparable to Krigstoms "zone further donwstream". The lack of distinct channel forms persisting through this facies, and the abundance of sandy lenses of a smaller nature, is reminiscent of "... a plain on which the channels can no longer be kept

together". (see above; and Krigstrom, 1962, p. 329-330). The third and final zones does not appear to occur at East or West Paris, nothing resembling lacustrine deposits have been found at all.

THE FINING UPWARD SEQUENCE

On the Icelandic sandar Krigstrom observed these facies laterally adjacent to one another down the length of the outwash plain or valley. At East Paris were the stratigraphic sequence is best seen, the zones are observed vertically one above the other, with the coarsest at the base. This would suggest, directly applying Johannes Walther's 'Law of Succession of Facies' (Blatt, Middleton and Murray, 1972, p. 187-188), that the aggradation of the outwash was associated with a retreat of the sediment source - the ice sheet. (Fig. 49). Rust (1972) also says that "a proximal-distal facies trend within the succession at any one locality could be due to recession of the source with time.." The distinct erosional break between units 1 and 2 could mean that the stratigraphic succession is not necessarily a single fining upwards sequence, but if one applies the idea of major "switching" of the channel systems the sequence is essentially unbroken.

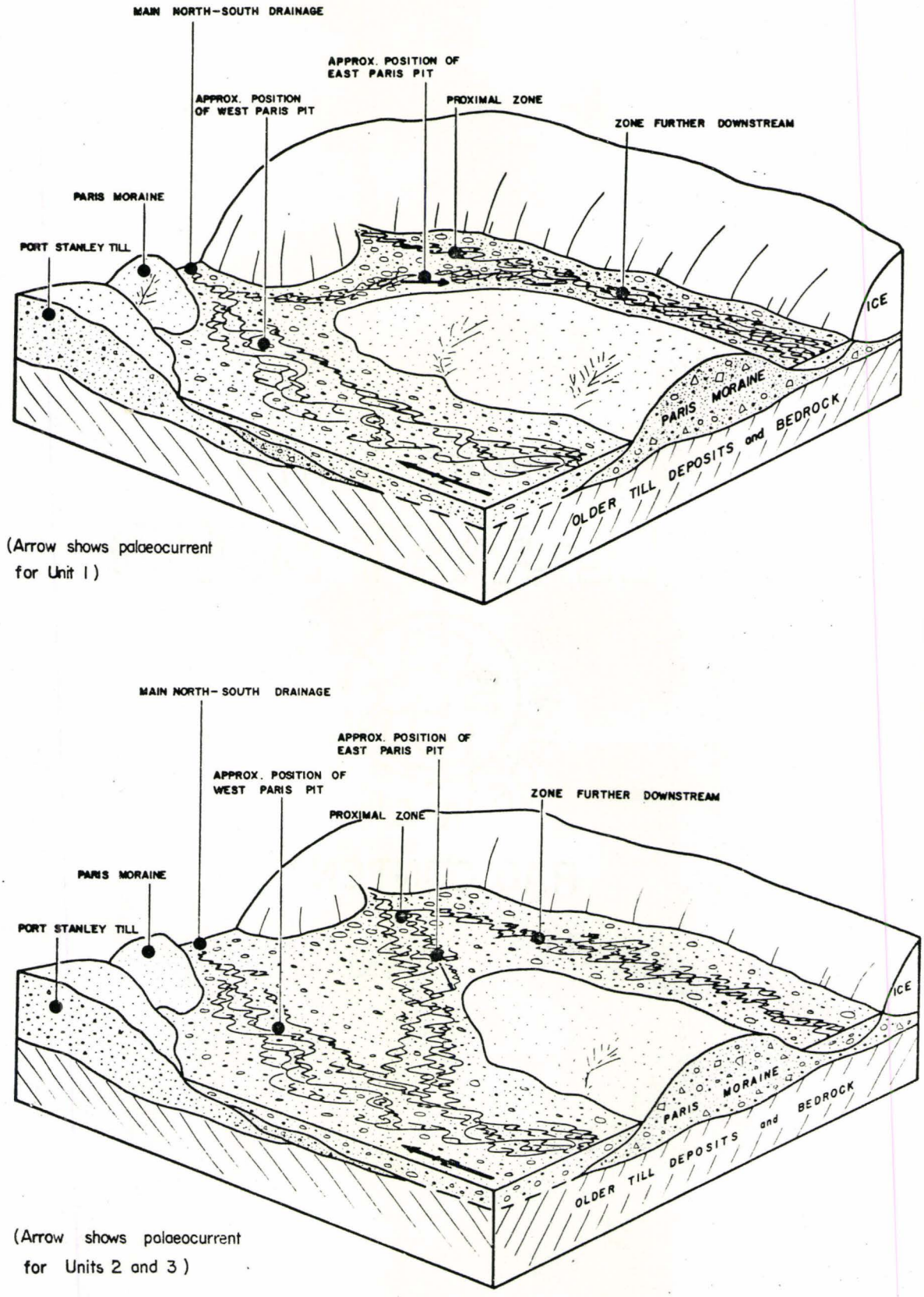

Fig. 49: Sandar zones related to the ice recession, the 'switching' of the drainage system, and the partial erosion of the Paris moraine

REFERENCES

REFERENCES

ARNBORG, L (1955) Hydrology of the glacial river Austerfljot. Geogr. Annaler. 37, p. 185-201.

BARENDSEN, G. W. et al (1957) Yale Natural Radiocarbon Measurements II. Science 126, p. 908-919.

BLATT, H, G. V. MIDDLETON and R. C. MURRAY (1972) Origins of Sedimentary Rocks. Prentice Hall, Englewood Cliffs. N.Y. 634p.

BOOTHROYD, J. C. (1970) Recent braided stream sedimentation, south Central Alaska. Abs. Bull. A.A.P.G. 54, p. 836.

BOOTHROYD, J. C. and GAIL M. ASHLEY (1972) Bedforms and sedimentary structures of braided outwash streams, Northeastern Gulf of Alaska. G.S.A. Abstract with program 4 (1). Northeastern section 7th Annual Meeting Buffalo, N.Y.

BRADLEY, W. C. et al (1972) Coarse sediment transport by flood flows on the Knik River, Alaska. G.S.A. Bull 83, p. 1261-1284.

BRICE, J. C. (1964) Channel patterns and terraces of the Loup Rivers in Nebraska. U.S.G.S. Prof. Paper. 442-D 41p.

BULL, W. B. (1968) Alluvial fans. Journal of Geol. Education. VXI (3) p. 101-106.

_____ (1972) Recognition of alluvial fan deposits in the stratigraphic record. in J. K. Rigby and W. K. Hamblin (Eds) Recognition of Ancient Sedimentary Environments S.E.P.M. Spec. Publ. 16.

CHAPMAN, L. J. and PUTNAM, D. F. (1966) The Physiography of southern Ontario. Toronto University Press. 2nd Edition. 386p.

CHIEN, N. (1961) The braided stream of the lower Yellow River. Scientra Sinica. 10. p. 734-754.

CHIEN, N. et al (1961) The characteristics and genesis analysis of the braided stream of the lower Yellow River. Acta Geographica Simica 27, p. 1-27 (English summary p. 26-27)

CHURCH, M. (1970) Baffin Island Sandar: A study of Arctic Fluvial Environments. (plus Appendices). Unpublished Ph.D. Thesis. University of British Columbia.

COLEMAN, J. M. (1969) Brahmaputra River: channel processes and sedimentation. Sed. Geol. 3, p. 129-239.

COLLINSON, J. D. (1970) Bedforms of the Tana River, Norway. Geogr. Annaler. 52(A) p. 31-56

COTTER, E. (1971) Palaeoflow characteristics of a Late Cretaceous River in Utah from analysis of sedimentary structures in the Ferron Sandstone. J.S.P. 41(1) p. 129-138

COSTELLO, W. R. (1970) Braided river deposits and their relationship to the Pleistocene history of the Credit River Valley, Ontario. Unpublished M.Sc. Thesis, McMaster University.

COSTELLO, W. R. and WALKER, R. G. (1972) Pleistocene Sedimentology, Credit River, Southern Ontario: A new component of the Braided River Model. J.S.P. 42(2) p. 389-400.

COWAN, W. R. (1970) Pleistocene Geology of the Brantford Area. Ontario Dept. of Mines. Open File Report 5048.

DAL CIN, R. (1968) Pebble Clusters: their origin and utilization in the Study of Palaeocurrents. Sed. Geol. 2 p. 233-247.

DANSGAARD, W. (1954) The O-18 abundance in Fresh Water. Geochim. Cosmochim.Acta. 6 p. 241.

_____ (1964) Stable Isotopes in Precipitation. Tellus. 16 p.436.

DANSGAARD, W. et al (1969) Ice cores and palaeoclimatology in I. U. Olson (Ed.) Twelfth Nobel Symp. Radiocarbon Variations and Absolute chronology, Uppsala, 1969. Wiley, N.Y.

DANSGAARD, W. et al (1971) Climatic record revealed by the Camp Century Ice Core in Lake Cenozoic Glacial Ages. K. K. Turekian (Ed.) Yale University Press, New Haven.

DAVIS, W. M. (1889) Structure and Origin of glacial sand plains. G.S.A. Bull. 1. p. 195-202.

DOEGLAS, D. J. (1962) The structure of sedimentary deposits of braided rivers. Sedimentology 1 p. 167-190.

FAHNESTOCK, R. K. (1959) Dynamics of stream braiding as shown by time lapse photographs. (abstract) G.S.A. Bull. 70 p. 1599.

_____ (1963) Morphology and hydrology of a glacial stream: White River, Mt. Rainier, Washington. U.S.G.S. Prof. Paper. 422-A 41p.

_____ (1969) Morphology of the Slims River. in V. C. Bushnell and R. H. Ragle (Eds.) Icefield Ranges Research Project: Scientific Results. Vol. 1 p. 161-172. Amer. Geogr. Soc. and Arctic Instit. of N. America.

FAHNESTOCK, R. K. and HAUSEHILD, W. L Flume studies of the transport of pebbles and cobbles on a sand bed. G.S.A. Bull. 73 p. 1431-1436.

FLINT, R. F. (1971) Glacial and Quarternary Geology. John Wiley and Sons. New York. 892p.

FOLK, R. L. and WARD, W. C. (1957) Brazos River Bar: A study in the significance of grain size parameters. J.S.P. 27, p. 3-26.

FOLK, R. L. (1968) Petrology of the sedimentary rocks. Hemphill's University of Texas. Austin, Texas.

GOLDTHWAIT, R. P. et al (1965) Pleistocene deposits of the Erie Lobe. in H. E. Wright and D. G. Frey (Eds.) The Quartenary of the U. S. Princeton University Press, Princeton, N. J.

GRIFFITHS, J. C. (1967) Scientific method in the analysis of sediments McGraw-Hill 508p.

HANCOCK, J. S. (1971) Studies of the late Wisconsinan Deposits of the West part of the City of London, Ontario. Unpublished senior Thesis. University of Western Ontario.

HARMS, J. C. and FAHNESTOCK, R. K. (1965) Stratification bedforms and flow phenomena (with an example from the Rio Grande). in G. V. Middleton (Ed.) Primary Sedimentary structures and their hydrodynamic interpretation. S.E.P.M. Spec. Publ. 12.

HEWITT, D. F. and COWAN, W. R. (1969) Sand and Gravel in Southern Ontario. Ind. Min. Rpt. 27. Ontario Department of Mines.

HEWITT, D. F. and KARROW, P. F. (1963) Sand and gravel in Southern Ontario. Ind. Min. Rpt. 11. Ontario Department of Mines.

HJULSTROM, F. (1952) The geomorphology of the alluvial outwash plains (sandar) of Iceland and the mechanics of braided rivers. Int. Geographers Union. Proc. 8th Gen. Ass. and 17th Int. Congress. p. 337-342.

JOPLING, A. V. (1964) Laboratory study of sorting processes related to flow sepations. J. Geophys. Res. 69. p. 3403-3418.

_____ (1965) Laboratory study of sorting processes in cross-bedded deposits in G. V. Middleton (Ed.) Primary Sedimentary structures and their hydrodynamic interpretation. S.E.P.M. Spec. Publ. 12.

_____ (1966) Some principles and techniques used in reconstructing the hydraulic parameters of a palaeoflow regime. J.S.P. 36(1) p.5-49.

JOPLING, A. V. and WALKER, R. G. (1968) Morphology and origin of ripple drift cross-lamination with examples from the Pleistocene of Massachusetts. J.S.P. 38 (4) p.971-984.

KARROW, P. F. (1963) Pleistocene Geology of Hamilton-Galt area. Ontario Department of Mines. Geol. Rpt. 16 68p.

KARROW, P. F. (1970) Quartenary Geology of the Stratford-Connestoga area, Ontario. Geol. Survey of Canada. Paper 70-34.

KELLERHALS, R. and BRAY, D. I (1967) Stable channels with gravel-paved beds. J. of the Waterways and Harbours Division. A.S.C.E. 93 No. WW1. Proc. Paper. 5091 p. 63-84.

KELLERHALS, R. and BRAY, D. I. (1971) Sampling procedures for coarse alluvial sediments J. of the Hydraulics Division. A.S.C.E. No. HY8. Proc. Paper. 8279. p. 1165-1180.

KRIGSTROM, A. (1962) Geomorphological studies of sandur plains and their braided rivers in Iceland. Geogr. Annaler. 34. p. 328-346.

LEOPOLD, L. B. and WOLMAN, M. G. (1957) River channel patterns: Braided, Meandering and Straight. U.S.G.S. Prof. Paper. 282-B p. 39-85.

LEOPOLD, L. B., WOLMAN, M. G. and MILLER, J. P. (1964) Fluvial processes in Geomorphology. W. H. Freeman & Co. San Francisco. 522p.

MACKIN, J. H. (1956) Cause of braiding by a graded river. (abs). G.S.A. Bull. 67. p. 1717-1718.

McCALLUM, K. J. (1955) Carbon - 14 age determinations at the University of Saskatchewan. Roy. Soc. Canada, Transactions. Ser. 3. (4) p.31-35.

McDONALD, B. C. and BANNERJEE, I (1971) Bedforms and sediments on a braided outwash plain. Can. J. Earth Science. 8 (10) p. 1282-1301.

McGOWAN, J. H. and GARNER, L. E. (1970) Physiographic features and stratification types of coarse grained point bars: modern and ancient examples. Sedimentology. 14 p77-111.

McGOWAN, J. H. and GROAT, C. G. (1971) Van Horne sandstone, West Texas: An Alluvial Fan Model for Mineral Exploration. Bureau of Econ. Geol. University of Texas, Austin, Texas. Report of Investigations No. 72.

MECKEL, L. D. (1967) Origin of the Pottsville Conglomerates (Penn.) in the Central Appalachians. G.S.A. Bull. 78. p. 223-258.

MIDDLETON, G. V. (1965) editor, Primary Sedimentary Structures and their Hydrodynamic interpretation. S.E.P.M. Spec. Publ. 12.

MORISAWA, M. (1968) Streams: their dynamics and morphology. McGraw-Hill.

OGDEN, J. G. and HAY, R. J. (1965) Ohio Wesleyan University, Natural Radiocarbon measurements II. Radiocarbon. 7. p. 166-173.

ORE, H. T. (1963) The braided stream depositional environment. Unpublished Ph.D. Thesis. Wyoming University.

ORE, H. T. (1964) Some criteria for recognition of braided stream deposits. Wyoming University. Dept. of Geology. Contributions to Geology 3(1) p.1-14.

PASSEGA, R. (1957) Texture as characteristic of clastic deposition. Bull. A.A.P.G. 41(9) p. 1952-1984.

PASSEGA, R. (1964) Grain size representation by C-M patterns as a Geological tool. J.S.P. 34. p. 830-874.

PICCIOTTO, E. et al (1960) Isotopic composition and temperature of formation of Antarctic snows. Nature. 187 p. 857.

PLUMLEY, W. J. (1948) Black Hills terrace gravels: A study in sediment transport. J. of Geol. 55. p. 526-577.

POPOV, I. V. (1965) Hydromorphological principles of the theory of channel processes and their use in hydrotechnical planning. Soviet. Hydrol. 1964: p. 188-195.

RIST. S. (1955) Skeiorarahlaup 1964 Jokulls. Icelandic Glaciological Society. p. 30-36.

RUST, B. R. (1972) Structure and Process in a braided river. Sedimentology 18, (3) p. 221-245.

SALISBURY, R. D. (1892) Overwash plain and valley trains. Geol. Survey of New Jersey, Annual Rpt. of the State Geologist. Section 7. p. 96-114.

SCHUMM, S. A. (1967) Palaeohydrology: application of modern hydrologic data to problems of the ancient past. Int. Hydrol. Symp. Fort Collum, Colorado. Proc. Vol. 1 p. 185-193.

_____ (1968 a) Speculations concerning palaeohydrologic controls of terrestrial sedimentation. G.S.A. Bull. 79. p. 1573-1588.

_____ (1968 b) River adjustment to altered hydrologic regimen: Murrambidgee River and palaeochannels, Australia. U.S.G.S. Prof. Paper. 598. 65p.

_____ (1969) River metamorphosis. A.S.C.E. J. of Hydraulics Division. Proc. Vol. 95. p. 255-273.

SCHUMM, S. A. and KAHN, H. R. (1972) Experimental Study of Channel Patterns. G.S.A. Bull. 83. p. 1755-1770.

SMITH, N. D. (1970) The braided stream depositional environment. Comparison of the Platte Rivers with some Silurian Clastics, North Central Appalachians. G.S.A. Bull. 81. p. 2993-3014.

_____ (1971) Transverse Bars and Braiding in the lower Platte River, Nebraska. G.S.A. Bull. 82, p. 3407-3420.

SMITH, N. D. (1972) Sedimentology of the Upper Kicking Horse River, British Columbia: a braided meltwater stream. G.S.A. Abstracts with Program 4 (1) Northeastern section, 7th Annual Meeting, Buffalo, N.Y.

SUNDBORG, A. (1956) The River Klaralven, a study of fluvial processes. Geogr. Annaler. 38. p. 125-316.

WAECHTER, N. B. (1970) Braided stream deposits of the Red River, Texas Panhandle. (Abs.) G.S.A. National Meeting, Milwaukee. p. 713.

WENTWORTH, C. K. (1922) A scale of crude and class terms for clastic sediments. J. Geol. 30. p. 377-392.

WILLIAMS, P. F. and RUST, B. R. (1969) The Sedimentology of a braided river. J.S.P. 39 (2) p. 649-679.

WOLF, K. H. et al (1967) Techniques of examining and analysing carbonate skeletions, minerals and rocks. in G. V. Chilingar H. J. Bissell and R. W. Fairbridge (Eds.) Carbonate rocks: Physical and Chemical aspects. Development in Sedimentology 9-B

ZNAMENSKAYA, N. S. (1963) Effect of average channel formation and local scouring at bridge piers. Soviet. Hydrol. 1962: p. 325-338.

APPENDIX A

SAND AND GRAVEL PITS IN THE AREA

APPENDIX A

SAND AND GRAVEL PITS IN THE AREA

The area contained in the western halves of the Galt and Brantford map area has a large number of gravel pits, associated predominantly with the outwash deposits of the late Wisconsinan ice which formed the Paris and Galt meraines.

The following pit descriptions, and the accompanying map indicate the extent of coverage which the Pleistocene geologist has locally. In a 35-40 mile long area south from Guelph there are more than 60 pits, 46 of which are described here. The remaining ones, unworked and without exposures at the time of visiting, are located on the map.

Most of the pits have previously been referred to by Hewitt and Karrow (1963), Hewitt and Cowan (1969) or Cowan (1970), and their reports should be consulted prior to further fieldwork.

With respect to further research, it is suggested that these exposures would possibly form the basis for a comprehensive study of a large portion of the Pleistocene outwash complex associated with the present Grand, Speed and Nith River Systems.

The numbers in parentheses alongside each pit name indicates the property number on map A.

(1) FORWELL LIMITED

Ref: Hewitt and Karrow 1963 p. 134

Lot 115. Waterloo Township. Fair Exposures of Grand River Spillway deposits, just south west of Breslau adjacent to the modern day Grand River.

(2) O'BRIEN PIT

1 mile south of Hwy 7 and the town of Breslau. This is a small

operation with fair exposures.

(Note: Map 2029 - Pleistocene Geology of Galt Area, from Karrow 1963, indicates 6 pits to the west of the Grand River and 3 more on the eastern side. All of these pits are badly overgrown with little or no exposures).

(3) ANGELSTONE LIMITED

Ref: Hewitt and Karrow 1963 p. 145

Predominantly sandy outwash exposed in the pit adjacent to the Angelstone plant. Good exposures.

(Note: Pits shown on Karrow's map (op. cit). in the area from Freeport to the Speed River also have little or no exposure).

(4) PRESTON SAND AND GRAVEL COMPANY LIMITED

Ref: Hewitt and Karrow 1963 p. 135

Operation in Lot 5 or Preston Township. The deposit forms part of a terrace of the Speed River Spillway System. Overburden is 60 cms. and the gravel is 7-10m at least. Water table is below pit base. Good exposures.

(5) MARTINI SAND AND GRAVEL LIMITED

Ref: Hewitt and Karrow 1963 p. 135

Operations in Lot 5 concession I, Waterloo Township. Part of some Spillway system terrace as (4) above. Overburden 30-60 cms. with gravel 8-10m. thick. Water table below pit base. Poor to fair exposures.

(Note: 2 other pits on Karrow's map adjacent to Hwy 401 have little or no exposures.)

(6) UN-NAMED PIT

Adjacent to "Loomcraft Wollens" factory north east of Galt. Has

good exposures of glacio-fluvial gravels. Small deposit being worked out.

(Note: 3 other pits indicated in this vicinity on Karrow's map have little or no exposures.)

(7) BLAIR SAND AND GRAVEL LIMITED

Property on Lot 29 Concession XII adjacent to Hwy 401 in North Dumfries Township. 5m. of gravels with little overburden. Good exposures.

(8) UN-NAMED PIT

Concession XII North Dumfries Township, 1 mile south of Blair. Kame-like deposits, exhibiting faulting. Good exposures.

(9) FORWELL LIMITED

2 miles south west of Preston and 1 mile north of Hwy 97 Concession XII, North Dumfries Township. Currently being worked and having good exposures of gravels.

(10) UN-NAMED PIT

Adjacent CPR and Hwy 401. Concession XI North Dumfries Township. 5 miles west of Galt. Fluvioglacial gravels with good exposures.

(11) UN-NAMED PIT

Concession XI, North Dumfries Township. North of Hwy 97 adjacent CPR, 2 miles west of Galt. Fair exposures in small pit.

(12) BLAIR SAND AND GRAVEL

Pit adjacent to Orr's Lake, Hwy 97 and CPR west of Galt. Good exposures of fluvioglacial gravels.

(13) GALT SAND AND GRAVEL LIMITED

Adjacent to Orr's Lake, Hwy 97 and CPR, 1 mile west of Galt. Fair to good exposures of fluvioglacial sands and gravels.

(Note: 5 other pits indicated on Karrow' map in the general vicinity all have little or no exposures.)

(14) UN-NAMED PIT

Adjacent to CPR and Nith River North of AYR. Concession VIII and IX North Dumfries. Small exposures of spillway gravels.

(15) UN-NAMED PIT

Adjacent to CPR northeast of Ayr. Small pit with good/fair exposures of spillway gravels.

(Note: Numerous other pits shown on Karrow's map in the areas adjacent to the Nith River and its tributary (Cedar Creek, all have little or no exposures.)

(16) UN-NAMED PIT

At Glen Morris on the Grand River in Concession VI, South Dumfries Township. Disused pit, with probable kame deposits.

(Note: Numerous other pits in the area between the Grand River and Cedar Creek had little or no exposures, at the time of visiting. They are, nevertheless located on map A as working may have recommenced since the summer of 1971)

(17) SOUTH DUMFRIES TOWNSHIP PIT

Ref: Cowan 1970 p. 115. Lot 3, Concession III South Dumfries Township, Brant County. Grand River terrace with deposits of fluvioglacial outwash. Fair exposures.

(18) McCOMB PIT

Ref: Cowan 1970 p. 109. Lot 17,Concession II South Dumfries

Township, Brant County. Small Pit, poorly exposed.

(19) UN-NAMED PIT

Adjacent to CNR and Nith River 4 miles west of Paris, Oxford County. Fair exposures of spillway gravels.

(20) SOUTH DUMFRIES TOWNSHIP PIT

Ref: Cowan 1970, p. 116. Lot 30, Concession III, South Dumfries Township, Brant County. Glaciofluvial/Glacio-lacustrine deposits. poor exposures.

(21) CONSOLIDATED SAND AND GRAVEL LIMITED (WEST PARIS)

Ref: Hewitt and Karrow 1963 p. 137, and Cowan 1970 p. 101 Lot 33, Concession II, South Dumfries Township. Overburden 1m. Gravel 8-10m. Water table at base of pit. Good exposures.

(22) CONSOLIDATED SAND AND GRAVEL LIMITED (EAST PARIS)

Ref; Hewitt and Karrow 1963 p. 138, and Cowan 1970 p. 100 Lot 26, Concession I, South Dumfries Township. Overburden 1-2m. Gravel 10-15 m. Water table at pit base. 1000m virtually continuous exposure.

(23) J. A. MARTIN

Ref: Cowan 1970 p. 106. Lot 22, Concession I, Brantford Township. Disused and poorly exposes outwash gravels.

(24) BLENHEIM TOWNSHIP

Ref: Cowan 1970. p. 95. Concession II, Oxford County. Shallow terrace deposit, poorly exposed.

(25) W. WILLIAMS

Ref: Cowan 1970 p. 121. Lot 1, Concession I, Burford Township Small, disused and poorly exposed.

(26) F. McKINNON

Ref: Cowan 1970. p. 109. Lot 2, Concession I, Brantford Township. No workings and poorly exposed.

(27) FLINTKOTE COMPANY OF CANADA

Ref: Hewitt and Cowan 1969 p. 41. Hewitt and Karrow 1963 p. 139 and Cowan 1970 p. 103. Lots 17 and 18, Concession II, Brantford Township. 13-15m of gravel, sand and till. Good exposures.

(28) BRANTFORD CITY

Ref: Cowan 1970 p. 97. Lot 19, Concession II, Brantford Township. Part of Paris-Brantford outwash gravels. Fair exposures.

(29) TELEPHONE CITY SAND AND GRAVEL (NO. 1)

Ref: Cowan 1970 p. 117. Lots 19 and 20, Concession III, Brantford Township. Outwash deposits on terrace of Grand River System. Good exposures, becoming worked out in large workings.

(30) D. ALBIN

Ref: Cowan 1970 p. 95. Lot 2, Concession II, Burford Township. Small pit and workings in outwash gravels.

(31) BRANTFORD TOWNSHIP

Ref: Cowan 1970, p. 98. Lot 11, Concession III, Brantford Township. Part of Paris-Brantford outwash gravels. Small pit with poor exposures.

(32) UN-NAMED PIT

Ref: Cowan 1970 p. 121. Lot 1, Concession III, Burford Township Small pit in glaciofluvial gravels poor-fair exposures.

(33) BRANT COUNTY, BURFORD TOWNSHIP PIT

Ref: Cowan 1970 p. 123. Lot 3, Concession V. Burford Township

fluvioglacial outwash gravels with fair exposures in small pit.

(34) BRANT COUNTY ROADS DEPARTMENT PIT

Ref: Cowan 1970 p. 96. Lot, 4, Concession IV, Brantford Township Probably ice-contact gravels. Small working. Poor-fair exposures.

(35) TELEPHONE CITY SAND AND GRAVEL LIMITED (NO. 2)

RefL Cowan 1970 p. 119. Lot 14, Concession V, Brantford Township. Worked out with poor-fair exposures of fluvioglacial gravels.

(36) TELEPHONE CITY SAND AND GRAVEL LIMITED (NO. 3)

The Company has leased an area south of Hwy 53 and south of Brantford Municipal Airfield.

Workings began in the late summer of 1972.

(37) MENARY CONSTRUCTION/CAYUGA QUARRIES

Ref: Cowan 1970 p. 108. Lot 22, Concession IV, Brantford Township. Highlevel terraces of Grand River. Poor exposures in disused pits.

(38) S. TOTA PIT

Ref: Cowan 1970 p. 210. Lot 6, Concession VIII, Burford Township. Outwash/deltaic gravels. Flooded

(39) BRANTFORD TOWNSHIP

Ref: Cowan 1970 p. 99. Lot 7, II Range West of Mount Pleasant Road, Brantford Township. Fluvioglacial/deltaic gravels.

(40) D. PEPPER PIT

Ref: Cowan 1970 p. 111. Lot, 1, Concession IV, Oakland Township Brant County. Disused pit in Paris meraine outwash apron. Poor exposures.

(41) POLZIER PIT

Ref: Cowan 1970 p. 111. Lot 7, Concession III Oakland Township.. Outwash gravels with till (?).

(42) E. MAGUIRE AND SONS PIT

Ref: Cowan 1970 p. 107. Lot 1, Concession II, Oakland Township Brant County. Ice-contact deposits of Paris meraine system. Part-time operations in pit. Fair exposures.

(43) UN-NAMED PIT

Ref: Cowan 1970 p. 122. Lots 4 and 5, Concession I, Oakland Township. Small pit in outwash gravels.

(44) UN-NAMED PIT

Ref: Cowan 1970 p. 122. Lot 5, Concession I , Oakland Township. Small pit in outwash deposits.

(45) R. L. STRICKLER

Ref: Cowan 1970 p. 114. Lot 6, Concession I , Oakland Township. Outwash sands and gravels. Poorly exposed

(46) G. I. NICHOLS PIT

Ref: Cowan 1970 p. 110. Lot 1, Concession I, Windham Township, Norfold County. Outwash gravels with fair-poor exposures

APPENDIX B

GRAIN SIZES: METHODS AND DATA

APPENDIX B

GRAIN SIZES: METHODS AND DATA

The quantitative description of the bed material of a gravel-bed river is a difficult task involving several subjective decisions. However, much of the subjectivity is removed when considering the sampling of the Pleistocene deposits of such rivers. According to Kellerhals and Bray (1971) the major difficulties in sampling gravels in active fluvial environments are the result of 5 major factors.

(1) Lateral and longitudinal variations in bed material composition

(2) Time variations

(3) Vertical variations and stage changes

(4) Wide bimodal size distributions

(5) Use of non-equivalent sampling procedures.

(1) Lateral and logitudinal variations in bed material composition occur even in a short reach of a gravel bed river. Frequently there are areas of the bed consisting only of gravel at the surface with no sand matrix, and other areas of sand size material with no gravel (see openwork gravels, and various sandy horizons in unit 1, Bar Top facies, and Shallow Braided facies of this study). Both extremes and the deposits in the middle of the spectrum have to be sampled to obtain a complete quantitative description of the bed load.

(2) Time variations in the prevailing rate of bed load transport can alter the composition of the gravel bed (Kellerhals and Bray, 1967; Fahnestock, 1963; and Church, 1970). However, the "frozen" nature of the Pleistocene gravels precludes any sampling through time, and a thorough sampling of the deposits should give a complete quantitative description

of the varying bed load.

(3) Vertical variations which occur as a result of stage changes in the flow can also cause difficulties in sampling. At low stages it is possible for virtually all the sand to be winnowed out of a gravel bed, and a distinct gravel pavement to be formed. Equally, winnowed sand accumulations can occur in shallow depressions and channel like forms (see (1) above), and a sand of a different population can be washed into the interstices of a gravel pavement. These features create difficulties when one tries to use Grid Sampling Techniques, but the problems are avoided in the Pleistocene where only bulk sampling is possible. As with the lateral variations, each sub-facies can be sampled, and the effect of winnowing on the size distribution can be carefully considered. It is almost impossible, however, to distinguish between a winnowed gravel with later infill of sand matrix and a gravel/matrix combination deposited together.

(4) Natural fluvial gravels have a wide grain size range, often exceeding 10 phi units. The vast majority are bimodal with separate modes in the gravel and sand ranges. A low content in the 1-4mm range (0 to -2.0 phi) is often reported for gravel distributions. The bimodality can create difficulties in the physical sampling procedure: there is often a danger of undersampling one or other of the fractions, or of actually losing part of the finer fraction altogether. The remedy attempted in this study was simply great care in sampling and the taking of a large sample (2 or 3 shovels full).

(5) The use of non-equivalent sampling procedures and its inherent difficulties was avoided by employing the customary bulk sieve analysis techniques. Thus comparisons between studies is facilitated, since the

majority of sediment transport and river engineering studies used this method. The major difficulty arises from the size of sample required for representativeness. The coarse fraction of the population is commonly not sampled. In this study the coarser fraction was always sampled by measuring the 10 largest particles in the immediate vicinity, and within the same sedimentation unit, as the bulk sample. The mean of the intermediate axes gives a good approximation of the coarsest percentile of the grain size distribution (Middleton, personal communication, 1970). It is this statistic which is used in the plotting of C-M diagrams (Passega, 1957; see Fig. 10).

The data is presented as raw weights held on each sieve (range from -6.5 to -4.0 phi) and in the pan, with a total weight for each sample. After sieving, moment statistics were calculated (Griffiths, 1967; and Data Processing and Computing Centre, McMaster University, Programme Library, 1971) along with Folk and Ward (1954) graphic statistics.

The first two moments and the first graphic statistics compare very closely, and consequently no reason was seen for the inclusion of all three. With the 3rd and 4th moments, and their graphic equivalents a wide range of variation was found. Folk (1968) attributed the inaccuracy of the method of moments in this area to the "open-endedness" of the distributions. (ie:- where there is a lot of material in the pan fraction of unknown grain size). Consequently the Folk and Ward statistics are given for all four measures: mean grain size, sorting, skewness and kurtosis. In the text too the use of such terms in connection with grain size invariably refers to the graphic statistics of Folk and Ward.

The verbal classifications of the values are given below:

M_2 (Graphic mean, in phi units; see Fig. 11).

σ_I (Inclusive graphic standard deviation in phi units)

less than 0.35	very well sorted
0.35 to 0.50	well sorted
0.50 to 0.71	moderat y well sorted
0.7. to 1.0	moderately sorted
1.0 to 2.0	poorly sorted
2.0 to 4.0	very poorly sorted
more than 4.0	extremely poor sorted

SK_I (Inclusive graphic skewness).

+1.0 to +0.3	strongly fine skewed
+0.3 to +0.1	fine skewed
+0.1 to -0.1	near symmetrical
-0.1 to -0.3	coarse skewed
-0.3 to -1.0	strongly coarse skewed

K_G (Graphic kurtosis).

less than 0.67	very platykurtic
0.67 to 0.90	platykurtic
0.90 to 1.11	mesokurtic
1.11 to 1.50	leptokurtic
1.50 to 3.00	very leptokurtic
more than 3.0	extremely leptokurtic

GRAIN SIZE DATA: EAST PARIS

TABLE 1 : BAR CORE FACIES

SAMPLE NO.	-6.5	-6.0	-5.5	-5.0	-4.5
EP 17/5 2	0.00	802.50	.01	682.32	.01
EP 22/6 8	0.00	0.00	0.00	0.00	0.00
EP 26/11 9	221.50	633.32	.01	212.73	.01
EP 26/11 1	0.00	731.01	.01	299.81	.01

TABLE 2 : BAR FRONT FACIES

SAMPLE NO.	-6.5	-6.0	-5.5	-5.0	-4.5
EP 26/11 11	0.00	0.00	0.00	134.06	.01
EP 26/11 12	0.00	0.00	0.00	192.34	.01
EP 26/11 13	0.00	0.00	0.00	0.00	0.00
EP 26/11 14	0.00	0.00	0.00	0.00	0.00
EP 26/11 3	0.00	0.00	0.00	0.00	0.00
EP 26/11 5	0.00	0.00	0.00	0.00	0.00

(TABLE 1 : cont'd.)

-4.0	-3.5	-3.0	-2.5	-2.0	-1.5
342.58	26.70	93.83	52.89	34.30	23.57
0.00	0.00	0.00	0.00	0.00	0.00
391.01	27.35	54.81	93.67	37.89	30.21
207.53	34.34	51.94	101.98	48.89	37.15

(TABLE 2 : cont'd.)

-4.0	-3.5	-3.0	-2.5	-2.0	-1.5
251.61	157.75	121.53	65.45	73.82	25.29
368.40	150.60	93.68	40.07	51.51	30.41
0.00	0.00	0.00	0.00	.49	1.61
0.00	0.00	0.00	0.00	.98	2.21
0.00	11.33	8.21	16.74	55.21	74.36
0.00	0.00	.79	.26	.52	1.27

(TABLE 1 : cont'd.)

-1.0	-0.5	0.0	0.5	1.0	1.5
22.70	23.18	38.75	46.49	64.59	106.80
.11	.35	2.08	6.77	11.18	15.98
21.39	19.01	21.81	22.48	46.31	72.47
25.39	18.04	16.07	21.48	51.48	74.33

(TABLE 2 : cont'd.)

-1.0	-0.5	0.0	0.5	1.0	1.5
26.62	15.50	27.71	47.71	26.66	12.21
28.38	36.67	55.54	79.99	34.43	12.71
3.91	6.87	12.43	16.02	7.37	2.30
3.99	7.54	13.31	17.04	6.91	3.04
79.51	63.80	53.60	44.70	36.90	82.60
2.01	13.18	26.95	44.90	80.62	180.92

(TABLE 1 : cont'd.)

2.0	2.5	3.0	3.5	4.0	PAN
49.25	26.96	0.00	0.00	0.00	58.40
6.86	2.43	.88	.39	0.00	.55
121.33	39.99	30.61	15.55	13.01	10.10
141.99	99.61	39.30	20.45	15.61	9.02

(TABLE 2 : cont'd.)

2.0	2.5	3.0	3.5	4.0	PAN
6.04	4.84	2.85	2.81	1.08	5.09
6.71	4.38	2.54	1.96	1.01	3.94
1.01	.43	.37	.06	.04	.21
1.58	.98	.57	.08	.07	.32
92.30	48.60	15.40	51.60	23.20	21.60
116.80	19.35	3.85	1.25	.81	3.34

(TABLE 1 : cont'd.)

TOTAL WT.	MEAN	ST. DEV.	SKEW.	KUR.	MEDIAN	C(PHI.1)
2495.83	-4.033	2.610	.651	1.215	-5.174	-7.25
47.58	1.078	.712	.001	1.155	1.103	-.50
2136.57	-3.441	2.529	.991	.591	-4.499	-7.50
2045.44	-3.266	3.281	.677	.714	-5.014	-7.50

(TABLE 2 : cont'd.)

TOTAL WT.	MEAN	ST. DEV.	SKEW.	KUR.	MEDIAN	C(PHI.1)
1008.64	-3.079	1.732	.469	1.271	-3.624	-6.25
1195.28	-3.091	2.056	.510	1.038	-3.878	-6.50
53.12	-.019	.812	-.078	1.230	.039	-2.00
58.62	-.005	.909	-.027	1.379	.038	-2.25
779.66	.298	1.960	.043	.799	.303	-3.75
496.82	1.127	.724	-.238	1.154	1.215	-1.00

TABLE 3 : STOSS-SIDE FACIES : CROSS-BEDDED GRAVELS

SAMPLE NO.	-6.5	-6.0	-5.5	-5.0	-4.5
EP 28/6 2	0.00	0.00	0.00	0.00	0.00
EP 28/6 7	0.00	0.00	0.00	0.00	0.00
EP 29/6 2	0.00	0.00	0.00	0.00	0.00
EP 29/6 8	0.00	0.00	0.00	0.00	0.00
EP 29/6 9	0.00	0.00	0.00	0.00	0.00
EP 29/6 13	0.00	0.00	0.00	0.00	0.00
EP 30/6 8	0.00	0.00	0.00	0.00	0.00
EP 30/6 9	0.00	0.00	0.00	0.00	0.00
EP 30/6 10	0.00	0.00	0.00	0.00	0.00
EP 30/6 13	0.00	0.00	0.00	0.00	35.83
EP 30/6 15	0.00	0.00	0.00	0.00	0.00
EP 30/6 17	0.00	0.00	0.00	0.00	0.00
EP 30/6 18	0.00	0.00	0.00	0.00	0.00
EP 30/6 19	0.00	0.00	0.00	0.00	0.00
EP 30/6 20	0.00	0.00	0.00	0.00	0.00
EP 30/6 21	0.00	0.00	0.00	0.00	0.00
EP 30/6 22	0.00	0.00	0.00	0.00	0.00
EP 30/6 23	0.00	0.00	0.00	0.00	0.00

TABLE 4 : STOSS-SIDE FACIES : IMBRICATE GRAVELS

SAMPLE NO.	-6.5	-6.0	-5.5	-5.0	-4.5
EP 30/6 1	0.00	0.00	0.00	129.67	.01
EP 30/6 7	0.00	0.00	0.00	0.00	87.41
EP 30/6 11	0.00	0.00	0.00	89.43	56.31

(TABLE 3 : cont'd.)

-4.0	-3.5	-3.0	-2.5	-2.0	-1.5
0.00	12.61	5.64	5.75	3.93	5.55
0.00	0.00	3.70	3.10	12.41	21.12
0.00	14.75	7.32	7.05	6.77	11.93
0.00	0.00	0.00	1.20	1.87	1.46
0.00	0.00	1.48	3.50	3.56	4.04
0.00	0.00	1.67	1.12	1.66	2.39
0.00	0.00	0.00	6.97	14.06	24.14
0.00	0.00	8.61	12.42	14.78	18.53
0.00	0.00	0.00	0.00	.34	.25
10.62	14.61	17.26	15.32	14.18	15.42
12.25	16.99	21.78	28.71	38.45	33.48
0.00	14.16	.01	.08	2.07	.48
12.41	.01	2.25	5.22	6.43	8.10
0.00	8.75	5.17	10.05	16.29	15.25
0.00	6.91	12.56	8.70	13.87	15.07
0.00	0.00	1.43	2.89	1.58	3.28
0.00	0.00	0.00	.81	2.04	3.36
0.00	0.00	12.83	10.69	10.26	13.12

(TABLE 4 : cont'd.)

-4.0	-3.5	-3.0	-2.5	-2.0	-1.5
502.72	91.03	106.27	110.48	79.02	56.82
21.98	20.32	40.66	26.11	26.80	25.77
89.99	73.38	37.21	51.08	34.00	25.97

(TABLE 3 : cont'd.)

-1.0	-0.5	0.0	0.5	1.0	1.5
20.54	49.93	87.20	108.87	43.94	18.89
35.74	62.68	77.21	50.29	22.55	12.77
20.56	42.57	62.06	82.22	71.10	26.03
2.21	4.76	11.81	20.32	37.81	82.23
4.21	7.93	14.44	20.89	34.11	77.50
3.55	11.67	29.89	62.37	61.83	48.82
35.59	74.13	78.05	55.73	27.12	12.31
20.24	24.31	37.05	51.79	48.31	18.41
.34	.93	3.31	11.02	28.70	31.70
18.29	32.50	50.29	66.74	61.66	47.23
41.52	46.20	45.88	47.43	40.57	33.70
1.70	5.40	22.96	50.34	66.94	35.86
12.38	13.99	26.25	43.07	50.10	43.16
17.77	18.09	25.97	53.46	79.45	43.76
16.88	28.46	34.14	45.13	54.10	29.33
3.74	7.70	11.95	15.16	17.55	35.38
8.76	16.23	21.85	26.43	32.22	62.75
20.79	33.22	43.70	51.63	41.72	20.99

(TABLE 4 : cont'd.)

-1.0	-0.5	0.0	0.5	1.0	1.5
49.70	73.51	104.50	135.25	108.26	130.52
32.28	38.20	46.27	42.91	26.12	12.17
22.55	24.19	40.54	70.86	51.36	33.12

(TABLE 3: cont'd.)

2.0	2.5	3.0	3.5	4.0	PAN
5.13	3.05	1.35	0.00	0.00	4.52
3.46	2.00	.84	0.00	0.00	2.11
3.61	1.67	.67	0.00	0.00	2.13
26.03	25.91	10.02	0.00	0.00	.83
27.92	9.94	7.49	0.00	0.00	6.01
26.91	12.66	3.69	1.33	.88	2.02
2.72	1.47	.60	.40	.41	.86
5.24	3.66	1.53	.77	.68	1.66
7.37	11.06	8.84	2.10	.78	1.63
18.53	10.51	4.35	2.46	1.43	3.03
19.05	9.31	3.18	1.35	.88	1.97
8.02	2.98	1.18	.64	.64	1.84
15.58	5.27	2.41	1.01	.55	1.02
11.05	4.00	1.22	.52	.45	1.29
10.27	3.95	1.39	.62	.48	1.42
8.89	2.27	1.20	.59	.33	.64
32.60	15.30	7.78	2.57	1.01	1.61
13.50	4.89	1.25	.49	.41	.99

(TABLE 4 : cont'd.)

2.0	2.5	3.0	3.5	4.0	PAN
48.33	12.86	6.01	3.82	4.42	20.55
2.82	1.60	.72	.47	.47	1.57
18.26	8.83	3.48	1.68	1.31	3.47

(TABLE 3 : cont'd)

TOTAL WT.	MEAN	ST. DEV.	SKEW.	KUR.	MEDIAN	C(PHI.1)
376.90	-.088	1.061	-.246	1.740	-.015	-5.50
309.98	-.441	.964	-.059	1.199	-.395	-5.25
360.44	-.127	1.218	-.347	1.391	.044	-5.50
226.46	1.174	.879	-.086	1.303	1.193	-4.00
223.02	.924	1.132	-.292	1.653	1.112	-4.50
272.46	.703	.903	.032	1.109	.677	-3.75
334.56	-.457	.944	-.066	1.161	-.421	-4.75
267.99	-.316	1.329	-.305	.970	-.026	-5.50
108.37	1.329	.895	.265	1.067	1.147	-.75
440.26	-.696	2.115	-.418	.998	-.042	-5.00
442.70	-.789	1.753	-.080	.881	-.695	-5.25
215.30	.514	1.194	-.341	2.431	.578	-4.25
249.21	.165	1.476	-.380	1.434	.436	-4.50
312.54	-.059	1.394	-.446	1.055	.364	-4.75
283.28	-.266	1.475	-.331	1.070	.056	-4.50
114.58	.520	1.130	-.385	1.130	.772	-4.00
235.32	.850	1.122	-.227	1.084	1.047	-4.00
280.48	-.218	1.353	-.212	1.185	-.050	-4.50

(TABLE 4 : cont'd.)

TOTAL WT.	MEAN	ST. DEV.	SKEW.	KUR.	MEDIAN	C(PHI.1)
1773.75	-2.118	2.291	.325	.644	-2.741	-6.25
454.65	-2.106	2.074	-.065	.657	-1.922	-6.00
737.02	-2.332	2.351	.259	.642	-2.783	-6.00

TABLE 5 : BAR TOP FACIES : SANDS

SAMPLE NO.	-6.5	-6.0	-5.5	-5.0	-4.5
EP 29/6 7	0.00	0.00	0.00	0.00	0.00

TABLE 6 : BAR TOP FACIES : GRAVELS

SAMPLE NO.	-6.5	-6.0	-5.5	-5.0	-4.5
EP 30/6 12	0.00	0.00	0.00	0.00	68.77
EP 30/6 14	0.00	0.00	0.00	0.00	177.79
EP 30/6 16	0.00	0.00	0.00	0.00	0.00

TABLE 7 : SIDE-CHANNEL FACIES : TROUGH CROSS-BEDS

SAMPLE NO.	-6.5	-6.0	-5.5	-5.0	-4.5
EP 17/5 1	0.00	0.00	0.00	0.00	0.00
EP 22/6 1	0.00	0.00	0.00	0.00	0.00
EP 22/6 2	0.00	0.00	0.00	0.00	0.00
EP 22/6 9	0.00	0.00	0.00	0.00	0.00
EP 22/6 11	0.00	0.00	0.00	0.00	0.00
EP 22/6 12	0.00	0.00	0.00	0.00	0.00
EP 28/6 4	0.00	0.00	0.00	0.00	0.00
EP 28/6 5	0.00	0.00	0.00	0.00	0.00
EP 28/6 6	0.00	0.00	0.00	0.00	0.00
EP 28/6 8	0.00	0.00	0.00	0.00	0.00
EP 29/6 1	0.00	0.00	0.00	0.00	0.00
EP 10/9 7	0.00	0.00	0.00	0.00	0.00

(TABLE 5 : cont'd.)

-4.0	-3.5	-3.0	-2.5	-2.0	-1.5
0.00	0.00	0.00	0.00	0.00	.12

(TABLE 6 : cont'd.)

-4.0	-3.5	-3.0	-2.5	-2.0	-1.5
30.52	26.33	27.92	30.14	34.08	32.45
78.85	8.44	3(.54	38.02	30.10	25.11
82.75	113.47	97.95	80.56	54.63	35.11

(TABLE 7 : cont'd.)

-4.0	-3.5	-3.0	-2.5	-2.0	-1.5
0.00	61.40	118.75	241.00	334.00	423.00
0.00	0.00	1.51	1.91	1.43	1.90
0.00	7.09	.66	1.83	1.00	.65
0.00	0.00	0.00	0.00	0.00	.25
0.00	0.00	0.00	2.30	4.54	7.63
0.00	0.00	0.00	0.00	0.00	0.00
0.00	5.19	14.63	29.99	32.53	42.88
0.00	0.00	0.00	.67	1.92	2.40
0.00	2.63	.00	2.56	3.21	4.47
0.00	6.82	1.67	11.08	13.30	21.59
0.00	0.00	4.46	11.29	12.31	16.75
13.44	4.38	4.36	10.36	13.78	11.62

(TABLE 5 : cont'd.)

-1.0	-0.5	0.0	0.5	1.0	1.5
.13	.13	.31	1.64	5.60	22.41

(TABLE 6 : cont'd.)

-1.0	-0.5	0.0	0.5	1.0	1.5
31.22	34.48	29.89	26.22	18.47	11.02
32.81	33.89	57.99	69.98	52.79	36.88
25.42	19.59	20.85	27.09	26.93	32.63

(TABLE 7 : cont'd.)

-1.0	-0.5	0.0	0.5	1.0	1.5
518.80	981.07	1133.35	1340.47	1279.00	697.34
3.58	13.30	31.05	53.87	74.92	149.05
.88	1.40	3.86	11.38	22.60	49.62
.44	.60	1.38	2.95	4.43	11.72
13.98	15.06	19.91	23.40	34.44	91.95
.29	.40	.68	1.56	3.59	15.30
60.66	62.89	57.89	53.47	49.09	48.54
6.62	20.92	47.11	81.77	74.14	45.00
9.00	19.14	34.27	51.83	53.77	46.56
35.40	40.83	53.98	54.56	50.23	19.99
16.66	18.43	24.91	36.12	29.04	16.69
15.01	21.13	27.27	35.30	41.80	59.95

(TABLE 5 : cont'd.)

TOTAL WT.	MEAN	ST. DEV.	SKEW.	KUR.	MEDIAN	C(PHI.1)
62.20	1.545	.543	.037	1.068	1.518	0.00

(TABLE 6 : cont'd.)

TOTAL WT.	MEAN	ST. DEV.	SKEW.	KUR.	MEDIAN	C(PHI.1)
409.38	-2.249	2.003	.023	.718	-2.192	-5.50
702.73	-2.108	2.270	.102	.563	-2.206	-6.25
659.82	-2.079	1.994	.488	.889	-2.778	-5.75

(TABLE 7 : cont'd.)

TOTAL WT.	MEAN	ST. DEV.	SKEW.	KUR.	MEDIAN	C(PHI.1)
7601.02	-.162	1.254	-.205	1.079	-.005	-3.50
494.59	1.114	.855	-.178	1.091	1.214	-2.00
128.81	.993	1.273	-.436	2.716	1.132	-4.00
36.21	1.325	1.079	.114	1.924	1.344	-1.25
303.60	.888	1.155	-.359	1.180	1.166	-2.50
36.68	1.395	.570	-.064	1.330	1.386	-1.00
476.13	-.591	1.413	-.040	.878	-.585	-5.00
319.15	.516	.873	.065	1.187	.489	-1.75
259.10	.475	1.003	-.114	1.107	.523	-3.50
320.05	-.336	1.202	-.173	1.002	-.228	-5.00
195.42	-.382	1.343	-.248	.878	-.143	-5.00
638.64	1.248	1.483	-.563	1.287	1.721	-4.50

(TABLE 5 : cont'd.)

2.0	2.5	3.0	3.5	4.0	PAN
20.64	8.82	1.42	.33	.15	.50

(TABLE 6 : cont'd.)

2.0	2.5	3.0	3.5	4.0	PAN
2.96	1.34	.81	.59	.56	1.61
15.77	6.57	2.55	1.30	1.07	2.28
25.10	10.20	2.96	1.22	.91	2.45

(TABLE 7 : cont'd.)

2.0	2.5	3.0	3.5	4.0	PAN
295.49	100.92	29.94	13.06	0.00	33.43
103.79	41.58	0.00	0.00	0.00	16.70
17.73	6.49	2.02	0.00	0.00	1.60
7.81	3.76	0.00	0.00	0.00	2.87
56.25	21.24	0.00	0.00	0.00	12.90
11.52	2.58	.36	.10	0.00	.30
10.04	2.58	1.37	0.00	0.00	4.38
19.52	12.93	3.03	0.00	0.00	3.12
18.55	7.74	2.43	0.00	0.00	2.94
6.12	1.50	0.00	0.00	0.00	2.98
4.75	1.51	.60	0.00	0.00	1.90
137.82	186.96	44.84	7.45	1.53	1.64

TABLE 8 : SIDE CHANNEL FACIES : PLANAR LAMINATION

SAMPLE NO.	-6.5	-6.0	-5.5	-5.0	-4.5
EP 10/9 1	0.00	0.00	0.00	0.00	0.00
EP 10/9 2	0.00	0.00	0.00	0.00	0.00
EP 10/9 3	0.00	0.00	0.00	0.00	0.00
EP 10/9 4	0.00	0.00	0.00	0.00	0.00
EP 10/9 5	0.00	0.00	0.00	0.00	0.00
EP 10/9 9	0.00	0.00	0.00	0.00	0.00
EP 10/9 10	0.00	0.00	0.00	0.00	0.00
EP 10/9 12	0.00	0.00	0.00	0.00	0.00

TABLE 9 : SIDE CHANNEL FACIES : RIPPLED SANDS

SAMPLE NO.	-6.5	-6.0	-5.5	-5.0	-4.5
EP 22/6 3	0.00	0.00	0.00	0.00	0.00
EP 22/6 7	0.00	0.00	0.00	0.00	0.00
EP 22/6 10	0.00	0.00	0.00	0.00	0.00
EP 10/9 8	0.00	0.00	0.00	0.00	0.00
EP 10/9 11	0.00	0.00	0.00	0.00	0.00

TABLE 10 : SHALLOW BRAIDED STREAM FACIES : IMBRICATE GRAVEL

SAMPLE NO.	-6.5	-6.0	-5.5	-5.0	-4.5
EP 8/9 11	0.00	0.00	0.00	173.43	120.31
EP 8/9 12	0.00	0.00	0.00	133.81	270.88
EP 8/9 13	0.00	0.00	0.00	45.34	61.48

(TABLE 8 : cont'd.)

-4.0	-3.5	-3.0	-2.5	-2.0	-1.5
0.00	0.00	0.00	0.00	0.00	0.00
0.00	0.00	0.00	0.00	0.00	0.00
0.00	0.00	0.00	0.00	0.00	0.00
0.00	0.00	0.00	0.00	0.00	.20
0.00	0.00	0.00	0.00	0.00	0.00
0.00	0.00	0.00	0.00	0.00	.16
0.00	0.00	0.00	0.00	.11	.06
0.00	0.00	2.17	.69	.00	.12

(TABLE 9 : cont'd.)

-4.0	-3.5	-3.0	-2.5	-2.0	-1.5
0.00	0.00	0.00	0.00	0.00	0.00
0.00	0.00	0.00	0.00	0.00	0.00
0.00	0.00	0.00	0.00	0.00	0.00
0.00	0.00	0.00	.78	.19	.47
0.00	0.00	0.00	1.20	1.05	2.00

(TABLE 10 : cont'd.)

-4.0	-3.5	-3.0	-2.5	-2.0	-1.5
169.83	146.83	74.21	102.80	71.01	56.97
507.93	264.37	110.47	102.40	99.91	63.36
93.97	95.80	110.71	91.48	62.68	48.21

(TABLE 8 : cont'd.)

-1.0	-0.5	0.0	0.5	1.0	1.5
0.00	0.00	.01	.01	.03	.41
0.00	.01	.00	.02	.06	.59
0.00	0.00	.01	.01	.03	.22
.31	1.14	1.18	3.09	9.61	73.95
0.00	.01	.02	.06	.44	4.34
.18	.06	.08	.12	.22	.50
.20	.09	.77	1.98	3.20	9.95
.80	.56	1.18	2.99	6.90	23.97

(TABLE 9 : cont'd.)

-1.0	-0.5	0.0	0.5	1.0	1.5
.11	.10	.05	.24	1.45	12.27
.11	.01	.09	.17	.22	.51
0.00	0.00	0.00	0.00	.01	.00
.08	3.79	8.03	17.80	33.40	88.13
2.91	4.96	6.67	12.12	19.33	49.75

(TABLE 10 : cont'd.)

-1.0	-0.5	0.0	0.5	1.0	1.5
46.55	48.19	79.45	93.68	102.70	66.21
61.48	72.55	81.56	93.63	146.61	130.41
35.27	30.47	86.91	44.93	48.01	102.05

(TABLE 8 : cont'd.)

2.0	2.5	3.0	3.5	4.0	PAN
3.59	13.53	13.79	6.37	1.92	.59
4.39	15.98	12.42	4.64	1.40	.51
2.36	10.10	9.87	5.34	1.86	.53
148.12	67.78	20.33	6.84	2.20	.88
24.24	25.33	5.81	1.13	.25	.09
3.24	21.39	10.55	2.89	.68	.15
39.57	136.83	86.60	21.13	5.83	2.17
61.89	88.41	42.09	14.14	4.39	3.07

(TABLE 9 : cont'd.)

2.0	2.5	3.0	3.5	4.0	PAN
18.88	3.50	.29	0.00	0.00	.47
7.25	18.29	27.91	12.36	0.00	5.54
.03	.47	3.78	12.34	17.59	25.48
109.72	115.81	46.03	10.20	2.07	.17
99.28	126.33	47.02	13.33	4.75	3.31

(TABLE 10 : cont'd.)

2.0	2.5	3.0	3.5	4.0	PAN
42.68	27.83	10.21	5.31	3.48	5.49
129.23	73.93	38.81	16.66	6.01	5.05
97.23	64.16	26.36	11.55	2.48	3.49

(TABLE 8 : cont'd.)

TOTAL WT.	MEAN	ST. DEV.	SKEW.	KUR.	MEDIAN	C(PHI.1)
40.25	2.624	.566	.085	1.067	2.592	1.50
40.02	2.508	.522	.119	1.067	2.467	1.25
30.33	2.668	.588	.121	1.051	2.623	1.50
335.63	1.783	.543	.112	1.164	1.764	0.00
61.74	2.029	.449	.017	1.034	2.034	1.00
40.22	2.426	.463	.166	1.212	2.363	-.50
308.49	2.386	.525	.058	1.188	2.359	.50
253.37	2.143	.697	-.035	1.271	2.144	-2.75

(TABLE 9 : cont'd.)

TOTAL WT.	MEAN	ST. DEV.	SKEW.	KUR.	MEDIAN	C(PHI.1)
37.36	1.579	.405	-.046	.995	1.618	.25
72.46	2.672	.670	.101	1.404	2.672	1.25
59.70	3.800	.519	-.252	.852	3.876	2.50
436.67	1.760	.758	-.128	1.060	1.799	-.50
394.01	1.891	.816	-.247	1.384	1.989	-1.50

(TABLE 10 : cont'd.)

TOTAL WT.	MEAN	ST. DEV.	SKEW.	KUR.	MEDIAN	C(PHI.1)
1447.17	-2.304	2.423	.289	.677	-2.810	-5.25
2409.06	-2.285	2.487	.559	.653	-3.375	-5.25
1162.58	-1.425	2.523	.172	.647	-1.794	-5.25

TABLE 11 : SHALLOW BRAIDED STREAM FACIES : TABULAR CROSS BEDDED GRAVELS

SAMPLE NO.	-6.5	-6.0	-5.5	-5.0	-4.5
EP 29/6 4	0.00	0.00	0.00	0.00	0.00
EP 29/6 5	0.00	0.00	0.00	0.00	0.00
EP 29/6 12	0.00	0.00	0.00	0.00	0.00
EP 30/6 3	0.00	0.00	0.00	0.00	0.00
EP 30/6 4	0.00	0.00	0.00	0.00	0.00
EP 30/6 5	0.00	0.00	0.00	0.00	0.00
EP 30/6 6	0.00	0.00	0.00	0.00	0.00
EP 8/9 1	0.00	0.00	0.00	0.00	0.00

TABLE 12 : SHALLOW BRAIDED STREAM FACIES : CHANNEL INFILLING

SAMPLE NO.	-6.5	-6.0	-5.5	-5.0	-4.5
EP 22/6 4	0.00	0.00	0.00	0.00	0.00
EP 22/6 6	0.00	0.00	0.00	0.00	0.00
EP 28/6 1	0.00	0.00	0.00	0.00	0.00
EP 28/6 3	0.00	0.00	0.00	0.00	0.00

TABLE 13:SHALLOW BRAIDED STREAM FACIES : SANDS

SAMPLE NO.	-6.5	-6.0	-5.5	-5.0	-4.5
EP 29/6 3	0.00	0.00	0.00	0.00	0.00
EP 29/6 6	0.00	0.00	0.00	0.00	0.00
EP 29/6 10	0.00	0.00	0.00	0.00	0.00
EP 29/6 11	0.00	0.00	0.00	0.00	0.00
EP 30/6 2	0.00	0.00	0.00	0.00	0.00

(TABLE : 11 cont'd.)

-4.0	-3.5	-3.0	-2.5	-2.0	-1.5
0.00	0.00	0.00	3.16	7.02	11.75
0.00	20.54	9.98	11.16	19.15	19.65
0.00	3.66	1.71	19.54	53.74	100.40
26.17	18.19	2(.81	31.27	24.99	21.13
13.80	15.07	13.16	22.87	35.50	57.72
22.42	23.50	35.90	98.99	125.01	71.17
206.11	68.27	49.38	34.70	29.10	16.54
17.13	6.56	4.04	10.86	10.70	8.90

(TABLE : 12 cont'd.)

-4.0	-3.5	-3.0	-2.5	-2.0	-1.5
0.00	53.45	20.47	28.11	26.98	30.94
0.00	51.28	6.09	18.29	27.39	23.41
0.00	13.17	5.78	13.73	27.92	43.69
0.00	7.15	14.15	64.42	117.93	108.23

(TABLE : 13 cont'd.)

-4.0	-3.5	-3.0	-2.5	-2.0	-1.5
0.00	0.00	0.00	0.00	0.00	.46
0.00	0.00	0.00	0.00	.30	1.20
0.00	0.00	0.00	0.00	0.00	.08
0.00	0.00	0.00	7.51	18.85	38.60
0.00	0.00	0.00	.48	2.24	4.05

(TABLE 11 : cont'd.)

-1.0	-0.5	0.0	0.5	1.0	1.5
22.88	29.83	33.46	36.78	26.09	8.02
24.58	30.98	48.97	67.41	56.24	47.18
144.68	135.43	90.99	68.03	39.13	23.93
21.05	21.40	18.14	29.26	51.22	44.45
63.93	55.93	27.34	16.40	8.77	4.97
25.55	8.88	4.54	4.60	3.34	2.59
13.79	14.82	11.23	7.80	4.97	4.05
11.99	214.88	49.48	77.20	88.07	78.35

(TABLE 12 : cont'd.)

-1.0	-0.5	0.0	0.5	1.0	1.5
36.48	50.72	56.44	55.00	39.99	32.94
21.89	31.90	30.21	32.36	15.76	8.12
50.45	52.92	38.83	26.24	16.04	8.69
79.07	79.23	78.66	99.20	69.05	26.28

(TABLE 13 : cont'd.)

-1.0	-0.5	0.0	0.5	1.0	1.5
.47	.79	1.72	3.25	5.40	12.93
6.94	16.54	27.19	30.69	25.89	28.62
.24	.43	.89	3.36	14.02	39.81
63.09	67.64	43.65	27.24	11.73	10.45
5.30	7.31	9.45	12.76	24.13	63.73

(TABLE 11 : cont'd.)

2.0	2.5	3.0	3.5	4.0	PAN
1.95	1.50	.75	.50	.43	1.21
11.20	3.70	1.71	1.08	.94	2.34
18.32	6.53	2.76	1.74	1.69	6.11
15.59	7.27	2.13	1.25	1.21	5.90
2.23	1.34	.80	.60	.72	2.17
1.64	1.25	.83	.71	.97	4.24
2.58	1.54	.76	.47	.56	1.35
28.84	7.81	3.39	1.36	1.03	2.31

(TABLE 12 : cont'd.)

2.0	2.5	3.0	3.5	4.0	PAN
11.21	3.01	1.15	0.00	0.00	3.50
3.68	2.05	1.14	0.00	0.00	6.36
2.40	1.30	.88	0.00	0.00	3.96
4.41	4.41	2.56	0.00	0.00	10.97

(TABLE 13 : cont'd.)

2.0	2.5	3.0	3.5	4.0	PAN
16.38	25.79	20.30	6.38	3.66	6.71
25.22	47.96	10.63	2.15	1.03	3.01
14.63	16.60	18.09	2.07	.64	1.09
12.36	10.10	2.79	1.11	.86	3.70
58.56	99.41	19.88	5.16	2.43	6.47

(TABLE 11 : cont'd.)

TOTAL WT.	MEAN	ST. DEV.	SKEW.	KUR.	MEDIAN	C(PHI.1)
185.33	-.285	1.022	-.082	.994	-.231	-4.00
376.81	-.302	1.553	-.353	1.058	.025	-4.00
718.39	-.766	1.148	.181	1.122	-.869	-4.25
361.43	-.851	2.031	-.164	.725	-.600	-4.50
343.32	-1.474	1.305	-.087	1.250	-1.394	-4.75
436.13	-2.364	.979	.054	1.552	-2.351	-4.75
468.02	-3.315	1.302	.645	1.143	-3.796	-4.50
622.90	-.005	1.214	.095	1.161	-.233	-4.50

(TABLE 12 : cont'd.)

TOTAL WT.	MEAN	ST. DEV.	SKEW.	KUR.	MEDIAN	C(PHI.1)
450.39	-1.005	1.741	-.201	.820	-.716	-6.00
279.93	-1.458	1.792	-.104	.823	-1.192	-6.00
306.00	-1.008	1.273	-.014	1.134	-1.017	-5.00
765.72	-.973	1.321	.094	.764	-1.051	-5.50

(TABLE 13 : cont'd.)

TOTAL WT.	MEAN	ST. DEV.	SKEW.	KUR.	MEDIAN	C(PHI.1)
104.24	2.130	1.039	-.068	1.270	2.208	-1.00
227.37	1.031	1.202	-.077	.749	1.086	-1.50
111.95	1.678	.780	.306	.827	1.464	-2.50
319.68	-.620	1.233	.253	1.299	-.765	-4.25
321.36	1.627	.984	-.300	1.308	1.767	-4.50

GRAIN SIZE DATA: WEST PARIS

TABLE 14 : BAR FRONT FACIES : SAND DRAPE (a)

SAMPLE NO.	-6.5	-6.0	-5.5	-5.0	-4.5
WP 2/9 1	0.00	0.00	0.00	0.00	0.00
WP 2/9 2	0.00	0.00	0.00	0.00	0.00
WP 2/9 3	0.00	0.00	0.00	0.00	0.00
WP 2/9 4	0.00	0.00	0.00	0.00	0.00

TABLE 15 : BAR FRONT FACIES : SAND DRAPE (b)

SAMPLE NO.	-6.5	-6.0	-5.5	-5.0	-4.5
WP 22/6 1	0.00	0.00	0.00	0.00	0.00
WP 22/6 2	0.00	0.00	0.00	0.00	0.00
WP 22/6 3	0.00	0.00	0.00	0.00	0.00
WP 22/6 5	0.00	0.00	0.00	0.00	0.00
WP 22/6 6	0.00	0.00	0.00	0.00	0.00
WP 22/6 7	0.00	0.00	0.00	0.00	0.00
WP 22/6 1≠	0.00	0.00	0.00	0.00	0.00
WP 22/6 2≠	0.00	0.00	0.00	0.00	0.00
WP 22/6 3≠	0.00	0.00	0.00	0.00	0.00

TABLE 16 : BAR FRONT FACIES : SAND DRAPE (c)

SAMPLE NO.	-6.5	-6.0	-5.5	-5.0	-4.5
WP 30/10 1	0.00	0.00	0.00	0.00	0.00
WP 30/10 3	0.00	0.00	0.00	0.00	0.00
WP 30/10 4	0.00	0.00	0.00	0.00	0.00
WP 30/10 5	0.00	0.00	0.00	0.00	0.00
WP 30/10 6	0.00	0.00	0.00	0.00	0.00
WP 30/7 10	0.00	0.00	0.00	0.00	0.00
WP 30/10 8	0.00	0.00	0.00	0.00	0.00

(TABLE 14 : cont'd.)

-4.0	-3.5	-3.0	-2.5	-2.0	-1.5
0.00	0.00	0.00	0.00	0.00	.22
0.00	0.00	0.00	0.00	0.00	0.00
0.00	0.00	0.00	0.00	0.00	0.00
0.00	0.00	0.00	0.00	0.00	0.00

(TABLE 15 : cont'd.)

-4.0	-3.5	-3.0	-2.5	-2.0	-1.5
0.00	29.15	7.88	14.25	8.95	12.07
0.00	0.00	0.00	0.00	0.00	.26
0.00	0.00	0.00	0.00	0.00	0.00
0.00	0.00	0.00	0.00	.18	.05
0.00	0.00	0.00	0.00	0.00	0.00
0.00	0.00	0.00	0.00	0.00	0.00
0.00	0.00	0.00	0.00	0.00	.13
0.00	0.00	0.00	0.00	0.00	.14
0.00	0.00	0.00	0.00	0.00	0.00

(TABLE 16 : cont'd.)

-4.0	-3.5	-3.0	-2.5	-2.0	-1.5
0.00	3.38	1.33	1.61	3.87	8.22
0.00	0.00	0.00	0.00	0.00	0.00
0.00	0.00	0.00	0.00	0.00	0.00
0.00	0.00	0.00	0.00	0.00	0.00
0.00	0.00	0.00	0.00	.08	.05
0.00	0.00	0.00	0.00	0.00	0.00
0.00	0.00	0.00	0.00	0.00	.26

(TABLE 14 : cont'd.)

-1.0	-0.5	0.0	0.5	1.0	1.5
.20	.53	1.16	2.69	5.92	15.52
0.00	0.00	.01	.02	.28	4.47
.13	.28	.61	2.68	15.66	45.97
.03	.24	1.14	2.98	8.65	16.58

(TABLE 15: cont'd.)

-1.0	-0.5	0.0	0.5	1.0	1.5
15.26	19.73	23.10	34.50	39.74	48.41
.16	.19	.46	.84	3.00	23.99
.04	.01	.01	.03	.28	6.44
.20	.40	.76	1.73	11.09	42.04
0.00	0.00	.02	.07	.34	1.69
0.00	0.00	0.00	0.00	.01	.04
1.07	3.51	6.67	9.99	13.19	20.65
.14	.30	.48	1.16	3.23	26.77
0.00	0.00	0.00	0.00	.01	.29

(TABLE 16 : cont'd.)

-1.0	-0.5	0.0	0.5	1.0	1.5
16.19	33.91	44.87	80.43	163.92	348.10
0.00	.02	.05	.33	1.28	5.58
0.00	.01	.15	.42	1.28	6.00
0.00	0.00	.02	.28	1.23	3.96
.46	.87	2.80	7.22	19.89	104.18
0.00	0.00	.01	.06	.42	2.73
.81	1.81	15.57	61.81	127.82	213.95

(TABLE 14 : cont'd.)

2.0	2.5	3.0	3.5	4.0	PAN
27.56	24.43	11.78	5.13	2.59	2.27
18.36	21.01	9.90	4.11	1.84	1.57
15.55	4.73	1.48	.56	.28	.61
13.07	9.12	3.95	1.88	1.00	1.01

(TABLE 15 : cont'd)

2.0	2.5	3.0	3.5	4.0	PAN
23.91	10.52	3.07	0.00	0.00	3.95
42.74	18.87	2.55	.58	.29	.48
21.95	31.10	12.42	3.27	.95	.61
40.95	24.88	7.25	2.25	.77	.97
4.84	18.79	24.29	12.19	7.74	6.37
.33	4.69	16.73	21.13	18.39	20.69
15.23	7.49	1.87	.48	.23	.53
44.27	17.17	4.04	1.06	.39	.45
1.73	7.38	21.34	18.65	15.67	14.38

(TABLE 16 : cont'd.)

2.0	2.5	3.0	3.5	4.0	PAN
186.33	55.89	15.11	4.10	2.00	3.44
10.04	9.59	3.97	1.33	.72	.53
10.12	7.45	2.23	.96	.72	.52
5.91	7.88	6.61	4.25	2.84	1.44
199.01	122.47	28.05	16.83	20.18	37.01
4.78	4.95	4.21	4.42	3.73	2.89
175.15	120.19	31.96	5.56	1.82	3.33

(TABLE 14 : cont'd.)

TOTAL WT.	MEAN	ST. DEV.	SKEW.	KUR.	MEDIAN	C(PHI.1)
100.00	1.949	.844	.041	1.250	1.931	-4.00
61.57	2.234	.657	.180	1.149	2.182	1.00
88.54	1.299	.515	.132	1.478	1.271	-4.50
59.65	1.571	.853	.141	1.156	1.508	-.25

(TABLE 15 : cont'd.)

TOTAL WT.	MEAN	ST. DEV.	SKEW.	KUR.	MEDIAN	C(PHI.1)
294.49	-.320	1.913	-.386	.918	.244	-5.00
94.41	1.710	.476	-.000	1.030	1.714	0.00
77.11	2.160	.553	.032	1.126	2.157	.75
133.52	1.668	.631	.102	1.069	1.626	0.00
76.34	2.839	.753	.157	1.063	2.756	1.00
82.01	3.459	.664	-.023	.787	3.454	2.00
81.04	1.049	.920	-.151	1.003	1.144	-1.00
99.60	1.701	.510	.048	1.125	1.699	0.00
79.45	3.292	.708	.055	.846	3.241	1.75

(TABLE 16 : cont'd.)

TOTAL WT.	MEAN	ST. DEV.	SKEW.	KUR.	MEDIAN	C(PHI.1)
972.70	1.082	.850	-.243	1.382	1.185	-2.00
33.44	1.984	.686	.099	1.129	1.971	.50
29.86	1.856	.689	.113	1.241	1.849	.25
34.42	2.409	.907	.073	.974	2.369	.50
559.10	1.955	.848	.301	1.574	1.862	.25
28.20	2.685	1.005	.058	.816	2.637	.75
760.04	1.412	.743	-.005	.996	1.402	-.25

TABLE 17 : BAR FRONT FACIES : GRAVEL CROSS-STRATA

SAMPLE NO.	-6.5	-6.0	-5.5	-5.0	-4.5
WP 26/11 1	0.00	0.00	0.00	116.01	.01
WP 26/11 3	0.00	0.00	0.00	65.21	.01

TABLE 18 : BAR FRONT FACIES : IMBRICATE GRAVELS

SAMPLE NO.	-6.5	-6.0	-5.5	-5.0	-4.5
WP 26/11 2	0.00	0.00	0.00	120.91	.01
WP 26/11 4	0.00	0.00	0.00	140.01	.01

TABLE 19 : LATERAL ACCRETION FACIES : GRAVELS

SAMPLE NO.	-6.5	-6.0	-5.5	-5.0	-4.5
WP 10/5 9	0.00	0.00	0.00	0.00	0.00
WP 10/5 10	0.00	0.00	0.00	0.00	0.00
WP 10/5 11	0.00	0.00	0.00	0.00	0.00
WP 10/5 12	0.00	0.00	0.00	0.00	0.00
WP 12/7 1	0.00	0.00	0.00	0.00	0.00
WP 12/7 2	0.00	0.00	0.00	0.00	0.00
WP 15/7 6	0.00	0.00	0.00	0.00	0.00
WP 20/7 3	0.00	0.00	0.00	31.68	58.70
WP 20/7 5	0.00	0.00	0.00	0.00	56.01
WP 20/7 6	0.00	0.00	0.00	0.00	0.00
WP 30/7 9	0.00	0.00	204.09	582.38	331.52
WP 30/7 10	0.00	199.83	368.42	275.10	499.75

(TABLE 17 : cont'd.)

-4.0	-3.5	-3.0	-2.5	-2.0	-1.5
217.21	63.36	56.67	23.34	30.44	16.99
120.34	38.58	26.86	13.73	18.70	10.10

(TABLE 18 : cont'd.)

-4.0	-3.5	-3.0	-2.5	-2.0	-1.5
190.87	116.42	81.45	92.51	85.38	77.71
201.10	136.91	92.34	101.10	67.91	89.99

(TABLE 19 : cont'd.)

-4.0	-3.5	-3.0	-2.5	-2.0	-1.5
0.00	208.40	48.80	42.80	51.23	45.76
0.00	157.30	30.40	36.29	39.90	31.31
0.00	69.58	14.40	11.29	13.98	8.68
0.00	42.77	16.47	12.21	7.34	7.40
0.00	226.80	66.02	59.29	48.65	33.57
0.00	195.96	59.69	28.12	15.96	9.73
49.74	62.22	83.82	86.72	67.75	54.81
242.49	110.98	65.52	40.92	21.06	18.44
80.20	122.39	114.42	71.19	48.91	28.33
0.00	68.20	58.39	67.80	52.92	56.79
415.67	209.36	245.36	184.62	92.47	63.18
381.43	185.20	278.02	234.83	116.19	56.14

(TABLE 17 : cont'd.)

-1.0	-0.5	0.0	0.5	1.0	1.5
17.92	22.04	33.90	52.83	21.94	7.61
9.70	12.08	35.82	26.29	11.23	3.34

(TABLE 18 : cont'd.)

-1.0	-0.5	0.0	0.5	1.0	1.5
65.55	61.04	63.03	134.31	109.32	56.61
75.54	71.11	68.01	154.70	90.53	21.84

(TABLE 19 : cont'd.)

-1.0	-0.5	0.0	0.5	1.0	1.5
43.92	40.88	38.75	43.38	48.61	45.42
30.08	27.03	23.48	20.33	18.57	16.35
6.85	6.88	9.75	21.73	44.83	60.43
11.59	15.00	18.20	24.74	25.05	20.51
28.14	24.01	23.82	25.00	29.61	57.33
9.95	13.42	38.25	88.09	125.39	58.77
43.38	38.19	43.35	62.20	62.97	37.90
17.72	18.57	25.57	23.54	38.15	86.00
26.10	24.06	32.61	53.18	74.14	83.71
70.33	87.20	114.51	116.76	64.48	39.40
46.28	42.66	47.94	61.95	87.26	161.79
34.03	28.72	31.91	47.38	124.12	261.48

(TABLE 17 : cont'd.)

2.0	2.5	3.0	3.5	4.0	PAN
4.01	1.44	1.63	.92	.81	2.45
2.95	1.55	.61	.66	1.00	2.01

(TABLE 18 : cont'd.)

2.0	2.5	3.0	3.5	4.0	PAN
21.62	10.06	8.07	6.71	5.71	6.09
8.67	4.04	2.68	2.21	1.97	3.01

(TABLE 19 : cont'd.)

2.0	2.5	3.0	3.5	4.0	PAN
24.23	12.04	4.27	0.00	0.00	4.31
6.37	2.96	1.38	0.00	0.00	2.05
28.09	12.02	3.88	0.00	0.00	2.59
10.43	5.15	1.77	0.00	0.00	1.79
43.71	26.31	12.87	7.71	5.69	14.07
18.77	7.72	3.05	1.24	.80	1.78
13.92	6.11	2.25	1.08	.87	1.86
42.34	15.36	5.04	2.20	1.57	3.52
36.31	14.85	6.55	3.44	2.60	6.28
19.05	7.26	2.85	1.34	1.14	2.36
146.43	67.18	22.90	9.00	5.48	9.08
115.16	34.49	9.48	4.02	2.84	7.95

(TABLE 17 : cont'd.)

TOTAL WT.	MEAN	ST. DEV.	SKEW.	KUR.	MEDIAN	C(PHI.1)
691.53	-3.058	2.101	.523	.906	-3.901	-6.25
400.77	-3.006	2.110	.494	.763	-3.808	-6.75

(TABLE 18 : cont'd.)

TOTAL WT.	MEAN	ST. DEV.	SKEW.	KUR.	MEDIAN	C(PHI.1)
1313.38	-1.961	2.217	.111	.676	-2.181	-6.50
1333.68	-2.198	2.071	.161	.680	-2.523	-6.25

(TABLE 19 : cont'd.)

TOTAL WT.	MEAN	ST. DEV.	SKEW.	KUR.	MEDIAN	C(PHI.1)
702.80	-1.652	1.976	.274	.630	-1.998	-5.50
443.80	-2.122	1.707	.392	.756	-2.529	-5.50
314.98	-.600	2.186	-.494	.557	.370	-4.50
220.42	-1.022	2.046	-.210	.618	-.586	-6.00
732.60	-1.552	2.290	.494	.620	-2.354	-6.25
676.69	-1.072	1.984	-.352	.520	-.428	-6.00
719.14	-1.601	1.854	.212	.712	-1.915	-5.00
869.37	-2.281	2.392	.642	.648	-3.541	-6.00
885.28	-1.806	2.241	.385	.631	-2.511	-6.50
830.78	-1.060	1.646	-.201	.812	-.765	-6.00
3036.60	-2.881	2.609	.575	.985	-4.018	-6.00
3296.49	-3.009	2.702	.504	1.137	-4.100	-6.50

TABLE 20 : LATERAL ACCRETION FACIES : TRANSITION SUB-FACIES

SAMPLE NO.	-6.5	-6.0	-5.5	-5.0	-4.5
WP 20/7 1	0.00	0.00	0.00	0.00	33.84
WP 20/7 2	0.00	0.00	0.00	0.00	0.00

TABLE 21 : LATERAL ACCRETION FACIES : SANDS

SAMPLE NO.	-6.5	-6.0	-5.5	-5.0	-4.5
WP 10/5 5	0.00	0.00	0.00	0.00	0.00
WP 15/7 8	0.00	0.00	0.00	0.00	0.00
WP 15/7 9	0.00	0.00	0.00	0.00	0.00
WP 30/7 3	0.00	0.00	0.00	0.00	0.00
WP 30/7 4C	0.00	0.00	0.00	0.00	0.00
WP 30/7 5	0.00	0.00	0.00	0.00	0.00
WP 30/7 8	0.00	0.00	0.00	0.00	0.00

TABLE 22 : SIDE CHANNEL FACIES

SAMPLE NO.	-6.5	-6.0	-5.5	-5.0	-4.5
WP 10/5 1	0.00	0.00	0.00	0.00	0.00
WP 10/5 3	0.00	0.00	0.00	0.00	0.00
WP 10/5 7	0.00	0.00	0.00	0.00	0.00
WP 10/5 8	0.00	0.00	0.00	0.00	0.00
WP 15/7 1	0.00	0.00	0.00	0.00	0.00
WP 15/7 2	0.00	0.00	0.00	0.00	0.00
WP 15/7 3	0.00	0.00	0.00	0.00	0.00
WP 15/7 4	0.00	0.00	0.00	0.00	0.00
WP 15/7 5	0.00	0.00	0.00	0.00	0.00
WP 30/7 1A	0.00	0.00	0.00	0.00	0.00
WP 30/7 2	0.00	0.00	0.00	0.00	0.00
WP 30/7 4F	0.00	0.00	0.00	0.00	0.00
WP 30/7 7F	0.00	0.00	0.00	0.00	0.00
WP 30/7 7C	0.00	0.00	0.00	0.00	0.00

(TABLE 20 : cont'd.)

-4.0	-3.5	-3.0	-2.5	-2.0	-1.5
40.57	40.11	20.13	9.88	4.84	5.70
11.62	5.73	4.10	1.35	3.01	1.90

(TABLE 21 : cont'd.)

-4.0	-3.5	-3.0	-2.5	-2.0	-1.5
0.00	34.37	6.65	18.24	10.67	7.28
0.00	0.00	0.00	1.04	1.96	1.44
0.00	0.00	0.00	.66	1.52	.30
0.00	0.00	0.00	0.00	0.00	0.00
0.00	0.00	0.00	0.00	0.00	.40
0.00	0.00	0.00	0.00	0.00	.04
0.00	0.00	0.00	0.00	0.00	.13

(TABLE 22 : cont'd.)

-4.0	-3.5	-3.0	-2.5	-2.0	-1.5
0.00	0.00	0.00	0.00	0.00	0.00
0.00	0.00	0.00	0.00	0.00	0.00
0.00	0.00	0.00	0.00	0.00	0.00
0.00	0.00	0.00	0.00	0.00	0.00
0.00	0.00	0.00	0.00	0.00	0.00
0.00	0.00	0.00	0.00	0.00	0.00
0.00	0.00	0.00	0.00	0.00	0.00
0.00	0.00	0.00	0.00	0.00	0.00
0.00	0.00	0.00	0.00	0.00	0.00
0.00	0.00	0.00	0.00	0.00	0.00
0.00	0.00	0.00	0.00	0.00	0.00
0.00	0.00	0.00	0.00	0.00	0.00
0.00	0.00	0.00	0.00	0.00	0.00
34.55	41.65	17.84	6.18	2.72	3.13

(TABLE 20 : cont'd.)

-1.0	-0.5	0.0	0.5	1.0	1.5
5.12	4.91	5.56	7.83	18.23	55.95
2.28	4.42	9.76	18.09	45.51	146.29

(TABLE 21 : cont'd.)

-1.0	-0.5	0.0	0.5	1.0	1.5
8.33	11.15	25.20	59.45	91.92	101.89
1.93	2.37	3.45	8.15	14.22	32.83
.11	.76	6.67	65.14	142.46	97.25
.14	.01	.12	.65	5.50	54.57
.25	.16	.43	.85	3.65	15.35
.14	1.33	3.37	5.10	6.79	11.37
.10	.19	.51	1.33	5.60	21.23

(TABLE 22 : cont'd.)

-1.0	-0.5	0.0	0.5	1.0	1.5
0.00	0.00	.08	.19	.55	3.16
0.00	0.00	0.00	.02	.23	1.86
0.00	0.00	0.00	0.00	.01	.02
0.00	.02	.07	.14	.13	.53
0.00	0.00	0.00	0.00	0.00	.09
0.00	0.00	0.00	0.00	0.00	.06
0.00	0.00	0.00	0.00	0.00	.08
0.00	0.00	0.00	0.00	.01	.12
0.00	.01	.01	.25	.13	1.64
.04	.04	.01	.06	.22	1.19
0.00	0.00	.07	.13	15.04	0.00
0.00	0.00	.01	.07	.22	1.09
.09	.18	.38	1.49	6.76	23.25
2.96	3.55	3.66	4.65	15.73	72.31

(TABLE 20 : cont'd.)

2.0	2.5	3.0	3.5	4.0	PAN
41.50	18.92	7.18	3.10	1.58	2.18
108.94	45.47	16.65	6.35	3.35	3.93

(TABLE 21 : cont'd.)

2.0	2.5	3.0	3.5	4.0	PAN
57.61	28.07	9.96	3.29	1.46	1.92
41.91	44.13	26.89	14.72	8.84	5.82
55.02	39.01	7.46	1.67	.68	1.57
69.09	35.29	13.37	4.97	2.32	1.32
17.40	9.16	2.86	1.09	.52	.50
18.04	15.58	6.72	2.25	.81	.55
14.73	6.55	2.51	1.06	.48	.49

(TABLE 22 : cont'd.)

2.0	2.5	3.0	3.5	4.0	PAN
9.15	16.91	16.93	10.44	6.26	2.64
5.46	15.69	29.56	21.15	11.86	4.89
.27	7.69	32.33	24.89	12.00	4.64
6.91	54.45	48.03	13.92	4.32	1.48
.63	3.21	9.89	14.16	17.11	27.84
.90	14.83	44.34	22.68	10.13	3.36
.95	15.80	33.75	13.03	5.35	1.78
1.32	21.36	31.40	11.59	3.54	.99
8.12	33.76	21.59	5.38	1.60	.49
2.73	7.59	16.57	13.96	9.33	4.67
0.00	29.74	18.58	8.91	4.31	2.34
5.47	12.85	23.44	22.77	19.66	18.64
11.35	3.27	1.01	.39	.21	.40
45.56	17.73	6.52	2.38	1.20	2.01

(TABLE 20 : cont'd.)

TOTAL WT.	MEAN	ST. DEV.	SKEW.	KUR.	MEDIAN	C(PHI.1)
327.13	-1.054	2.600	-.169	.552	-.656	-5.25
438.75	1.343	1.212	-.293	2.725	1.381	-5.25

(TABLE 21 : cont'd.)

TOTAL WT.	MEAN	ST. DEV.	SKEW.	KUR.	MEDIAN	C(PHI.1)
477.46	.327	1.733	-.463	1.684	.812	-4.50
209.70	1.945	1.093	-.053	1.256	1.947	-2.25
420.28	1.087	.699	.232	1.046	.974	-5.00
187.35	1.780	.587	.190	1.025	1.737	.75
52.62	1.683	.660	.080	1.179	1.650	-1.25
72.09	1.598	.945	-.196	1.091	1.719	-.75
54.91	1.553	.639	.222	1.228	1.461	-.25

(TABLE 22 : cont'd.)

TOTAL WT.	MEAN	ST. DEV.	SKEW.	KUR.	MEDIAN	C(PHI.1)
66.31	2.624	.776	.062	1.015	2.592	.75
90.72	2.896	.694	.027	1.080	2.874	1.25
81.85	3.060	.542	.172	1.017	3.012	2.00
130.00	2.546	.455	.132	1.004	2.529	1.50
72.93	3.643	.650	-.265	.798	3.748	2.00
96.30	2.937	.515	.202	1.095	2.865	2.00
70.74	2.813	.520	.161	1.236	2.775	1.75
70.33	2.712	.487	.117	1.091	2.697	1.75
72.98	2.438	.486	.132	1.141	2.390	1.25
56.41	3.024	.737	.021	1.088	2.993	1.25
79.12	2.162	1.045	-.224	1.613	2.409	.50
104.22	3.210	.798	-.024	.875	3.197	1.50
48.78	1.380	.532	.149	1.255	1.333	-.25
284.33	-.334	2.445	-.653	.540	1.038	-5.50

APPENDIX C

PALAEOCURRENTS: METHODS AND DATA

APPENDIX C

PALAEOCURRENTS: METHODS AND DATA

To obtain estimates of the palaeocurrents that deposited the sands and gravels a number of different sedimentary structures and fabrics were measured.

(i) The imbricate fabric of the crudely horizontally stratified gravels.

(ii) The tabular-and trough-cross bedded foresets of the sands and gravels.

(iii) The crest lines, cross-laminae and 'rib and furrow' structures of rippled and ripple drift cross laminated sands and silts.

The following accout gives a brief outline of the way in which the data was collected in the field, analysed and plotted.

THE IMBRICATE FABRICS

Any one sample was taken in what was designated to be a single sedimentation unit. This in itself can be quite difficult to determine in the case of the more "massive" gravels, but a reasonable guide was obtained from the frequent sandy horizons found within these gravels. Sets of data were then taken between two of these sandy lenses which were vertically adjacent in the more dubious 'beds'. All the pebbles and cobbles measured had a ratio of b:c axes of more than 3:1, and a b-axis of more that 5cm. In nearly all the cases the a-axes were oriented transverse to the inferred palaeocurrent direction, and the a-b planes (maximum projection planes) dipped upstream. Using a specially designed instrument (see Fig. 50) for the field measurement it was possible to take both the direction and the angle of maximum dip of the

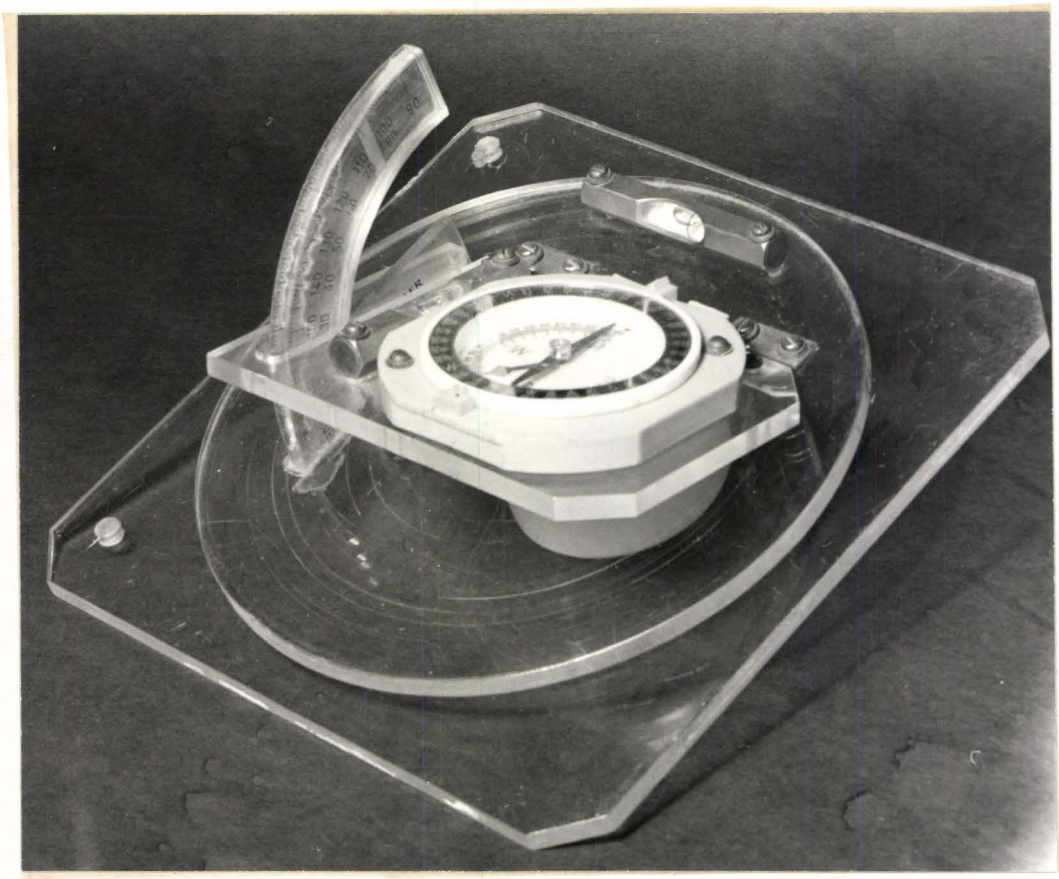

Fig. 50: Instrument used for measuring pebble orientations.

a-b plane on any pebble or cobble.

At each sampling site 20 to 35 particles were measured, depending on the quality of the fabric. If the gravel was "well imbricated" fewer pebbles were measured than if it were "poorly imbricated". The particles chosen were the 20 (to 35) closest to the starting point of the sampling, within the sedimentation unit, and rarely spread over more than 1 square metre.

The individual measurements were plotted stereographically on a Schmidt net as the point at the intersection of the azimuth of the maximum dip direction and the projection of the a-b plane, in the northern hemisphere. The resulting scatter of points was then contoured at 1, 2.5, 5, 7.5,10 and 12.5 percent per one-percent area. This method results in "girdle" toward the edge of the plot on the downstream side of the centre, and gives a better visual effect than plotting the more conventional 'poles to the plane of maximum projection', which would group closely near to the centre.

The vector means of these and all other palaeocurrent data were calculated by standard programmes from the McMaster University Data Processing and Computing Centre Programme Library.

THE CROSS-BEDDING

The cross-bedding measured was of several different types and in widely varying grain sizes of material. Where the coarsest gravels had developed large scale foresets, as in the Bar Front Facies at East Paris, and the Bar Front and Lateral Accretion facies at West Paris, an approximation of the corss-bedding had to be made.. In this case pebbles and cobbles were measured which had a pronounced elongation of the a-b plane (tabular or discoid in shape), and which lay in the plane

of the foresets. For each particle the direction and angle of the maximum dip of the a-b plane were measured. A similar procedure was commonly used where sandy cross-strata had pebbles on the foreset slopes.

Where the deposits were partially consolidated the foresets themselves were measured directly. This was commonly the case with coarse sand and granule sized sediments. In unconsolidated sands the task of collecting palaeocurrent data was much simplified. A small trench could be dug and plane of the foresets approximated very well from their traces on two mutually perpendicular faces.

The difficulty of getting good palaeocurrent data from trough cross-bedding was minimized by the fact that excavation and trenching were normally possible. Hence data could be collected from both sides of the troughs. Commonly this would mean neglecting the cross-strata of the axial portion and a bimodal plot would result. But the bisector of the two modes give a good indication of the axial position of the troughs.

All this type of data was plotted on rose diagrams as percent per 15 degree class interval.

THE RIPPLED SANDS

The sediments were invariably unconsolidated so that trenching was very easy. In the case of small-scale trough cross-bedding the sands were planed off to the horizontal and the directions obtained from the "rib and furrow" structures exhibited. With more tabular or straight crested ripples the crest line was often measured and the palaeocurrent direction taken at right angles to it. Surfaces, such as the stoss-side surface in ripple drift cross-laminated sands could be measured by the outcrop of the plane on two mutually perpendicular surfaces

cut into the sands.

Again, this type of data was plotted on rose diagrams as per cent per 15 degree class interval.

In the following tables all the bearings of the raw data are magnetic. Local magnetic declination is 6° west of True North. The vector means are corrected for true north. (*) denotes figure corrected for true north. (1) denotes either mean of dip angles; or vector mean of directions corrected for true north; or inferred palaeocurrent directions corrected for true north. (2) denotes standard deviation in degrees.

PALAEOCURRENT DATA: EAST PARIS

TABLE 23: BAR CORE FACIES - IMBRICATION

5 samples 119 readings vector mean 138° (*)

F5		F27		F36		F47		F48	
Dip	Dirn	Dip	Dirn	Dip	Dirn	Dip	Dirn	Dip	Dirn
24	292	13	328	9	321	21	310	17	322
23	312	35	046	27	294	17	326	18	331
25	329	21	292	16	060	44	312	42	316
17	334	21	009	30	342	28	303	33	310
31	348	10	266	23	317	21	254	27	259
18	308	9	187	12	277	31	306	29	302
26	010	13	092	22	312	43	307	49	317
32	332	5	244	26	002	29	332	30	306
15	356	4	079	32	304	21	356	23	352
19	044	48	331	46	336	20	332	14	350
16	335	8	238	14	327	16	013	17	340
21	314	9	274	47	318	15	347	26	305
45	321	13	043	28	324	33	303	23	335
35	352	23	316	25	322	34	338	24	314
24	308	29	017	26	294	32	305	14	352
17	342	24	313	30	324	21	012	8	314
7	047	28	326	20	298	8	301	10	008
14	346	32	274	29	332	8	352	16	333
23	324	23	015	29	312	21	001	16	286
27	334	17	332	28	024	17	322		
26	312	10	358	9	008				
25	292	3	159	6	274				
19	332	17	285	25	014				
34	002	26	297	23	028				
11	310	23	323	13	297				
34	336								
28	254								
27	289								
15	348								
28	316								
(1) 23	139	23	140	24	135	24	140	24	136
(2) 8	33	11	33	10	35	10	29	10	26

TABLE 24: BAR FRONT FACIES - GRAVEL CROSS-STRATA

7 samples 140 readings vector mean 177 (*)

	F 40		F 41		F 42		F 43		F 44		F 45		F 46	
	Dip	Dirn	Dip	Dirn	Dip	Dirn	Dip	Dirn	Dip	Dirn	Dip	Dirn	Dip	Dirn
	25	261	29	166	35	261	29	280	36	190	21	270	27	264
	22	187	34	253	34	201	34	213	23	192	29	248	36	239
	28	173	34	190	17	177	33	187	27	197	12	228	34	219
	29	145	16	167	13	186	17	184	29	211	33	190	15	212
	44	091	15	144	6	187	16	128	43	215	34	190	14	208
	26	149	8	229	29	161	22	172	39	194	28	199	27	193
	30	173	21	244	27	180	22	192	37	194	34	198	24	192
	9	199	23	189	43	209	31	221	31	231	30	201	39	190
	14	211	31	165	41	241	9	231	23	237	23	204	34	189
	30	174	34	159	33	191	33	195	27	260	22	211	40	186
	39	156	29	142	22	177	29	172	27	165	33	189	25	181
	38	137	27	211	22	148	28	134	16	173	40	167	35	169
	33	244	27	131	31	138	28	146	39	174	42	168	28	159
	23	184	38	165	34	135	37	143	26	189	28	173	24	157
	27	179	26	174	28	116	26	181	26	187	28	174	29	157
	28	121	28	198	34	169	37	174	27	175	7	131	31	139
	17	232	28	128	34	182	39	199	31	140	13	135	11	120
	37	139	37	109	11	183	41	197	9	151	16	136	31	180
	25	175	39	161	29	211	26	231	16	153	33	151	23	220
	27	159	49	167	21	273	27	259	30	127	34	121	25	189
(1)	28	169	29	169	27	176	28	187	28	182	27	172	28	182
(2)	9	41	9	38	10	40	8	39	8	33	9	45	8	34

TABLE 25: BAR FRONT FACIES - SIDE CHANNEL SAND BODY

3 samples 40 readings vector mean 217° (*)

DE 32	DE 33(A)	DE 33 (B)
axes of troughs	orthogonals to crest lines of foresets	
263	210	231
275	216	222
251	226	227
253	205	226
245	211	229
257	206	206
261	191	207
271	201	211
265	208	213
266	197	212
	214	205
	222	200
	222	191
	220	197
	216	199
(1) 256	205	206
(2) 9	10	13

	F 1		F 2		F 3		F 4		F 6		F 7	
	Dip	Dirn	Dip	Dirn	Dip	Dirn	Dip	Dirn	Dip	Dirn	Dip	Dirn
	12	315	8	010	40	070	5	035	19	014	38	306
	25	304	7	022	25	026	35	014	33	011	29	342
	40	010	24	344	28	334	23	100	27	046	21	016
	21	359	14	296	13	022	40	045	21	108	8	080
	17	290	32	018	20	002	22	030	21	034	26	353
	27	342	19	004	19	006	11	060	10	324	20	357
	15	318	19	341	13	080	10	020	37	012	28	300
	16	343	26	318	26	026	14	344	17	320	23	342
	16	020	25	018	44	002	26	024	28	007	33	323
	50	360	12	060	27	050	34	092	12	017	34	321
	38	285	33	014	19	085	14	338	14	359	24	347
	15	288	36	065	17	008	20	026	43	034	26	072
	11	340	22	090	25	010	15	020	46	338	27	082
	25	302	15	322	16	008	17	016	11	022	27	359
	48	260	38	350	19	352	44	034	17	076	25	004
	13	329	17	310	19	346	32	042	46	358	38	027
	17	020	12	346	19	310	39	328	37	318	44	358
	26	080	17	330	15	052	36	014	26	023	43	012
	24	350	19	340	25	032	31	009	27	354	16	049
	20	120	22	012	44	359	6	070	25	014	26	342
	19	394	24	360	12	030	14	328	24	061	18	103
	19	339	34	350	25	332	11	342	23	049	39	023
	23	356	12	024	27	330	13	013	23	311	19	010
	28	060	30	014	40	318	15	010	29	028	18	082
	32	342	33	018	24	002	33	306	30	332	17	003
(1)	24	161	22	176	24	187	22	194	25	193	26	186
(2)	11	34	9	36	9	36	12	37	10	38	9	44

TABLE 27: STOSS-SIDE FACIES - CROSS STRATA

4 sample 46 readings vector mean 176° (*)

	DE 10		De 13(A)		DE 13 (B)		DE 26	
	Dip	Dirn	Dip	Dirn	Dip	Dirn	Dip	Dirn
	24	170	35	170	6	190	26	233
	26	160	18	166	19	226	19	191
	22	180	21	136	30	250	21	201
	15	280	21	148	17	216	23	196
	17	200	26	138	27	218	24	162
	26	173	6	210	19	272	22	169
	26	173			21	210	20	164
	25	186			11	170	23	197
	13	311			24	148	25	191
	16	112			32	170	22	223
	7	132			7	184	21	197
	13	106			7	220	27	175
	22	160					25	184
	25	126						
	17	134						
(1)	19	167	21	155	18	200	23	185
(2)	6	37	9	28	9	35	3	21

TABLE 28: BAR TOP FACIES - REWORKED BAR CORE UPPER SURFACE

2 samples 51 readings vector mean 249° (*)

F 37		DE 24	
Dip	Dirn	Dip	Dirn
		23	287
34	271	31	209
27	312	32	217
26	004	26	228
24	334	27	234
14	358	28	199
14	290	29	276
13	296	26	270
21	168	28	194
11	284	23	213
26	294	21	200
6	129	22	196
15	016	22	236
33	282	24	204
33	261	24	234
28	258	26	218
31	219	25	217
32	322	21	252
23	297	25	259
41	210	17	203
30	322	11	237
32	294	13	292
24	253	20	284
3	010	11	256
29	255	18	129
13	286	11	161
(1)23	276	22	220
(2)10	39	6	39

TABLE 29: BAR TOP FACIES - SAND LENSES (CROSS STRATA)

5 samples 70 readings vector mean 180° (*)

DE 15		DE 28		DE 30		DE 30	DE 31
Dip	Dirn	Dip	Dirn	Dip	Dirn	Rib and Furrow	
14	160	32	182	20	183	185	189
18	218	28	175	19	186	186	195
18	210	28	188	25	186	185	194
30	268	25	153	24	181	191	189
28	172	30	174	23	192	190	196
24	096	29	169	26	193	179	179
33	246	30	163	27	194	177	185
28	178	28	171	28	196	191	183
				24	195	176	184
				21	196	185	181
				21	191	184	191
				26	189	191	195
				28	187	172	197
				27	186	177	198
				31	191	185	198
						183	179
						181	179
						184	189
						180	188
							189
24	188	29	166	25	183	177	182
7	54	2	11	3	5	6	7

TABLE 30: BAR TOP FACIES - IMBRICATION

4 samples 95 readings vector mean 179° (*)

	F 25		F 39		F 49		F 50	
	Dip	Dirn	Dip	Dirn	Dip	Dirn	Dip	Dirn
	13	328	20	018	25	001	36	332
	35	046	30	337	24	016	40	358
	21	292	25	356	22	101	41	002
	21	009	17	339	28	032	23	010
	10	266	37	003	26	034	23	034
	9	187	22	028	25	356	27	025
	13	092	21	309	5	301	25	021
	5	244	20	225	25	348	9	021
	4	079	12	346	21	356	38	016
	48	331	10	326	27	360	27	019
	8	238	6	048	42	032	17	060
	9	274	25	006	35	016	20	071
	13	043	23	037	15	025	30	103
	23	316	11	349	15	048	19	309
	29	017	14	065	13	061	20	356
	24	313	4	089	20	056	25	358
	28	326	5	222	21	034	24	360
	32	274	26	342	17	028	23	358
	23	015	21	023	24	016	21	016
	17	332	29	011	19	017	24	021
	10	358	6	208	10	010		
	3	159	16	051	21	001		
	17	285	21	214	18	009		
	26	297	29	172	15	010		
	23	323	20	033	18	017		
(1)	19	157	19	189	21	204	26	201
(2)	11	54	9	33	8	29	8	33

DE 16		DE 2A		DE 2B		DE 8A		DE 9		DE 1		DE 1 (cont'd.)	
Dip	Dirn	Dip	Dirn	Dip	Dirn	Dip	Dirn	Dip	Dirn	Dip	Dirn	Dip	Dirn
21	230	25	070	26	206	21	248	15	220	24	190	27	168
22	230	17	210	16	207	18	251	3	193	14	240	29	177
33	235	28	148	19	164	26	328	13	200	17	238	29	183
28	250	29	105	12	178	20	212	15	199	22	190	22	207
29	230	30	260	16	179	25	186	15	259	13	194	30	191
27	255	12	270	25	189	30	188	23	210	12	270	27	190
32	156	17	156	11	180	14	223	12	212	13	294	23	222
		23	180	13	120	21	254	31	170	16	259	15	243
		29	168	14	245	14	249	29	130	26	188	24	216
		20	283	17	266	19	203	27	118	11	120	13	264
		27	090	6	192	17	201	15	240	22	230	16	229
		23	120	8	264					23	218	25	206
		27	185	12	120					13	189	27	202
		29	160	23	250					24	193	11	118
		22	180	16	150					19	208	28	190
		30	162	13	130					4	252	25	218
		15	223	6	144					9	114	11	134
		26	191	12	110					20	210	14	155
		12	199	25	178					23	178	27	170
		27	132	12	177					28	181	28	173
		26	180	18	164					17	159	14	170
		21	150							9	196	36	184
		21	180							17	151	31	178
										21	194	14	189
										12	199	22	202
										20	184		
(1) 27	220	23	171	15	179	20	216	18	190			20	190
(2) 4	33	6	51	6	50	5	26	9	42			7	37

TABLE 32: SIDE CHANNEL FACIES -RIPPLED SANDS

4 samples 56 readings vector mean 218° (*)

DE 4	DE 5	DE 18	DE 6
Rib and Furrow Structures			orthoganals to crest lines
236	212	192	240
230	234	174	236
215	231	204	231
215	209	206	
210	205	148	
220	249	151	
185	226	187	
195	249	202	
218	208	176	
232	222	208	
226	208	203	
236	220		
	225		
	225		
	209		
	215		
	240		
	235		
	244		
	222		
	222		
	231		
	292		
	242		
	281		
	305		
	306		
	283		
	283		
(1) 212	232	185	235
(2) 16	30	32	5

TABLE 33: SHALLOW BRAIDED FACIES - IMBRICATION

5 samples 125 readings vector mean 196° (*)

F 21		F 22		F 23		F 24		F 26	
Dip	Dirn	Dip	Dirn	Dip	Dirn	Dip	Dirn	Dip	Dirn
22	045	12	358	22	003	2	279	26	016
7	054	12	262	8	353	16	339	5	281
31	013	8	008	16	356	35	077	25	009
5	026	8	007	24	013	15	349	21	040
6	048	21	002	25	099	12	337	27	032
8	146	8	107	4	124	34	013	42	029
7	083	14	311	29	020	29	011	35	066
15	314	16	326	6	347	31	042	15	031
9	302	24	026	18	293	28	358	15	002
9	108	20	305	30	045	14	359	13	019
12	030	21	196	6	360	21	332	20	091
10	316	26	358	8	343	19	002	21	307
5	153	29	065	12	015	15	063	17	010
14	084	11	214	16	111	17	015	24	029
7	093	12	226	41	157	12	330	19	044
19	125	18	222	22	179	5	049	10	087
7	224	8	125	13	105	37	304	21	048
15	034	28	017	4	164	13	337	18	343
16	182	24	021	8	148	12	346	15	294
24	024	11	341	19	089	22	041	18	057
22	014	36	347	10	096	41	040	25	041
14	020	30	030	11	299	38	029	24	010
13	030	16	067	40	080	41	057	22	007
5	182	6	016	18	026	9	192	28	355
3	080	15	028	14	044	31	351	28	360
1) 12	192	17	182	17	227	22	183	21	191
2) 7	44	8	39	10	50	11	41	8	41

TABLE 34: SHALLOW BRAIDED FACIES - CHANNEL INFILL CROSS-STRATA

5 samples 21 readings vector mean 229 (*)

	DE 11		DE 17		DE 19		DE 20		DE 23	
	Dip	Dirn	Dip	Dirn	Dip	Dirn	Dip	Dirn	Dip	Dirn
	33	272	34	242	30	266	29	223	27	208
	22	268	35	242	28	251	31	219	30	217
	15	194	21	250	28	206	28	218	21	219
	32	270	14	252					28	231
			23	241					21	195
			25	250						
(1)	26	245	25	241	28	235	29	214	25	208
(2)	8	38	8	5	1	31	2	3	4	14

TABLE 35: SHALLOW BRAIDED FACIES -TABULAR CROSS-STRATA

3 samples 47 readings vector mean 205° (*)

	DE 34		DE 35		DE 36	
	Dip	Dirn	Dip	Dirn	Dip	Dirn
	26	210	21	229	17	239
	29	215	19	241	17	214
	18	210	17	235	19	211
	16	212	16	221	21	208
	21	221	17	227	35	207
	25	230	19	224	34	201
	24	229	21	196	29	224
	27	195	24	191	29	223
	29	200	23	200	27	219
	31	196	23	201	29	200
	33	199	31	199	17	184
	34	201	33	197	31	201
	29	206	32	210	16	195
	35	221	29	206	25	196
	17	216	27	215	24	199
	16	211	28	216		
(1)	26	205	24	207	25	202
(2)	6	11	6	15	6	14

TABLE 36: SHALLOW BRAIDED FACIES - CROSS BEDDED SANDS

3 samples 48 readings vector mean 198° (*)

	DE 37		DE 38		DE 39	
	Dip	Dirn	Dip	Dirn	Dip	Dirn
	6	174	14	184	5	200
	16	186	11	196	4	201
	10	229	9	211	16	201
	9	216	21	201	17	211
	31	217	17	197	11	221
	32	224	16	210	30	232
	16	227	19	217	27	217
	21	196	21	206	21	200
	16	197	23	214	23	184
	11	210	27	197	19	184
	19	199	29	196	17	186
	17	210	30	210	18	188
	21	239	10	221	17	199
	22	241	3	159	6	212
	23	210	6	160	10	221
	24	196			11	241
	24	183				
(1)	19	203	17	193	16	200
(2)	7	19	8	19	8	17

PALAEOCURRENT DATA: WEST PARIS

TABLE 37: BAR FRONT FACIES - IMBRICATION

3 samples 70 readings vector mean 236° (*)

	F 28		F 29		F 32	
	Dip	Dirn	Dip	Dirn	Dip	Dirn
	35	076	13	086	43	059
	19	041	11	056	25	075
	21	039	15	087	38	102
	44	128	13	073	31	074
	22	031	15	074	10	102
	20	302	19	114	22	069
	28	017	6	103	26	073
	32	098	15	073	19	078
	23	077	36	072	40	047
	28	121	32	045	27	058
	23	336	22	134	26	051
	15	016	23	031	29	048
	15	034	23	049	29	031
	20	332	26	087	23	055
	14	116	39	067	31	075
	12	339	34	058	20	113
	17	015	32	025	17	063
	21	013	31	034	31	061
	18	022	36	086	24	077
	18	319	12	025	23	035
	26	103	15	353		
	20	346	17	060		
	13	027	38	048		
	5	084	32	061		
	30	338	28	073		
(1)	21	206	24	242	27	242
(2)	8	54	10	27	8	21

TABLE 38: BAR FRONT FACIES - GRAVEL FORESETS

6 samples 165 readings vector mean 274° (*)

F 14		F 15		F 30		F 31		F 34		F 35	
Dip	Dirn	Dip	Dirn	Dip	Dirn	Dip	Dirn	Dip	Dirn	Dip	Dirn
38	210	11	251	16	241	36	314	8	312	27	233
24	252	26	334	12	024	40	311	20	142	37	324
39	247	30	296	17	102	41	306	9	125	28	332
23	214	23	330	20	040	23	254	32	354	22	327
41	248	24	250	20	121	23	234	48	014	14	268
12	278	17	322	12	013	25	219	32	012	23	315
33	252	35	318	20	302	17	282	34	064	41	291
11	302	17	194	25	033	9	306	42	105	36	287
33	196	6	322	23	300	38	268	29	236	34	329
20	302	15	341	14	109	37	285	26	226	28	306
13	308	14	244	13	254	17	262	21	232	22	300
20	253	30	247	33	318	20	274	39	235	37	301
13	272	23	317	19	089	30	275	45	214	33	296
11	206	16	360	12	328	19	298	26	226	27	282
17	275	12	074	39	305	20	221	39	296	33	261
14	233	8	351	22	070	15	206	39	268	32	258
38	202	23	332	26	093	25	231	15	264	9	271
18	212	21	002	33	059	18	246	32	170	35	299
27	327	21	340	29	037	34	202	45	021	14	266
24	281	32	004	18	107	21	204	32	026	29	332
17	253	41	002	30	289			35	009		
38	268	28	292	20	240			32	288		
12	232	14	040	40	321			28	058		
8	195	21	341	28	236			14	284		
17	273	25	336	27	273			27	271		
		14	310	31	217			24	354		
		14	308	10	221			14	321		
		36	335	35	055			12	233		
		15	281	25	123			22	252		
		11	270	14	103			14	229		
		11	084	20	039						
		3	010	18	093						
		28	325	23	041						
		40	360	21	340						
		24	010	23	312						
22	246	21	320	23	261	25	254	28	248	28	288
11	37	9	52	8	43	9	38	11	49	9	28

TABLE 39: BAR FRONT FACIES - MINOR BARS

2 samples 28 readings each

DW 10		DW 11/F 16	
Dip	Dirn	Dip	Dirn
15	171	9	087
33	157	31	018
23	169	38	358
26	151	25	337
20	141	36	026
22	171	35	067
12	184	36	012
16	203	28	061
22	162	30	025
28	159	23	360
26	167	15	335
10	136	22	045
16	171	23	051
14	139	19	004
24	103	7	312
32	279	40	316
44	257	22	208
28	248	20	318
28	272	32	289
25	241	18	215
21	234	26	230
41	237	31	212
18	246	12	232
28	206	11	279
8	243	16	236
29	217	30	280
37	186	25	270
29	251	24	266
24	190	24	317
9	47	9	72

(1)
(2)

TABLE 40: BAR FRONT FACIES - SAND DRAPE (a) RIPPLES

5 samples 52 readings

DW 2	DW 12	DW 13	DW 14	DW 15
Rib & Furrow	orthogonals to crest lines of ripples			
220	286	206	188	264
249	283	211	192	260
237	262	216	194	266
255	263	196	194	268
239	284	193	191	266
	288	191	207	261
	263	201	242	259
	261	202	238	258
	271	202	231	246
	265	206	239	248
	276	206		
	275	208		
		203		
		201		
		192		
(1) 234	264	196	204	253
(2) 13	10	7	22	7

TABLE 41: BAR FRONT FACIES - SAND DRAPE (b) RIPPLES

7 samples 60 readings

DW 18	DW 19(A)	DW 19(B)	DW 20	DW 21(A)	DW 21(B)	DW 22
Rib and Furrow Structures			Orthoganals to ripple crests		Rib and Furrow Structures	
183	217	186	191	217	199	203
184	183	208	197	221	202	226
202	194	217	171	219	194	219
194	173	176	168	220	209	206
		192	173	206	207	207
		195		212	211	178
		199		208	211	231
		195		227	231	237
		200		219	196	209
		199		204	227	184
		199			214	207
					233	190
					199	
					221	
(1) 185	186	191	174	209	205	202
(2) 9	19	11	13	7	13	18

TABLE 42: BAR FRONT FACIES - SAND DRAPE (c) RIPPLES

7 samples 82 readings

DW 4(A)	DW 4(B)	DW 4(C)	DW 5	DW 6	DW 7	DW 8
Ribs and Furrow Structures				Orthoganals to crest lines		
182	038	215	116	271	288	284
185	013	183	113	264	274	289
186	001	179	118	262	262	287
211	353	178	164	253	305	286
193	352	207	109	242	297	287
184	015		085	247	199	289
182	025			261	283	
193	354			248	266	
191	054			255	268	
186	024			247	289	
177	341			236	273	
198	006			305	286	
191	350			244	312	
190	342			247	273	
174	359				268	
	007				296	
	016					
	004					
	040					
	354					
(1) 182	002	186	112	250	277	281
(2) 9	19	17	25	17	15	2

TABLE 43: LATERAL ACCRETION FACIES - IMBRICATION (i)

5 samples 135 readings vector mean 188° (*)

F 9		F 11		F 12		F 13		F 20	
Dip	Dirn	Dip	Dirn	Dip	Dirn	Dip	Dirn	Dip	Dirn
39	057	20	067	19	342	25	047	30	038
25	086	42	062	13	292	17	355	38	097
21	057	36	081	34	016	10	332	29	024
11	106	35	042	23	145	11	234	24	043
20	039	22	174	22	072	15	360	21	044
10	026	30	072	20	348	38	032	17	331
13	271	13	074	19	018	42	082	25	037
25	248	19	336	10	014	42	020	26	051
55	360	28	048	25	062	6	330	3	020
15	317	21	018	33	339	13	334	26	229
14	007	10	274	17	317	15	218	10	050
17	092	22	012	15	336	29	346	14	061
31	004	7	347	27	319	36	007	7	259
34	021	23	348	40	086	15	054	12	013
33	034	38	336	28	333	18	056	9	055
42	314	10	190	13	302	23	070	16	324
27	027	11	270	40	320	11	024	6	027
27	326	29	012	40	040	16	325	9	050
6	021	17	334	22	174	40	060	27	051
27	006	26	039	37	113	13	352	12	031
13	029	26	030	30	029	38	078	10	236
27	308	29	046	9	212	49	069	37	018
18	304	32	055	25	347	33	010	16	100
13	358	16	328	23	328	18	013	12	347
46	026	16	294	30	052	10	141	32	026
		17	022						
		19	012						
		18	292						
		25	292						
		16	348						
		19	140						
		9	079						
		18	358						
		9	027						
		23	322						
1) 24	180	21	180	25	185	23	188	19	209
2) 12	54	9	48	9	71	12	62	10	59

TABLE 44: LATERAL ACCRETION FACIES - IMBRICATION (ii)

2 samples 50 readings vector mean 248° (*)

	F 10		F 17	
	Dip	Dirn	Dip	Dirn
	22	131	14	088
	31	074	26	072
	34	013	14	046
	20	119	34	110
	30	098	15	135
	11	160	14	065
	31	093	18	148
	41	065	36	028
	42	145	18	124
	32	133	10	001
	16	079	35	355
	16	164	6	121
	15	036	34	056
	10	109	23	143
	14	304	17	086
	17	357	25	076
	14	132	16	151
	20	100	4	358
	21	252	3	101
	24	076	33	330
	25	064	16	065
	22	338	7	100
	15	128	17	144
	18	025	6	065
	25	074	29	310
(1)	22	247	18	248
(2)	9	34	10	57

TABLE 45: LATERAL ACCRETION FACIES - CROSS STRATA

2 samples 50 readings vector mean 317° (*)

	F 18		F 19	
	Dip	Dirn	Dip	Dirn
	40	339	24	035
	46	324	26	064
	28	254	25	120
	11	280	8	132
	18	024	21	295
	12	281	35	180
	27	322	39	288
	27	304	12	266
	27	330	19	278
	33	338	5	084
	32	314	74	276
	9	044	16	288
	41	273	30	242
	30	032	13	331
	28	344	22	342
	8	061	37	240
	33	001	23	214
	22	354	16	280
	18	056	14	355
	22	329	15	286
	18	337	23	324
	27	346	28	228
	24	328	21	302
	32	341	11	240
	25	346	17	308
(1)	25	333	21	308
(2)	10	43	9	59

TABLE 46: LATERAL ACCRETION FACIES - TRANSITION SUB-FACIES

1 sample 25 readings

DW 28	
Dip	Dirn
10	289
9	295
17	345
16	270
13	267
21	347
31	358
11	360
26	004
19	271
21	281
23	276
11	313
13	331
16	319
19	321
19	295
21	286
17	284
23	302
26	346
30	348
21	351
17	354
18	303
6	37

TABLE 47: LATERAL ACCRECTION FACIES - CROSS BEDDED SANDS

1 sample 15 readings

	DW 27	
	Dip	Dirn
	25	305
	24	301
	31	291
	32	254
	30	265
	29	281
	29	288
	26	280
	28	279
	24	255
	21	263
	22	277
	25	278
	24	291
	30	279
(1)	27	273
(2)	3	15

TABLE 48: SIDE CHANNEL FACIES - RIPPLES

2 samples 40 readings

	DW 23	DW 24
	Orthogonals to crest lines.	
	229	004
	211	302
	213	331
	207	333
	191	329
	195	328
	195	346
	186	353
	217	356
	221	357
	228	348
	211	331
	206	333
	204	329
	199	327
	190	301
	197	311
	199	309
	211	316
	207	317
(1)	200	325
(2)	47	49

TABLE 49: SIDE CHANNEL FACIES - CROSS-BEDDED SANDS

2 samples 30 readings vector mean 253°(*)

	DW 25		DW 26	
	Dip	Dirn.	Dip	Dirn.
	21	270	19	275
	26	295	30	261
	27	243	21	253
	29	271	23	251
	31	263	25	226
	31	259	26	245
	28	287	29	271
	28	288	31	251
	27	261	26	255
	21	270	24	256
	26	263	28	231
	25	288	28	233
	31	265	27	234
	29	263	23	251
	28	251	24	268
(1)	27	262	26	245
(2)	3	14	3	15

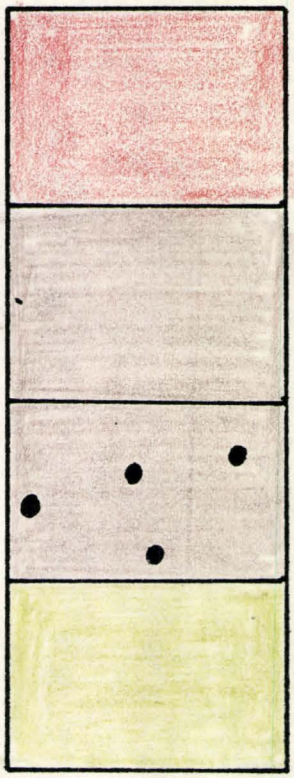

OUTWASH GRAVELS

WENTWORTH TILL

PORT STANLEY II

PORT STANLEY I

Loc. 2

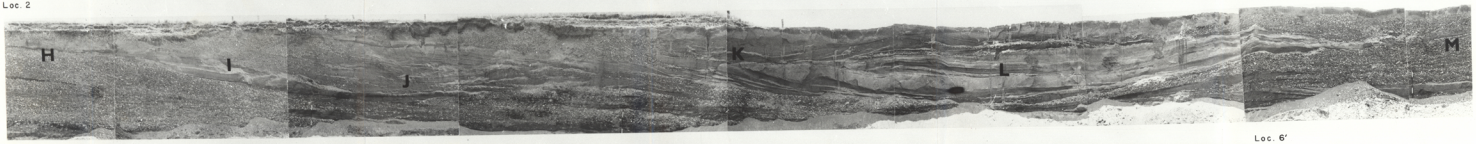

Loc. 7

Loc. 6'

Loc. 5'

Loc. 5

Loc. 5'

Loc. 4'

Location numbers refer to Fig.

WEST PARIS PIT: PHOTOLOG

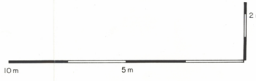

NATIONAL TOPOGRAPHIC SERIES 1:50,000

CANADA

EDITION 4 ~~THIRD EDITION~~

CANADA, SHEET 40 P/8 WEST HALF

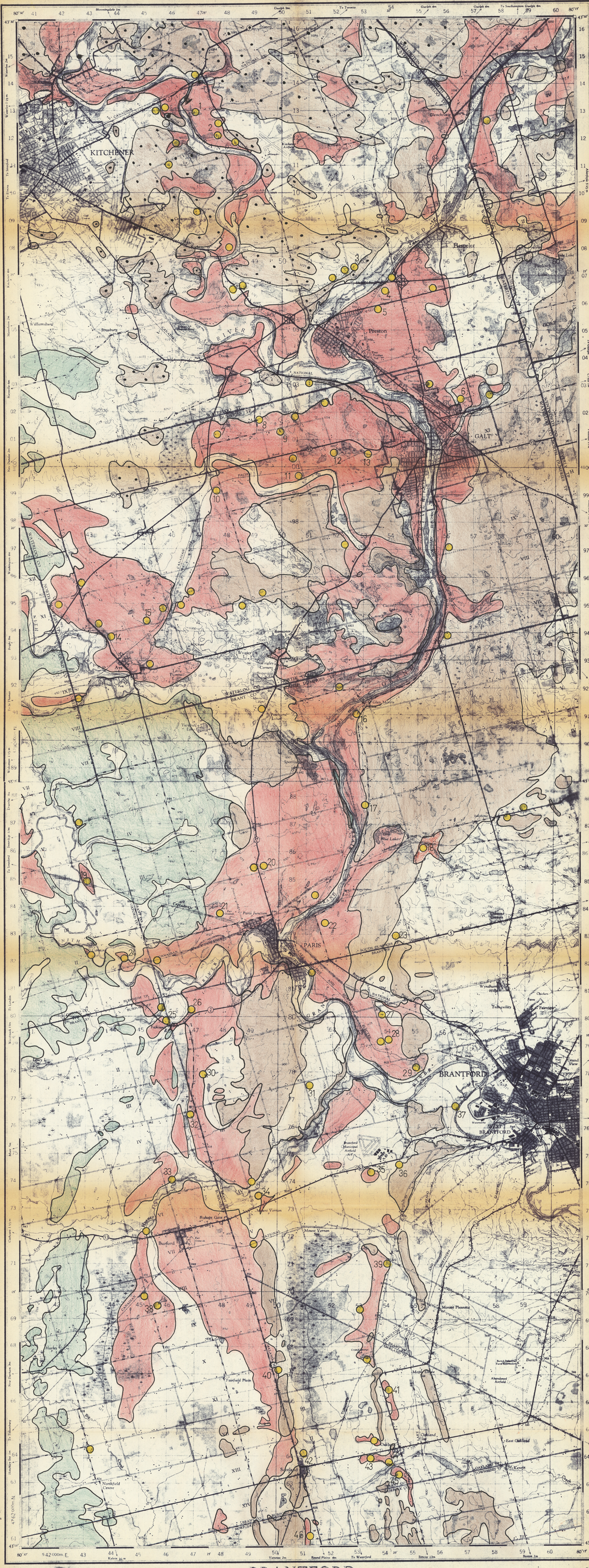

Original Survey by the Army [illegible] Establishment, R.C.E. 1909
Aerial photography by the R.C.A.F. 1951

DECLINATION 1956

BRANTFORD

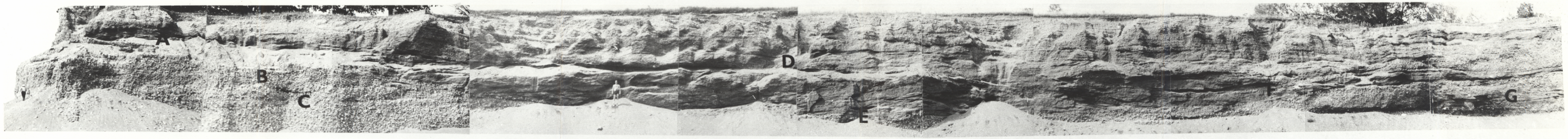

Loc. 2

Loc. 3

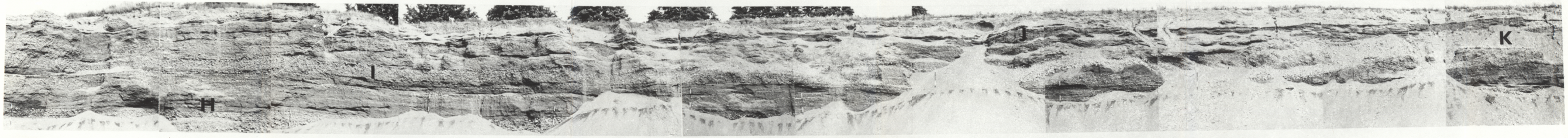

Loc. 3

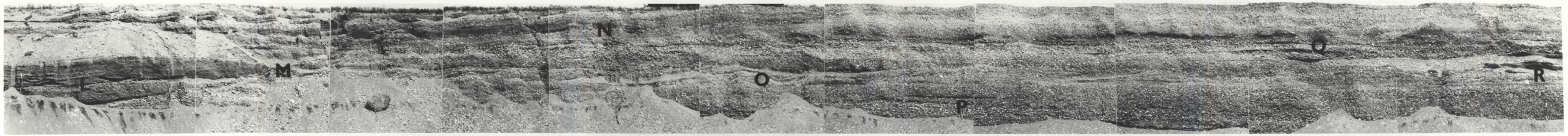

Loc. 4

EAST PARIS PIT: PHOTOLOG

5m

20m 10m

Location numbers refer to Fig.10